“Nuclear hormone receptor regulation of microRNAs”

Dissertation

zur Erlangung des Grades eines Doktors
der Naturwissenschaften (Dr. rer. nat.)
an der Universität Osnabrück

vorgelegt
von Axel Bethke
aus Osnabrück in Niedersachsen, Deutschland
Juni 2009

Externer Betreuer: Prof. Dr. Adam Antebi
Baylor College of Medicine
Houston, Tx
USA

1. Berichterstatter : Prof. Dr. Helmut Wieczorek

2. Berichterstatter: Prof. Dr. Achim Paululat

Abstract

The progression of multicellular organisms through different genetically defined developmental programs requires temporal control. Endocrine regulation of this temporal control is achieved by small molecules that originate from endocrine tissues and diffuse throughout the whole body of the animal to coordinate program execution by activating cell specific gene expression patterns. These programs then define cascades of successive, distinct developmental stages or the choice between alternative fates for the same stage.

A model for temporal control of development is found in the *C. elegans*, environmental cues signal through insulin and TGF-beta cascades to regulate the hormone synthesis of *daf-12*/nuclear hormone receptor (NHR) that then coordinates organism wide developmental timing and fate choice.

For cell intrinsic aspects of *C. elegans* temporal control of development, microRNAs play an important role for regulation of developmental progression but their connection to organism wide endocrine control is unknown. This work shows how the DAF-12/NHR directly activates *let-7* family microRNAs during the L3 stage to actively repress translation of *hbl-1*, a mediator of L2 stage fates, to prevent L2 stage fates from reoccurring during L3 stage. The interaction of upstream transcription factors with the downstream *cis*-regulatory elements in promoters of the *let-7* family microRNAs, are further analyzed in detail and identify potential DAF-12 co-regulators that might connect *daf-12* endocrine signaling also to later stage developmental control.

These observations are the first to integrate microRNAs into the currently established endocrine signaling cascades. In addition they reveal specific details about how organism wide upstream, endocrine signaling pathways connect to downstream cell intrinsic changes of gene expression and developmental progression throughout the organism. Through these observations, this work postulates a “molecular switch” to be active in driving stage transitions. This switch consists of a NHR that directly activates microRNAs to actively repress mediators of old stages while activating translation of genes mediating the new stage.

Table of Contents

ABSTRACT ..... **I**

TABLE OF CONTENTS ..... **II**

TABLE OF FIGURES ..... **VI**

TABLE OF TABLES ..... **VII**

ABBREVIATIONS ..... **VII**

1 . INTRODUCTION **1**

1.1 Nuclear Hormone Receptors *1*

1.1.1 Type I and type II nuclear receptors 2

1.1.2 Nuclear receptor co-regulators 2

1.1.3 Hormonal signaling in development 3

1.1.3.1 Control of developmental progression in insects 3

1.1.3.2 Control of developmental progression in chordates 4

1.1.3.3 Control of developmental progression in mammals 5

1.2 Nematodes *6*

1.3 Caenorhabditis elegans *6*

1.3.1 Life cycle 7

1.3.2 Dauer formation 8

1.3.3 How is dauer formation regulated? 8

1.3.4 TGF-beta signaling in *C. elegans* 9

1.3.5 Insulin-like signaling in *C. elegans* 10

1.3.6 Steroidal ligands for DAF-12/NHR 10

1.3.7 Dauer signaling converges on a nuclear hormone receptor 11

1.3.8 Dauer formation overview 12

1.3.9 Conservation of the *C. elegans* dauer signaling cascade 13

1.3.10 Heterochronic regulation 13

1.3.10.1 Tissues with heterochronic phenotypes 13

1.4 MicroRNAs *15*

1.4.1 MicroRNAs and the L1 to L2 stage transition 16

1.4.2 MicroRNAs and the L2 to L3 stage transition 16

1.4.3 MicroRNAs and the L4 to adult stage transition 17

1.4.4 Heterochronic regulation by DAF-12 signaling 18

1.5 Questions addressed in this dissertation *19*

2 . NUCLEAR HORMONE RECEPTOR REGULATION OF microRNAs CONTROLS DEVELOPMENTAL PROGRESSION **21**

INTRODUCTION 22

RESULTS 24

2.1 NHR activates microRNAs *24*

2.1.1 *In vitro* promoter interaction 24

2.1.1.1 Direct transcriptional activation of microRNA-promoters by DAF-12 and ligand 24

2.1.1.2 Direct physical DAF-12 interaction with response elements in the promoter fragments 26

2.1.2 *In vivo* promoter activation 29

2.1.2.1 *Mir-241* promoter regulation and *daf-12* signaling mutations 29

2.1.2.2 *Mir-84* promoter regulation in *daf-12* signaling mutant backgrounds 30
2.1.2.3 Mature microRNA dose measured by Q-PCR 31
2.1.2.4 MicroRNA promoter activation in *daf-12* upstream signaling mutants 34
2.1.3 MicroRNAs and their involvement in signaling cascades 36
2.1.3.1 HBL-1 drives developmental progression in seam cells and is microRNA regulation target 36
DISCUSSION 38
2.2 Overview *38*
2.3 Transcription factor and microRNA act as a "molecular switch" *40*
2.3.1 Mammalian p53 and the "molecular switch" 40
2.3.2 Consequences of the "molecular switch" idea 41
2.4 NHR-signaling paradigms *42*
2.4.1 *Mir-241* promoter regulation 43
2.4.2 *Mir-84* regulation and dafachronic acid independent activation 43
2.4.3 *Lin-12*/notch receptor in hypodermal differentiation 44
2.5 Feedforward and feedback loops *45*
2.5.1 *Lin-12* activates *mir-61* to form a feedback loop 46
2.5.2 Neuronal differentiation in *C. elegans* and feedback 46
2.5.3 EcR and feedback 47
2.5.4 C/EBP alpha and NFI-A and feedback 47
OUTLOOK 48
2.6 Cell non-autonomy of microRNAs *48*
2.7 Ligand independent activation of DAF-12 / mir-84 promoter *49*
2.7.1 Alternative transcription factors: *lin-12* 49
2.8 Feedback regulation by let-7 ..... *50*

3 . DAF-12 ACTIVATION OF *CIS*-REGULATORY ELEMENTS IN microRNA PROMOTERS 51
INTRODUCTION 52
3.1 Promoter regulation studied in C. elegans *53*
3.2 Initial studies of the myo-2 promoter *53*
3.3 The "gene battery" define the tissue characteristics *54*
3.3.1 DAF-19/x-box binding factor defines ciliated neurons 55
3.3.2 PHA-4/forkhead factor defines a specific organ 55
3.3.3 TTX-3 and CEH-10 homeodomain factors define gustatory neurons 56
3.4 Repeat generation of defined promoter regions *57*
3.5 Transcription factors influencing expression of let-7 family microRNAs *58*
3.5.1 Tissue specifity of *mir-84* promoter regulation 58
3.5.2 *Daf-12* independent activation of the *mir-241* promoter 58
3.5.3 DAF-12 influence on the *let-7* promoter 59
3.5.4 FLYWCH transcription factors regulate microRNA promoters 59
3.5.5 *Daf-12*/nhr regulates microRNA promoters 59
3.5.6 *Lin-12*/notch regulates microRNA promoters 59
RESULTS 59
3.6 DAF-12 dependent cis-regulatory elements *59*
3.7 Repeat generating PCR strategy *60*
3.8 Repeats of isolated mir-84 promoter regions *62*
3.8.1 The nomenclature of CRMs within the *mir-84* promoter 62
3.8.2 Increased repeat number enhances activation 64
3.8.3 84d and 84e repeat reporters 64
3.9 Repeats of isolated mir-241 promoter regions *66*
3.10 Let-7 TRE reporter *68*
3.11 Conserved elements in analyzed promoters *70*
3.11.1 *Daf-3*/co-smad 71
3.11.2 Forkhead transcription factors *pha-4* and *daf-16* 71

3.11.3 *Ceh-22*/homeobox domain 71
3.12 Lin-12/notch receptor *72*
3.13 FLYWCH transcription factors flh-1, flh-2, flh-3 ..... *73*
DISCUSSION 74
3.14 Regulation of CRMS present in the mir-84 and the mir-241 promoters *74*
3.15 Candidate TFs for let-7 family microRNA regulation *74*
3.15.1 *Lin-12*/NOTCH receptor is a candidate for *daf-12* interaction 75
3.15.2 Direct *let-7* promoter regulation through DAF-12 76
OUTLOOK 76
3.16 Connecting CRMs to signaling cascades *76*
3.17 Lin-12 in terminal differentiation *77*
3.18 Daf-12 in terminal differentiation *77*

4 . DAF-12 AND ITS CO-REGULATOR LIN-29 FORM A "MOLECULAR SWITCH" DRIVING TERMINAL DIFFERENTIATION OF THE HYPODERMIS 79
INTRODUCTION 80
RESULTS 81
4.1 Co-activation assay of LIN-29 and DAF-12 on the mir-84 promoter *81*
4.2 EMSA with LIN-29 and DAF-12 on DAF-12 regulated CRMs *83*
4.3 Mammalian two hybrid assay for Lin-29 and DAF-12LBD interaction *83*
4.4 GFP reporter analysis for LIN-29 and DAF-12 co-activation in vivo *85*
DISCUSSION 86
OUTLOOK 90
4.5 Epistasis experiments of daf-12 signaling, microRNA expression and molting phenotype *90*
4.6 LIN-29 activation of the mir-84 promoter independent of DAF-12 ..... *91*
4.7 Molecular switch homolog functions in mammalian tissue differentiations *91*

5 . MATERIALS & METHODS 93
DNA MANIPULATION 93
5.1 PCR protocols *93*
DNA CONSTRUCTS 93
5.2 Expression vectors for mammalian cell culture *93*
5.2.1 Luiferase reporter vectors 94
5.2.2 Site directed mutagenesis of *daf-12*-like CRMs 95
5.3 CRM-repeat generation *95*
5.4 Double-tagging constructs *98*
NEMATODES 101
5.5 RNAi knock-out *101*
5.6 Analysis of GFP expression *101*
5.7 Worm transformation *101*
5.8 Worm lines transgenic with reporter used in Chapter 2 ..... *102*
5.9 Worm lines transgenic with CRM-repeat reporter constructs *102*
5.10 Worm lines transgenic with double tagging constructs *103*
GENE ALLELES / STRAINS 104
MICROSCOPY 105
5.11 Microscope *105*
5.12 Fluorescence microscopy filter sets *105*
5.13 Bionocular *105*
CELL CULTURE AND LUCIFERASE ASSAY 105

5.14 Luciferase assay data *106*
5.15 Gel Shift *107*
RNA EXTRACTION 109
TAQMAN Q-PCR 109
DATA ANALYSIS 110

6 . APPENDICES 111
APPENDIX 1: *HIM4*/HEMICENTIN IS TRANSCRIPTIONALLY REGULATED BY *DAF-12* 111
APPENDIX 2: DAFACHRONIC ACID DERIVATIVES AND THEIR EFFECT ON DAF-12 113
6.1 Glycinoeclepin A drivatives as DAF-12 ligand *113*
6.2 Ascr#3 interact and DAF-12/NHR or DAF-9/CYP450 ..... *115*
6.2.1 Ascr#3 and DAF-12/NHR 116
6.2.2 Ascr#3 and DAF-9/CYPp450 116
6.3 Δ^4- and Δ^7-dafachronic and DAF-9/CYPp450? *117*
APPENDIX 3: TRANSCRIPTIONAL ACTIVATION VERSUS UTR-MEDIATED REPRESSION 119
APPENDIX 4: CONSERVATION OF *CIS*-REGULATORY MOTIFS IN *LET-7* FAMILY MICRORNA PROMOTERS 123
APPENDIX 5: DIMERIZATION MIGHT INFLUENCE DAF-12 TRANSCRIPTIONAL ACTIVATION 128
APPENDIX 6: LIST OF HETEROCHRONIC GENES IN *C. ELEGANS* 130
APPENDIX 7: PUBLICATION IN "SCIENCE" 135
APPENDIX 8: PUBLICATION IN "ORGANIC LETTERS" 139

7 . ERKLÄRUNG ÜBER DIE EIGENSTÄNDIGKEIT DER ERBRACHTEN WISSENSCHAFTLICHEN LEISTUNG 143
7.1 Publication of Data presented in Chapter 2 ..... *144*
7.2 Publication of Data presented in Appendix 2 ..... *144*

8 . REFERENCES 145

Table of Figures

Figure 1: C. elegans life cycle from hatching till adulthood 7
Figure 2: Structures of dafachronic acids 11
Figure 3: *Daf-9*, *daf-12* and *din-1* downstream of TGF-beta / insulin signaling 12
Figure 4: Seam cells of the hypodermis and their cell lineage 14
Figure 5: Distal tip cell migration in hermaphordites 15
Figure 6: V1-4 and V6 seam cell lineages in wild type and mutant backgrounds 19
Figure 7: Luciferase assay of microRNA promoters 24
Figure 8: Shostak-response element for DAF-12 25
Figure 9: Deletion analysis of *mir-241* and *mir-84* promoters 26
Figure 10: EMSA of 241a and 241b 27
Figure 11: EMSA of 241cd 28
Figure 12: DAF-12 and dafachronic acid regulate *mir-241* promoter *in vivo* 29
Figure 13: DAF-12 and dafachronic acid regulate *mir-84* promoter *in vivo* 31
Figure 14: Relative quantification of *let-7* family microRNAs by Q-PCR 32
Figure 15: Quantitative PCR of *mir-1* 33
Figure 16: *mir-84* regulation during dauer recovery 34
Figure 17: microRNA promoter regulation in different dauer signaling mutant backgrounds 35
Figure 18: *Hbl-1* UTR reporter is regulated by *daf-12* signaling 38
Figure 19: Model for NHR-microRNA signaling cascades 40
Figure 20: Models of regulatory loops 45
Figure 21: DAF-12-like CRM 60
Figure 22: Repeat-generation PCR scheme 61
Figure 23: CRMs of the *mir-84* promoter 62
Figure 24: CRM repeats of the *mir-84* promoter 65
Figure 25: CRM repeats of the *mir-241* promoter 66
Figure 26: Re-analysed luciferaseassay of the *let-7* promoter 68
Figure 27: *Let-7* "TRE" element 68
Figure 28: EMSA of TRE-element 69
Figure 29: CRM repeat of the TRE 70
Figure 30: CEH-22 and DAF-12 response elements 72
Figure 31: Luciferase assay of LIN-29/DAF-12 co-activation 82
Figure 32: EMSA with DAF-12 and LIN-29 84
Figure 33: Mammalian Two Hybrid Assay with LIN-29 and DAF-12 85
Figure 34: *In vivo gfp* reporter analysis in *daf-12* and *lin-29* mutant backgrounds 86
Figure 35: EGR2-like CRM in the *mir-84* promoter 87
Figure 36: Revised regulation model for larvae-to-adult transition 89
Figure 37: A391 and A424 vector map 97
Figure 38: Cross reactivity of TaqMan Q-PCR primers and probes 110
Figure 39: *Him-4* regulation is *daf-12* dependent 112
Figure 40: Dafachronic acid derivatives 114
Figure 41: DAF-12 activation by dafachronic acid derivatives 115

Figure 42: Ascaroside asc#3 does not interact with DAF-12 or DAF-9 117
Figure 43: CFP/YFP tagging..... **Error! Bookmark not defined.**
Figure 44: Cross-species alignment of *myo-2* promoter 123
Figure 45: Cross-species alignment of 84e 124
Figure 46: Cross-species alignment of 84d..... 124
Figure 47: Cross-species alignment of 241ab 125
Figure 48: species alignment of 241cd 126
Figure 49: Cross-species alignment of TRE 126
Figure 50: Luciferase assay of repeated response elements..... 128

Table of Tables

Table 1: Seam cell counts 37
Table 2: List of *cfp* / *yfp* tagging vector constructs..... 99
Table 3: Double tagging injected extra chromosomal arrays..... 103
Table 4: Gene alleles / strains 105
Table 5: Double-tagging plasmid constructs 120

Abbreviations

AMH	anti-Muellerian hormone
CFP / *cfp*	*cyan fluorescent protein*
CRM	*cis*-regulatory element
DA	dafachronic acid
Daf-c	dauer constitutive phenotype
Daf-d	dauer defective phenotype
DBD	DNA binding domain of a NR or NHR
DIC	differential interference contrast microscopy
DR	direct repeat
DTC	distal tip cell
EcR	ecdysone receptor
EMSA	electrophoretic mobility shift assay
ER	everted repeat
EtOH	ethanol
gf	gain-of-function mutation
GFP / g*fp*	*green fluorescent protein*
HEK	human embryonic kidney cells
20E	20-hydroxyecdysone
IR	inverted repeat
JH	juvenile hormone
L1/L2/L3/L4/Ad	larval stage 1 / larval stage 2 / larval stage 3 / larval stage 4 / Adult

L3d	dauer larva
LBD	ligand binding domain of a NR or NHR
lf	loss-of-function mutation
Mig	migration phenotype of the DTC
miR	microRNA
na	not applicable
NHR	nuclear hormone receptor
NR	nuclear receptor
kb	kilo base pair – length of a DNA fragment
nt	nucleotide
PCR	polymerase chain reaction
PPAR delta	peroxisomal proliferation factor delta
PTTH	prothoracicotrophic hormone
Q-PCR	quantitative polymerase chain reaction
RAR	retinoic acid receptor
RE	response element
RISC	RNA mediated Silencing Complex
RLU	Relative Luciferase Units
RXR	retinoic X receptor
s	shit
ss	super shift
TF	transcription factor
TR	thyroid receptor
TRE	temporal regulatory element in the let-7 promoter
TRM	*trans*-regulatory element
VDR	vitamin D receptor
VPC	vulva precursor cell
YFP / *yfp*	*yellow fluorescent protein*

1. Introduction

Many examples have been described of how endocrine regulation controls developmental progression. However, it is still not well understood how organism-wide endocrine signals are converted into cell-intrinsic responses and changes of developmental programs. The aim of this dissertation is to investigate hormonal control of intracellular developmental programs and its relation to environmental influences. In this introduction, I will explain the background necessary to understand how nuclear hormone receptors convert these endocrine hormone signals into changes in target gene expression-- which constitute developmental plasticity. I proceed by applying this knowledge to several model systems for development and hormonal control, before I focus on one specific model organism, *Caenorhabditis elegans*. In *C. elegans*, the nuclear hormone receptor DAF-12 together with "dafachronic acid" hormones control developmental progression through different larval stages as well as the choice between two alternative larvae of the same stages. I connect this developmental control to environmental conditions by reviewing how synthesis of dafachronic acids is regulated by several conserved upstream signaling cascades on an organism wide level. Next I examine the developmental stages at the cellular level and explain how a group of genes, called heterochronic genes, regulates timely execution of cell specific developmental programs. I will show that microRNAs, a newly discovered class of regulatory genes, have important functions as heterochronic genes. This will lead to the question of what mechanisms connect the upstream hormonal signals to the downstream cell-specific developmental programs.

1.1 Nuclear Hormone Receptors

In order to understand hormone activity, it is necessary to understand what nuclear receptors are and how they react to their ligands. Nuclear receptors (NRs) are transcription factors (TFs) that bind to lipophilic ligands such as steroids, bile acids or fatty acids to regulate gene expression. The term "nuclear hormone receptor" more specifically refers to NRs that bind steroid ligands, like the estrogen or the glucocorticoid receptors. The protein structure of NRs contains a DNA binding domain (DBD) near the N-terminus and a LBD at the C-terminus. The DBD of a NR recognizes promoters of target genes by binding to a short DNA sequence, called the "response element" (RE), which typically consists of six nucleotides. NRs can homodimerize

with the same NRs, (e.g. RXR/RXR) or more commonly, heterodimerize with other NRs (e.g. RXR/VDR or RXR/RAR) (Mangelsdorf and Evans, 1995). These NR-dimers can bind repeats that are direct, as well as inverted or everted palindromes (DR, IR, ER). In addition, the choice of dimerization partners can influence the RE that the complex binds to (Mader et al., 1993), but different arrangements of the REs relative to each other influence the nuclear receptor dimer that can bind the promoter, and with it the promoter activation state (Kurokawa et al., 1994). The LBD of NRs consists of 12-alpha helices and ligand binding induces conformation changes that trigger activation (Bourguet et al., 1995; Tanenbaum et al., 1998).

1.1.1 Type I and type II nuclear receptors

Nuclear receptors are grouped into two classes, type I and type II (Mangelsdorf and Evans 1995). Type I NRs bind to steroids and activate transcription in the presence of a ligand while being inactive in the absence of ligands, such as estrogen and glucocorticoid receptors. Type II NR activate in presence, but repress in the absence of a ligand. Examples of these include the thyroid receptor or vitamin D receptor. The regulation of type II NRs is achieved by the NR interacting in a ligand dependent way with co-regulators that enhance transcription of the NR target genes. An example of a co-activator that activates transcription is SRC-1 (Onate et al., 1995) and an example for a co-repressor is N-Co-R (Zamir et al., 1996) that causes transcriptional repression. But how do ligands regulate the interaction of nuclear hormone receptors and their co-regulators?

1.1.2 Nuclear receptor co-regulators

As stated previously, the results of ligand binding to NRs are dependent on co-regulators that interact with multiple areas of the DNA ligand binding domain. These include both co-activator and co-repressor proteins. For example, during ligand binding, the highly mobile helix 12 of the LBD re-arranges to make contact with helix 3, forming a "charge clamp" and exposing charged amino acid residues that interact with LXXLL-motif of a protein structure called "NR box" that is found in co-activator proteins (Savkur and Burris, 2004). The details of this mode of interaction were first described for estrogen (ER) (Shiau et al., 1998) and thyroid receptor (TR) (Darimont et al., 1998) binding to co-activator GRIP1.

Co-activator complexes enhance transcription through a variety of mechanisms including histone modification, chromatin remodeling, and bridging with components of basic transcriptional machinery. Co-activators induce transcription of a target gene after recruitment to

the corresponding promoter by interaction with a bound NHR. Conversely, co-repressor proteins, such as NCoR and SMART, contain LXX I/H IXX I/L motifs called "CoRNR box" that LBDs of NRs interact with. (Rosenfeld et al., 2006). Usually, NCoR and SMART are recruited to type II NRs like TR, RARs in the absence of a ligand and interact with other proteins like SHARP that recruits enzymes such as histone deacetylases HDAC1 and HDAC2 to decrease transcription, (Shi et al., 2001). Other co-repressors like LCor, RIP140 or REA are recruited in the presence of an antagonist molecule in the LBD (Rosenfeld et al., 2006) to repress transcriptional activation. These factors can be further regulated by posttranscriptional modifications-- such as phosphorylation, acetylation, SUMOylation, or ubiquitinylation-- (Rosenfeld et al., 2006) all of which serve to enhance or decrease transcriptional activation of the TFs. One example is increasing the protein turnover-rate of the TF.

1.1.3 Hormonal signaling in development

Hormone signaling during development is complex and multifaceted. The effects of hormone signaling on nuclear hormone receptors and their transcriptional targets are most obvious during metazoan development. Metazoans, which include *C. elegans*, undergo extensive tissue remodeling during maturation from juvenile to reproductive adult. Most of these processes are regulated by NR ligands, such as steroids, thyroids, or retinoic acids, which promote two different kinds of maturation processes, metamorphosis or non-metamorphotic transitions (Paris and Laudet, 2008).

Metamorphosis is a drastic remodeling of organs, which often goes along with a change in ecosystem and food source. One example includes frogs, which are land living insectivores, but develop through metamorphoses into a submerged herbivorous tadpole.

Normal development and maturation, in addition to metamorphosis, is subject to endocrine control. Endocrine signals that regulate metamorphosis in insects are ecdysteroids and juvenile hormones, while thyroid hormones drive amphibian metamorphosis. An example of a less defined metamorphotic development is mammalian sexual differentiation and maturation driven by steroids like estradiol or testosterone (Gilbert, 2003). The following paragraphs review the hormonal control of development in insects, amphibians and mammals.

1.1.3.1 Control of developmental progression in insects

Insects that have a larvae stage that is very distinct from the adult stage, also called holometabolous insects, transition between larval and adult stages, which involve

metamorphoses and the formation of an immobile pupae, of which the differentiated adult emerges. Hemimetabolous insects develop without a specific metamorphosis stage through a succession of molts from a small larvae into the larger, sexually reproducing adult with similar morphology (Gilbert, 2003).

The general regulation of insect molting and metamorphosis differs between species, but follows the general mechanism: Neurosecretory cells in the brain release a peptide hormone called prothoracicotrophic hormone (PTTH) that acts on the prothorarcic gland which produces ecdysone. Ecdysone is modified in peripheral tissue into the biologically active 20-hydroxyecdysone (20E) which binds to a heterodimer of the ecdysone receptor (EcR) and ultraspirical, an RXR homolog. (Thomas et al., 1993; Yao et al., 1993). Larval molts are accompanied by a pulse of juvenile hormone (JH) excreted from an endocrine organ known as corpora allata. Inhibition of this JH pulse during the ecdysone pulse leads to pupae formation and induction of metamorphosis (Adam et al., 2003). The 20E diffuses throughout the whole organism, but tissues react very differently to this single signal. For example, imaginal cells that give rise to adult organs are stimulated to grow, whereas larval tissues die. One reason for this diverse response is thought to be the presence of different EcR isoforms in different tissues. These isoforms share the same DBD and LBD, but differ in their *N*-terminus (Talbot et al., 1993; Truman et al., 1994).

1.1.3.2 Control of developmental progression in chordates

In contrast to insect steroid hormones, thyroid hormones are responsible for the control of development and metamorphosis in amphibians. Thyroid hormones are found only in chordates and are excreted from the thyroid glands (Brown and Cai, 2007) where they are derived from tyrosine (unlike steroid hormones, which are derived from cholesterol). They act on the thyroid receptor to promote metamorphosis from tadpole to frog which involves extensive tissue remodeling, such as limb growth and tail resorption. The most common model for metamorphosis in chordates is amphibian metamorphosis. *Xenopus laevis* is the currently favored model organism: embryogenesis takes 1 week, tadpole stage 6 weeks or more, depending on environmental conditions, metamorphosis takes 8 days, and the adult stage is approximately 6 months (Brown and Cai, 2007). The major endogenous thyroid hormone, called thyroxine, was initially extracted from thyroid glands, and subsequently chemically synthesized (Harington, 1928). This compound was able to induce precocious metamorphosis while removal

of the thyroid gland of tadpoles inhibits it (Allen, 1925). Ectopic expression of a transgene coding for a dominant negative TR suppresses thyroid hormone induced gill and tail resorption, gut remodeling, limb outgrowth and DNA replication in several tissues. This does so by assembling co-repressor complexes to thyroid hormone and TR regulated genes to inhibit target gene transcription (Buchholz et al., 2003; Hsia et al., 2003).

1.1.3.3 Control of developmental progression in mammals

In contrast to metamorphotic development in insects and amphibians, sex determination and maturation in mammals is determined by steroid hormones. During development the gonadal rudiment passes through a bipotential stage, 4 to 7 weeks after fertilization, where it can form gonads of one of either sexes. In absence of a Y chromosome, the gonadal primordium develops into ovaries that produce estrogens, steroid hormones that promote female secondary sex characteristics and enable the "Muellerian duct" to develop into parts of the female sex organs, like uterus and oviduct. In presence of a Y chromosome, testis are formed that secrete two major hormones: "anti-Muellerian hormone" (AMH), a TGF-beta ligand that leads to destruction of the Muellerian duct, and testosterone that promotes formation of male secondary sex characteristics like penis, male duct system and scrotum (Couse et al., 1999; Couse and Korach, 2001; Fisher et al., 1998). This process is initiated by wnt4/Wnt gene (Vainio et al., 1999) activating *dax-1*/nhr (Muscatelli et al., 1994; Zanaria et al., 1994) that competes with Y-chromosomal *sry*/tf and autosomal *sox9*/tf (Nachtigal et al., 1998; Swain et al., 1998) to prevent *sry*/tf and *sox9*/tf dependent formation of AMH.

Production of estrogen or testosterone during puberty drives the maturation of sexual organs as well as other maturation processes, e.g. termination of bone growth. The growth spurt of bones during early puberty is caused by growth hormones activating the epiphyseal growth plates of the long bones to produce insulin-like growth factor-I (IGF-I), which together with the growth hormone increases bone growth by activating chondrocyte proliferation of the proliferative zone of the growing bone (Gilbert, 2003). The increased dose of steroid hormones induces a progression in development of the epiphyseal growth plates into mature chondrocytes that stop producing insulin. The chondrocytes further differentiate into hypertrophic chondrocytes and at this point the growth spurt is terminated through the steroid hormone induced differentiation.

The above are examples of hormonal control of development. However, to study the mechanisms of their action, it often is beneficial to use more rapidly developing organisms than mammals. A useful model organism for this research turned out to be the nematode *Caenorhabditris elegans*.

1.2 Nematodes

Nematodes live in many different ecosystems including marine, soil and plant environments or in animals as parasites that pass through one or more different hosts during their life cycle (Anderson, 1984). They are often referred to as roundworms, have a thread like shape, their mouth opening at the front tip is followed by a pharynx that continues into the gut that opens to the exterior near the rear end of the worm. They have a complex nervous system and excretory-secretory systems (Lee, 2002).

Most nematode species develop through four successive larval stages (L1-L4), separated by molts, into a reproducing adult, and can exit the direct development, usually after the second larval stage to form an alternative, arrested larva, that stops in development and is protected by a strong cuticle that shields it from environmental stresses. The formation of this arrested larva is a response to environmental signals. In parasitic nematodes, the arrested larvae is often the infective form and often occurs during the change from a non-infective stage or an intermediate host to the final host (Anderson, 1984). The endocrine regulation of this choice between developmental progression or arrested larva formation is best studied in the model organism *Caenorhabditis elegans* in the case of the dauer diapause (Motola et al., 2006).

1.3 Caenorhabditis elegans

C. elegans is a soil living nematode with a rapid generation time of 3 days in which a single adult can produce >300 offspring (Riddle et al., 1997). Adults consist of less then 1000 cells but still have defined organ systems as for example the nervous system with more then 300 cell. All cells are transparent and follow an invariable pattern of cell divisions during development, called the cell lineage. All these characteristics are encoded in a small, diploid genome with 100 Mega base pairs. *C. elegans* reproduces mostly by parthenogenesis, but 1 in 1000 worms is male, providing the researcher with the benefits of both sexual recombination as well as inbreeding by self-fertilization. Very successful were genetic screens using mutagenic reagents like e.g. ethyl methane sulfonate (EMS), followed by screening for worms that showed aberrations of the

normal developmental pattern resulting from a single genomic lesion. Classic and modern genetic procedures can be applied to find then the molecular identity of the gene behind the affected function (Hodgkin, 2007). This process lead to major scientific advances in understanding the nematode biology and along the homolog functions in higher animals and humans. This success is reflected in the Nobel Prices that were awarded to scientists working on *C. elegans* in the years 2002, 2006 and 2008.

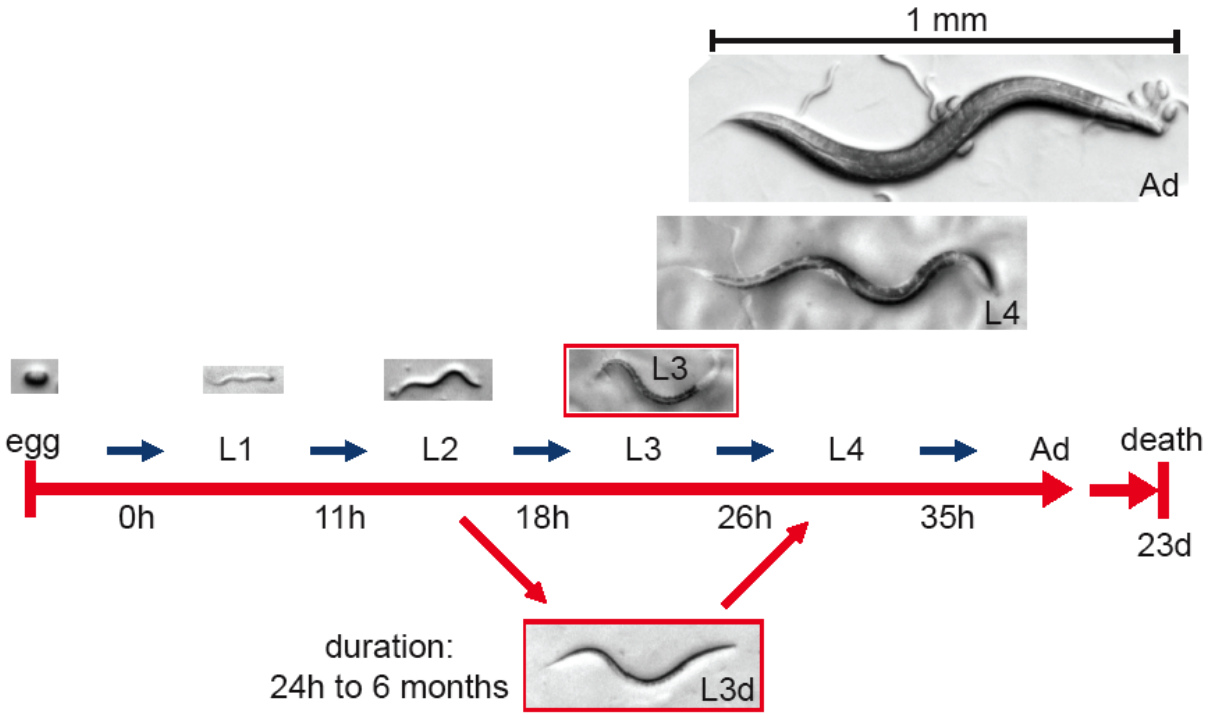

Figure 1: C. elegans life cycle from hatching till adulthood
Development progresses from left to right and arrows symbolize hatching or molts between stages. Worm images are to scale. The hour numbers indicates the hours post-hatching at which the molt to the next stage occurs. Unfavorable environments can cause developmental arrest and dauer larvae formation (L3d stage) that lasts until environmental conditions improve which induces developmental progression and molting into the L4 stage.

1.3.1 Life cycle

One of the many processes that *C. elegans* acts as a model for is the regulation of developmental progression – the focus of this dissertation. Previous research led to the discovery of a complex network of signaling cascades and genes involved. I will discuss several aspects of these cascades, and start out with the developmental timeline during wild type development and normal conditions.

Under favorable growth conditions, *C. elegans* develops rapidly from an egg through four different larval stages into an adult (Figure 1). At 25°C, this process takes 48h. Most cell division and organogenesis occurs during embryogenesis. After larvae hatch from the eggs, a subset of tissues undergo further division, differentiation and growth, mostly oriented towards reproduction. The transition from one larval stage to the next is marked by a molt, in which the old cuticle is shed, and the new cuticle formed underneath by the hypodermis. At the transition to adult, hypodermal cells exit the cell cycle and terminally differentiate causing the molt cycle to cease. Adults lay fertilized eggs during a three day period, and continue to live for a maximum of 17 more days while the body morphology progressively deteriorates (Girard et al., 2007; Herndon et al., 2002). During the entirety of development, *C. elegans* cell lineages follow an invariant division pattern (Sulston and Horvitz, 1977; Sulston et al., 1983). This invariant cell division pattern allowed for example the discovery of mutants that lead to cell lineage modifications (called *lin*) and helped elucidate their underlying regulatory mechanisms.

1.3.2 Dauer formation

In contrast to the rapid life cycle described above, *C. elegans* development also includes the option to exit developmental progression and molt into an arrested larval stage, called "dauer," which occurs during unfavorable conditions such as temperature extremes, starvation or in the presence of a pheromone that induces dauer formation called "dauer pheromone". This dauer pheromone is an indicator of high population density and is excreted during the L1-L2 stages. In its presence, the *C. elegans* will molt into an alternative third larval stage, called the dauer larvae (L3d). Dauer larvae are arrested in development and are stress resistant and long lived. They can survive for up to six months, while normal developmental progression leads to a maximum life span of approximately two to three weeks (Cassada and Russell, 1975). When the dauer larva senses improved environmental conditions, it resumes developmental progression and within 24h molts into an L4 stage worm that then continues with normal development and reproduction.

1.3.3 How is dauer formation regulated?

Several forward genetics mutant screens have been performed in order to find out about the mechanisms regulating dauer formation. Those screens revealed several classes of genes that when mutated affect "dauer formation". Also known as "daf"-genes, the members of this gene class are numbered according to chronological order of discovery. Daf-mutants fall into two classes: dauer defective mutants (Daf-d) fail to form dauer larvae, while dauer constitutive

mutants (Daf-c) constitutively form dauer larvae, independent of environmental conditions (Riddle et al., 1981). Identified genes were grouped by epistasis and phenotypical analysis into different classes that correspond to separate signaling reviewed by Fielenbach (Fielenbach and Antebi, 2008).

The most upstream events influencing the dauer formation decision are environmental factors like temperature, food availability and dauer pheromone, which are detected by sensory neurons. During favorable environmental conditions that promise successful reproduction, these neurons express DAF-7/TGF-beta ligand (Schackwitz et al., 1996) and DAF-28/insulin peptide (Zhang et al., 2003), which activate TGF-beta and insulin signaling cascades, respectively, to prevent dauer formation. Both cascades converge onto hormone biosynthetic enzymes regulating the production of "dafachronic acids"- the bile acid-like steroid ligands for the nuclear hormone receptor DAF-12 (Motola et al., 2006). Liganded DAF-12 then promotes developmental progression. Conversely, under unfavorable environmental conditions or mutations that reduce TGF-beta or insulin signaling dafachronic acid production is shut down and the unliganded DAF-12 causes dauer larvae formation and developmental arrest. These two cascades represent the connection of environmental conditions to endocrine regulation of development, and the mechanism of action is known in great detail for both TGF-beta and insulin cascades.

1.3.4 TGF-beta signaling in *C. elegans*

DAF-7/TGF-beta ligand is expressed in the ASI sensory neuron only during favorable conditions. It promotes developmental progression and the bypass of dauer arrest (Savage-Dunn, 2005). Repression of *daf-7*/TGF-beta ligand expression during unfavorable conditions, genetic deletion, or ablation of the expressing neuron lead to dauer arrest (Bargmann and Horvitz, 1991). DAF-7/TGF-beta ligand activates TGF-beta receptors DAF-1 and DAF-4 that phosphorylate smad proteins DAF-8 and DAF-14 causing their nuclear import. Transcriptional activity of DAF-8/smad and *daf-14*/smad during developmental progression is antagonized by *daf-3*/co-smad (Patterson et al., 1997) and *daf-5*/sno-ski (da Graca et al., 2004; Tewari et al., 2004). Deletion of *daf-1*/type I receptor, *daf-4*/type II receptor, *daf-8*/SMAD, *daf-14*/smad inhibit TGF-beta signaling and cause the Daf-c phenotype, while deletions of *daf-3*/co-smad are *daf-5*/sno-ski have a Daf-d phenotype (Inoue and Thomas, 2000; Larsen et al., 1995).

1.3.5 Insulin-like signaling in *C. elegans*

The *Daf-28*/insulin ligand is one of many insulin-like proteins in the *C. elegans* genome and is only expressed in the ASI and ASJ sensory neurons during favorable conditions (Li et al., 2003). It binds to DAF-2/insulin receptor in target tissues, which then activates AGE-1/phosphoinositol-3-kinase and leads to the production of Phosphatidylinositol 3-phosphate (PIP3). The DAF-2/insulin receptor protein of *C. elegans* is 35% and 34% identical to the human insulin receptor and the human insulin-like growth factor-I receptor, respectively (Kimura et al., 1997). This equidistant relation results in this signaling cascade being most accurately referred to as "insulin/IGF signaling" which is to be kept in mind when, for simplicity, *daf-2* signaling will in this dissertation be referred to simply as "insulin signaling".

PIP3, together with kinases PDK-1, AKT-1, AKT-2 and SGK-1, phosphorylate DAF-16/FOXO and cause it to be retained in the cytoplasm (Henderson and Johnson, 2001; Lee et al., 2001; Lin et al., 2001). Therefore, decreased insulin signaling leads to the de-phosphorylation and subsequent nuclear localization of DAF-16/FOXO where it activates its transcriptional target genes (Paradis and Ruvkun, 1998). Hypomorphic alleles, *e1370* and *e1368*, of the *daf-2*/insulin receptor have a temperature sensitive Daf-c phenotype. While growth at 25°C causes constitutive dauer formation, growth at the permissive temperature of 15°C does not cause dauer formation--instead development progresses with an increased resistance against heat stress, oxidative stress, UV, hypoxia and pathogen infection. Unchallenged *daf-2(e13768)* or *daf-2(e1370)* mutant worms show a two-fold extended lifespan compared to wild type (Gems et al., 1998; Kenyon et al., 1993; Larsen et al., 1995). Enhanced stress resistance and increased life span due to decreased insulin signaling mutations were shown to be conserved across taxa (Kenyon, 2005). Loss of DAF-16/FOXO transcriptional activity suppresses these phenotypes, as well as dauer formation, identifying DAF-16/FOXO as the main downstream factor for insulin signaling (Kenyon et al., 1993).

1.3.6 Steroidal ligands for DAF-12/NHR

These two upstream signaling cascades intersect with endocrine regulation of development via their control over a steroid hormone synthetic pathway that produces bile acid-like steroids, called "dafachronic acids", which bind to and activate the nuclear hormone receptor DAF-12. DAF-9/CYP p450, the most downstream enzyme of this pathway, is expressed in two neurons

called XXX. In addition, DAF-9 is expressed in the hypodermis in a manner dependent on environmental conditions and insulin and TGF-beta inputs (Gerisch et al., 2001; Jia et al., 2002).

Two DAF-12 ligands were identified, Δ4-dafachronic acid and Δ7-dafachronic acid, which differ by the position of a double bound (Motola et al., 2006) (Figure 2) and their potency in activating DAF-12 dependent transcription (Figure 41 A and following page: Figure 42 D). The more potent Δ7-dafachronic acid was chemically synthesized later (Giroux and Corey, 2007); therefore, experiments in this study were initiated with Δ^4-dafachronic acid. Structurally related compounds were also tested for in vitro and in vivo activation of DAF-12, but were found to be not as potent as the previously identified (Figure 41) (Giroux et al., 2008).

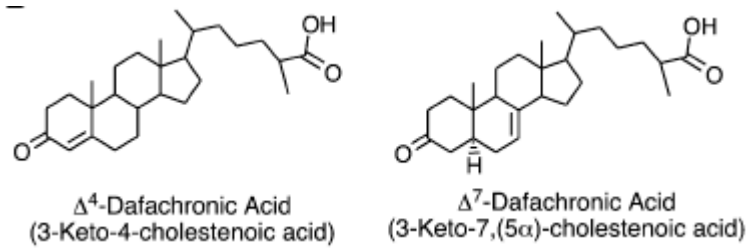

Δ^4-Dafachronic Acid
(3-Keto-4-cholestenoic acid)

Δ^7-Dafachronic Acid
(3-Keto-7,(5α)-cholestenoic acid)

Figure 2: Structures of dafachronic acids
(Motola et al., 2006)

1.3.7 Dauer signaling converges on a nuclear hormone receptor

After discussing the DAF-12 ligand and its regulation, I proceed to compare the nuclear hormone receptor DAF-12 itself to the paradigms of nuclear receptor signaling. DAF-12 is a class-II-like nuclear receptor with a predicted 12 helix ligand binding domain homologous to known steroid receptors (Antebi et al., 1998; Antebi et al., 2000). DAF-12 regulates dauer formation, developmental progression, fat metabolism and life span. For dauer formation, null alleles of *daf-12* are Daf-d which suppress all other known Daf-c loci as well as natural dauer formation; it is therefore considered the most downstream factor of dauer signaling. Null alleles for *daf-9* constitutively form dauers, suggesting that the unliganded receptor promotes the dauer state. Accordingly, this Daf-c allele class is suppressed by *daf-12* null alleles as well as null alleles of the nuclear receptor co-repressor *din-1*/sharp, identified as a *daf-12* interacting factor (Ludewig et al., 2004). This suppression supports the hypothesis that a complex of DAF-12 and DIN-1 works together to repress transcriptional targets, in the absence of DAF-9 biosynthetic products. *Daf-9;din-1* double null mutants allow bypassing dauer arrest even in the presence of unliganded DAF-12. Thus, hormone availability regulates the state of the *daf-12*-dauer-switch

(Gerisch and Antebi, 2004; Mak and Ruvkun, 2004), with the liganded receptor promoting reproductive development and the unliganded receptor promoting dauer formation.

1.3.8 Dauer formation overview

Taken altogether, the data suggest the following model for environmental control of developmental progression or arrest.

In favorable environments, sensing neurons ASI and ASJ express ligands DAF-7/TGF-beta ligand and DAF-28/insulin ligand to activate TGF-beta and insulin cascades. These cascades, through their downstream effectors, regulate expression of DAF-9 in the endocrine XXX cells. The XXX cells themselves regulate dafachronic acid production in the hypodermis via *daf-12*, which modulates hypodermal DAF-9 expression in a feed forward circuit. This hypodermal DAF-9 expression generates the dafachronic acid dose required to overcome dauer formation induced by unliganded DAF-12 throughout each cell of the whole organism. In unfavorable environments, decreased DAF-7/TGF-beta ligand and DAF-28/insulin ligand expression in the sensory neurons decreases the activity of the involved cascades, ultimately leading to DAF-12 mediated repression of its transcriptional targets to cause dauer formation (Figure 3).

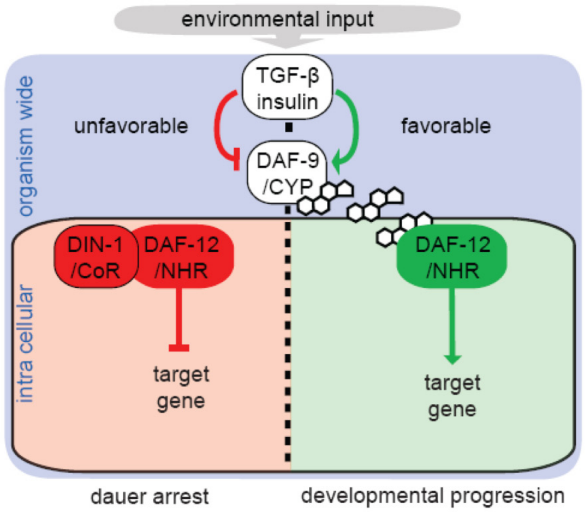

Figure 3: *Daf-9*, *daf-12* and *din-1* downstream of TGF-beta / insulin signaling
Sensing of favorable environmental condition increases TGF-beta and insulin signaling, which then activate DAF-9/CYP p450 and dafachronic acid synthesis. Daf-12 binds Dafachronic acid and activates is target genes to promote developmental progression. Sensing of an unfavorable environment leads to loss of TGF-beta and insulin signaling, resulting in repression of DAF-9/CYPp450 activity and dafachronic acid production. Unliganded DAF-12 represses its transcriptional targets to cause dauer formation.

1.3.9 Conservation of the *C. elegans* dauer signaling cascade

Evidently, this model of a steroid ligand operated switch that executes the decision between developmental progression and arrest is conserved in other nematodes as well, including free-living *Pristionchus pacificus* and parasitic *Strongyloides papillosus* (Ogawa et al., 2009). In these species, *C. elegans* dafachronic acid hormones are functional to inhibit formation of the arrested and infective larval stage, respectively. However, this conservation seems to be less true for the upstream signaling cascades, such as TGF-beta and insulin signaling.

1.3.10 Heterochronic regulation

In the sections above I described how signaling cascades connect environmental conditions to endocrine regulation of developmental progression and fate choice on a global, whole-animal scale. In the sections below, I will introduce findings on genes that regulate the timing of developmental progression at the cellular level. When these genes are mutated they affect the temporal regulation of development in certain tissues. This class of genes is called "heterochronic genes". Heterochrony was first used to describe differences in developmental timing between two species. An example for this is brain development in humans and chimpanzees that starts at similar developmental timing, but ends years earlier in chimpanzees compared to human brain development (Mitteroecker et al., 2004). In *C elegans*, mutations of heterochronic genes affect the timing of developmental programs compared to wild type background. Many mutations are known to affect the development of different tissues but for simplification the focus will be on two specific tissues: the gonad and the hypodermis. Many aspects of temporal control over developmental progression became obvious by looking at the mutations of different genes, the consequences of these mutations for developmental timing, and the epistasis of these genes to each other.

1.3.10.1 Tissues with heterochronic phenotypes

C. elegans became an important model organism for research on heterochronic regulation due to its invariable patterns of cell divisions during development. Each larval stage is defined by stage specific developmental programs and each of these programs is reflected in its own cell specific divisions and differentiations, all of which can easily be observed by light microscopy (Sulston and Horvitz, 1977; Sulston et al., 1983). Genes that regulate the time point in development at which a specific program is executed are called "heterochronic" genes. Mutations of these genes cause stage specific programs to be expressed either earlier or later than normal

(Ambros and Horvitz, 1984). In particular, precocious mutants cause a program of an early stage to be skipped and the programs of the succeeding stage to be executed instead. Conversely, retarded mutants repeat stage-specific programs one or more times, and delay the execution of the succeeding program. The main characteristic of these mutations is that they do not change the nature of a stage specific program but only the timing of its occurrence.

A tissue with obvious heterochronic phenotypes is the hypodermis. Hypodermal seam cells follow an invariant and asymmetric stem cell like division pattern with stage specific variations that have been used to track developmental progression (Figure 4). During this stem cell like division pattern, one daughter cell maintains stem cell character and continues to divide, while the other daughter cell exits the cell cycle and fuses to the hypodermal syncytium. Specifically during the L2 program, the seam cells first undergo a proliferative division directly followed by the stem cell like division pattern – acting as an easily identifiable developmental program executed during this stage only. Repetition or loss of this hypodermal L2 program leads to changes in overall seam cell numbers during later stages. The L4 to adult transition also has unique character, leading to exit from the cell division cycle, fusion to the hypodermis, and terminal differentiation (Figure 4).

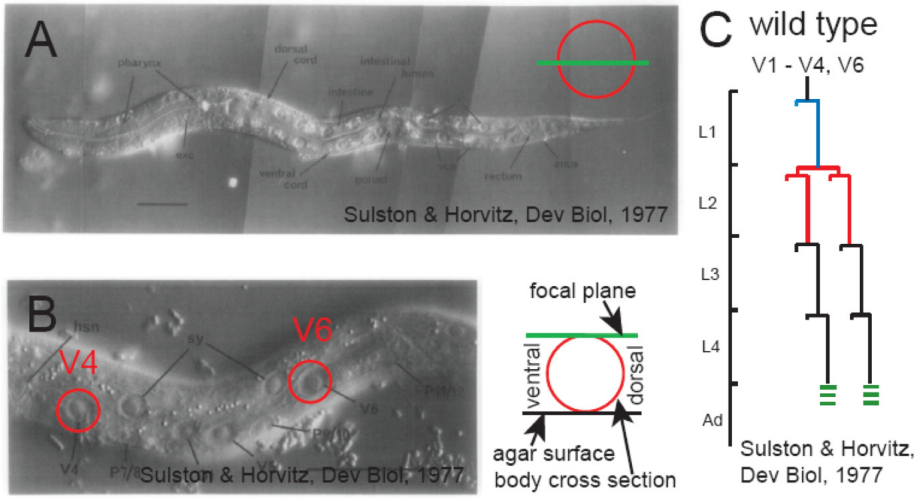

Figure 4: Seam cells of the hypodermis and their cell lineage
DIC micrograph of a C. elegans L1 stage larva with the focal plane through mid body, showing a.o. the pharynx and nuclei of the gut cells. Worms crawl on their side (A). DIC micrograph of an L1 stage worm with the focal plane through the hypodermis, with seam cells "V4" and "V6 circled (B). Division pattern of hypodermal seam cells with developmental progression from top to bottom (C). Marks indicate molts between stages. The L2 stage marked with an arrow has a proliferative and a stem cell like division pattern. Seam cells fuse into a seam syncitium and

form cuticle structures called "alae", symbolized as green lines. Images taken from (Sulston and Horvitz, 1977)

A second tissue with heterochronic phenotypes is the gonad. During L2 and early L3 stages, the two arms of the gonad grow out from the mid body towards head and tail along the ventral side of the body, led by migratory distal tip cells (Hedgecock et al., 1987; Kimble and Hirsh, 1979). During mid L3, the distal tip cells change direction and migrate from ventral to dorsal sides, where they then turn back towards mid body, and stop by L4.

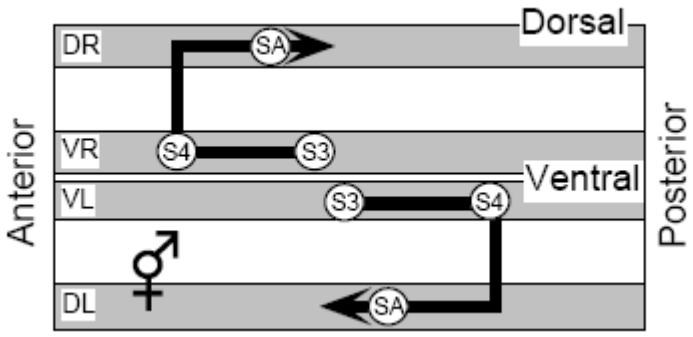

Figure 5: Distal tip cell migration in hermaphordites
Cylindrical projection of distal tip cell migration on the body wall of the animal, opened at the the dorsal midline. Dorsal is up and down, ventral is central. "S3" refers to L3 stage programs, "S4" to L4 stage programs, and "SA" to adult stage programs. The arrow symbolizes the migration path of the gonad, away from mid body along the ventral side during S3, turning dorsal during S4 program and reflexing back towards midbody along the dorsal side. Figure taken from (Antebi et al., 1998).

Heterochronic genes belong to diverse functional categories and include transcription factors, translation factors, chromatin factors, posttranslational regulators and microRNAs (Moss 2007). MicroRNAs represent a recently discovered class of regulatory genes, that is estimated to regulate 30% of the vertebrate genome (Lewis et al., 2005).

1.4 MicroRNAs

microRNAs were first discovered for their involvement in the heterochronic regulation of hypodermal development in *C. elegans*. Several different microRNAs and their target protein coding genes act at several different stage transitions during *C. elegans* development. In the following section, microRNAs involved in heterochronic regulation and what genes they have to interact with in order to achieve their function are described. These interactions will highlight mechanisms of heterochonic regulation in general.

1.4.1 MicroRNAs and the L1 to L2 stage transition

The first microRNA described was *lin-4*/microRNA (Chalfie et al., 1981) through its interaction with *lin-14*/nuclear protein (Liu and Ambros, 1989). LIN-14/nuclear protein is translated during L1, but translation is repressed during L2 stage in wild type, despite the mRNA still being present. Loss of the coding region of *lin-14*/nuclear protein causes a loss of L1 programs and hypodermal seam cells precociously execute the L2 stage programs during L1 stage (Arasu et al., 1991). The opposite phenotype results from loss or reduced function mutations of *lin-4*/miroRNA, a consequence of *lin-14*/nuclear protein translation persisting during the L2 stage. The hypodermis of these mutants fails to timely progress from L1 to L2 stage program. Loss of LIN-14/nuclear protein is epistatic to loss of *lin-4*/microRNA, while loss of the 3'UTR of *lin-14*/nuclear protein acts as a *lin-14*-gain-of-function mutation exhibiting the same phenotypes as *lin-4*/microRNA. This indicates that *lin-4*/microRNA suppresses translation of LIN-14/nuclear protein mRNA (Figure 6 A).

These observations can be interpreted as LIN-14/nuclear protein driving L1 stage programs. Termination of L1, and progression to L2 stage programs requires *lin-4*/microRNA mediated repression of *lin-14*/nuclear protein translation. This *lin-4* microRNA mediated translational repression is mediated by *lin-4*/microRNA interacting with the 3'UTR of *lin-14*/nuclear protein. Two publications (Lee et al., 1993; Wightman et al., 1993) were critical to the discovery and mechanism of microRNAs. In a groundbreaking work, Lee et al. 1993 showed that *lin-4*/microRNA gene is not a protein coding mRNA, but a non-translated RNA that is made as a larger precursor that is processed into 21-23 nucleotide long microRNA. Wightman et al. observed that *lin-4*/miroRNA was partly complementary to the *lin-14* 3'UTR, and demonstrated that *lin-4* post-transcriptionally inhibits *lin-14*/nuclear protein through its 3' end, providing the fundamental mechanism of microRNA target regulation (Wightman et al., 1993). Later work showed that the mature microRNA is incorporated into a RNA-induced Silencing Complex (RISC) (Hutvagner et al., 2001), where it represses translation of genes that contain antisense elements in their 3'UTR (Olsen and Ambros, 1999). As a summary, *lin-4*/microRNA is required for a transition from L1 to L2 programs.

1.4.2 MicroRNAs and the L2 to L3 stage transition

L2-L3 transitions are primarily regulated by the *C. elegans* hunchback, *hbl-1*. Hunchback proteins are transcription factors containing cys2-his2 zinc finger motifs, and are important for

early embryonic pattern formation, as first described in Drosophila (Lehmann and Nusslein-Volhard, 1987; Tautz et al., 1987). In *C. elegans*, the hunchback homolog *hbl-1* also plays a later role in larval developmental timing, promoting the hypodermal L2 program (Abrahante et al., 2003; Lin et al., 2003) *hbl-1*/hunchback directed RNAi leads to a loss of hypodermal L2 programs and precocious execution of L3 programs directly following the L1 stage (Table 1). Transition from the hypodermal L2 stage to the L3 stage is dependent on the disappearance of *hbl-1*/hunchback protein mediated by three *let-7* family microRNAs: *mir-48, -84, -241* (collectively referred to as "*let-7s*") (Abrahante et al., 2003; Lin et al., 2003). Loss of *let-7s*/microRNAs leads to persistent HBL-1/hunchback expression during L3 and failure of the L2 to L3 transition (Abbott et al., 2005). Thus, *let-7s* microRNAs are normally required for a transition from L2 to L3 programs (Figure 6 B).

1.4.3 MicroRNAs and the L4 to adult stage transition

The L4-to-adult transition is marked by the end of molting, with the seam cells exiting the cell cycle, terminally differentiating and fusing into a seam syncitium, which excretes a ridged cuticular structure called “alae” – a convenient marker for the adult fate (Page and Johnstone, 2007). Loss or reduction of function of several heterochronic genes cause failure of the L4-adult switch, including *let-7*/microRNA (Reinhart et al., 2000) and zinc-finger protein LIN-29/ZnFi (Figure 6 C) (Ambros and Horvitz, 1984).

Lin-29 regulation is complex. mRNA transcription already starts during the L2-L3 stage, but translation is suppressed by the *lin-41*/RBCC ring finger protein. *Lin-29*/ZnFi expression is derepressed when *lin-41*/RBBC itself is translationally suppressed by *let-7*/microRNA as it comes on during the L3-L4 stage. Thus, LIN-41/RBBC disappearance allows LIN-29/ZnFi translation during L4 stage and promotion of terminal differentiation in hypodermis, as well as in the vulva (Reinhart et al., 2000). However, more recent studies show that varying the expression level of *mir-84* can modulate the phenotypes of *let-7* and *lin-29* mutants (Hayes et al., 2006), placing the microRNAs further downstream in the herterochronic pathway. RNAi knock down of several heterochronic genes - including those acting earlier in the pathway - can suppress the microRNA deficiency phenotypes of inhibited terminal differentiation. This highlights how complicated heterochronic regulation networks can be, consisting of multiple parallel branches of regulation.

1.4.4 Heterochronic regulation by DAF-12 signaling

Another regulator of the L2 to L3 transition is the nuclear hormone receptor *daf-12*. Loss of function alleles of *daf-12* lead to retarded developmental progression, reflected in a repetition of L2 stage specific programs in the hypodermal seam cells. Alleles like *daf-12(rh61*), which affects the ligand binding domain, cause both stronger hypodermal phenotypes and gonadal migration phenotypes when the distal tip cell continues outwards migration during L3 stage and fail to turn back towards midbody (Antebi et al., 1998). These phenotypes are associated with weak repressing activities of DAF-12 and its co-repressor DIN-1 (Ludewig et al., 2004), when dafachronic acid synthesis or binding to the receptor is diminished. Indeed, gonadal heterochronic phenotypes are also caused by mutations affecting dafachronic acid synthesis such as *daf-9(rh50)* (Gerisch et al., 2001; Jia et al., 2002). Loss of dafachronic acid synthesis of the *daf-9(dh6)* null allele or alleles that severely decrease DAF-12 ligand binding domain affinity for dafachronic acid, like *daf-12(rh273)* or *daf-12(rh274)* lead to either constitutive dauer formation (Daf-c) or severe retarded phenotypes in the gonad (Antebi et al., 2000). All phenotypes of reduced dafachronic acid production or LBD affinity can be suppressed by knock-out of DIN-1, indicating that they are caused by various degrees of *daf-12* target repression. The function of *daf-12* in these tissue specific heterochronic phenotypes is not only to globally arrest development as described earlier, but also to actively promote tissue specific developmental progression.

From the discussion above, it is known that a loss of the cell specifically acting *let-7s* microRNAs causes the same phenotype as a loss of the global acting nuclear hormone receptor *daf-12*—an increase in the number of seam cells. By contrast, a loss of microRNA repression target *hbl-1* causes the opposite phenotype, a decrease in the number of seam cells.

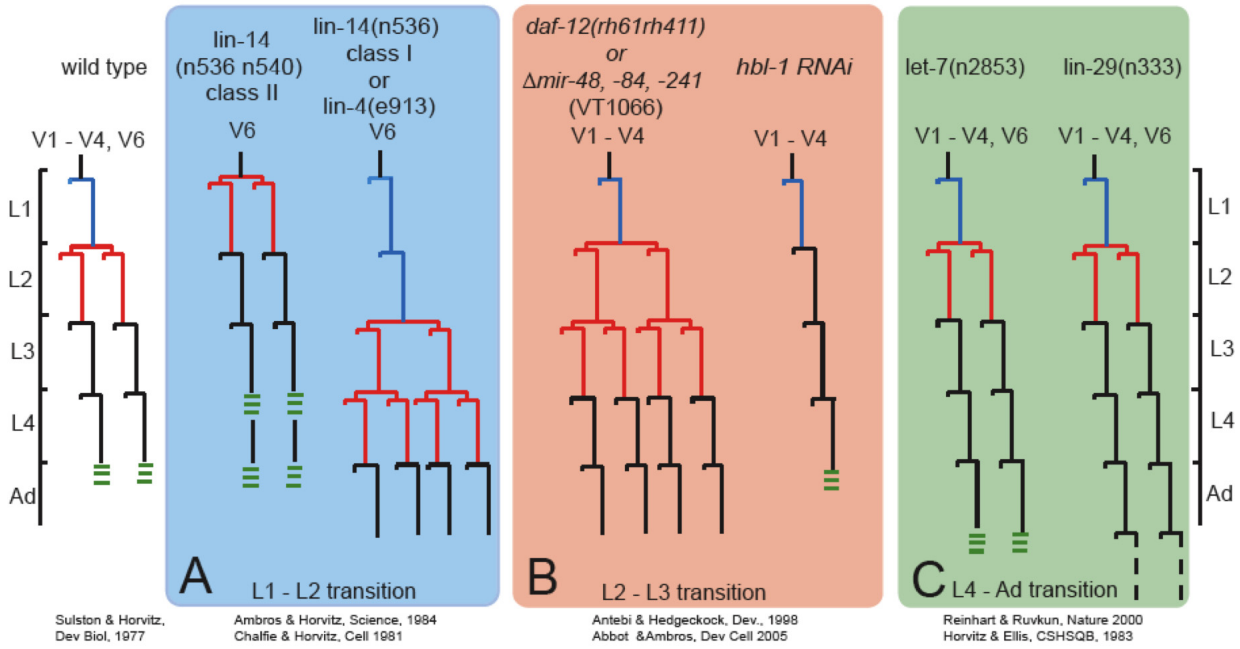

Figure 6: V1-4 and V6 seam cell lineages in wild type and mutant backgrounds
lin-14(n536n540) loss-of-function (lf) mutants fail to execute hypodermal L1 programs while *lin-14(n536)* gain-of-function (gf) and *lin-4(e913)* lf fail to progress timely to L2 stage (A). RNAi against *hbl-1* results in a loss of L2 programs, while *daf-12(rh61rh411)* lf and *mir-48 -84, -241* triple deletion mutants fail to timely progress to L3 stage (B). *lin-29(n333)* lf and *let-7(n2853)* temperature sensitive (ts) lf mutant fail to terminally differentiate and timely progress to adult stage (C).

The above mentioned microRNAs are so far known as cell specific regulators of heterochronic development, which due to their tight spatial control of expression only affect a subset of tissues. Other heterochronic factors are listed in Appendix 6 or reviewed elsewhere (Moss, 2007; Rougvie, 2001).

1.5 Questions addressed in this dissertation

MicroRNAs were discovered only recently, but it is clear that they are involved in many important biological processes such as stem cell maintenance, development and cancer. Despite their importance, many aspects of their regulation and function remain unknown so far. Only few examples are described for *trans*- and *cis*- acting regulatory factors that coordinate their transcriptional regulation. A connection of microRNA transcriptional regulation to upstream signaling allows an understanding of a broad regulatory cascade in a physiologic context.

In *C. elegans*, the loss-of-function phenotype of *let-7s*/microRNAs resembles a loss-of-function of the nuclear hormone receptor DAF-12. In Chapter 2 of this dissertation, I

investigated the possibility that this phenotypic similarity is a result of the *let-7s*/microRNAs being direct transcriptional targets of DAF-12. This connection would link DAF-12, an important regulator of global developmental progression, as a trans-regulatory factor to the *let-7s*/microRNAs, which act principally as cell type specific heterochronic genes.

To understand the hormone dependence of microRNA regulation, it is important to understand the extent of nuclear hormone receptor regulation of microRNAs and how much other transcription factors contribute. Because hormone receptor/microRNA promoter interactions have not been described in detail so far, I isolated predicted *daf-12* regulated cis-regulatory elements from microRNA promoters and tested the dependence of their activation on *daf-12* and other transcription factors, as described in Chapter 3 .

The activity of nuclear receptors depends on their interaction with co-regulating factors, and in Chapter 4 , I test a candidate DAF-12 co-regulator, LIN-29/ZnFi for its *in vitro* and *in vivo* influence on DAF-12 dependent transcriptional regulation.

Altogether these studies shed light on fundamental aspects of microRNA regulation during metazoan developmental progression.

2. Nuclear hormone receptor regulation of microRNAs controls developmental progression

This work was published as:

Science. 2009 Apr 3;324(5923):95-8.
Axel Bethke, Nicole Fielenbach, Zhu Wang, David J. Mangelsdorf, Adam Antebi :
"Direct nuclear hormone receptor regulation of microRNAs controls developmental progression"

Nicole Fielenbach contributed data to Figure 12, Figure 13 and Figure 17

Adam Antebi contributed data to Figure 17, Figure 18 and Table 1

Introduction

Many examples are known of how environmental input can influence the progression of development of an organism, e.g. the delayed sexual maturation of humans caused by starvation, or the delay of metamorphosis of starving tadpoles (Gilbert, 2003).

The environment achieves this by influencing the endocrine regulation that is driving development. The endocrine signal originates from endocrine tissues that excrete signaling compounds like steroid or thyroid hormones that can diffuse throughout the whole body to orchestrate changes across different tissues. Environmental conditions influence these endocrine organs and hormone syntheses and influence organism wide progression or fate choices. In target tissues, nuclear hormone receptors convert this signal into local changes of gene expression patterns that define the morphology changes and developmental programs executed within each tissue. How exactly the hormone signals are converted into cell specific developmental programs, and how those are responsive to environmental changes remains mostly unclear and a lot of research on both mammalians as well as model organisms has been done to identify these hormones, their downstream targets and how they regulate them. In the model organism *C. elegans*, this research lead to the identification of steroid like hormones called dafachronic acids (Motola et al., 2006). Dafachronic acids are synthesized by a cascade of hormone synthetic genes only in presence of food and favorable environmental conditions. Hormone synthesis is regulated by insulin and TGF-beta signaling cascades that convey environmental sensing information and repress it e.g. in absence of food (Gerisch and Antebi, 2004). Dafachronic acids signal throughout the whole worm body to activate the nuclear hormone receptor DAF-12 and its target genes. In absence of dafachronic acids, DAF-12 tightly represses its transcriptional targets and causes developmental arrest and dauer larva formation. This repression seems to be the main function of DAF-12 for developmental regulation, since null mutants of *daf-12* fail to arrest, and show overall normal morphology. DAF-12 transcriptional activation seems to be required for developmental progression at least in one tissue, the hypodermal seam cells, that fail to properly transit from larval stage L2 to L3 absence of DAF-12 transcriptional activation (Antebi et al., 1998).

It is not well understood what target genes DAF-12 regulates to transduce the presence or absence of the global dafachronic acid signal into cell intrinsic gene expression changes.

However, knowing the identity of these genes and the dynamic of their regulation is fundamental to understanding this model system for not only how hormone signaling drives development, but also for how it connects to upstream signaling cascades that link development to environmental conditions.

The main purpose of this study was to gain insight into these processes by identification of direct DAF-12 target genes and their regulation. The primary aim was to find transcriptional activation targets of DAF-12 and connect them to upstream hormone signaling and downstream tissue specific effects. A starting point for this aim was to identify genes that cause a similar loss-of function phenotype as *daf-12*, hinting a functional connection. Candidates are *mir-48, -84*, and *-241*, members of the *let-7* family of microRNAs, since their deletion leads to a loss of developmental progression from L2 to L3 stage programs in the seam cells (Abbott et al., 2005) as seen in *daf-12* null mutant background. MicroRNAs are a recently discovered class of cell autonomously acting translational regulators coding for small hairpin RNA molecules that get processed and incorporated into a protein complex whose sequence specifically interferes with RNA translation of its target genes. Several repression targets for the *let-7* family microRNAs have already been described, one of which is hunchback homolog *hbl-1*, which is required for L2 specific seam cell program execution (Abrahante et al., 2003). This functional connection of translational regulator genes and their repression targets to DAF-12 and hormone signaling dependent functions is the reason why I tested these genes for DAF-12 dependent regulation. A direct connection would integrate cell specific factors like the microRNAs and *hbl-1* into a *daf-12* and hormone dependent signaling cascade. This cascade would not only span the gap between tissue specific development and organism wide hormonal control, but it would also connect it to already established cascades for environmental sensing. The final cascade would span from environmental sensing, through the insulin and TGF-beta cascade, onto the steroid synthesis pathway and *daf-12* dependent regulation of tissue specific regulators that are part of cell specific developmental programs. In addition to this, it would be the first time that microRNAs are found to be integral parts of a signaling cascade.

In this chapter, I will present experiments that I undertook to test the promoters of the *let-7* family microRNAs for direct DAF-12 regulation, and how this regulation affects microRNA downstream targets. I will test if the microRNAs are part of a cascade connecting global *daf-12* hormone signaling to seam cell specific program execution, and if this cascade reacts

accordingly to signaling mutant backgrounds. Finally, I will look for literature examples to test if this regulation motif is conserved in other organisms.

Results

2.1 NHR activates microRNAs

2.1.1 *In vitro* promoter interaction

2.1.1.1 Direct transcriptional activation of microRNA-promoters by DAF-12 and ligand

To test the above stated hypothesis, I cloned promoter regions of several microRNA genes into a luciferase reporter construct and performed luciferase assays in Human Embryonic Kidney cells (also known as 293T cells). I tested promoters of *lin-4* and *lin-4* homolog *mir-237*, as well as *let-7* and its homologs *mir-48, -84, -241* (referred to as *let-7s*) promoters. Co-transfected was either DAF-12 or GFP expression vector, and activation was assayed in presence of either 400nM Δ^4-dafachronic acid or EtOH as vehicle control. I found that only *mir-241p* and *mir-84p* reporters gave strong luciferase activation (Figure 7).

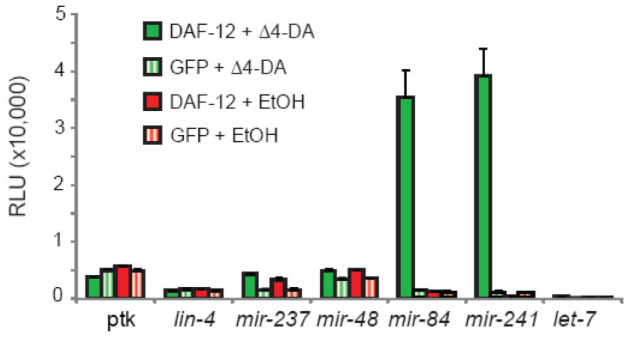

Figure 7: Luciferase assay of microRNA promoters
Expression vectors for DAF-12 or GFP as control were transfected into Human Embryonic Kidney cells, along with vectors containing luciferase cDNA downstream of a microRNA promoter followed by a minimal promoter. Dafachronic acid (Δ^4-DA) strongly activates *mir-84* and *mir-241* promoters in the presence of DAF-12 *in vitro*, whereas other promoters were not visibly activated. Assay was repeated twice with similar results.

Activation was dependent on the presence of both DAF-12 and ligand, suggesting that DAF-12 can physically interact with both promoters, as well as with the basic mammalian transcriptional machinery.

To find the location of the DAF-12 response elements (RE) in the promoters, I generated a deletion series of the *mir-241* promoter to map the DAF-12 response elements. I found that a 500bp long truncation #4 retains highest DAF-12 and ligand dependent activation making it likely for DAF-12 response elements to be present in these 500bp.

To define a canonical RE that DAF-12 can bind to, Shostak (Shostak et al., 2004) used an approach testing *in vitro* DNA binding of genomic fragments to immobilized DAF-12 DBD. I generated a consensus DAF-12 response element by using the "Weblogo.com" tool of the UC Berkeley to combine various REs defined by Shostak. I will refer to this element as ”Shostak-RE” (Figure 8).

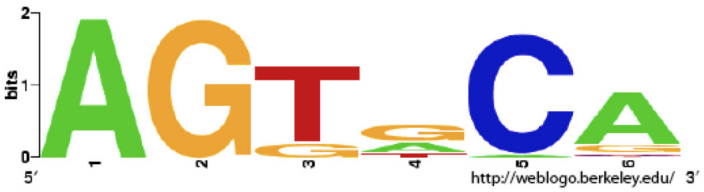

Name	fold induction	DAF-12 REs present
4.2	182x	AGGACA AGTGCA AGTGCG AGGACA AGGACA
4.19	152x	AGTACT AGTGCA
4.15	53x	AGTTCA AGTAAC AGTACA
4.1	41x	AGTTCA AGGACA AGTGCA AGTACA
4.14	24x	AGTTCA AGTGCG AGTTCA AGTGCG AGTTCA AGTGCG
4.3	20x	AGTGCA AGTGCA AGTGCA AGTGCA AGTGCA AGTGCA AGTGCA AGTGCA

Figure 8: Shostak-response element for DAF-12
DAF-12 response elements identified by Shostak were combined independent of their fold-induction potential to generate a canonical response element using the “Weblogo.com” tool.

EMSA experiments by Daniel Motola also showed an increased DAF-12 affinity to the RE when the Shostak-RE was preceded by a stretch of several adenosine nucleotides (Motola, personal communication). The #4 truncation fragment of the *mir-241* promoter contains four potential DAF-12-response-elements (REs) that fulfilled the above mentioned criteria. The two separately located sites were called 241a and 241b, and an inverted repeat with 9 nucleotides

spacing between response elements (IR9) was called 241cd. Two potential response elements were identified for the *mir-84* promoter and called 84d and 84e.

In the full-length promoter context, deletion or mutation of the 241a and 241b elements of the *mir-241* promoter and 84d and 84e elements of the *mir-84* promoter led to a ~7 and ~3 fold decrease in activation, respectively (Figure 9). This was interpreted as DAF-12 and ligand dependent activation to depend on the presence of the identified response elements in the promoter *in vitro*.

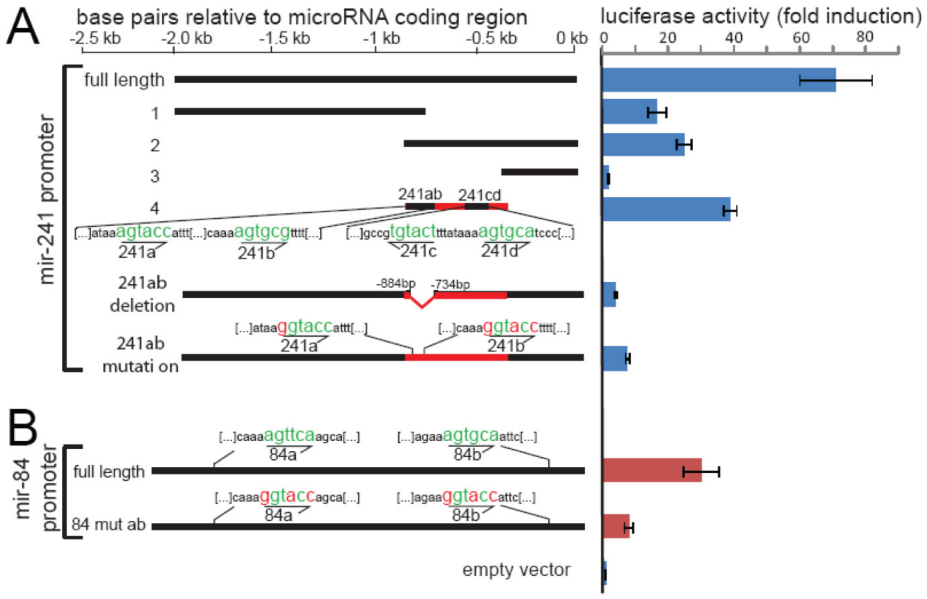

Figure 9: Deletion analysis of *mir-241* and *mir-84* promoters
Deletion fragments 1 to 4 of the *mir-241* promoter retained DAF-12 and dafachronic acid (400nM) dependent partial activation. The strongest activating fragment #4 harbored four Shostak-response elements, called 241a, 241b, 241c, 241d. Deletion or point mutation of 241a and 241b abolished most activation (A). Mir-84 promoter lost most activation after deletion of 84a and 84b sites. Due to different promoters used, the nomenclature of the 84a and 84b site changes in Chapter 3 to "84c" and "84e". Assay was repeated twice with similar results.

2.1.1.2 Direct physical DAF-12 interaction with response elements in the promoter fragments

To test if DAF-12 can physically interact with those candidate DAF-12 response elements, I performed electrophoretic mobility shift assay (EMSA). Human Embryonic Kidney cells were transfected with expression vectors for either GFP or Flag-tagged DAF-12. Nuclear extract of transfected cell cultures were incubated with radio labeled, 30 nucleotides long oligo nucleotides spanning candidate DAF-12 response elements. I found that among unspecific background shift signals, specific shift signals were induced only by nuclear extract of *daf-12* transfected cultures.

These specific shifts were super shifted by incubation with anti-Flag antibody as proof of DAF-12 being the shift causing protein. The shift was sequence specific, since unlabeled wild type sequence oligo competed away the shift signal, while oligos with a mutated *daf-12* response element failed to do so (Figure 10 A).

The 241b element caused a clear shift signal, while the 241a element produced in addition to a specific signal an unspecific background band. The specific signal gained in intensity when incubated with *daf-12* transfected nuclear extracts, and was super shifted after anti-Flag antibody incubation (Figure 10 B).

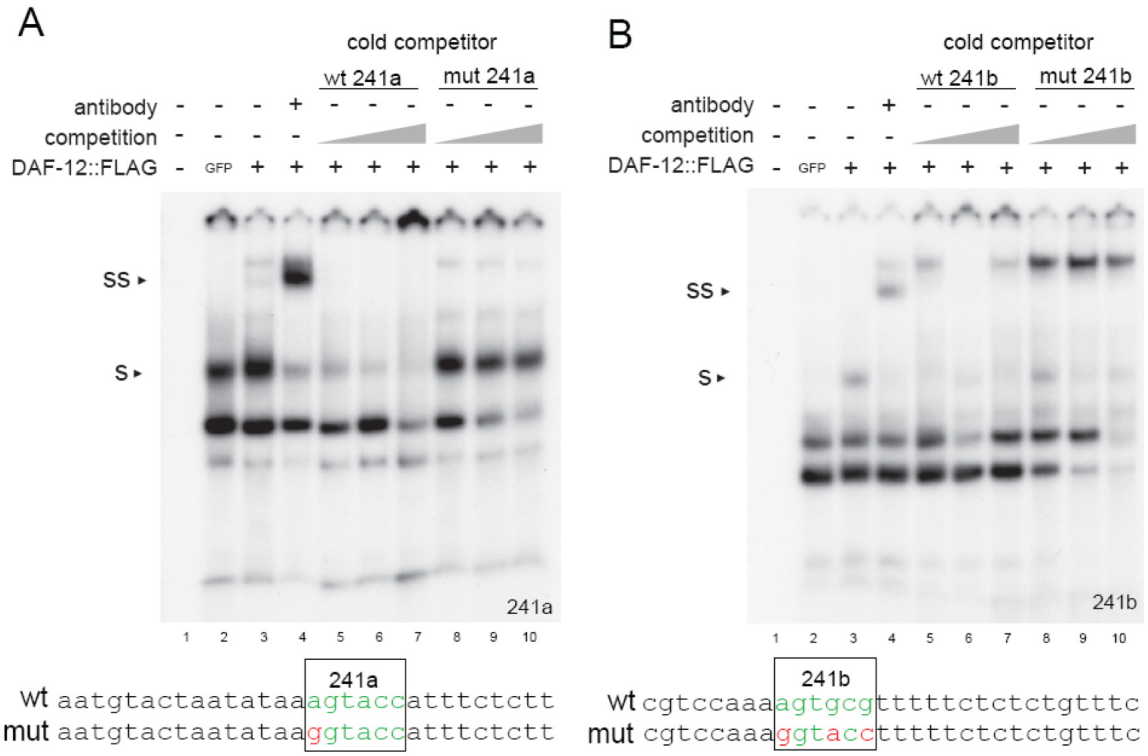

Figure 10: EMSA of 241a and 241b
Nuclear extract of cells expressing Flag-tagged DAF-12 induced a shift (s) of 241a element containing radio-labeled oligo that was partially over layered by a non-DAF-12 dependent shift. The DAF-12 specific signal was super shifted (ss) after incubation with anti-Flag antibody, competed away by non-labeled wild type sequence oligo, but not competed away by oligos with point-mutated 241a (A) while shift and super shift of 241b are not over layered (B). Green letters indicate DAF-12-REs while red letters represent mutated nucleotides. EMSA was repeated once with similar results.

The oligo containing the 242cd sites produced a more complex shift pattern, since either one (causing the "monomer s") shift or both (causing the "dimer s") shift response elements can be occupied to induce a shift by DAF-12 protein. Double occupancy resulted in a higher shift and was the predominant condition as seen by the more intense shift band. Anti-Flag antibody also generated a super shift even though more diffuse than the super shift signal observed for the single-response element containing oligos. Competition with cold wild type oligo competed DAF-12 away from the labeled oligos, while single or double mutated competitor oligo partially competed with the result of a more equal distribution between single and double DAF-12 occupancy of the oligo that is reflected in the more equal intensity between the two different shift signals (Figure 11).

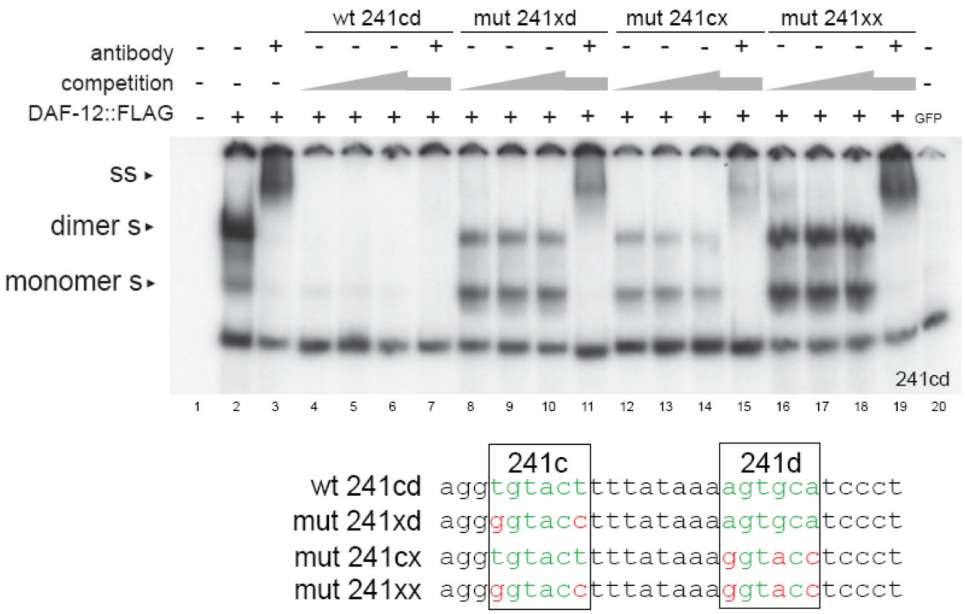

Figure 11: EMSA of 241cd
Nuclear extract of cells expressing Flag-tagged DAF-12 induced two shift signals (s) of radio labeled oligo containing 241cd element. "monomer" shift (s) signal is caused by oligos bound to a single DAF-12 protein, while "dimer" shift (dimer s) is caused by oligos bound to two DAF-12 proteins. The DAF-12 specific signal was super shifted (ss) after incubation with anti-Flag antibody. Incubation with non-labeled wild type (wt) competitor oligo competed away the shift. Addition of oligo with one (mut 241xd or mut 241cx) or both (mut 241xx) *daf-12* response elements mutated changed the ratio of "monomer" and "dimer" shift towards monomer bound, labeled oligo. Green letters indicate DAF-12-REs while red letters represent mutated nucleotides. EMSA was repeated once with similar results.

The 241c and 241d elements are spaced 9 nucleotides apart, which reflects nearly one complete turn of the DNA helix, positioning the two DNA bound DAF-12 proteins in direct proximity possibly reflecting direct DAF-12-DAF-12 homo-dimerization or hetero-dimerization with one alternative nuclear hormone receptor. Dimerization is common for NHRs and modifies transcriptional output (Forman & Evans 1995). The context of possible dimerization and *in vivo* transcriptional activation generated by these two sites are investigated in more detail in Appendix 5.

2.1.2 *In vivo* promoter activation

2.1.2.1 *Mir-241* promoter regulation and *daf-12* signaling mutations

To examine microRNA promoter activation *in vivo*, I generated transgenic worm lines containing the microRNA promoters fused to a *gfp* reporter gene (termed *mir-241p::gfp* or *mir-84p::gfp*). I found that wild type worms transgenic with the *mir-241p::gfp* reporter gave a broad expression pattern as described (Esquela-Kerscher et al., 2005).

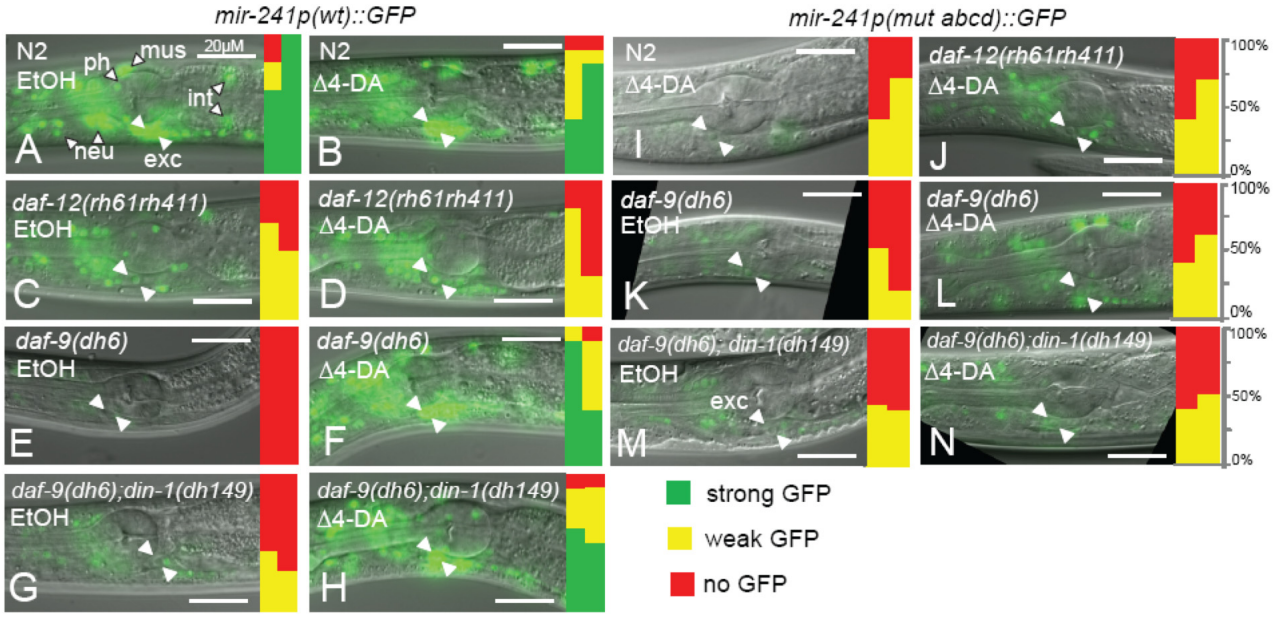

Figure 12: DAF-12 and dafachronic acid regulate *mir-241* promoter *in vivo*

(A to H) *mir-241p::gfp*. Images show representative L3 animals, with indicated cell types (white arrowheads and exc, excretory cell; outlined arrowheads, neu, neuron; mus, muscle; int, intestine; ph, pharynx). Bar graphs alongside the images quantify the percentage of worms with excretory cell GFP expression as either strong (green), weak (yellow), or off (red) (two independent experiments, left and right, n = 10 animals each, and representative images are shown). Wild type (N2, A and B) grown without ethanol (EtOH) or with dafachronic acid (250nM Δ^4-DA) showed equal expression levels. Expression was decreased in *daf-*

12(*rh61rh411*) null (C), strongly repressed in *daf-9*(*dh6*) null (E), or not activated in *daf-9*(*dh6*);*din-1*(*dh149*) double null (G), but was rescued nearly to wild type level by growth on 250 nM Δ^4-DA (F and H). In wild type (B) or *daf-12* null (D) animals, dafachronic acid supplementation had no effect. Point mutation of all four DAF-12 REs abolished differences of tested genetic backgrounds or dafachronic acid (I to N).

daf-12(rh61rh411) null mutants showed decreased expression most noticeably in the excretory cells (exc), as well as muscles (mus), pharynx (ph) and intestine (int) whereas neuronal expression (neu) seemed less affected, revealing tissue selectivity of *daf-12* regulation (Figure 12 C-D). Previous research revealed that null mutants for cytochrome P450 *daf-9(dh6)* fail to produce dafachronic acid, and the unliganded DAF-12 interacts with its co-repressor DIN-1/SHARP to repress its transcriptional targets. According to this, *mir-241p::gfp* expression was tightly repressed in most tissues in *daf-9* null background (Figure 12 E). Supplementation with dafachronic acid rescued this arrest and increased *mir-241p::gfp* expression back to wild type levels (Figure 12 F). Tight repression was also relieved in *daf-9(dh6);din-1(dh149)* double null mutants lacking both, the ligand and the co-repressor. *Mir-241p::gfp* expression levels in this double mutant strain were similar to *daf-12* null mutants (Figure 12 G, H). Unlike *daf-12* null mutants, dafachronic acid supplementation of *daf-9;din-1* worms restored *mir-241p::gfp* expression back to wild type levels. Point mutation of all four *daf-12*-REs in *mir-241p* (termed *mir-241p(mut abcd)::gfp*) resulted in the same weak expression level in wild type, *daf-12* null, *daf-9* null, and *daf-9*;*din-1* doubles with or without ligand, as previously seen of the *mir-241* wild type promoter *gfp* construct in *daf-12* null background (Figure 12 I-K).

This was interpreted as liganded DAF-12 acting through its REs to mildly activate *mir-241p* in some issues, whereas unliganded DAF-12 together with DIN-1 tightly represses expression in nearly all tissues. The loss of any influence of *daf-12* signaling onto the point mutated reporter constructs further shows that DAF-12 does not interact with any other response elements in the promoter than the mutated four to mediate activation and repression.

2.1.2.2 *Mir-84* promoter regulation in *daf-12* signaling mutant backgrounds

As reported (Esquela-Kerscher et al., 2005; Hayes et al., 2006), *mir-84p::gfp* was expressed in pharynx, somatic gonad, seam cells, vulva cells, and occasionally in the intestine. The phenotype of *daf-12* null or the *let-7s* deletion overlaps in the seam cells, and direct

transcriptional activation of the microRNAs would show as de-regulated *mir-84p::gfp* seam cell expression.

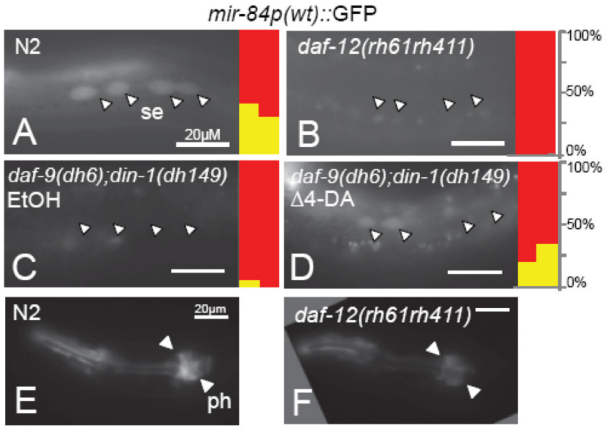

Figure 13: DAF-12 and dafachronic acid regulate *mir-84* promoter *in vivo*
Images show representative L3 animals. Bar graphs alongside the images quantify the percentage of worms with excretory cell GFP expression as either strong (green), weak (yellow), or off (red) (two independent experiments, left and right, n = 10 animals each, and representative images are shown). Epidermal seam cells (arrowheads) expressed *mir-84p::gfp* in wild type (N2, A), but not in *daf-12* null mutants (B). Seam cell expression was absent in hormone-deficient *daf-9;din-1* animals (C), but restored to nearly wild type levels by dafachronic acid (Δ^4-DA) supplementation (D).

Indeed, seam cell expression was absent in *daf-12* null and *daf-9;din-1* double null mutants, with expression increased to almost wild type levels in *daf-9;din-1* animals grown on dafachronic acid supplemented plates (Figure 13 A-D). This finding possibly explains *daf-12* heterochronic phenotypes as a failure to activate the microRNAs in tissues subject to temporal control of development. In contrast to seam cell expression, expression in other tissues such as the pharynx was less affected (Figure 13 E, F), again showing tissue-specifity of *daf-12* regulation.

2.1.2.3 Mature microRNA dose measured by Q-PCR

Promoter fusions to *gfp* reporter genes reflect the transcriptional activation of the promoter, but do not account for regulation during the microRNA maturation process, which was also found do be highly regulated (Newman et al., 2008). To quantify mature microRNAs, I used Taqman Quantitative PCR (Q-PCR) and found that the transcriptional regulation of the *let-7s* is also reflected in the abundance of total mature microRNAs detected. *daf-12* mutants and *daf-9;din-1* animals without ligand showed decreased levels compared to wild type, whereas *daf-9*

null mutants showed tight repression of *let-7*s microRNAs (Figure 14 A-D). As expected, expression in *daf-9*, *daf-9;din-1*, but not *daf-12* mutants was rescued by dafachronic acid. *mir-1* was used as an endogenous control as it was reported to be not regulated during development of *C. elegans* (Lau et al., 2001).

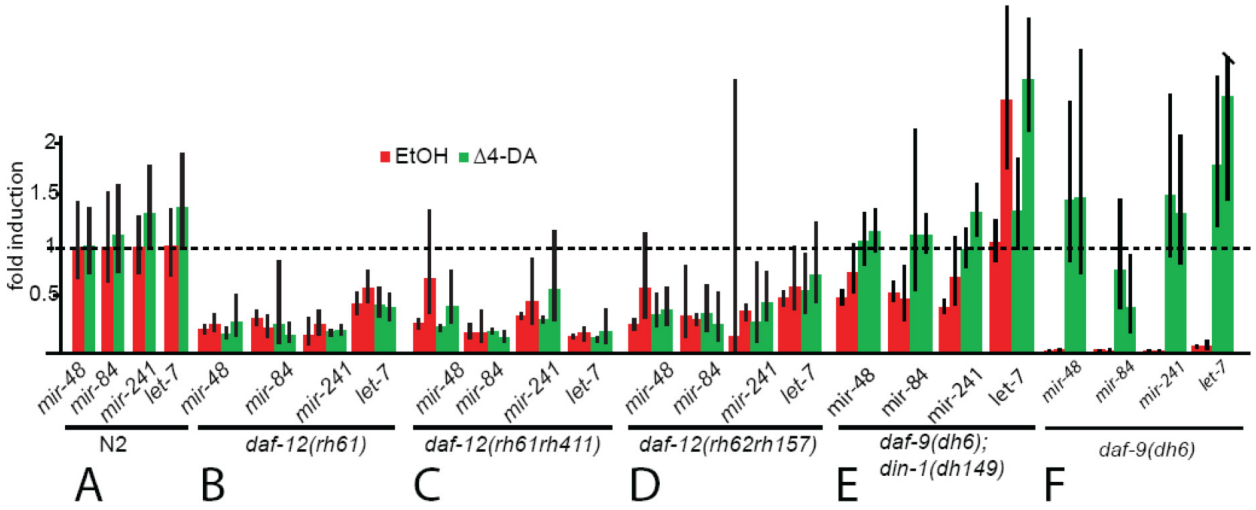

Figure 14: Relative quantification of *let-7* family microRNAs by Q-PCR
microRNA expression was decreased in *daf-12(rh61)* (B), *daf-12(rh61rh411) null* (C), *daf-12(rh62rh157) null* (D), *daf-9;din-1* double null mutants (E) and repressed in *daf-9* mutants (F) relative to wild type expression (A). In *daf-9* genotypes, expression was dependent on growth in presence of 250nM Δ^4-dafachronic acid. Q-PCR was carried out using the TaqMan system, using *mir-1* quantification as endogenous control.

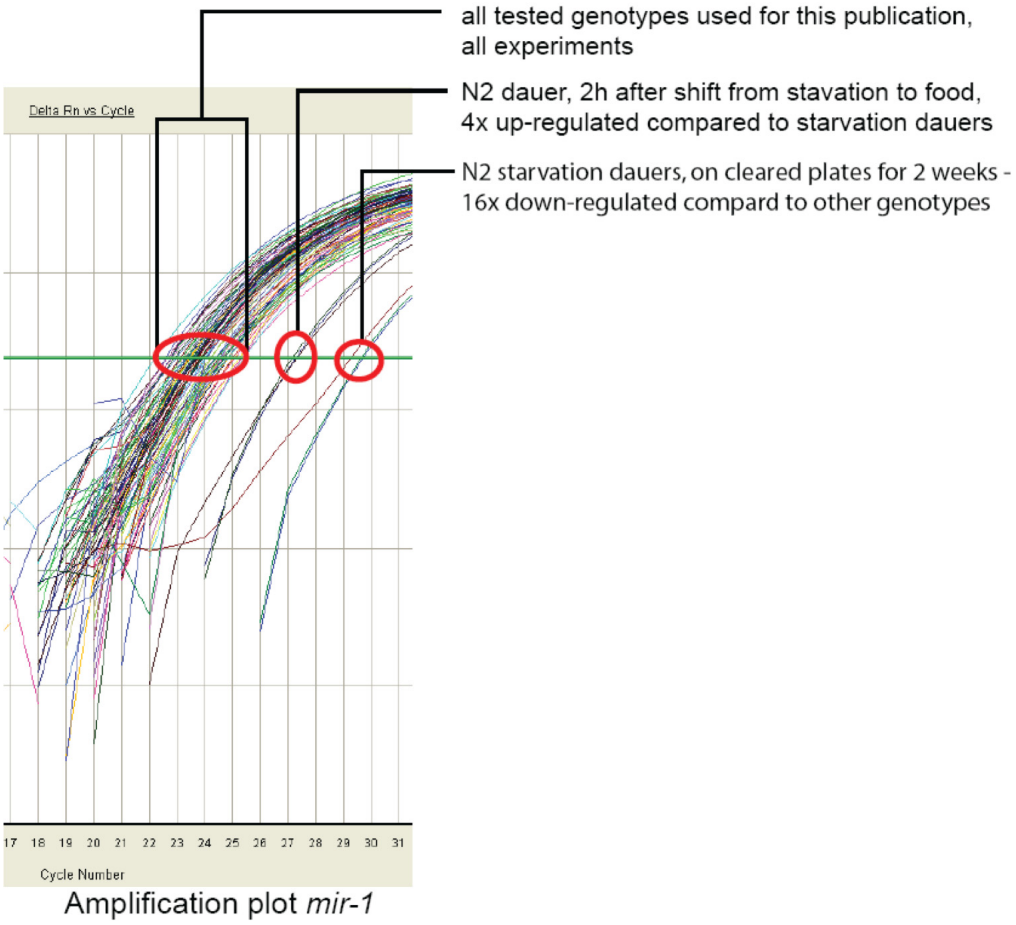

Figure 15: Quantitative PCR of *mir-1*
The amplification plot for miR-1 detector shows overlapping CT values for *mir-1* in all genotypes tested i.e. *daf-9(dh6)* in presence versus absence of 250nM Δ^4-dafachronic acid. Therefore *mir-1* expression does not change substantially in the genetic backgrounds used in this publication. In contrast to this, N2 dauers on starved plates express ~ 16x reduced amount of *mir-1*, which after 2h of re-feeding already increases 4x (A).

The only RNA purifications showing drastic changes of *mir-1* content judged by the Q-PCR amplification plot were derived from starvation dauers. However, the absolute RNA amount used as template was below minimum concentration necessary for accurate quantification and therefore was not quantified prior to use, instead equal number of worms were extracted (100 animals per condition) (Figure 15). Variations in RNA input concentrations might be responsible for a general over- or underrepresentation of all four measured *let-7s*, but this specific misrepresentation is identical for all four microRNAs quantified for a specific condition.

However, relative quantification of the four *let-7* family microRNAs indicates a specific regulation of *mir-84* relative to the other three quantified miRs (Figure 16).

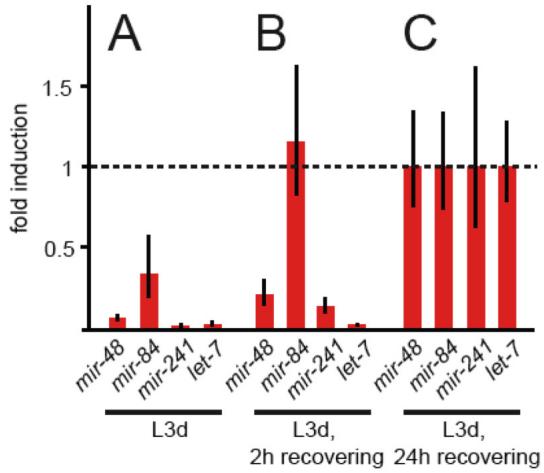

Figure 16: *mir-84* regulation during dauer recovery
Quantification of let-7 homologs in N2 starvation dauers (A), 2h after re-feeding (B) and 24h after re-feeding (C) on a single biological replicate consisting of 100 hand-picked worms. Fold change of *let-7* homologs relative to endogenous control miR-1 and calibrated to 24h of re-feeding. Note that miR-1 RNA is less abundant in RNA preparations of starvation dauers (Figure 15). One biological replicate of n=100 animals each condition.

2.1.2.4 MicroRNA promoter activation in *daf-12* upstream signaling mutants

In the introduction, I describe evidence for upstream neuronal input through TGF-beta and insulin signaling onto the global decision between developmental progression or arrest. This influence converges onto *daf-12* ligand production. Direct DAF-12 dependent *mir-84* and *mir-241* activation connects these upstream signaling cascades through *daf-12* and its ligand to cell intrinsic program execution in the hypodermis. To further investigate this dependence onto upstream cascades, and to show how the downstream, cell intrinsic *let-7s* expression is affected by global acting TGF-beta and insulin signaling, the regulation dynamics of *mir-84p::gfp* and *mir241p::gfp* reporter construct were analyzed in dauer constitutive mutant backgrounds of *daf-7*/TGF-beta, *daf-2*/Insulin/IGF-I Receptor, and *daf-9*. *Daf-2(e1368)* and *daf-7(e1372)* alleles are temperature sensitive and cause dauer formation only when cultivated at non-permissive temperature of 25°C, while *daf-9* is a null allele that does not produce dafachronic acid under any condition and constitutively causes dauer formation.

In *daf-2* and *daf-7* dauer larvae grown at non-permissive temperatures, *mir-241p::gfp* expression was nearly completely repressed, whereas *mir-84p::gfp* was down regulated in some

tissues such as the pharynx (Figure 17 A-D) but consistently up-regulated and expressed more penetrantly in others tissues such as the seam cells (Figure 17 E-G).

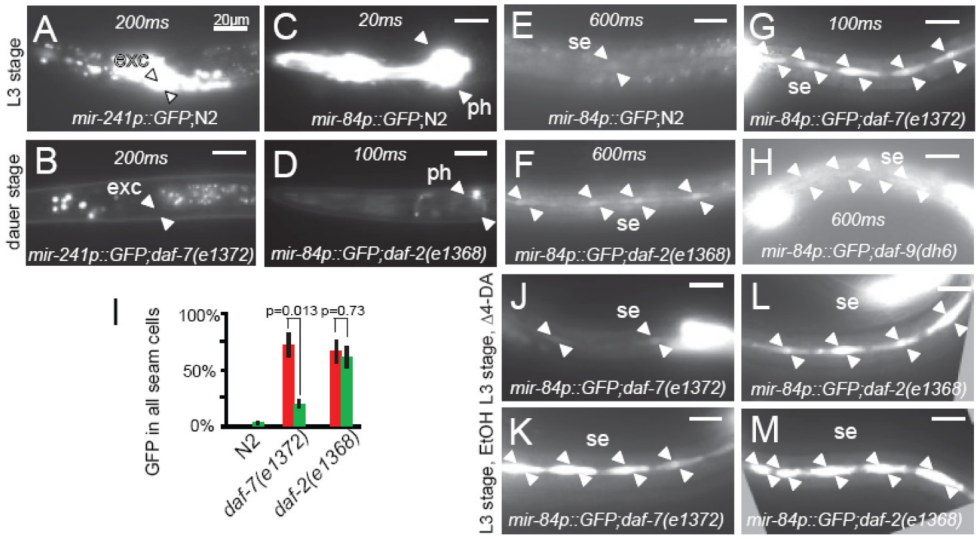

Figure 17: microRNA promoter regulation in different dauer signaling mutant backgrounds
Mir-241p::gfp showed high expression in continuously growing wild type (A), but low expression in *daf-7(e1372)* dauer larvae (B). *mir-84p::gfp* showed high expression in the pharynx of continuously growing wild type (C) but low expression in *daf-2(e1368)* dauers (D). *mir-84p::gfp* seam cell expression (E) was elevated in *daf-2* and *daf-9* mutants during dauer stage (F and H) and was even higher in *daf-7* mutants during reproductive growth at 20°C (G). Penetrant seam expression was reversed by 500 nM dafachronic acid in *daf-7*, but not *daf-2*, during reproductive growth (I to M). Animals were assayed during L3 and/or L3d stages, *n*> 20 animals, and representative images are shown. Red bars represent percentage of worms showing expression when grown on ethanol vehicle, while green bars represent the same during growth on Δ^4-dfachronic acid (SEM).).

Mir-84 seam cell expression is increased even in the total absence of ligand synthesis in *daf-9* null mutants (Figure 17 H). These findings are in contrast with the existing model of *daf-12* signaling where the absence of ligand causes DAF-12 to tightly repress transcription of its target genes and to induce dauer formation.

It was found that in *daf-2(e1368)* and *daf-7(e1372)* mutant L3 worms grown under permissive temperature, seam cell expression was more penetrant than in wild type background, arguing for a ligand independent transcriptional activation of *mir-84p* in this tissue (Figure 17 G).

To test ligand influence on the expression in this tissue, worms grown under permissive temperature that were either ligand supplemented or non-supplemented were compared.

Dafachronic acid supplementation largely suppressed the increased expression in seam cells in *daf-7*, but not in *daf-2* background (Figure 17 I-M). These findings suggest that insulin/IGF and TGF-beta signaling distinctly regulate *mir-84p* expression in a dafachronic acid dependent and independent manner.

2.1.3 MicroRNAs and their involvement in signaling cascades

2.1.3.1 HBL-1 drives developmental progression in seam cells and is microRNA regulation target

The zinc finger protein *hbl-1*/hunchback is responsible for L2 proliferative programs of seam cells (Fay and Wood, 1999), and the protein is present during L2 stage but not during L3. *Hbl-1* loss during L2 stage leads to loss of proliferative L2 seam cell program, and a decreased seam cell number in later stages. *Let-7s* mutants result in both increased seam number and *hbl-1::gfp* expression during L3 stage, interpreted as *let-7s* repressing *hbl-1* through binding and repressing its 3'UTR (Abbott et al., 2005; Li et al., 2005). To examine if *daf-12*, *let-7s* and *hbl-1* form a continuous regulatory cascade, changes in L2 program repression during L3 stage in *daf-12* signaling mutant backgrounds were looked at by monitoring seam cell numbers in later stages as an indicator for L2 stage program repetition. Expected was an increased HBL-1 expression during decreased *let-7* transcription, with a resulting increase in L2 program repetition and seam cell numbers. Consistent with this idea of NHR signaling promoting *hbl-1* inhibition, an increase in seam cell number was observed in *daf-12(rh61)* and *rh61rh411* mutants and in *daf-9;din-1* double mutants. *Daf-12(rh61)* exhibits a penetrant extra seam phenotype interpreted as a more severe failure to inhibit L2 programs during L3 stage than seen in *daf-12* null mutant background (Table 1). The seam cell phenotype was dependent on functional *hbl-1(+),* an observation that by genetic epistasis places *daf-12* upstream of *hbl-1*. Restoring *daf-12* transcriptional activation back to wild type level by ligand supplementation of *daf-9;din-1* double null mutants also reversed seam cell number back to wild type level.

Genotype	Seam Number	P-value
Wild type N2	12±0	na
daf-12(rh61rh411)	13±1.4	.00022
daf-9(dh6);din-1(dh149)	13±1.1	<.0001
daf-9;din-1 + DA	12±0	na
let-7s: mir-48 mir-241(nDf51); mir-84(n4037)	16±1.5	<.0001
daf-12(rh61)	22±1	<.0001
hbl-1RNAi	9±.7	<.0001
daf-12(rh61) hbl-1RNAi	10±1.3	<.0001

Table 1: Seam cell counts
Seam cells between posterior pharyngeal bulb and the anus were counted by DIC microscopy during the L3 stage. n≥20 animals, mean and SD are shown, P-values were calculated by T-test relative to wild type. (na, not applicable)

GFP-reporter fusions to *hbl-1*-UTR in *daf-12* signaling mutant background that was shown to decrease let-7s microRNA transcription (Esquela-Kerscher et al., 2005) were analyzed to show that these phenotypes are caused by *hbl-1*-UTR mediated repression. In this background, expression level of two different *gfp* reporter constructs were analyzed, that both contained the *hbl-1*-promoter: the *hbl-1p::gfp::unc-54*-UTR reporter contained the unrepressed *unc-54*-UTR and is insensitive towards *hbl-1*-UTR mediated repression so that it only reflects transcriptional activation. The *hbl-1p::gfp::hbl-1*-UTR construct contained the *hbl-1*-UTR and is subject to *bhl-1*-UTR mediated repression. This reporter therefore reflects transcriptional activation minus *hbl-1*-UTR mediated translational repression.

Comparison of these reporters shows changes in *hbl-1*-UTR mediated repression. When compared to wild type and *daf-12* signaling mutant background, expression of *hbl-1p::gfp::hbl-1*-UTR was up-regulated during L3 only in *daf-12(rh61)* background with decreased *let-7s* transcription, but not in wild type (Figure 18). Interestingly, the *hbl-1*-UTR reporter containing strain showed up-regulation in the ventral nerve cord in the *daf-12(rh61)* background, while the *unc-54*-UTR reporter containing strain showed strong body muscle up-regulation – pointing towards direct or indirect *daf-12* regulation of *hbl-1* in this tissue.

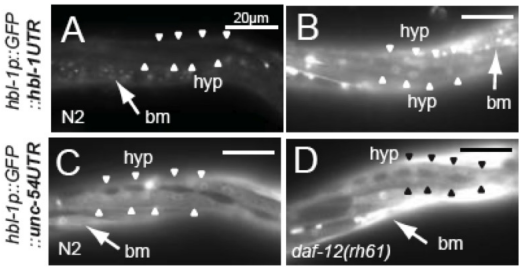

Figure 18: *Hbl-1* UTR reporter is regulated by *daf-12* signaling
A *gfp*-fusion to *hbl-1* promoter and UTR was repressed in the hypodermis at mid L3 (28 hours) in wild type (A). In the *daf-12*(*rh61*) mutants, reporter signal was up-regulated in the hypodermis (hyp) and other tissues (B) (exposure 250 ms). A *gfp*-fusion to the *hbl-1* promoter, containing the *unc-54*–UTR lacked substantial up-regulation in the hypodermis (C and D), although body muscles (bm) showed modest reporter up-regulation (D) (exposure time 50 ms). n>10 animals were observed and representative images are shown.

The observed up-regulation in the seam cells was interpreted as caused by reduced *hbl-1*-UTR-mediated repression due to decreased *let-7s* transcription. The observation of equal hypodermal expression levels of the construct without *hbl-1*-UTR in both wild type and *daf-12(rh61)* background verifies that the difference is caused by *hbl-1*-UTR mediated repression.

Discussion

2.2 Overview

In this work, I show that the nuclear hormone receptor DAF-12 directly regulates the *let-7* family members *mir-84* and *mir-241*. Direct regulation of a microRNA has not been shown so far for NHRs, only few TFs are known, e.g. *lin-12* and *lag-1* in *C. elegans* and *p53* in mammals, to directly regulate microRNA transcription (Chang et al., 2007; He et al., 2007; Raver-Shapira et al., 2007; Tarasov et al., 2007; Yoo and Greenwald, 2005).

Let-7s microRNAs mediate tissue specific programs of developmental progression and their absence leads to arrest or failure to progress in development. By showing direct DAF-12 and dafachronic acid mediated activation of these microRNAs, animal wide endocrine regulation of development was connected to the cell autonomous activity of microRNAs. These findings were interpret as a "molecular switch" explained further down and it was proposed that this "molecular switch" is a model for the regulation of stage transitions and how the combined function of DAF-12/NHR and its directly activated *let-7s* microRNAs is required (Figure 19).

But before talking about the molecular switch idea, I explain in more detail the integration of these hormone regulated microRNAs into signaling cascades. I begin this explanation by looking at the most upstream components of TGF-beta and insulin signaling that are expressed in sensory neurons. These components are regulated according to environmental input, and favorable environment increase, while unfavorable environment reduce signaling of both cascades that then activate the biosynthesis of dafachronic acids through transcriptional control over DAF-9 in the endocrine tissues XXX neurons and hypodermis (Gerisch and Antebi, 2004). Dafachronic acids activate the type II clear receptor DAF-12 that acts as a switch between two states: liganded DAF-12 activates transcription of its targets to cause developmental progression while unliganded DAF-12 represses them and causes developmental arrest/ dauer formation. The mechanism behind this process was analyzed in hypodermal seam cells, where a loss of *daf-12* activation during L3 stage leads to a failure to progress and a repetition of L2 programs. The same phenotype is observed in absence of the *let-7s* (Abbott et al., 2005), while the opposite phenotype is observed in absence of the *let-7s* repression target *hbl-1* (Abrahante et al., 2003). It was found that direct DAF-12 mediated transcriptional activation of the *let-7s* is necessary to suppress *hbl-1* during L3 to prevent L2 fates from reoccurring, and that loss of *daf-12* transcriptional activation leads to a failure to suppress L3 expression of *hbl-1* and a failure to progress (Figure 19). This connection integrates the cell autonomous acting *let-7s* into global insulin/TGF-beta signaling cascades, and spans regulation from animal wide to cell type specific program execution.

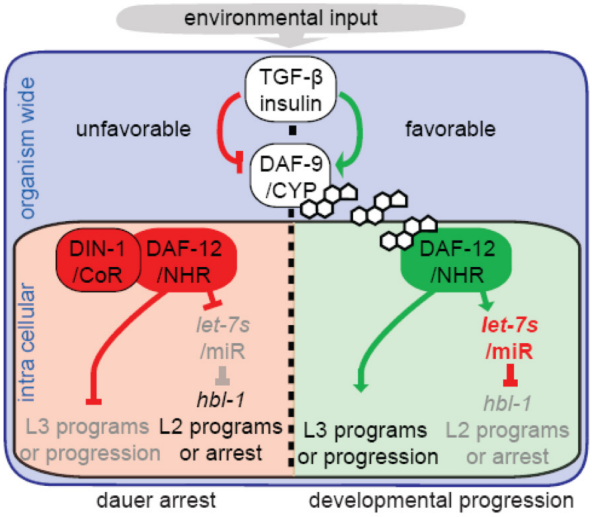

Figure 19: Model for NHR-microRNA signaling cascades
In response to favorable environmental signals, activated insulin/IGF and TGF-b pathways induce Δ^4-DA biosynthesis through DAF-9/CYP450. (Right) DAF-12 with the ligand activates L3 programs and expression of *let-7s* and thereby inhibits HBL-1 and genes of L2 programs, which result in developmental progression. (Left) During unfavorable conditions, DAF-12 without the ligand, together with DIN-1, repress L3 programs and *let-7s*, which allows de-repression of L2 programs or developmental arrest. Dauer signaling also has Δ^4-dafachronic acid–independent outputs onto microRNAs.

2.3 Transcription factor and microRNA act as a "molecular switch"

Within the regulatory context that was analyzed, NHR transcriptional activation prevents arrest, while the direct NHR mediated activation of microRNAs as "activated repression" of "old programs" drives developmental progression. These two functions could be interpreted as a combined "molecular switch" that mediates stage transitions or the discrimination between two stages in a single tissue. To see if this hormone regulated "molecular switch" function is involved in other important processes in other systems, the "molecular switch" hypothesis was tested by reviewing several similar cases from the literature. However, to date there are no NHRs described to directly activate microRNAs.

2.3.1 Mammalian p53 and the "molecular switch"

An important TF mediating the decision between continued development or cell cycle arrest, DNA repair, senescence or apoptosis is p53 (Zhao et al., 2000). After cell stresses like UV or ionizing irradiation, p53 is activated and induces cell cycle arrest, DNA repair, senescence or apoptosis. This is a vital protection mechanism, and absence or decrease of p53 function is

associated with 50% of all known cancers (Harris, 1996). p21 is an important transcriptional activation target of p53, and p21 deletion represses major aspects of p53 mediated cell stress responses (Waldman et al., 1995) but does not completely suppress p53 mediated growth arrest (Brugarolas et al., 1995), indicating that p21 redundant functions also are important for the p53 cell stress response. Recently, He (He et al., 2007) and others (Chang et al., 2007; Raver-Shapira et al., 2007; Tarasov et al., 2007) showed that p53 directly activates transcription of *mir-34a-c*. *mir-34* microRNAs repress genes that promote cell cycle progression - the opposing function to p53 - and *mir-34* transfection into cells leads to cell cycle inhibition and senescense. These observations can be interpreted as *miR-34s* silencing genes that oppose the effects of p21 by supporting the transition from cell cycle progression to arrest. In other words, *mir-34s* and p21 mediate similar functions to achieve p53 downstream effects. When looking at p53 and the *mir-34s* with the "molecular switch" hypothesis in mind, the above mentioned findings can be interpreted as p53 and *mir-34* forming a "molecular switch": p53 directly activates transcription of mRNAs for genes like p21 that promote a.o. cell cycle arrest, while it simultaneously activates *mir-34* microRNAs that repress translation of genes with opposite function, e.g. cell cycle progression. The conclude is that the "molecular switch" can be considered as being conserved in this system and that it indeed might be a paradigm for understanding not only hormone dependent developmental progression as in this case, but also the function of other TFs involved in fundamental processes such as tumor formation, stem cell differentiation or maturation in metazoans.

2.3.2 Consequences of the "molecular switch" idea

A general goal of the "molecular switch" idea is to understand the function of microRNAs that are directly activated by certain TF as the "activated repression" function of this TF, as p53 in the above example. As a consequence, the investigation of the function of a TF would at an early time point already involve experiments to identify directly activated microRNAs. This would facilitate the understanding of more integrated functions of the TFs in question, as it did in example shown in this chapter, where it was essential to identify the *let-7s* microRNAs as direct transcriptional targets and as an "activated repression" function of *daf-12* in order to make sense of the hypodermal heterochronic phenotypes of *daf-12*.

The application of the "molecular switch" idea may be especially important in understanding how progression of development is controlled. Progression from one developmental stage to the

next also involves actively terminating the previous stage to prevent overlap. When this switch involves a nuclear hormone receptor, this transition can be achieved by a single signal in the form of a hormone, acting on a type II nuclear receptor that changes from active repression in absence, to activating transcription in presence of the ligand. But also non-hormonally induced changes of the functional status of a TF can achieve the goal to mediate a transition from one program to different one, as the p53 example shows. The invariant cell lineage of *C. elegans* facilitated the discovery of this regulation principle, and it is likely to be less apparent in more complex animals whose cell lineages are more dynamically regulated and less well known.

2.4 NHR-signaling paradigms

DAF-12 signaling dependent regulation of the *mir-84* and *mir-241* promoters also validates nuclear hormone receptor signaling paradigms set up by several key publications over the last three decades (Mangelsdorf et al., 1995).

Abundance of the dafachronic acid ligands is ultimately regulated by a single, non-redundant gene, cytochrome p450 *daf-9* (Gerisch et al., 2001; Jia et al., 2002). The ligand products of this enzyme bind to the NHR DAF-12, a type II nuclear receptor that in the presence of its ligand activates transcription of its target genes (Motola et al., 2006) to allow progression through development (Antebi et al., 1998). *C. elegans* co-activators for DAF-12 have not been identified, but ligand bound DAF-12 can interact with mammalian co-activator SRC-1 (Motola et al., 2006). In the absence of ligand, DAF-12 interacts with co-repressor DIN-1 (Ludewig et al., 2004; Motola et al., 2006), an homolog of human co-repressor SHARP, to suppress transcriptional activation of its target genes. The importance of active activation and active repression is reflected in the severity of phenotypes of mutations affecting different components of this cascade: a null allele of *daf-12* leads to less severe phenotypes like increased seam cell divisions or loss of dauer formation, while an increase of DAF-12 interaction with DIN-1 causes constitutive target gene repression that leads to migration defects of the gonad, reduced bruit size or increased dauer formation. These phenotypes result from two different types of mutations, one type effecting the DAF-12 ligand binding domain e.g. *daf-12(rh61)* or *daf-12(rh273)* (Antebi et al., 2000), and the other limiting or abolishing the synthesis rate of DAF-12 ligand e.g. *daf-9(rh50)* or *daf-9(dh6)* (Gerisch and Antebi, 2004). Constitutive DAF-12 repression, in e.g. *daf-9(dh6)* null background, involves constitutive dauer formation, and can be completely suppressed by either additional loss of *din-1* function or ectopic hormone supplementation. The

daf-9;din-1 double null mutant exhibits in most parts phenotypes resembling *daf-12* null alleles in absence, and wild type phenotypes in presence of supplemented *daf-12* hormone. These hypotheses based on genetic epistasis experiments were validated by quantifying *gfp* reporter fusions to the *mir-241* and *mir-84* promoters in various *trans*-mutant backgrounds in Figure 12 and Figure 13, discussed in further detail below.

2.4.1 *Mir-241* promoter regulation

mir-241p::gfp reporter showed moderately reduced activation in several tissues in a *daf-12* null background, but no tissue lost all activation, indicating that *daf-12* is only one TF among others contributing to the overall transcriptional activation of this promoter. Loss of ligand production in the *daf-9(dh6)* null allele causes DAF-12 to interact with co-repressor DIN-1 to mediate unconditional, tight transcriptional repression of the *mir-241* promoter in nearly all tissues, with the exception of a few head neurons. This demonstrates that unliganded DAF-12 actively represses its target promoters throughout most of the worm body. The strong *daf-9* null phenotype is changed to the weak *daf-12* null phenotype in *daf-9(dh6);din-1(dh149)* double null mutant background since this genetic background is deficient for both, *daf-12* activation as well as repression. Activation was restored back to wild type levels by ligand supplementation of *daf-9(dh6)* and *daf-9(dh6);din-1(dh149)* mutant backgrounds, validating that *daf-9* is a non-redundant step in the dafachronic acid synthesis pathway.

DAF-12 regulates the *mir-241* promoter by interacting with a defined number of *cis*-regulatory elements present in the DNA sequence of the promoter, called response elements (Mangelsdorf and Evans, 1995). All DAF-12 mediated transcriptional control of the *mir-241* promoter passes through four response elements, and their deletion renders the promoter completely insensitive to mutations affecting *daf-12* signaling, like *daf-9* null and *daf-9;din-1* double null background with or without ligand supplementation. The epistatic relation of these factors is shown in the model in Figure 19.

2.4.2 *Mir-84* regulation and dafachronic acid independent activation

Pharyngeal expression of the *mir-84p::gfp* reporter was regulated in a similar way as the *mir-241* promoter, but seam cell expression was completely lost in *daf-12* null. Seam cell expression was also lost *in daf-9;din-1* double nulls, but restored to wild type levels by ligand addition, and surprisingly increased in *daf-9(dh6)*, *daf-2(e1368)* and *daf-7(e1372)* constitutive dauer mutants or *daf-2(e1368)* and *daf-7(e1372)* mutants growing at permissive temperature as non-arrested

worms. Ligand supplementation was able to suppress up-regulation of seam cell expression in *daf-7*, but not *daf-2* background. This indicates a *daf-12* ligand independent promoter activation following distinct mechanisms for TGF-beta or insulin cascades.

One possible explanation is DAF-12 hetero dimerization with alternative NHRs as (Forman et al., 1995) described for mammalian RXR with VDT, TR, PPAR delta, that - when hetero dimerized - render the receptor dimer insensitive to the RXR ligand, but responsive to the ligand of the hetero dimerization partner. This effect relied on interaction between ligand binding domains, independent of the DNA binding capacity of the second dimerization partner. Given that the *C. elegans* genome contains 284 genes coding for NHRs (Antebi, 2006), the possibilities are vast and might not even rely on actual presence of a second ligand, since many NHRs are suspected to be orphan receptors. This observation poses an interesting opportunity to further study general NHR signaling functions and their intercalation with insulin and TGF-beta cascades. To our knowledge, no other experimental system integrates all these functions into a single, *in vivo* model with as drastic outcomes as the ones observed here.

An alternative explanation is that other transcription factors act in these genetic backgrounds. Dependence on DAF-12 *trans*-regulatory action is supported if the increased seam cell GFP expression in these backgrounds is suppressed by loss of DAF-12. This *trans*-regulatory influence of DAF-12 or other factors binding to DAF-12-REs can be tested by using a *gfp* reporter fused to a *mir-84* promoter that has both DAF-12-REs point mutated, as seen in Figure 9 B. One candidate for an alternative TF activating promoter of the *let-7s* family is notch-receptor *lin-12*, described in the following paragraph.

2.4.3 *Lin-12*/notch receptor in hypodermal differentiation

Despite its best described function during vulva development (see below), a recent publication connects *lin-12* also to seam cell differentiation (Solomon et al., 2008). *Lin-12* gain-of-function mutants exhibit molting phenotypes during all molts, and seam cells precociously underwent terminal differentiation not after the L4 stage but already after the L3 stage. *Lin-12* gain-of-function mutations also show enhanced *let-7* transcription which might explain the precocious phenotype, since *let-7* is required for terminal differentiation in the hypodermis and loss of *let-7* results in delayed phenotypes in vulva and hypodermis. How the increased *let-7* levels affect *daf-12* signaling requires further investigation since *daf-12* and *let-7* interaction is complex, as discussed in the following section.

2.5 Feedforward and feedback loops

While DAF-12 transcriptionally activates *let-7* family members (Bethke et al., 2009) and temporally regulates *let-7* itself (Johnson et al., 2003), several lines of experiments also showed that DAF-12 itself is a repression target of *let-7* during later stages. Current bioinformatic prediction algorithms indicate the presence of *let-7* seed-regions inside the *daf-12*-UTR (e.g. http://pictar.mdc-berlin.de/ or http://microrna.sanger.ac.uk). Experimental investigation showed that phenotypes caused by loss of *let-7* activity are suppressed in *daf-12* null mutant background, placing *daf-12* downstream of *let-7* (Grosshans et al., 2005). These observations suggest that *daf-12* and the *let-7* family microRNAs are involved in both, feedback- and forward loops, to drive stage transitions.

To date, many microRNAs are described to be involved in feedback inhibition, and to better understand the *daf-12* involvement into these regulatory loops, I will shortly discuss several cases of microRNAs feedback and – forward loops that mostly involve either hormone signaling or heterochronic regulation.

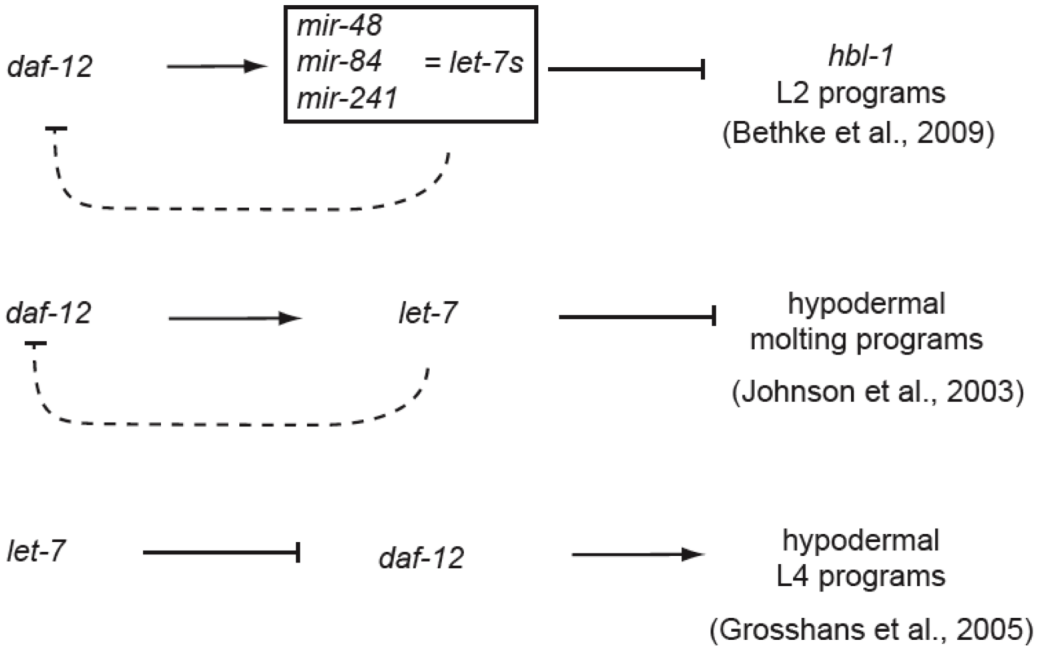

Figure 20: Models of regulatory loops
In this work it was shown that DAF-12 directly activates the *let-7s*, while Johnson et al (2003) showed *let-7* transcriptional regulation by DAF-12, and Grosshans et al (2005) showed experiments that suggest DAF-12 to be downstream of *let-7*. The dashed lines symbolize possible *let-7* suppression of DAF-12 through *let-7* binding sites in the DAF-12 UTR.

2.5.1 *Lin-12* activates *mir-61* to form a feedback loop

During vulva formation, *lin-12*/notch is directly activating *mir-61*/microRNA in vulva precursor cells (VPCs) while they are induced to follow three different cell fates during vulva formation (Yoo and Greenwald, 2005). One central cell, the p6 cell, follows primary vulva cell fates, while the two adjacent p5 and p7 cells follow secondary vulva cell fates, all three cells giving rise to cells forming the vulva, while p3, p4 and p8 cells follow tertiary cell fate to fuse into the hypodermal syncytium. EGFR-Ras-MAPK signals onto vulva precursor cells p5, p6, p7 with highest intensities in p6 promoting primary vulva cell fates, while *lin-12*/notch is up-regulated in p5 and p7 to promote secondary cell fates. One direct target of *lin-12*/notch is *mir-61*, a microRNA that represses the negative regulator of *lin-12*/notch, *vav-1*. This cascade acts as a feedback loop to enhance *lin-12* signaling once it reaches a certain threshold. However, this feedback loop has only a dispensable function during vulva formation, since for example loss of negative regulator *vav-1* does not prevent proper vulva formation.

Applying the "molecular switch" idea, *lin-12* can be interpreted as the TF that initiates the transition from "precursor" to "differentiation" programs in the VPCs, namely secondary vulva precursor cell fates. *Vav-1* belongs to the program that suppresses secondary vulva precursor cell fate formation and therefore is target of the "activated repression" mediated by *lin-12* activated *mir-61*. At the same time as repressing *vav-1*, *lin-12* mediates direct activation of protein coding genes that are already part of the vulva differentiation programs, as LIN-11/homeodomain transcription factor (Marri and Gupta, 2009). As a summary, *lin-12* activates the repression of *vav-1* that opposes differentiation, while directly activation *lin-11* that contributes to differentiation.

2.5.2 Neuronal differentiation in *C. elegans* and feedback

A second example of a non-hormonal loop involving TFs and microRNAs is the double negative feed back loop described by (Johnston et al., 2005) that regulates bilateral cell fate decision of two gustatory neurons, ASE left and ASE right, during *C. elegans* development. This feedback loop involves two pairs of TF/microRNA combinations, with the microRNA being a direct activation target of the TF. Each pair defines one of two possible cell fates in a pair of gustatory neurons. The downstream microRNA of one pair suppresses the upstream TF of the other pair. To define a choice between the two possible states, outside influence enhances one TF to unbalance the loop and to increase expression of the regulated microRNA that in turn

represses the other TF of the alternative fate choice. This repression leads to a loss of repressing microRNA counteracting the primarily enhanced TF, and the system reaches a stable output.

2.5.3 EcR and feedback

An example for a feeback loop involving hormone signaling involves the Ecdysone receptor (EcR) that is feedback inhibited by *mir-14*. Deletion of *mir-14* leads to several phenotypes, a.o. increased adult survival and an increase of EcR expression levels. A genetic decrease of EcR dose in an EcR +/- background suppresses the adult survival of a *mir-14* null background (Varghese and Cohen, 2007). The authors interpreted this as a lack of *mir-14* mediated EcR repression causing an over expression that ultimately leads to the observed phenotype. However, the majority of *mir-14* deletion phenotypes remained unaffected by decreasing EcR levels. Unfortunately, it was not investigated if 20-OH-Ec mediated repression of *mir-14* activation is a direct effect of EcR and its ligand ecdyson, or if other intermediate regulators are necessary.

2.5.4 C/EBP alpha and NFI-A and feedback

Another example for hormonal induction of a microRNAs involving a feedback loop has been described in mammals. It involves the interplay of retinoic acid, C/EBP alpha, NIF-A and *mir-223* in "acute promyelocytic leukemia" (APL) (Fazi et al., 2005). In APL cell lines, blood cells are arrested during their development into different blood cell lineages, but a high dose of retinoic acid overcomes this block and induces developmental progression and terminal differentiation, involving expression of several microRNAs, among others *mir-223*. The factor NFI-A binds to a response element in the *mir-223* promoter and transcriptionally activates it to generate a constant baseline expression level, while at the same time, NFI-A also is a repression target of *mir-223*, and these two components form a negative feedback loop. Retinoic acid application up-regulates C/EBP-alpha which then binds to response elements in the *mir-223* promoter that overlap the REs of NFI-A, which is displaced from the promoter, while increasing *mir-223* expression at the same time increases repression of NFI-A. This is an example of an indirect hormone induction of microRNA up-regulation that drives development and differentiation, including a feedback inhibition loop involving TFs driving transcription of microRNAs that at the same time repress those TFs.

The literature shows examples of feedback loops that, involving TFs and miRs, regulate temporal coordination of stage transitions in one cell type (e.g. *mir-223* in mammalian blood cell lineage), or amplify regulatory input that drives the decision towards one of two possible fates

(e.g. neuronal or vulva cell fates in *C. elegans*). Direct hormonal involvement into microRNA feedback loop regulated differentiation processes has been shown in this work for *C. elegans* hypodermal cells, but not yet for the mammalian blood cell lineage differentiation. The results from the *C. elegans* model in this Chapter 2 might point the way for mammalian research on this area.

Outlook

2.6 Cell non-autonomy of microRNAs

The observed spatial separation of *mir-84* regulation and HBL-1 translational repression is most likely caused by either of three possibilities:

a) cell non-autonomous microRNA function

b) low level HBL-1 expression and repression in the seam cells

c) low level HBL-1 regulation in the hypodermal syncytium and signaling into seam cells

In order to test hypothesis a) of cell non-autonomous microRNAs activity, it is necessary to identify the mode of microRNA transportation between cells. The hypothesis is supported if inactivation of this transport mechanism leads to *let-7s* loss-of-function phenotypes in the seam cells while maintaining wild type like microRNA expression levels. In recent literature, two different transport mechanisms for small RNAs have been described, assuming that microRNA procession takes place inside the transcribing cell and not the target cell.

One cell-to-cell transport mechanism for small RNA molecules has been described in context of global RNAi effects in *C. elegans* that require the function of *sid-1* and *sid-2* proteins involved in uptake of small double stranded RNA molecules into cells (Winston et al., 2002; Winston et al., 2007). For these genes to be involved in the cell non-autonomous microRNA effect, the seam cell expressed microRNA would be required to get excreted and taken up by the hypodermis via a *sid*-protein based mechanism. However, *sid*-protein independent effects were also observed, and no genes have been assigned to these alternative functions.

A second cell-to-cell transport mechanism for small RNA molecules is hinted by the observation that endosomes or microvesicles described for mammalian cell culture contained not only protein coding mRNA, but also microRNAs (Valadi et al., 2007; Yuan et al., 2009).

Differences in RNA content between the vesicles and the cell they originate from suggests that regulated deposition of RNAs into the budding vesicles occurs.

An alternative approach for testing hypothesis a) is to do *in situ* hybridization for mature and precursor "pri-miRNAs" in seam cells and hypodermis tissue at the L3 stage. The hypothesis would be supported if mature microRNAs are detected in hypodermal syncytium and seam cells, while premature microRNAs are only detected in the seam cells. This can be further tested by knocking out the transport mediating genes and detecting mature microRNAs only in the same tissue as the pri-miRNAs. Those findings would be the first proof of microRNA function requiring directed microRNA transportation across cell membranes.

2.7 Ligand independent activation of DAF-12 / *mir-84* promoter

The observed *mir-84* reporter activation in a *daf-12* ligand less background might be caused by ligand independent activation of DAF-12, or by alternative transcription factors like LIN-12/LAG-1.

DAF-12 *trans*-dependence can be tested by observing *mir-84* seam cell expression of *daf-7*, *daf-2* or *daf-9(dh6)* alleles in *daf-12(rh61rh411)* background: loss of ligand less activation in *daf-12* null background strongly indicates *daf-12* dependence. *Cis*-dependence on *daf-12* response elements in the *mir-84* promoter can be tested by observing a *mir-84p::gfp* reporter with all *daf-12* REs point mutated and crossed into the above mentioned genetic backgrounds. Remaining seam cell GFP expression in *daf-12* null background of wild type promoter reporter, but loss in mutant promoter reporter would argue for non-DAF-12 TF mediating the initially observed, ligand independent activation.

2.7.1 Alternative transcription factors: *lin-12*

Independent of DAF-12 dependence for the ligand-independent activation, *mir-84* reporter activation in *lin-12* gain- and loss-of-function mutant background needs to be established.

lin-12 gf activates *let-7* precociously (Solomon et al., 2008), but *mir-84* has partly redundant function with *let-7* for terminal differentiation in the hypodermis (Hayes et al., 2006), and *mir-84* might also be subject to *lin-12* dependent activation. The influence of *lin-12* onto *mir-84* promoter regulation will be investigated in further detail in Chapter 3.12, while a possible connection of *mir-84* and *let-7* mediated terminal differentiation will be investigated in Chapter 4

.

2.8 Feedback regulation by *let-7*

Epistasis places *daf-12* upstream and downstream of *let-7* family microRNAs, of which some are transcriptionally regulated by *daf-12*, making *daf-12* in combination with its target microRNAs a candidate for feedback repression.

Feedback repression of *daf-12* directly involving microRNA activity will modify *daf-12* translation independently of transcriptional activation of the *daf-12* promoter. Analysis of these parameters would require measurement of translation independent of transcription. Due to the tight control of spatial expression of *let-7* family microRNAs, tissue specific measurement would help identify involved, partially redundant microRNAs. A technique to achieve this is tested in Appendix 3. The described reporter for translational repression needs to lose feedback-repression in deletion background of either the involved microRNAs, or *daf-12* null background.

The biological function of the *daf-12* feedback control can be revealed by looking at what phenotypes loss-of-feedback regulation has. This can be done by successively mutating *let-7* binding sites in the *daf-12*-UTR of a *gfp* reporter construct, and testing it for an increase in expression in response to let-7 site mutations. Additionally, a construct containing the *daf-12* genomic region instead of a *gfp* can be tested for *in vivo* phenotypes caused by *let-7* site mutations and the resulting DAF-12 upregulation. Expected phenotypes include abnormal seam cell division, dauer formation or precocious terminal differentiation of the hypodermis – see Chapter 4 .

3. Daf-12 activation of *cis*-regulatory elements in microRNA promoters

Introduction

Chapter 2 showed how the nuclear hormone receptor DAF-12 directly activates microRNAs of the *let-7* family. Through this connection, global nuclear hormone receptor signaling exerts temporal and cell type specific control of microRNA gene activation. However, the observed dependence of microRNA promoter activation upon *daf-12* signaling was limited in many tissues, with most of the activation during developmental progression depending on non-DAF-12 TFs. In addition to that, some of the observed regulation dynamics contradicts the current model of dafachronic acid dependent activation of DAF-12 target genes. These observations prompted a more detailed investigation of the mechanisms of microRNA promoter activation by *daf-12* signaling and by alternative cascades or transcription factors.

Previous research has shown how the transcriptional activation of a gene is regulated by *trans*-regulatory modules ("TRM") i.e. the transcription factors (TF) and co-regulators that bind to *cis*-regulatory modules ("CRM") i.e. TF binding sites within the promoter region of the regulated gene (Davidson, 2006). In this chapter, specific CRMs were tested for activation by DAF-12 or non-DAF-12 TFs. This was done by using a new technique to isolate single CRMs out of the full length promoter, while enhancing their individual transcriptional activation of *in vivo* reporter assays. Each of the isolated CRMs was tested for transcriptional activation in genetic backgrounds of mutants either for *daf-12* signaling or alternative TFs candidate for *daf-12* signaling interaction. The aim was to identify tissues with high and low dependence on *daf-12* and hormone dependent regulation. A tissue with high *daf-12* signaling dependence is a candidate for showing phenotypes that connect *daf-12* signaling and the microRNAs to biological functions. Identification of non-DAF-12 TFs regulating microRNA transcription was expected to link their upstream cascade to the downstream acting microRNA promoters and functions and was hoped to reveal how these cascades intersect with *daf-12* mediated hormonal regulation.

The following section of the introduction reviews several key publications for the theory of promoter regulation in *C. elegans,* with several examples of *trans*- and *cis*- regulatory modules and their function as well as recently described factors involved in *let-7* family promoter regulation. This is done in order to build the background for a detailed analysis of DAF-12 and

hormone dependent and independent regulation of *cis*-regulatory modules present in promoters of *let-7* family microRNAs.

The result section discusses possible new sequences for DAF-12 CRMs and presents experimental data of reporter activation by the CRMs from Chapter 2 after they were isolated out of full length promoter context. A candidate DAF-12 CRM from the *let-7* promoter was investigated in the same way, and reporters for all isolated CRMs were tested in various genetic backgrounds, including new candidate *daf-12* interacting.

3.1 Promoter regulation studied in *C. elegans*

C. elegans as a model organism offers several advantages for the study of transcriptional regulation. One important advantage is that the natural expression pattern of most *C. elegans* genes is sufficiently recapitulated by small promoter regions: Null mutants of most genes are rescued by re-introduction of a wild type copy that requires only 2kb of upstream promoter sequence to rescue the null allele (Okkema and Krause, 2005). Further more, stable trans-formation of reporter constructs into *C. elegans* by germline DNA injection is a fast and reliable process that requires less than two weeks to obtain strains that stably transmit the injected DNA as an extra chromosomal array (Fire, 1986). In addition to this, the *C. elegans* genome is simple and most functions are executed by non-redundant genes (Wood, 1988), so that the activation of a promoter in a specific tissue often relies on a single TF, and null mutant background for this TF causes a complete loss of activation (Flames and Hobert, 2009). Below I review some of the literature on transcriptional regulation in *C. elegans*.

3.2 Initial studies of the *myo-2* promoter

Initial research on the mechanisms of promoter activation was done on the myosin heavy chain gene *myo-2* that has yielded many important insights of which several will be mentioned here. The *myo-2* promoter studies revealed that tanscriptional activation in a specific tissue nis caused by defined, few hundred base pair long sequence elements in a promoter, and that several genes expressed in the same tissue share these elements in their promoters (Okkema et al., 1993). A combination of multiple, different CRMs, each bound and activated by a different TF, defines the "full length" expression profile of a promoter, and isolated fragments containing only a subset of CRMs activate expression only in a subset of tissues. In particular, enhancer elements smaller than 200bp were discovered that were able to direct transcription activation to the

downstream transcription start site on their own. By various *in vitro* binding experiments, *ceh-22*/homeobox domain protein (Okkema and Fire, 1994), TGF-beta signaling component *daf-3*/co-smad (Patterson et al., 1997; Thatcher et al., 1999) and *pha-4*/forkhead factor (Kalb et al., 1998) were identified as proteins binding and contributing to regulation of defined enhancer elements present within a 127bp stretch of the *myo-2* promoter, called C183. It is important to notice that each factor is bound to its own individual CRM, the short sequence of DNA its DNA binding domain recognizes, and that the C183 contained multiple, seperated CRMs, each being bound by a different factors. *In vivo* regulatory interaction of those factors with the C183 element were validated for all three factors. A bioinformatic approach further revealed DAF-12 to bind and regulate elements in the *myo-2* as well as the *ceh-22* promoter (Ao et al., 2004). Interestingly, the identified *daf-12* dependent *cis*-regulatory element, (CACACA) is different from the DAF-12-RE defined by Shostak (Shostak et al., 2004), (AGTGCA), the one used in this work. Deletion of this binding site decreased both, pharyngeal activation during normal growth conditions, as well as repression during dauer stage or in mutant backgrounds that set *daf-12* signaling to repression rather then activation. Research like this revealed the combinatorial nature of specific promoter regions or CRMs and gave rise to the idea of the "gene battery".

3.3 The “gene battery” define the tissue characteristics

The character and properties of a terminally differentiated tissue are defined by the genes expressed in it, collectively described as a "gene battery" (Davidson, 2006). Promoters of genes belonging to this gene battery can share the same CRMs. Application of current laboratory techniques like microarrays and cell sorting techniques have helped to first identify the set of genes expressed in a specific tissue. Analysis of the promoter regions of these genes led to the identification of *cis*-regulatory promoter elements that are required for this tissue specific expression. These CRMs are not only conserved between genes of the same gene battery, but also between species as different as yeast and mammals. Of importance for this study is that the presence and function of a CRM contributes the gene to a gene battery, and subsequently to a biological function. The importance of this is reflected in two key publications involving *daf-19*/x-box binding factor and *pha-4*/forkhead factor.

3.3.1 DAF-19/x-box binding factor defines ciliated neurons

RFX-type transcription factors are highly conserved and involved in processes as distinct as DNA damage checkpoint regulation in yeast or MHC class II gene regulation in humans. They share a characteristic DNA binding domain distinct from other described DBDs that recognizes sequences called "x-box", which are as well highly conserved. The *C. elegans* genome codes for one x-box binding factor, called "*daf-19*" due to its constitutive dauer forming phenotype. However, *daf-19* was initially discovered during a screen for mutations that affect dye-filling, a characteristic of ciliated sensory neurons in *C. elegans* (Perkins et al., 1986) that make up 60 out of a total of 302 hermaphrodite neurons. Loss of function mutants of *daf-19* cause a failure to form these cilia while other aspects of neuron morphology seem little unaffected, making *daf-19* the key factor for the induction of cilia formation (Swoboda et al., 2000). The sequence of the DNA recognition motif of human RFX factors was described (Emery et al., 1996; Reith et al., 1994), with very similar motifs present in promoters of known ciliated neuron expressed factors of *C. elegans,* leading to the identification of a consensus DAF-19-CRM. Reporter constructs containing a DAF-19-CRM were expressed in ciliated neurons, and expression was lost either by point mutating the DAF-19-CRM in the reporter or by crossing the wild type sequence reporter into *daf-19* null allele background. In an attempt to define a ciliary transcriptome, genome wide searches for genes bearing this consensus CRM in their promoter led to the discovery of many more candidate cilia related genes with a high percentage of experimentally validated positives (Blacque et al., 2005).

These observations underline the potency of a single factor that binds to well defined consensus DNA motifs spanning only few base pairs. These consensus CRMs then activate their target genes that define a precise morphological feature of their cell, in this case cilia formation. However, individual characteristics of variations of a consensus CRM can also have functional consequences, as was shown by the differences in function of variant forms of the CRM of the forkhead factor *pha-4*.

3.3.2 PHA-4/forkhead factor defines a specific organ

The *C. elegans* forkhead transcription factor PHA-4 is a homolog of human FoxA and acts as an organ identity gene defining the pharynx and the foregut. The precursor cells that during embryogenesis in wild type give raise to pharynx/forget cell lines fail to do so in loss of function alleles, while over expression of PHA-4 leads to an excess of pharyngeal/foregut cells (Horner et

al., 1998). The PHA-4 response element was defined with help of the homology to human FoxA response elements and was identified in nearly all members of the pharynx and foregut defining gene battery (Gaudet et al., 2004; Kalb et al., 1998). Pharyngeal expression of PHA-4 begins during early embryogenesis and lasts until late larval stages, a time span reaching from initial cell fate decisions to post embryogenic development. This long lasting presence of PHA-4 raises the question if all target genes of *pha-4* are activated evenly during this time span or if gene battery members are regulated differentially and if this is still achieved through the PHA-4-CRM. The answer to this question came from analysis of promoters of the pharynx/foregut gene battery that revealed the presence of different variations of PHA-4-CRMs. These variations differed in PHA-4 binding affinity, with high affinity sites driving early expression and low affinity sites driving late activation (Gaudet et al., 2004). This way it is possible that different CRMs are activated by the same upstream factor and connect their promoter to the same upstream cascade, but can still maintain individual features that distinguishes their function from other CRMs for the same *trans*-acting factor, in this case differing in temporal onset of expression.

3.3.3 TTX-3 and CEH-10 homeodomain factors define gustatory neurons

Fragmentation of a single promoter can be reveal a CRM that activates expression in a specific tissue of interest. A bioinformatic search looking for genes that harbor this specific CRM in their promoter reveal other members of the gene battery that contribute to the characteristics of this tissue of interest, an approach more sensitive then forward genetics. Wenick and Hobert (Wenick and Hobert, 2004) used this approach in their work on the gene battery defining the gustatory AIY neuron in *C. elegans*, and the corresponding CRMs that were activated by the homedomain proteins *ttx-3* and *ceh-10*. During this study, the authors again showed that the architecture of promoters is highly modular, and that separate CRMs each activate transcription in a single type of cell or tissue. They also validated that within a promoter, separate CRMs behave in an additive manner to yield the spatial and temporal expression profile seen for the full length promoter. General observations were that the identified CRMs usually did not have repressive function. Nor did promoter truncations lead to expression in other tissue types than the full length promoter. A third observation was that most CRMs behaved in an enhancer like manner in that the orientation or distance to the transcription start site varied.

3.4 Repeat generation of defined promoter regions

This introduction chapter explained so far that CRMs connect promoters to upstream signaling cascades (3.2) and that genes required to define the characteristics of a tissue or an organs are grouped into a "gene battery" with all members of this gene battery having the same CRMs (3.3) in their promoters. One factor can be sufficient to drive a specific gene battery to define morphological features of a tissue or a whole organ (3.3.1). But despite the sequence similarities of a consensus CRM for a specific *trans*-factor, individual CRMs still have individual function (3.3.2). Single CRMs only partially recapitulate the expression pattern of a full length promoter, while each additional CRM for the same *trans*-factor increases the intensity of the promoter activation (3.3.3). A consensus CRM for DAF-12 was discussed in Chapter 2 , but *daf-12* signaling alone does not define a specific tissue or organ, but rather influences activation of many gene batteries according to animal wide dafachronic acid signaling activity and developmental fate choices.

This DAF-12 and dafachronic acid dependence of DAF-12-CRMs is one of the two main topics of this chapter. The other point of interest is to find other TFs and signaling cascades that connect to either DAF-12-CRMs or CRMs in close proximity.

To address the first topic, genomic promoter regions were isolated to *in vivo* investigate the transcriptional activation DAF-12-CRMs in context of their direct adjacent sequences and CRMs.

The second topic is investigated by crossing reporters for these isolated CRMs into mutant backgrounds of signaling cascades that are candidate to functionally interact with DAF-12 signaling. The hope is to connect the microRNAs to new cascades via those new *trans*- or *cis*-connections.

Since Chapter 2 shows that DAF-12 influence on the investigated promoters is limited, a low transcriptional activation of an isolated DAF-12-CRM alone is expected that requires an enhancement of this transcriptional activation. Previous observations (Wenick and Hobert, 2004) showed an additive effect of CRMs onto overall promoter activation, indicating that generation of multiple tandem repeats of short promoter fragment covering the CRM of interest could already lead to an increase in signal output of a one specific CRM in its genomic sequence environment.

In order to generate two-, four- or six-fold repeats of any genomic sequence in a time efficient way, a PCR technique was established that rapidly generates repeats from genomic DNA templates arranged in identical orientation. Those PCR-generated repeats were placed upstream of a *pes-10* minimal promoter (Fire et al., 1990) that provides a transcription start site able to recruit the basal transcription apparatus, followed by a *yfp* coding region.

3.5 Transcription factors influencing expression of *let-7* family microRNAs

In the this part of the introduction I will introduce the promoter characteristics to be investigated in this chapter, and TFs that are candidates for daf-12 signaling interaction on the let-7 microRNA family promoters.

With the importance and function of CRMs in mind, it becomes clear that the interaction of *trans*-acting factors (TFs) with CRMs of the *let-7s* microRNA promoters will show how *daf-12* dependent and independent upstream signaling converges onto the *let-7s* microRNAs. Several of these DAF-12-independent *trans*-acting factors and CRMs for the *let-7* family promoters have already been described and will be discussed further below.

3.5.1 Tissue specifity of *mir-84* promoter regulation

In Chapter 2.4.2, *mir-84* promoter reporter regulation in seam cells and pharynx was discussed and how the regulation in the seam cells, but not the pharynx, contradicts the current idea of ligand dependent DAF-12 activation. This chapter describes experiments that try to find if the unexpected seam cell regulation originates from a distinct *cis*-regulatory module than the one responsible for the pharyngeal regulation, and if DAF-12 or non-DAF-12 TFs act through those CRMs or CRMs in their direct proximity.

3.5.2 *Daf-12* independent activation of the *mir-241* promoter

Chapter 2.1.2.1 showed that a reporter with the *mir-241* promoter fused to *gfp* continues to be expressed in many tissues like neurons, body muscle, excretory cells even in absence of *daf-12* signaling. The remaining "background" activation was interpreted as not DAF-12 dependent, indicating that non-DAF-12-TFs can activate CRMs in the *mir-241* promoter region. To test if these CRMs are the same or different from DAF-12-like CRMs, DAF-12-like CRMs were isolated from the remaining promoter sequence to either separate background and *daf-12* dependent activation or to reavel if these isolated CRMs respond to both *daf-12* dependent and independent activation.

3.5.3 DAF-12 influence on the *let-7* promoter

Several experiments discussed in Chapter 2.5 indicate that DAF-12 acts upstream as well as downstream of *let-7*, and might be part of a feedback regulation loop involving *let-7*. This ambiguity could be solved by showing that DAF-12 is capable of directly regulating CRMs of the *let-7* promoter.

3.5.4 FLYWCH transcription factors regulate microRNA promoters

Ow and Ambros (Ow et al., 2008) identified by yeast-one-hybrid assays three FLYWCH zinc finger protein like TFs that bind promoters of microRNAs *lin-4*, *mir-48* and *mir-241*. Simultaneous knock-out of multiple FLYWCH TFs lead to precocious expression of microRNA repression targets, e.g. *lin-14*, but also embryonic lethality. To find heterochonic phenotypes further downstream in the pathway, the authors monitored seam cell proliferation and expression level of specific collagen genes that mark the adult stage. However, they were unable to record FLYWCH gene dependent heterochronic phenotypes. This indicates that the FLYWCH TF regulation of the *let-7s* microRNAs does not play an essential role in miR target regulation.

The identified FLYWCH CRMs are located in close proximity to DAF-12 regulated CRMs described in Chapter 2 , indicating a possible functional interaction with *daf-12* signaling. This was the reason to test RNAi knock-out of *flywch* genes in *daf-12* signaling background for synthetic phenotypes.

3.5.5 *Daf-12*/nhr regulates microRNA promoters

Regulatory influence of DAF-12 on promoters of the *let-7* microRNA family was already discussed in Chapter 2.5.

3.5.6 *Lin-12*/notch regulates microRNA promoters

Regulatory influence of *lin-12* on promoters of the *let-7* microRNA family was already discussed in Chapter 2.5.1.

Results

3.6 DAF-12 dependent *cis*-regulatory elements

The first canonical DAF-12 RE (referred to as “Shostak-RE”) sequence was defined by Shostak et al through *in vitro* DNA affinity assays of an immobilized DAF-12 DNA binding domain (Shostak et al., 2004). The authors showed *in vivo* DAF-12 dependent activation of promoters containing this RE and I was able to verify the function of these Shostak-REs in

Chapter 2 . However, the REs present in the tested microRNA promoters differed from the conserved core of the Shostak-RE. This resulted in a changed canonical RE that I from now on refer to as "DAF-12-like CRM" (Figure 21), which I try to detect and analyze in the promoters of members of the *let-7* family of microRNAs.

After discussing the results of previously analysed protein coding genes, and before presenting the results from my work on microRNA promoters, I will shortly discuss the reason for choosing specific promoters to analyse, namely promoters of *mir-84, mir-241* and *let-7*.

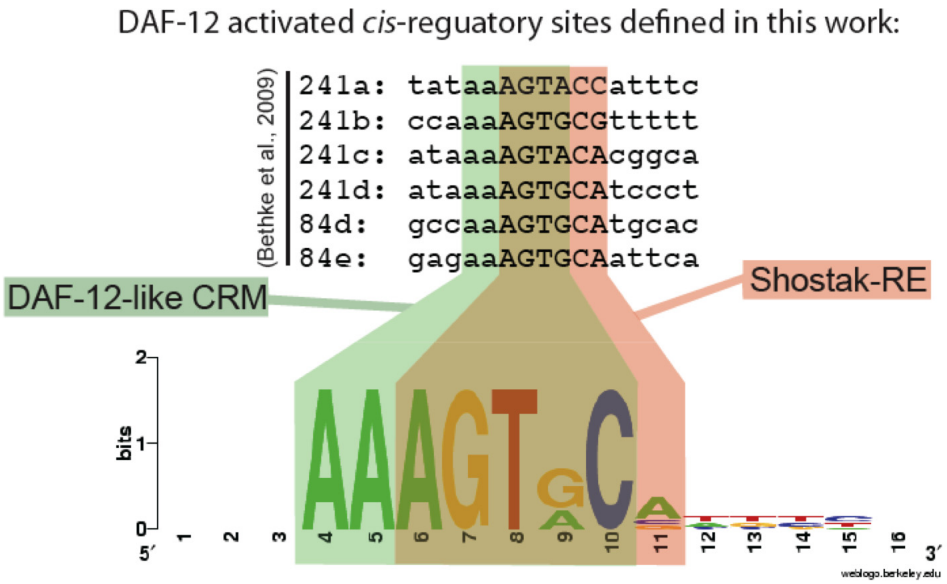

Figure 21: DAF-12-like CRM
Validated DAF-12 response elements from Chapter 2 were combined using the "Weblogo" tool to give the canonical sequence of the DAF-12-like *cis*-regulatory module. The previously published Shostak-sequence (Shostak et al., 2004) is overlayed in red, while the DAF-12-like CRM resulting from this study (Bethke et al., 2009) is overlayed in green.

3.7 Repeat generating PCR strategy

Promoter stretches between 100 and 150bp length surrounding DAF-12-like CRMs were isolated out of the promoters of *mir-84*, *mir-241* and *let-7* and converted to multiple repeats to enhance signal intensity. For this repeat generation via PCR, a novel method was used based on primers that contain the 5' and 3'tag DNA sequence juxtaposed. Inclusion of this tag renders the PCR product capable of self-priming after completion of the first round for amplification of the genomic DNA template to generate repeats of the desired length (Figure 22).

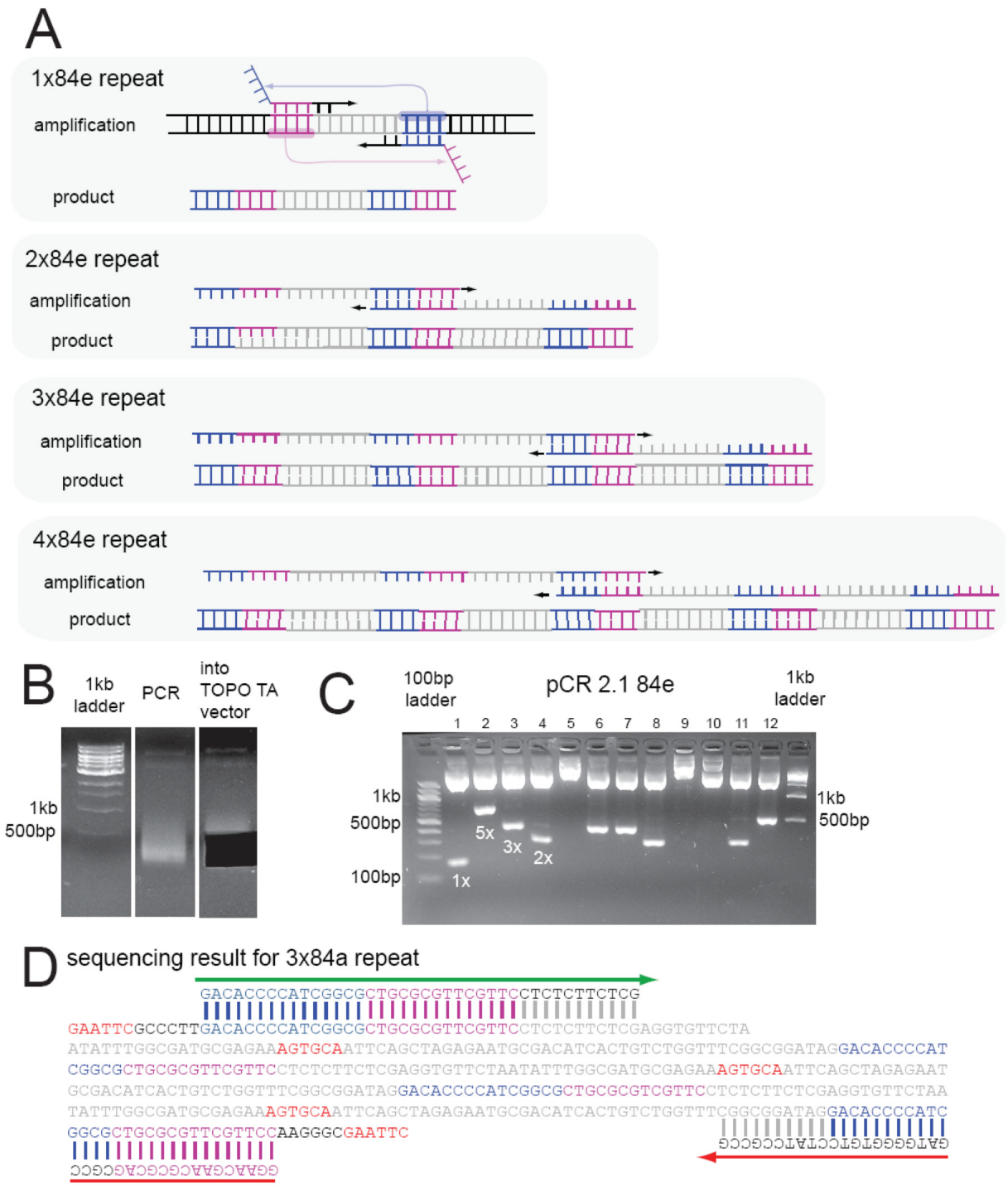

Figure 22: Repeat-generation PCR scheme

Colorcoded regions show homolog sequences independent of their orientation. Primers bind to the template DNA and define the content and the length of the repeated promoter fragment. 5' tags of the primers were chosen to bind to the sequence at the opposite end of the targeted promoter fragment, allowing the initial PCR product to self-prime and generate repeats with a defined orientation (A). PCR product was separated by agarose gel electrophoreses, DNA with the length of the desired repeat length was gel extracted (B) and sub-clonated into TOPO vector,

where it was excised with restriction enzymes cutting on both sides of the insert (C). The result of the sequencing reaction of the vector containing a three fold repeat of the 84e element shows the orientation of the color coded primer regions within the generated repeat (D). Red highlights the Shostak-REs for DAF-12.

3.8 Repeats of isolated *mir-84* promoter regions

The PCR repeat generation was used on two 120bp long stretches of the *mir-84* promoter surrounding the 84d or the 84e elements (following page: Figure 23) to generate repeats of different repeat lengths.

3.8.1 The nomenclature of CRMs within the *mir-84* promoter

The nomenclature of CRMs within the *mir-84* promoter differs between Chapter 2 and 3 because the promoter region analyzed changed during the course of this work (following page: Figure 23). The initial luciferase assay was performed on a 2.8kb promoter element, as described by Esquela-Kerscher (Esquela-Kerscher et al., 2005). The worm line transgenic with the 2.8kb promoter *gfp* reporter lacked seam cell expression, while a 1kb and a >8kb *mir-84* promoter reporter showed similar seam cell expression (Hayes et al., 2006). Therefore, worm lines were chosen that are transgenic with the described 1kb promoter reporter. Two Shostak-REs were identified within the initially used 2.8kb promoter fragment, and site directed mutagenesis of these two sites showed 3x reduced DAF-12 and ligand dependent activation in luciferase assay (see Chapter 2 , Figure 7). The 1kb promoter used for the *in vivo gfp* reporter construct contained one of those two Shostak-REs, but site directed mutagenesis did not severely affect *in vivo* reporter activation according to observation by eye in n>10 worms. Reanalysis of the 2.8kb promoter identified five Shostak-REs, of which two - named 84d and 84e (following page: Figure 23 and Figure 24) - fall into the 1kb promoter fragment present in the *in vivo* reporter construct. Worm strains transgenic with a reporter that has these two Shostak-REs point mutated are pending detailed analysis if they indeed loose DAF-12 dependent transcriptional activation.

following page: Figure 23: CRMs of the *mir-84* promoter

A 2.8kb and a 1kb promoter region of the *mir-84* microRNA were used in this study. DAF-12-like and other CRMs are marked in red, with an arrow indicating the CRM orientation. Note that the "84a" from Chapter 2 is now called "84c", and the "84b" element of Chapter 2 is now called "84e".

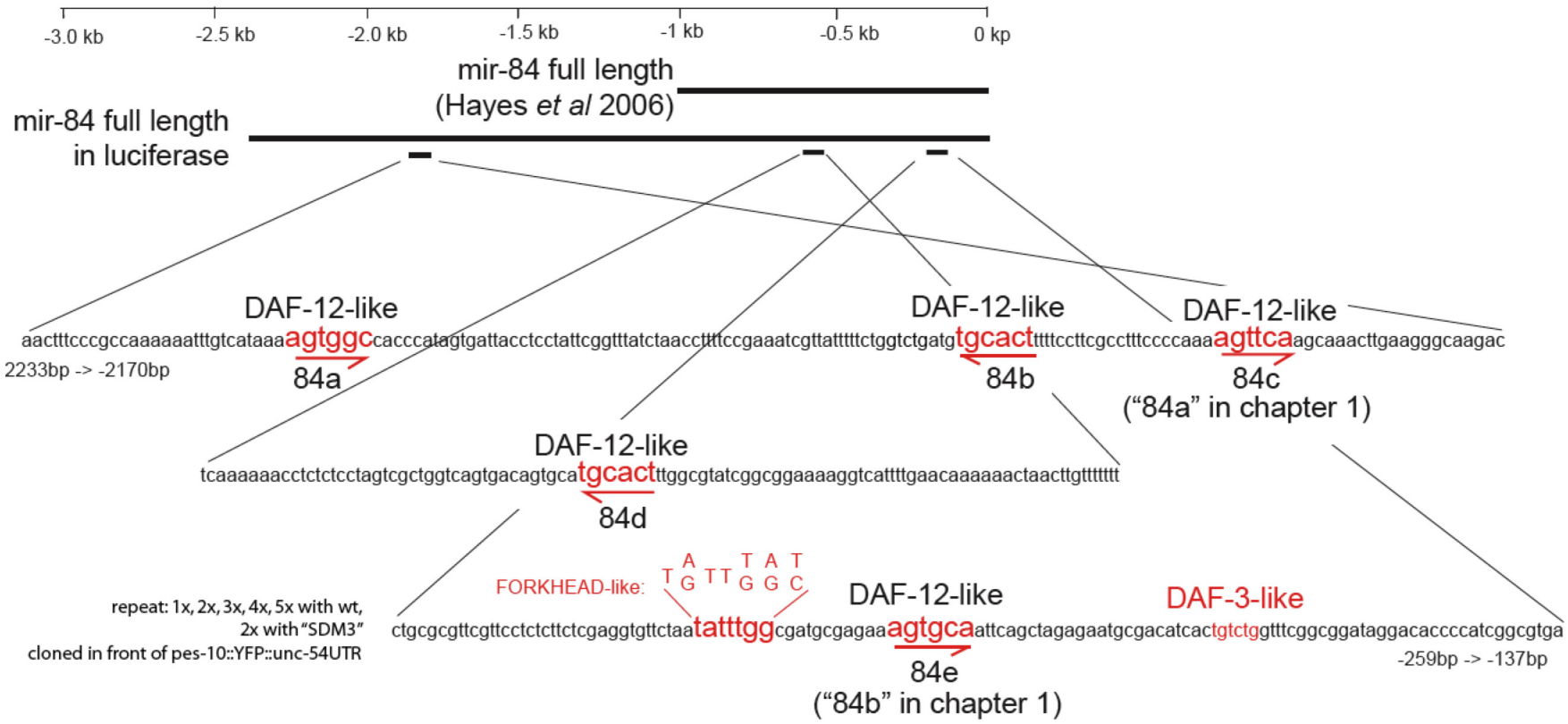
-3.0 kb
-2.5 kb
-2.0 kb
-1.5 kb
-1 kb
-0.5 kb
0 kp
mir-84 full length
(Hayes et al 2006)
mir-84 full length
in luciferase
DAF-12-like
DAF-12-like
DAF-12-like
aactttcccgccaaaaaatttgtcataaaagtggccacccatagtgattacctcctattcggtttatctaacctttccgaaatcgttatttttctggtctgatgtgcacttttccttcgcctttccccaaaagttcaagcaaacttgaagggcaagac
2233bp -> -2170bp
84a
84b
84c
("84a" in chapter 1)
DAF-12-like
tcaaaaaacctctctcctagtcgctggtcagtgacagtgcatgcacttggcgtatcggcggaaaaggtcattttgaacaaaaaactaacttgtttttt
84d
FORKHEAD-like:
T A T T A T
G TT G G C
repeat: 1x, 2x, 3x, 4x, 5x with wt,
2x with "SDM3"
cloned in front of pes-10::YFP::unc-54UTR
DAF-12-like
DAF-3-like
ctgcgcgttcgttcctctcttctcgaggtgttctaatatttggcgatgcgagaaagtgcaattcagctagagaatgcgacatcactgtctggtttcggcggataggacaccccatcggcgtga
-259bp -> -137bp
84e
("84b" in chapter 1)

3.8.2 Increased repeat number enhances activation

To test the principle that increased repeat number increases promoter activation, worm lines were generated that are transgenic with constructs containing one-, two- or a four-fold repeat of the 84e element (Figure 24 A). The 1x84e gave very low GFP intensity in the pharynx, that was increased by 2x84e, and even further increased by 4x84e. The 4x84e is an extremely potent transcriptional activator, of which germline injection of only 2.5ng/ul DNA concentration resulted in transgenic lines with high GFP intensity. Injection of higher concentrations led to no transgenic offspring - this was probably caused by a lethal phenotype due to sequestration of vital TFs away from their endogenous target genes to the 4x84e DNA present in high dose. Conclusion was that increased number of repeats of a CRM strongly increases expression level, facilitating the analysis of tissue specific expression and regulation.

3.8.3 84d and 84e repeat reporters

The 4x84e reporter is expressed only in the pharynx (Figure 24 A). In comparison to this, a 4x84e and a 6x84 reporter were analysed, of which the 6x84e reporter was oriented in reverse orientation to the 4x84e reporter. The 6x84e reporter showed no obviously different tissue specifity than the 4x84e reporter (n>100 animals, observation by eye). In contrast to the 4x84e reporter, the 4x/6x84d reporters lack expression in the pharynx, and instead shows weak expression in excretory cell, and rectal gland under favorable growth conditions (Figure 24 B-F). However, under dauer inducing conditions, the 4x/6x84d reporter showed strong seam cell expression in preliminary experiments (Figure 24 G), and starved worms show a strong vulva expression after refeeding (Figure 24 H).

Consistent with the full length reporter construct, the 4x84e reporter does not show strong DAF-12 dependence, pointing to non-DAF-12 TRMs being responsible for expression in this specific tissue. Candidate TFs for this function will be discussed later in this chapter.

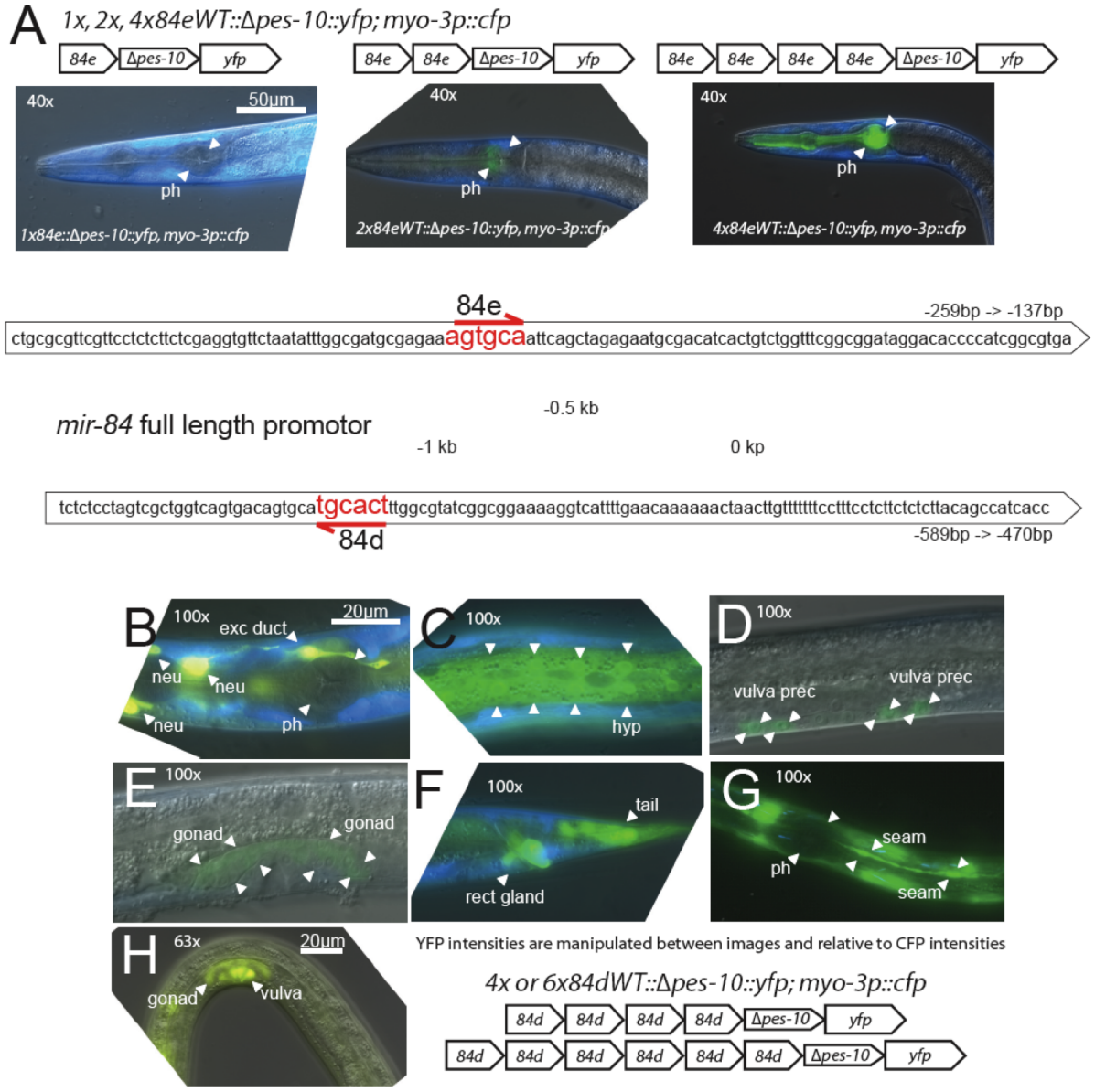

Figure 24: CRM repeats of the *mir-84* promoter

Sequence of the 84d and 84e elements and their location within the 1kb full length promoter of the *mir-84p::gfp* reporter used in Chapter 2 . Red highlights the Shostak-REs for DAF-12. Repeated promoter elements are fused to a *pes-10* minimal promoter (Fire et al., 1990) and a *yfp* reporter gene. Expression of the 84e reporters *in vivo* increases drastically with increasing numbers repeated 84e elements. 4x/6x84e show strong activation in the pharynx only (= ph, A) while 6x84d was expressed weaker and in more cell types: neurons (= neu, B), excretory cell (= exc duct, B), hypodermis (= hyp, C), vulva precursor cells (= vulva prec, D), gonad (E), rectal gland and tail (F), but not in the pharynx (= ph, B). Dauer worms showed strong expression in seam cells (G) and stared worms show strong expression in vulva cells (H) after re-feeding. Panels D, E and H show 4x84e, while panels B, C, F, G show a 6x84e reporter that is oriented in opposite orientation. Change of orientation did not have any obvious effect on expression

pattern. Expression in each shown tissue was observed in n>10 animals and representative images are shown.

3.9 Repeats of isolated *mir-241* promoter regions

Two repeats were generated of a 150bp region surrounding 241ab and a 100bp region surrounding 241cd.

The 4x241ab reporter shows expression only in the excretory cell and a few head neurons (following page: Figure 25 A). The excretory duct expression is completely abolished in *daf-12* null mutant background (following page: Figure 25 B) and is therefore 100% *daf-12* signaling dependent, while in *daf-9;din-1* double null mutant background it is low. Ligand supplementation to the latter genotype induced a strictly ligand dose dependent increase of expression level, while very high ligand dose led to a total loss of expression (following page: Figure 25 C). The 2x241cd reporter showed expression only in the pharynx and the gut cells (following page: Figure 25 D), with an incomplete DAF-12 dependence in *daf-12* null mutant background (following page: Figure 25 E), and a moderate ligand dependent rescue of the decreased expression in a *daf-9;din-1* double null mutant background.

\

following page: Figure 25: CRM repeats of the *mir-241* promoter
Sequence of the 241ab and 241cd elements and their location within the 2kb full length promoter of the *mir-241p::gfp* reporter used in Chapter 2 . Red highlights the Shostak-REs for DAF-12. Repeated promoter elements are fused to a *pes-10* minimal promoter (Fire et al., 1990) and a *yfp* reporter gene. The 4x241ab reporter is expressed in the excretory cell (exc, white arrows) and several head neurons (A), while excretory cell expression is completely lost in *daf-12(rh61rh411)* null mutants (B). In a *daf-9;din-1* double null background, expression level is dependent on ligand dose (C). The 2x241cd reporter is expressed in the pharynx and the gut (C), and shows moderate decrease of expression level in *daf-12* null background (D) compared to wild type. Binding site of the *flh-1* between the 241a and 241b elements discussed below is shown in blue. Expression in each shown tissue was observed in n>20 animals with one replicate and representative images are shown.

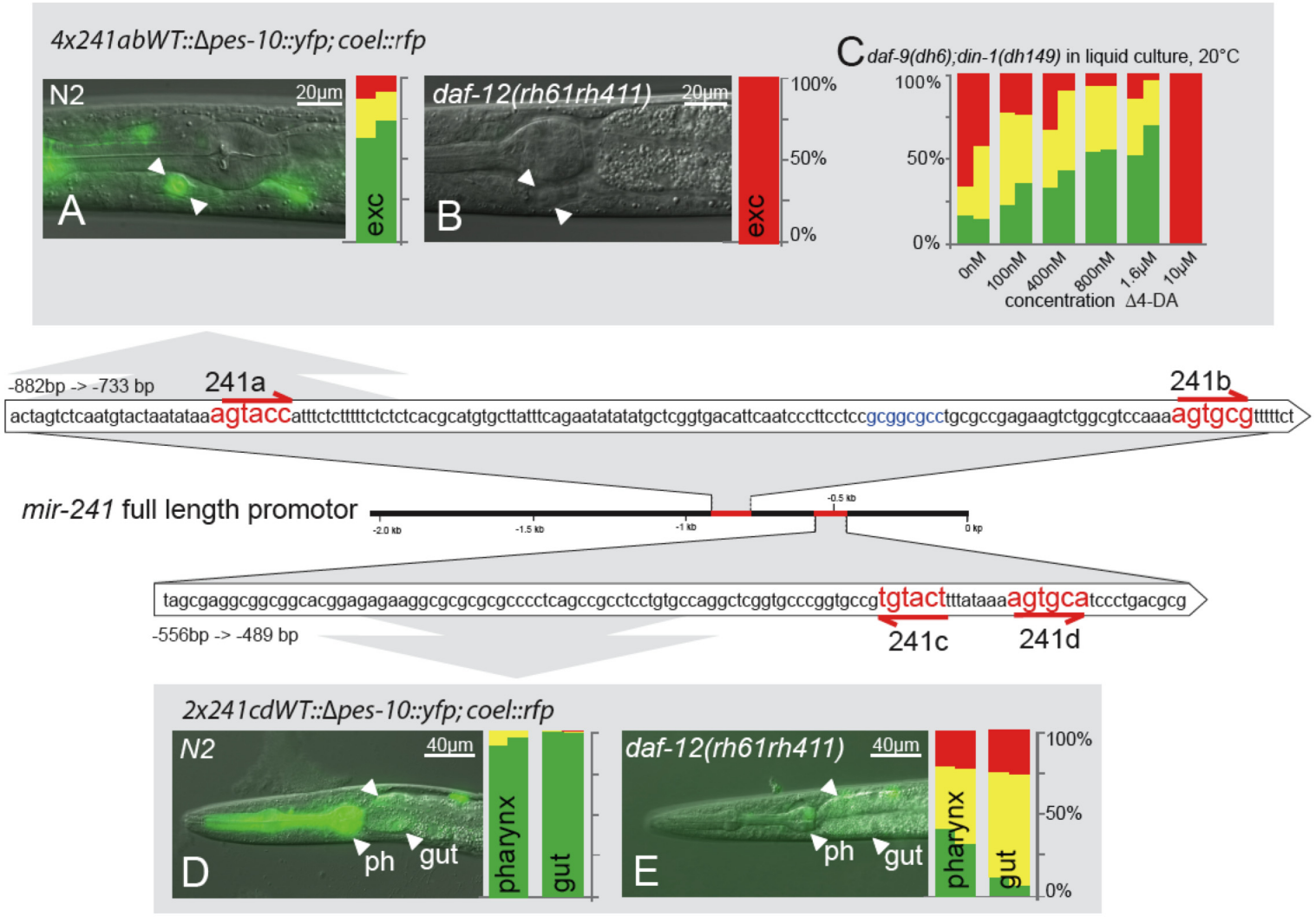
4x241abWT::Δpes-10::yfp; coel::rfp
N2
20µm
A
exc
daf-12(rh61rh411)
20µm
B
exc
100%
50%
0%
C daf-9(dh6);din-1(dh149) in liquid culture, 20°C
100%
50%
0%
0nM
100nM
400nM
800nM
1.6µM
10µM
concentration Δ4-DA
-882bp -> -733 bp
241a
241b
actagtctcaatgtactaatataaagtaccatttctcttttctctctcacgcatgtgcttatttcagaatatatatgctcggtgacattcaatcccttcctccgcggcgcctgcgccgagaagtctggcgtccaaaagtgcgttttct
mir-241 full length promotor
-2.0 kb
-1.5 kb
-1 kb
-0.5 kb
0 kp
tagcgaggcggcggcacggagagaaggcgcgcgcgcccctcagccgcctcctgtgccaggctcggtgcccggtgccgtgtacttttataaaagtgcatccctgacgcg
-556bp -> -489 bp
241c
241d
2x241cdWT::Δpes-10::yfp; coel::rfp
N2
40µm
D
ph
gut
pharynx
gut
daf-12(rh61rh411)
40µm
E
ph
gut
pharynx
gut
100%
50%
0%

3.10 *Let-7* TRE reporter

Luciferase assays discussed in Chapter 2 show a very low absolute activation of the *let-7* promoter for all four conditions tested (Figure 26 A). However, plotting the fold induction of ligand supplemented condition versus control indicated a 10 fold DAF-12 and ligand dependent transcriptional activation of the tested *let-7* promoter fragment (Figure 26 B).

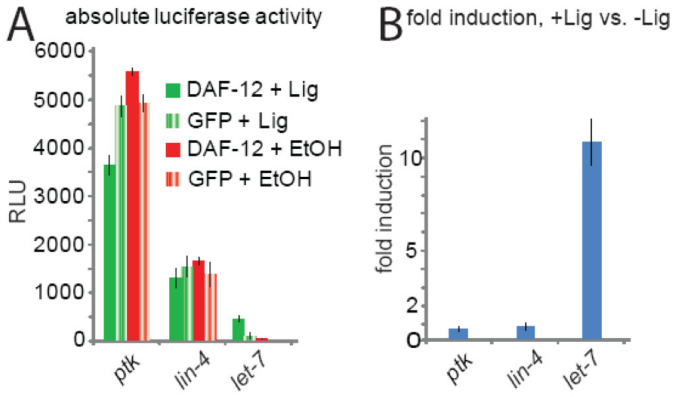

Figure 26: Re-analysed luciferaseassay of the *let-7* promoter
Plotting the data presented in Figure 7 with decreased unit size of the y-axis (A) reveals DAF-12 and ligand dependent activation of the *let-7* promoter construct in terms of absolute activation and ligand dependent fold induction (B).

The TRE element was identified as an important CRM for *let-7* transcriptional regulation (Johnson et al., 2003) (Figure 27 A). Closer examination reveals similarities of the TRE to the Shostak daf-12 RE (Figure 27 B).

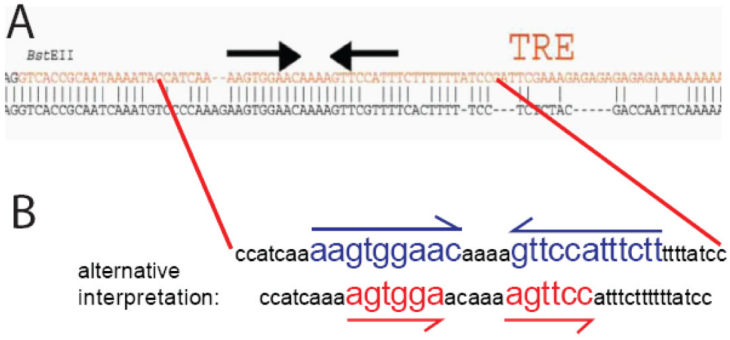

Figure 27: *Let-7* "TRE" element
A *let-7* promoter element that is important for *let-7* reporter expression was called "temporal regulatory element" or "TRE" (Johnson et al., 2003) (A), and can also be interpreted as a direct repeat of two DAF-12-like CRMs with 5 nucleotides pacing (DR5) (B).

EMSA with oligos containing wild type TRE sequence showd weak DAF-12 specific shift signals that were supershifted by antibody incubation and competed away by incubation with cold competitor oligo. Oligos with a TRE mutated to the same sequence shown to abolishe DAF-12 DNA interaction in Chapter 1 failed to show any shift signal, while oligos with a TRE sequence mutated into a perfect Shostak-RE revealed strongly enhanced DAF-12 specific shift signals (Figure 28).

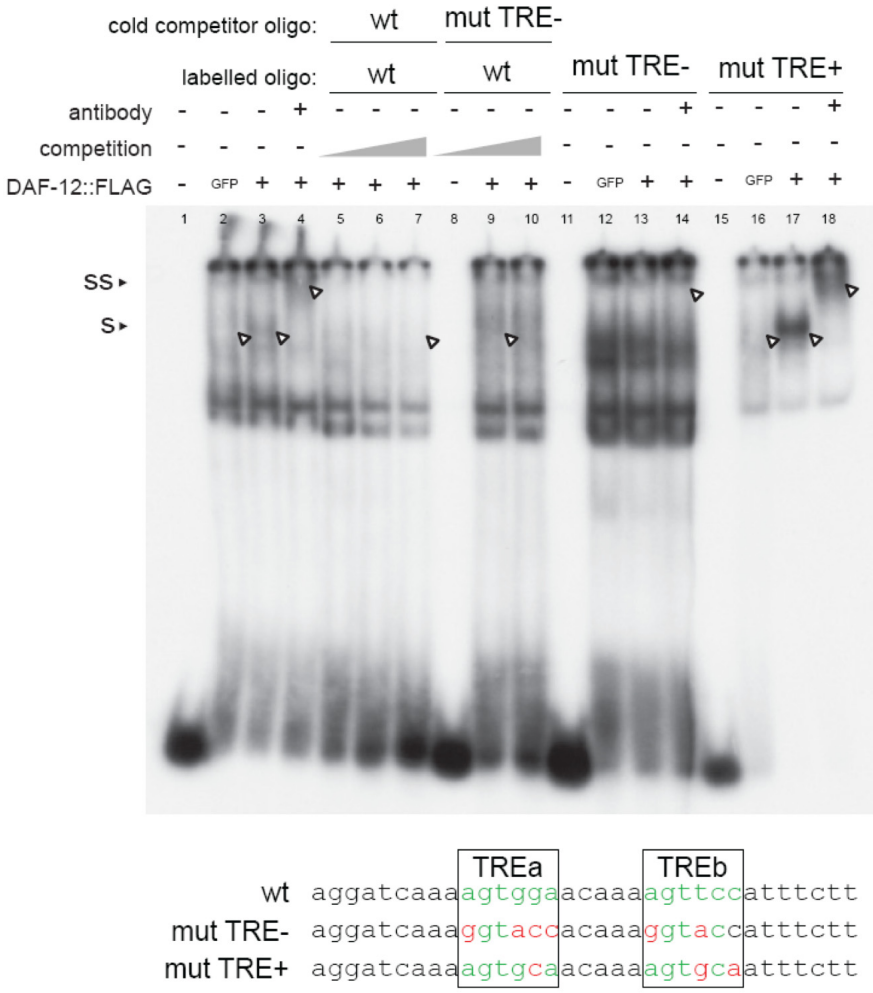

Figure 28: EMSA of TRE-element
Nuclear extract of cells expressing Flag-tagged DAF-12 induced a shift (s) of TRE element containing, radio labeled oligos. Weak shift (s) and super shift (ss) signals are obtained with the wild type TRE sequence, that are lost completely when the TRE site is mutated to a validated non-DAF-12-interacing sequence ("mut TRE -"), while they are strongly enhanced by mutating the TRE into a canonical DAF-12-like CRM sequence ("mut TRE +"). Grey bars represent a dose increase of the non-labeled competitor oligos. Green letters indicate DAF-12-REs while red letters represent mutated nucleotides. EMSA was done once.

To test for *in vivo* tissue specifity of the TRE-CRM, a 4xTRE reporter strain was generated and found expression in head neurons, weak expression in seam cells, and very strong expression in the rectal gland (Figure 27).

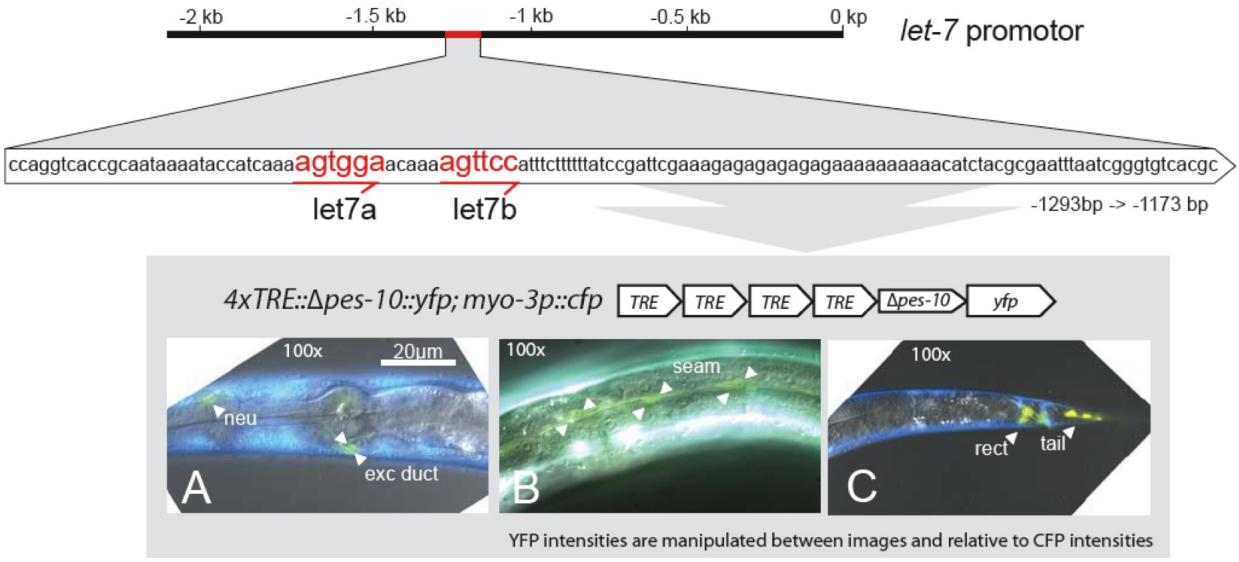

Figure 29: CRM repeat of the TRE
Sequence of the TRE element and their location within 2kb of promoter. Red highlights the Shostak-REs for DAF-12. Repeated promoter elements are fused to a *pes-10* minimal promoter (Fire et al., 1990) and a *yfp* reporter gene. The 4xTRE reporter is expressed in excretory duct (= exc duct, A), neurons (=neu, A), seam cells (= seam, B), and strongest in the rectal gland and tail (= rect / tail, C). Expression in each shown tissue was observed in n>10 animals and representative images are shown.

Preliminary rectal gland expression analysis of this reporter construct in DAF-12 null background (observation by eye, n>10 animals) did not reveal strong expression level changes, pointing again towards non-DAF-12 TRMs as the main source of activation in rectal gland expression. A *daf-12* dependent regulation of the 4xTRE would link the regulation to heterochronic phenotypes of *let-7* and the effects of *daf-12* null mutant background on reporter expression in this tissue remain to be tested.

3.11 Conserved elements in analyzed promoters

The above described DNA elements were chosen with the aim of isolating DAF-12 dependent *cis*-regulatory elements, and therefore are located around the identified DAF-12 binding sites. By extending the searching to binding motives that were assigned previously to TFs other then

DAF-12, several genes were identified as candidates for interaction with CRMs present in the 84e element.

3.11.1 *Daf-3*/co-smad

A DAF-3-like CRM present in the 84e element is similar to a CRM described for the *myo-2* promoter (Horner et al., 1998; Thatcher et al., 1999) (following page: Figure 23). Pharyngeal expression of the repeat reporter overlaps with the expression pattern of *daf-3* regulation target *myo-2* and also connects the repeat reporter expression pattern to a tissue with *daf-3* dauer regulation function (Patterson et al., 1997). Based on those findings, *daf-3(e1376)* mutant allele background was expected to cause a loss or gain of 4x84e reporter expression level during developmental progression or arrest. However, preliminary analysis (observation by eye, n>10 animals) indicated no change of expression level in mutant background compared to wild type.

3.11.2 Forkhead transcription factors *pha-4* and *daf-16*

A potential forkhead transcription factor binding site was also identified (following page: Figure 23). Loss-of-function of forkhead factor *pha-4* leads to a loss of pharynx formation (Horner et al., 1998), and pharyngeal expression of several reporter constructs was shown to be PHA-4 mediated (Gaudet et al., 2004). Forkhead factor *daf-16* is an important dauer regulator with expression and function in the pharynx (Ogg et al., 1997). Previous studies, using *in vitro* binding experiments with degenerated oligos found a 8nt long sequence of the elements that DAF-16 and three mammalian forkhead factors can physically bind. However, in 25 of 25 cases, the identified sequence differed in the most 3' nucleotide from the one present in the 84e element (Furuyama et al., 2000). To still test influence of *daf-16* null mutant background, the 4x84e reporter was rossed into *daf-16(mu86)* background and compared reporter expression level to that observed in wild type. Preliminary analysis (observation by eye, n>10 animals) indicated no clear loss or gain of reporter expression level in *daf-16(mu6)* mutant background during normal growth. Promoter activation *in pha-4* knock-out background still remains to be tested.

3.11.3 *Ceh-22*/homeobox domain

The homeobox domain protein CEH-22 regulates promoter activity in the pharynx. It binds to DNA sequences very similar to the canonical DAF-12 REs (Okkema and Fire, 1994) (Figure 30). CEH-22 function as well as activation of DAF-12-like CRMs 241cd and 84e all locate to the

pharynx, which raise the possibility of regulatory CEH-22 and DAF-12 interaction on DAF-12-like CRMs in this tissue.

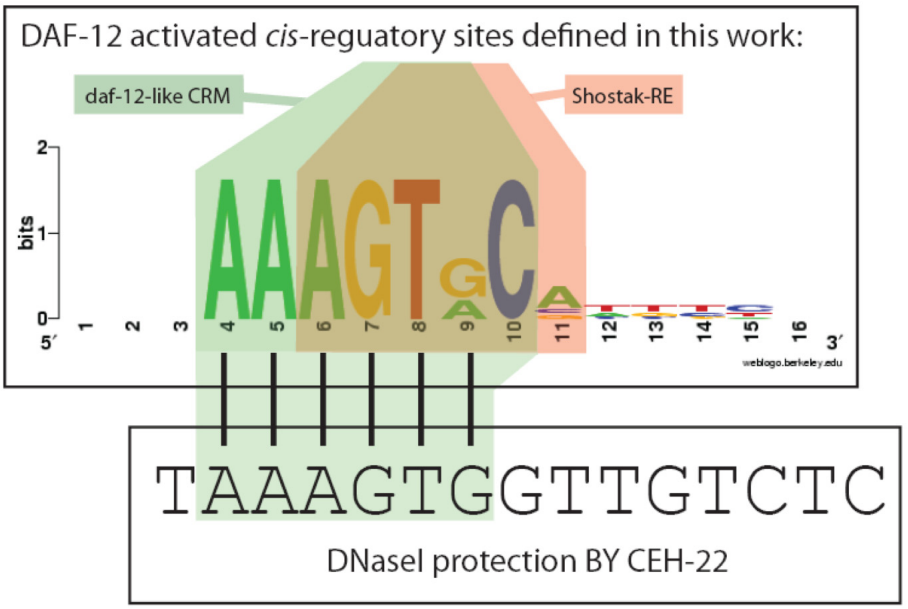

Figure 30: CEH-22 and DAF-12 response elements
A sequence protected from DNAseI degradation by CEH-22 protein incubation (Okkema and Fire, 1994) (below) shows high similarity to the consensus DAF-12-like CRM when compared to the Shostak-RE sequence and the sequence defined in Figure 21 (above).

3.12 *Lin-12*/notch receptor

Other TFs are interaction candidates not based on CRM sequence but on functional connection to microRNA regulation. Solomon et al describe heterochronic seam cell phenotypes of the *lin-12*/notch gain-of-function (gf) allele *n137n460* discussed in Chapter 2.7.1 (Solomon et al., 2008). The authors observed increased *let-7* promoter reporter expression in the seam cells, accompanied by a precocious terminal differentiation phenotype in the hypodermis. This precocious hypodermal differentiation is also known to involve *mir-84* function (Hayes et al., 2006). A second link of *lin-12* to *mir-84* is the overlapping expression of mir-84 CRM reporter 4x84d in vulva precursor cells (Figure 24 D) and reported *lin-12* dependent activation of *mir-61* (Solomon et al., 2008). For those reasons, the reporter 4x84d and 4xTRE were crossed into the *lin-12(n137n460) gf* mutation background and tested for *lin-12gf* regulatory effects on hypodermal expression. Both reporters and genotypes were assayed at the non-permissive temperature of 15°C during food availability. Preliminary observations indicate that *daf-12* null

(n=15) and *lin-12gf* (n=5) background decreased expression of the 4x84d CRM reporter during L3 stage in seam cells, vulva precursor cells and cells of the excretory system when compared to wild type background (n=33). The 4xTRE CRM reporter seemed to be unaffected in *daf-12* null background (n=8), while *lin-12gf* background during L4 stage (n=13) decreased the number of animals expressing the reporter in the seam cells compared to wild type. This decrease of the 4xTRE is unexpected, since published phenotype and full length promoter reporter regulation in *line-12gf* allele suggested to expect an increase. However, these are only preliminary observations and the experiments need to be repeated to give conclusive results. Other growth conditions need to be assayed in addition to this, since strong seam cell expression was only observed in dauer larvae and strong vulva expression was only observed in L4 worms recovering from starvation. The whole regulation dynamics of dauer / starvation recovery has not been investigated, conditions under which the *mir-84* full length promoter displays very interesting regulatory dynamics (see Chapter 2.4.2. and 2.7).

3.13 FLYWCH transcription factors *flh-1*, *flh-2*, *flh-3*

Previous publications describe that *flh-1(bc374)* loss-of-function leads to precocious expression of *mir-241* (Ow et al., 2008). The identified FLYWICH-CRM is located between the 241a and 241b sites of the 150bp long promoter sequence of the 241ab repeat (following page: Figure 25), and it resembles closely a CRM identified to be present in all *C. elegans* microRNA promoters (Ohler et al., 2004). The co-localization of the CRMs makes it appear likely that this is the place where FLYWCH and DAF-12 signaling converge. For those reasons it was decided to test the influence of *flh*-gene knock-down onto reporter constructs of DAF-12 dependent and independent 241ab, 241cd, 84d and TRE CRM repeats. Knock-down of either one or both TFs regulating the CRMs was expected to cause a change in expression intensity or pattern. However, worms transgenic with either of those reporter constructs grown on *flh-1*, *flh-2*, *flh-3*, or *flh-1/flh-2* double RNAi (observation by eye, n>20 per condition) did not show striking changes in expression pattern when compared to the same worm lines grown on L4440 empty RNAi vector control. To observe a reporter regulation effect, a more precise measurement of GFP expression level might be required. Another possibility is that RNAi might decrease *flh-1* dose insufficiently to generate a reporter phenotype.

Discussion

3.14 Regulation of CRMS present in the *mir-84* and the *mir-241* promoters

Daf-12 signaling is not the only signaling cascade regulating the *let-7* family microRNA promoters. A DAF-12-like CRMs of 100 to 150bp length was isolated to test for tissue specifity and dependency of transcriptional activtion onto DAF-12 or non-DAF-12 TFs. Increasing repeat length clearly enhanced the reporter signal of the DAF-12-like CRM constructs and facilitated analysis. With the help of these constructs I found that isolated DAF-12-like CRMs activate transcription only in a subset of tissues compared to the full length promoter. DAF-12 and ligand dependence of transcriptional activation of those isolated DAF-12-like CRMs greatly varied. Complete dependence was observed for the 241ab-CRM expressed in the excretory cell, while pharyngeal and gut expression of the 241cd-CRM and pharynx expression of the 84e-CRM show only partial dependence, but reflects tissue specific recapitulation of full length promoter regulation. The same seems to be true for the 84d-CRM, that appears recapitulate some of the *mir-84* regulation aspects described in 2.1.2.4 and Figure 17. No obvious *daf-12* dependence was found for the TRE-CRM expressed a.o. in seam cells and rectal gland. This led to the assumption that other TFs regulated by other cascades activate those CRMs, and two ways of determining the importance of the observed activation were tested: knock-down of candidate TFs discussed below and analysis of promoter sequence conservation presented in Appendix 5.

The chosen strategy of CRM-isolation and amplification appears to be successful for the *mir-84* promoter in separating two very distinct regulatory pattern, namely pharyngeal and seam cell regulation, as well for the *mir-241* promoter, where it successfully isolated DAF-12 and dafachronic acid dependent regulation, namely regulation in the excretory cell, away from other, hormone independently activating factors. These regulatory functions of the full length promoters can now be assigned to specific CRMs, given that the preliminary results can be validated by repeated experiments.

3.15 Candidate TFs for *let-7* family microRNA regulation

Several TFs were tested that are, based on prior publications, candidates to regulate *let-7* family promoters. Several TFs are candidates to directly bind to DAF-12- and non-DAF-12-like CRMs present in the repeated promoter sequences, while others were found to have a strong functional connection to *let-7* microRNA promoter regulation. Candidates for non-DAF-12-like CRM binding are DAF-3/co-smad, DAF-16/foxo, PHA-4/foxo and FLYWCH TFs. Candidate

for interaction with DAF-12-like CRMs is CEH-22/homodomain protein, and TF connected via function to *let-7* family promoter regulation is LIN-12/notch. However, *daf-3*/co-smad, *daf-16*/foxo and *flywch* mutant alleles as well as RNAi knock-down did not noticeably affect reporter activation and might need to be re-examined in more stringent ways, while candidates *pha-4*/foxo, *ceh-22*/homeodomain protein remain to be tested. Preliminary observations for *lin-12*/notch dependent regulation will be discussed below.

3.15.1 *Lin-12*/NOTCH receptor is a candidate for *daf-12* interaction

The notch receptor *lin-12* has important functions in vulva differentiation and uterus-seam connection (Greenwald et al., 1983), dauer recovery (Ouellet et al., 2008) and terminal differentiation of the hypodermis (see Chapter 2.4.3 and 2.7.1), the latter by activating expression of the *let-7* microRNA (Solomon et al., 2008). Several observations made during this work suggest potential interaction of *mir-84* and *lin-12*. Q-PCR data indicates that *mir-84* is the only *let-7* family member to be up-regulated during and directly after induction of dauer recovery (Figure 16). Based on the observations of strong dauer-related up-regulation in the seam cells of reporters for both, *mir-84* full length promoter (Figure 17 G-M) as well as the 4x/6x84d CRM (Figure 24 G), the expectation is that the up-regulation observed by Q-PCR to take place in the hypodermis - suggesting a function for *mir-84* during dauer recovery in the seam cells. *Mir-84* together with *let-7* drive terminal differentiation in the hypodermis (Hayes et al., 2006), further connecting *mir-84* to this process. Activation of the *mir-84* promoter during these *lin-12* influenced processes in *lin-12* target tissues makes functional interaction possible, and suggests that *lin-12* might act through not only regulating *let-7*, but also *mir-84* to drive developmental progression and terminal differentiation of the hypodermis. Preliminary observations presented in Chapter 3.12 underline these expectations but need to be repeated.

LIN-12 drives transcriptional activation by interaction with the DNA binding LAG-1. LAG-1 binds to DNA sequence RTGGGA (Christensen et al., 1996), but these sites are absent from the repeated promoter fragments. However, presence of several LAG-1 binding sites in the *ins-18* promoter that were conserved in *C. briggsea* did not result in *lag-1* dependent reporter construct regulation (Ouellet et al., 2008), raising the possibility of a TRTGGGA-CRM independent regulation function of *lag-1*. This still leaves room for a direct or indirect *lin-12* regulation of these CRMs that require further investigation.

3.15.2 Direct *let-7* promoter regulation through DAF-12

EMSA of the DR5 containing TRE CRM shows a much weaker DAF-12 binding to DNA than observed for tested CRMs of the *mir-241* promoter. However, the full length *let-7* does induce a DAF-12 and ligand dependent transcriptional activation in luciferase assays. These two findings support a direct interaction of DAF-12 with the *let-7* promoter. However, preliminary data presented in Chapter 3.12 rather disproof a daf-12, and suggest a lin-12 involvement, pending further analysis.

Also interesting is the low over-all luciferase activity specifically observed for the *let-7* promoter. This could be interpreted as endogenous mammalian factors present in the Human Embryonic Kidney Cells binding and suppressing the promoter activation, possibly through a high degree of conservation of CRM / TRF couples, as observed by Flames (Flames and Hobert, 2009). Loss of this activation after point mutation of the TRE CRM would clarify if DAF-12 activates the *let-7* promoter by interacting with the TRE.

Outlook

The reporter constructs described in this chapter still need to be accurately analyzed for loss of expression intensity relative to wild type background when loss-of-function is induced for the following genes:

3.16 Connecting CRMs to signaling cascades

Let-7 microRNA family regulation has so far not been connected to TGF-beta signaling directly, only through TGF-beta influence on dafachronic acid synthesis and DAF-12 activity. Identifying the potential *daf-3*/co-smad binding site adjacent to the 84e CRM (following page: Figure 23 and Figure 45) as an actually functional one of would show this direct connection of TGF-beta downstream signaling and *let-7* family microRNA regulation.

Forkhead transcription factors play an important role in developmental regulation, insulin signaling, stress resistance and longevity. However, no *daf-16*/foxo or *pha-4*/foxo forkhead factor dependence has been shown to date. Identifying the potential forkhead binding site adjacent to the 84e CRM (following page: Figure 23 and Figure 45) as actually functional would directly connect forkhead transcription factors to *let-7* microRNA regulation, a direct connection that has not yet been described, either.

A functional, linear interaction of *ceh-22*/homoedomain protein and DAF-12 has already been described in the pharynx (Ao et al., 2004). Finding that a canonical DAF-12-CRM (Figure 30)

has a very similar sequence to a CEH-22-CRMas regulation would indicate that these two factors also can act in parallel to regulate the same gene battery, connecting homeo domain protein function to DAF-12 hormonal control. This possible connection needs to be established by showing direct CEH-22 can interact with the DAF-12-like CRMs by EMSA.

A *flh-1, -2, -3 flywch* gene regulation would validate already published gene functions (Ow et al., 2008).

3.17 *Lin-12* in terminal differentiation

The *let-7* regulation through *lin-12* described previously (Solomon et al., 2008) together with the *gfp* reporter regulation of the 84e CRM repeat shown in Figure 24 indicate a possible functional interaction of *lin-12* with *mir-84* as well. This interaction needs to be analyzed in a *lin-12(n137n460)* gain-of-function mutant background, with an increase in *mir-84* promoter activation as expected outcome. This *lin-12* dependent activation would connect *lin-12* to *mir-84* regulation and complement the *let-7/mir-84* mediated suppression of larval programs described earlier (Frand et al., 2005; Hayes et al., 2006; Ouellet et al., 2008). Testing a *lin-12(n137n460);daf-12(rh61rh411)* for suppression of precocious alae formation of *lin-12* alone would directly establish epistasis between the these two factors.

Positive results of any of the suggested experiments would also make *lin-12* a candidate for influencing the unexpected ligand independent DAF-12 activation of the *mir-84* promoter in the seam cells observed in Chapter 2.1.2.4.

3.18 *Daf-12* in terminal differentiation

I showed luciferase assay (Figure 26) and EMSA (Figure 28) experiments that indicate a direct DAF-12 interaction with the *let-7* promoter. If *daf-12* influence onto the *let-7* promoter is mediated by direct interaction with the TRE (Johnson et al., 2003), DAF-12 and hormone dependent luciferase activation shown in Figure 26 should be abolished by point-mutating the TRE sites from the full length promoter. This would connect *daf-12* directly to the *let-7* mediated terminal differentiation of the hypodermis, in addition to the already established role of *daf-12* in hypodermal seam cell differentiation during L2 to L3 stage transition.

4. DAF-12 and its co-regulator LIN-29 form a “molecular switch” driving terminal differentiation of the hypodermis

Linyan Meng contributed data to Figure 31, Figure 33 and Figure 34

Introduction

DAF-12 is ubiquitously expressed, but transcriptional activation of DAF-12 target genes described in Chapter 2 and 3 shows extensive tissue specifity that is brought about by the promoter sequences. *Trans*-regulatory modules (TRMs = TFs) that act on different *cis*-regulatory modules (TF binding elements in promoters of regulated proteins, called CRMs) present in the promoter have been connected to tissue specify promoter activation. However, tissue specific differences in the cellular co-regulator pool can also modulate the transcriptional output of a TF (O'Malley, 2006) in a tissue specific way. For this reason, it was investigated to what extend tissue specific and temporally coordinated changes in transcriptional output of DAF-12 are caused by co-regulators influencing DAF-12, perhaps even independent of dafachronic acid.

The only known DAF-12 co-regulator is co-repressor DIN-1 (Ludewig et al., 2004), but DAF-12 also interacts *in vitro* with human co-activator SRC-1 (Motola et al., 2006). However, no *C. elegans* co-activator for DAF-12 has been described so far. DAF-12 and its ligand dependent activation is implicated in heterochronic regulation during L2 to L3 stage transitions (Antebi et al., 1998), when *let-7* family microRNAs, as its direct targets, also play a role during larva-to-adult transition (Hayes et al., 2006). For these functional roles of DAF-12, potential DAF-12 co-regulators were expected to also be involved in heterochronic regulation and to exhibit heterochronic phenotypes.

The chosen candidate, LIN-29, is a zinc finger protein with homology to mammalian EGR2. *Lin-29* null alleles continue to execute larval programs during the adult stage, for example continued seam cell division and molting, interpreted as failure of terminal differentiation in hypodermis and vulva (Liu et al., 1995; Rougvie and Ambros, 1995). Loss-of-function of *let-7* leads to similar phenotypes as *lin-29* null, a constellation similar to the seam cell division pattern of *daf-12* null alleles and the *let-7s* (*mir-48, -84, -241*) microRNA deletions discussed in Chapter 2 that were explained by DAF-12 directly activating the *let-7s*. One of the *let-7s* microRNAs, *mir-84*, was recently connected to hypodermal terminal differentiation as well. Hayes et al. found that molting phenotypes of hypomorphic *let-7* alleles are enhanced by further loss-of-function of *mir-84*, while over-expression of *mir-84* not only rescues *let-7* hypomorph phenotype, but also the molting phenotype of *lin-29* null alleles (Hayes et al., 2006). This already connects one direct

target of *daf-12* during L3 to the L4 to adult transition. However, the *mir-84* phenotypes are much weaker than those of *let-7* or *lin-29*, suggesting a smaller role of *mir-84* in this process.

Current epistasis models place *lin-29* at the most downstream position of the heterochonic pathway and suggesting it to be the ultimate factor driving terminal differentiation (Hayes et al., 2006). However, finding that *lin-29* acts upstream of *mir-84* and *let-7* microRNAs would change this model and place the microRNAs rather then *lin-29* to the very end of the heterochronic. According to this new model, the two microRNAs would act downstream of *lin-29* as the "activated suppression function" to repress larval genes while *lin-29* directly activates protein coding genes for the adult stage to mediated terminal differentiation. Loss-of-function of either the microRNAs or the TF activating the microRNA transcription would both result in failure to suppress larval programs and failure to drive adult programs, which could explain the continued molting during the adult stage. The observation that over-expression of *mir-84* rescues the continued molting of *let-7* and *lin-29* null mutants partially verifies this model (Hayes et al., 2006). However, it is still not clear if this happens by direct microRNA activation through LIN-29, or LIN-29 acting as a co-factor that can interact with the promoters of both genes. A candidate for the latter option is DAF-12, since the direct activation of *mir-84* thorough DAF-12 is validated in Chapter 2 , and Chapter 3 suggests a potential direct *let-7* activation by DAF-12, despite the fact that loss of DAF-12 alone does not cause defects in terminal differentiation.

This led to the question of whether the microRNA promoters are directly activated by LIN-29, or co-activated by LIN-29 acting through DAF-12. To address this question, the *mir-84* promoter was *in vitro* tested in luciferase assays for direct LIN-29 dependent activation, or LIN-29 co-activation of DAF-12. To complement the *in vitro* assays, *in vivo* assays were performed for transcriptional activation of a *mir-84* promoter fusion to *gfp* in wild type, *daf-12, lin-29*, and *daf-12;lin-29* double mutant background.

Results

4.1 Co-activation assay of LIN-29 and DAF-12 on the *mir-84* promoter

It was found that LIN-29 co-transfection leads to a two fold increased DAF-12 and ligand dependent activation of the *mir-84* promoter during *in vitro* luciferase assays, while *lin-29* transfection in absence of DAF-12 does not cause promoter activation (Figure 31). This was interpreted as LIN-29 co-activating DAF-12. However, it cannot be ruled out that the failure of

LIN-29 alone to activate the *mir-84* promoter is due to the lack of an activation domain compatible with the mammalian transcriptional machinery.

Point mutation of the DAF-12 CRMs leads to a strong loss of DAF-12 and ligand dependent activation, but *lin-29* co-transfection still enhances the remaining activation. This observation rules out the possibility that LIN-29 binds to a CRMs other than the DAF-12 CRMs to indirectly recruit liganded DAF-12 to result in activation. However, it does not distinguish whether LIN-29 binds to the DAF-12 CRM or directly to DAF-12 to enhance activation.

The *lit-1* promoter is DAF-12 and ligand activated, but co-transfection of *lin-29* decreases transcriptional activation instead of increasing it as it did with the *mir-84* promoter. This points towards a sequence specifity of the LIN-29 and DAF-12 co-activation that is only achieved by the *mir-84* promoter.

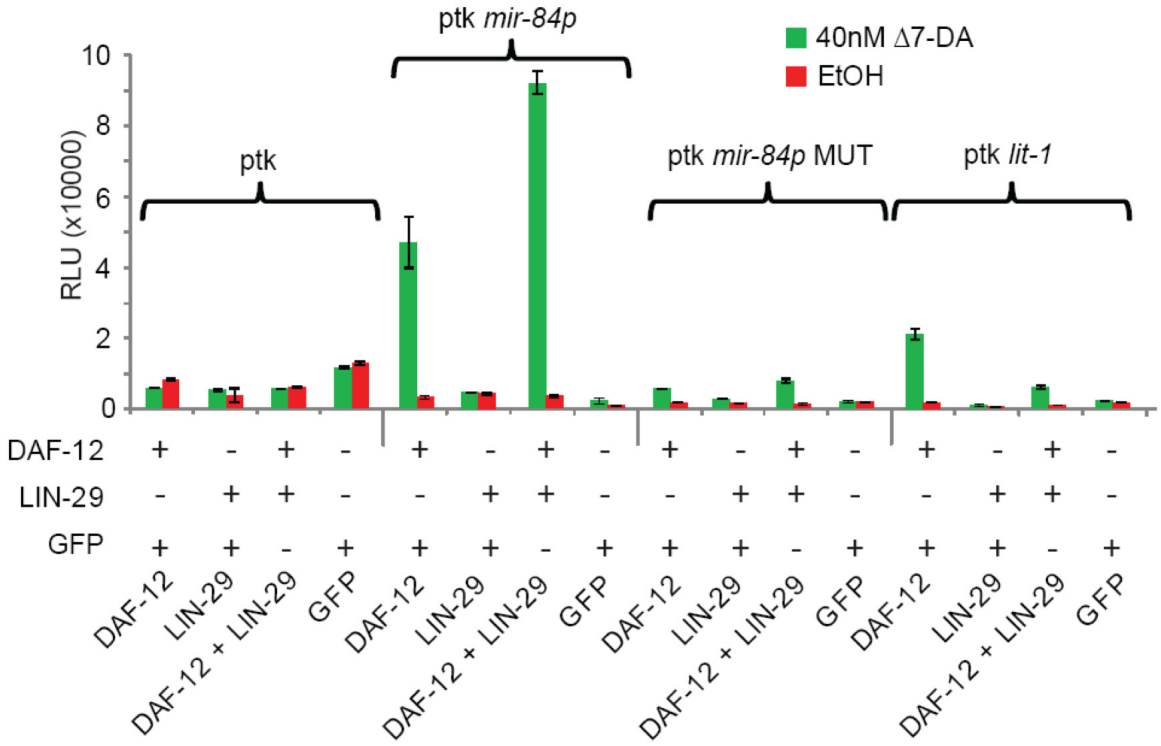

Figure 31: Luciferase assay of LIN-29/DAF-12 co-activation
Expression vectors for DAF-12, LIN-29 or GFP as control were transfected into Human Embryonic Kidney cells, along with luciferase reporter vectors containing the *mir-84* promoter and the *lit-1* promoter as used in Chapter 2 . Positive control *lit-1* promoter and the wild type *mir-84* promoter were used in Figure 7, while the mir-84 promoter with point mutated DAF-12-CRMs was used in Figure 9 B. LIN-29 co-transfection increased DAF-12 and ligand dependent activation of both *mir-84* promoters, but decreased *lit-1* promoter activity. Assay was repeated once with similar results.

4.2 EMSA with LIN-29 and DAF-12 on DAF-12 regulated CRMs

The question was addressed if LIN-29 can *in vitro* interact either with the DAF-12 CRM directly or with DAF-12 protein and EMSA was performed with oligos containing the 241cd CRM validated in Figure 11 to interact with DAF-12. The expectation was a shift signal in LIN-29 presence if LIN-29 can bind the oligo directly. If LIN-29 binds to DAF-12, a further increase of the DAF-12 induced shift in presence of both, LIN-29 and DAF-12 was expected. To test if this interaction is hormone dependent, shift experiments were performed in presence of both, DAF-12 and LIN-29, and in absence and presence of ligand (Figure 32). No LIN-29 mediated changes in shift pattern were detected under any of the experimental conditions. However, presence or absence of the ligand during EMSA changed the ratio of the DAF-12 induced monomer and dimer shift bands towards single occupancy in this experiment. Whether this was LIN-29 dependent or independent remains to be tested with EMSA in the presence of only DAF-12 and presence or absence of ligand.

4.3 Mammalian two hybrid assay for Lin-29 and DAF-12LBD interaction

Mammalian two hybrid assay were performed to test if the co-activation is caused by physical interaction of LIN-29 with DAF-12 (Figure 33). The *daf-12* ligand binding domain was fused to the *vp16* activation domain, and *lin-29* was fused *to gal-4dbd*. When only the *lin-29* construct is transfected, LIN-29::GAL-4DBD binds to the promoter of the luciferase reporter, but fails to activate transcription due to lack of an activation domain. This can change when the *daf-12lbd* construct is co-transfected. Under these conditions, physical interaction of LIN-29 with the DAF-12LBD locates the fused VP16 activation domain to the LIN-29::GAL-4DBD bound to the luciferase reporter. Once the VP16 domain is located to the luciferase promoter, it will induce activation of the luciferase gene. This activation is only achieved by interaction of the proteins that were fused to the GAL-4DBD and the VP16 domain, in this case interaction between LIN-29 and the DAF-12LBD. Negative controls were transfected with the empty vectors either expressing GAL-4::DBD or VP16 tag only. DNA was transfected into Human Embryonic Kidney Cells, as done in Chapter 2 .

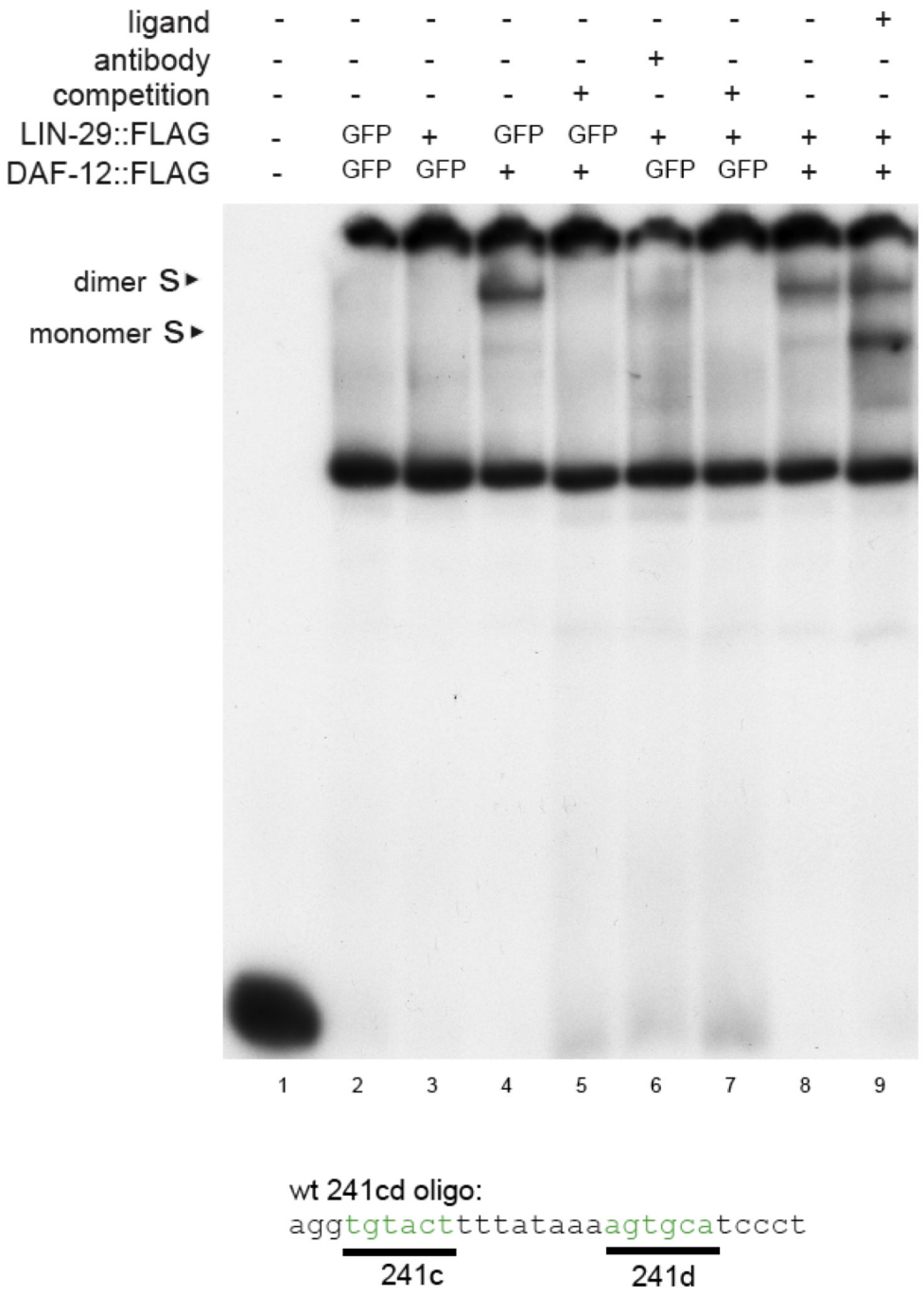

Figure 32: EMSA with DAF-12 and LIN-29
Nuclear extract of Human Embryonic Kidney cells expressing Flag-tagged DAF-12 induced two shift signals (s) of radio labeled oligo containing 241cd element as discussed in Figure 11. LIN-29 expression did not cause a shift alone or in presence of DAF-12, while ligand presence enhanced "monomer" binding over "dimer" binding. Green letters indicate DAF-12-REs. EMSA was done once.

Lin-29::gal-4dbd and *daf-12lbd::vp16* co-transfected cultures showed strong ligand dependent luciferase activation, indicating the possibility of ligand dependent, direct protein-protein interaction of LIN-29 and DAF-12LBD. However, DAF-12LBD::VP16 alone also caused noticeable ligand dependent luciferase activation, raising the possibility of unspecific interaction of the DAF-12LBD with the GAL-4::DBD.

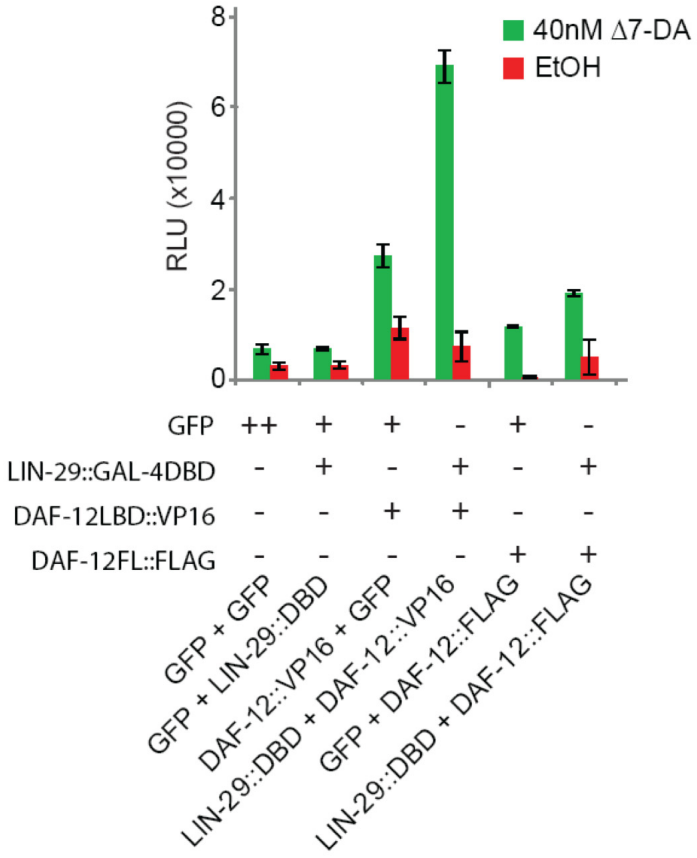

Figure 33: Mammalian Two Hybrid Assay with LIN-29 and DAF-12
Expression of GFP or LIN-29::GAL-4DBD very weakly activated a GAL-4 response element regulated luciferase reporter while luciferase in DAF-12-LBD::VP16 expressing cultures was activated weakly in absence, and strongly in presence of LIN-29::GAL-4DBD. DAF-12::FLAG expressing cultures showed tweak activity in absence and presence of LIN-29::GAL-4DBD. Assay was repeated once with similar results.

4.4 GFP reporter analysis for LIN-29 and DAF-12 co-activation *in vivo*

After testing for co-activation and physical interaction *in vitro*, in vivo co-activation was investigated next. The *mir-84p::gfp* promoter reporter was crossed into *daf-12(rh61rh411)* or *lin-29(n546),* or the double mutant *daf-12(rh61rh411);lin-29(n546)*, and GFP expression in the pharynx was measured during the L3 stage. D*af-12* null mutants were found to express less reporter than wild type, as reported in Chapter 2 (Figure 13). *Lin-29* null mutants expressed less

GFP than *daf-12* null mutants, and double mutants hardly expressed any reporter. This experiment shows that depletion of *daf-12* has a weak, and depletion of *lin-29* has a strong effect on *mir-84p::gfp* reporter expression level. The double mutant shows a further decrease of reporter expression. This experiment indicates that DAF-12 and LIN-29 both individually activate the *mir-84* promoter, and that LIN-29 dependent *in vivo* reporter activation is partially or totally independent of DAF-12.

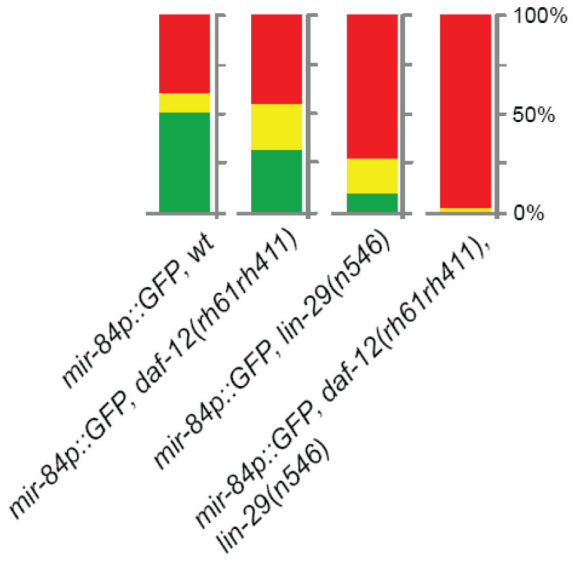

Figure 34: *In vivo gfp* reporter analysis in *daf-12* and *lin-29* mutant backgrounds
Expression of a *mir-84* promoter activated *gfp* reporter in the pharynx at L3 stage was weaker in *daf-12(rh61rh411)* null mutant background then in wild type. Expression in *lin-29(n5463)* null mutant background was further decreased and *daf-12;lin-29* double null mutant background nearly abolished all detectable GFP expression. n=20, GFP intensities were quantified once and relative GFP intensities observed multiple times.

Discussion

The *in vitro* co-activation assays show that LIN-29 presence enhances DAF-12 and ligand dependent transcriptional activation of *mir-84* promoter luciferase reporter, while LIN-29 alone does not have any *in vitro* effect. Daf-12 CRM deletion decreases activation but retains LIN-29 co-activation capacity. The *lit-1* promoter reporter shows a reduction of ligand dependent luciferase activation in the presence of LIN-29, indicating that co-activation is promoter sequence specific. These results were interpreted as LIN-29 acting as a co-activator for DAF-12 *in vitro* for the *mir-84* promoter, by either acting through DAF-12 CRMs or through DAF-12. However, these experiments do not clarify if LIN-29 is able to bind directly to the DNA, or if it binds to DAF-12 to achieve its co-activator function. And even if LIN-29 can bind to the

promoter tested by luciferase assay, it might not be able to recruit mammalian co-activators and the basic transcriptional machinery as DAF-12 is able to. At least for a human LIN-29 homolog, EGR2, it was shown to activate luciferase reporters containing two EGR2 response elements (Crosby et al., 1991), proving that this human LIN-29 homolog is able to bind its CRM and cause transcriptional activation in luciferase assays. It remains unclear whether the conservation between EGR2 and LIN-29 is high enough that LIN-29 maintains this capacity.

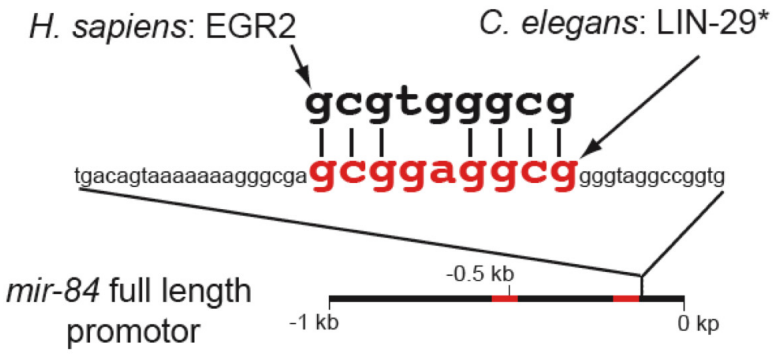

Figure 35: EGR2-like CRM in the *mir-84* promoter
Human ZincFinger protein and closest *C. elegans* LIN-29 homolog EGR2 binds to sequences (Crosby et al., 1991) similar to those found in *mir-84* promoter regions 89bp downstream of the 84e CRM.

241cd oligos only interacted with DAF-12, but not with LIN-29, and LIN-29 was not able to influence the DAF-12 dependent shift pattern, indicating that under the chosen conditions, LIN-29 cannot interact with either DAF-12 regulated 241cd, nor with DAF-12 protein itself. However, it was the *mir-84* promoter that showed co-activation, and the EMSA needs to be repeated on oligos containing CRMs present in this promoter to rule out sequence-specific effects on the LIN-29 mediated co-activation.

While the *in vitro* experiments show that LIN-29 acts through DAF-12, *in vivo* analysis of *mir-84* promoter expression indicates at least a partially DAF-12 independent activation of the *mir-84* promoter by LIN-29 in the pharynx. Further analysis of reporter expression in phenotype related tissues like seam cells is necessary to establish epistasis of lin-29 and *daf-12* in context of terminal differentiation of the hypodermis.

The results together place *mir-84* activation downstream of *lin-29*, in contrast to previously published models (Hayes et al., 2006). The new interaction of *lin-29* and *mir-84* allow

modifications to the published model of late stage heterochronic regulation pathway. The presented data can be interpreted as a re-occurrence of "molecular switch" with a combination of TFs and microRNAs driving developmental progression. However, further experiments described in the outlook below are necessary to solidify this hypothesis.

According to this hypothesis, the molecular switch would use the activation of microRNAs *mir-84* and *let-7* to suppress molt-activating genes, most likely *nhr-23/-25*, belonging to the old stage. At the same time it would activate programs of the new, adult stage. As the molecular switch described in Chapter 2 , the transcriptional activation of *let-7* family microRNAs would lead to terminal differentiation and a loss of stem cell character of the target tissue, while loss of microRNAs or the TFs activating them causes a failure of both developmental progression and terminal differentiation. This simplified model does not account for all regulatory functions of the larval-to-adult transition in the hypodermis, which becomes clear by looking at the regulation of adult specific genes: Larval and adult cuticles contain different collagens. The collagen gene *col-19* is specific for dauer larvae and adult stage and appears to be downstream of *mir-84*, *let-7* and *lin-29* since COL-19 expression is decreased in *let-7(mg279)* and further decreased in *let-7(mg279);mir-84* mutants (Hayes et al., 2006) as well as in lin-29 mutant background (Liu et al., 1995). This can be interpreted as the loss of repressing microRNAs leading to the loss of a hypothetical TF activating *col-19*, rather then *col-19* being directly activated by *lin-29* as the "molecular switch" idea would suggest, shown in Figure 36. Also DAF-12 may be repressed by feedback loops involving *mir-84* and *let-7* (Grosshans et al., 2005) as discussed in Chapter 2.5.

If the modified model holds true, it would connect *daf-12* signaling to terminal differentiation of the hypodermis. If the LIN-29 co-activation of DAF-12 is ligand dependent, these experiments would identify, for the first time, a steroid hormone that is directly regulating aspects of nematode molting. All DAF-12 transcriptional activation described so far is ligand dependent, but the pesented data does not support a ligand dependence of hypodermal terminal differentiation so far.

Our results imply that the larval to adult transition of the hypodermis in *C. elegans* requires the ligand dependent or independent DAF-12 mediated activation of *mir-84* and *let-7* microRNAs to suppress larval program promoting genes like *nhr-23, nhr-25*, *hbl-1* etc to prevent re-occurrence of molting during adult stage (Frand et al., 2005).

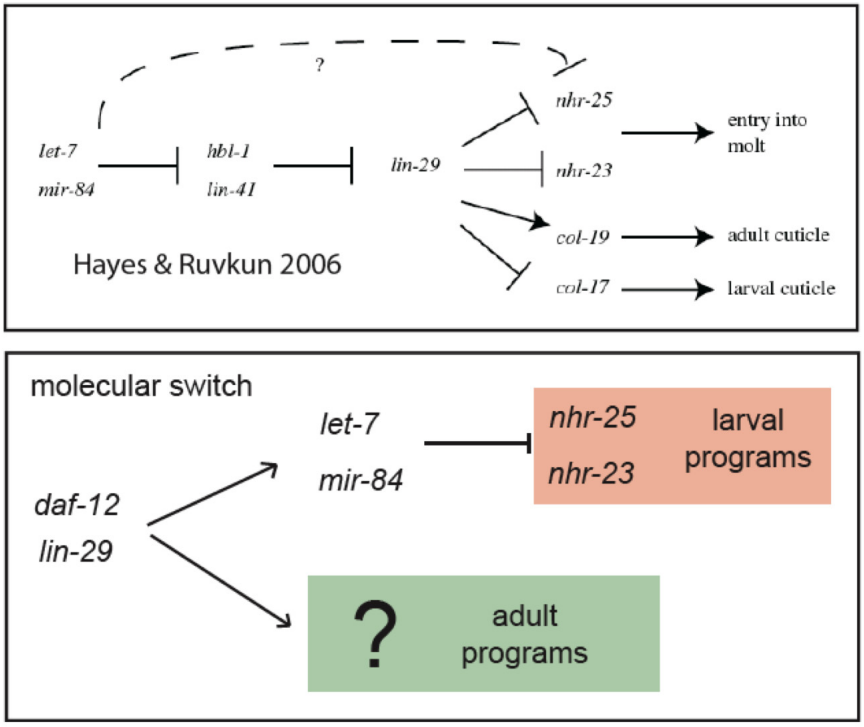

Figure 36: Revised regulation model for larvae-to-adult transition
Upper box is a current regulation model (Hayes et al., 2006), while the lower box is a new model based on the results of this work that suggest that the *mir-84 / let-7* microRNAs act downstream of *lin-29 / daf-12* that together might form a "molecular switch" discussed in Chapter 2 . This "molecular switch" would activate microRNAs to suppress the old programs – molting in this case – while it directly activates adult programs.

The homology between nematode LIN-29 to mammalian EGR2, and nematode LIN-29 co-regulator MAB-10 (Harris and Horvitz, 2007) to mammalian EGR2 co-regulators NAB1/-2 (Le et al., 2005) and their role in terminal differentiation of stem cell like cells allows to hypothesize that EGR2 could be part of a molecular switch in mammals mediating transitions between successive developmental programs. Experiments testing this possibility are explained in detail in the outlook to this chapter below. If this connection can be shown experimentally, it would link the *C. elegans* observations to mammalian stem cell differentiation processes and underline the conservation of the "molecular switch" idea. This conservation would also implicate that this mechanism is present in various vital processes of mammalian biology already mentioned in the discussion of Chapter 2 .

Outlook

4.5 Epistasis experiments of *daf-12* signaling, microRNA expression and molting phenotype

Epistasis experiments need to be performed to reveal the *in vivo* connection of *daf-12* signaling to the suppression of larval stage programs during adult stage. A hypomorph *let-7(mg279)* allele shows 30% supernumerary molts (Hayes et al., 2006). And additional loss of *mir-84* increases the molting phenotype to 100% penetrance, while over expression of *mir-84* reverses this and rescues *let-7(mg279)* to 0% penetrance. It needs to be shown how modulating DAF-12 transcriptional activation modulates *mir-84* levels at the L4 stage and the penetrance of supernumerary molting of *let-7(mg279)* at the same time. The ideal mutant background for this would be a *let-7(mg279);daf-9(dh6);din-1(dh149)* triple mutant. This background lacks endogenous dafachronic acid production as well as DAF-12 repressor function. As a result, transcriptional activation of DAF-12 is dependent on the ligand dose supplemented in the growth medium, as shown in Chapter 2 . Loss of DAF-12 transcriptional activation of *mir-84* should increase penetrance of the molting phenotype of *let-7(mg279)*, as *mir-84* loss did in *let-7(mg279);mir-84* double mutants. Supplementation of DAF-12 ligand to this mutant background will restore DAF-12 transcriptional activation and *mir-84* transcription to wild type levels and should rescues the increased supernumerary molting phenotype, at least back to *let-7(mg279)* penetrance.

Since clues for DAF-12 activation of *let-7* are discussed in Chapter 3 , a control is necessary to show that this is due to DAF-12 activating *mir-84*, or activating *mir-84* and *let-7*. This control would be the *daf-9(dh6);din-1(dh149);mir-84(tm1304)* triple mutant, tested for molting phenotype increase on non-ligand supplemented plates. An increase in penetrance in this case is likely due to decreased DAF-12 activation of *let-7*.

Contradicting with this model is a publication that describes rescue of *let-7* null allele phenotypes in a *daf-12* null allele background (Grosshans et al., 2005), placing *daf-12* downstream of *let-7*, while results presented in Chapter 2 place *daf-12* upstream of *let-7* family members (Bethke et al., 2009). These contradicting phenotypes might be due to modifications of the feedback inhibition involving *mir-84*, *let-7* and *daf-12*. To circumvent the feedback loop, an alternative approach might be necessary that involves *lin-29* hypomorphic alleles to modulate the activity of the molecular switch. A pilot experiment would monitor expression level of a *let-7*

promoter fusion to *gfp* in *lin-29* null background. Regulation according to the model would result in a decrease in expression, while the epistasis suggested by Grosshans places the *daf-12*, now including its co-activator *lin-29*, downstream of *let-7* regulation, in which case *let-7* reporter activation would remain unaffected. Not taken into account however is the regulatory loop which connects *daf-12* and *let-7* discussed in Chapter 2.5.

4.6 LIN-29 activation of the *mir-84* promoter independent of DAF-12

EMSA of oligos containing the so far identified DAF-12-CRMs present in the co-activated *mir-84* promoters would rule out sequence specific effects onto LIN-29 co-activation.

A VP16 domain fused to LIN-29 would force transcriptional activation, as long as the LIN-29DBD can bind the luciferase promoter, making transcriptional activation independent of the ability to recruit co-activators through LIN-29 itself. Luciferase assays with *mir-84* promoter reporter and LIN-29::VP16 would reveal the presence of any LIN-29 regulated CRM.

The DBD of LIN-29 shows high homology to mammalian EGR2, and a DNA motif resembling a validated EGR2 CRM is located in direct proximity of the 84e CRM (Figure 35). This potential CMR is as a candidate for direct regulation by LIN-29. EMSA of this putative LIN-29 CRM will establish if LIN-29 physically interacts with the CRM. As a second step, luciferase assays with LIN-29::VP16 and the *mir-84* promoter luciferase reporter will show if LIN-29 also activates this CRM in full length promoter context. Sequence specifity of LIN-29 for this CRM can be shown by luciferase assay with a *mir-84* promoter that has the putative LIN-29 CRMs point mutated – a loss of luciferase activation would support sequence specifity.

Promoters of *col-7*, *col-17* and *col-19* were published as *lin-29* targets (Liu et al., 1995; Rougvie and Ambros, 1995), but the presented experiments did not completely rule out the possibility of an indirect activation. If these promoters are in deed direct targets, they can act as a positive control for LIN-29 activation in luciferase assays.

4.7 Molecular switch homolog functions in mammalian tissue differentiations

To test the model of molecular switch driven terminal differentiation in mammals, a system is needed where activation of TFs homolog to *lin-29* is required for terminal differentiation. A well studied and potentially homologous differentiation process is the myelination of neurons of the mammalian periferal nervous system that occurs after neurons transit from premyelination program to myelination program. EGR2 and NAB1, -2 regulated transcription is required for

differentiation of neuronal Schwann cells past the premyelination state, as well as keratinocytes and chondrocyte differentiation (Le et al., 2005). The myelination program is suppressed by EGR2 mutations (Topilko et al., 1994), analog to LIN-29 loss-of-function that suppresses the terminal differentiation of the hypodermis in *C. elegans* (Liu et al., 1995; Rougvie and Ambros, 1995). The implication is that EGR2 directly activates mammalian microRNAs to suppress the neuronal outgrowth program in order to allow for myelination program execution and terminal differentiation. A test for this model would be the quantification of *let-7* family microRNAs in EGR2-/- animals to show that their transcription is indeed lost.

The next step would be to test if forced expression of the down-regulated *let-7* microRNAs can suppress the EGR2 -/- myelination defect. These experiments would validate or falsify the conservation of the molecular switch in mammals.

5 . Materials & Methods

DNA manipulation

Standard techniques were used to manipulate DNA (J. Sambrook, 1989).

Plasmid DNA was purified with QIAprep Spin Miniprep Kit (Qiagen 27106) or GeneElute HP Plasmid Midiprep Kit (Sigma NA0200-1KT). Restriction enzymes were purchased from NewEnglandBiolabs, used according to manufacturer's protocols. Shrimp alkaline phosphatase (Promega M820A), *Taq* plus Precision (Stratagene 600210-51), *Pfu* ultra HF (Stratagene 600380-51), Roche rapid ligation kit (11635379001), Primers were standard ordered oligo nucleotides" purchased from Integrated DNA Technology or Sigma Genosys.

5.1 PCR protocols

Primers used in this work were generated without software support. Most primers had 25-30 nucleotides homolog to the target sequence with a 5' extension containing restriction enzyme recognition sequences. Primers or primer lengths were chosen that the four most 3' nucleotides contained two guanidine or cytosine, with most 3' nucleotide being of them. It also was a criteria that the homolog region contained no more than four identical nucleotides directly adjacent to each other, and that all nucleotides were present in equal ratio. For most PCR reactions, melting temperature was 92°C with one initial 2 minute melting step and a 30 seconds melting step during cycling, annealing temperature was 50°C for 1 minute, extension temperature was72°C with 1 minute for 1 kb product length.

DNA constructs

5.2 Expression vectors for mammalian cell culture

DAF-12 cDNA was amplified with primers 326166 (cgggatccatgggcacaaatgga ggagtc) and 326164 (ccgctcgagctatttgattttgaaaaattctc) and cloned into *pCMVTag2b* (Stratagene #211172). *Lin*-29 cDNA was excised from vector Ba 282 using *XmaI*, *XhoI* and cloned into *pCMVTag2b* (Stratagene #211172). *Lin*-29 cDNA was sub-clonated into pCMX gal-4DBD to give pCMX lin-29::gal-4DBD.Vectors *pCMX gal-4-dbd*, *pCMX vp16*, *pCMX vp16::daf-12-lbd* and *pCMX daf-9* were obtained from the Mangelsdorf lab (Motola et al., 2006).

5.2.1 Luiferase reporter vectors

microRNA promoters were PCR amplified using the following primers: *mir-48* (JRP6, JRP3) and *mir-241* (JRP7, JRP2, (Esquela-Kerscher et al., 2005)),

mir-84 with primers 27723-001 (GGATCC gatgccacaggcagacgtatgatgaatagt) and 27723-002 (gtcgacctccaaaattatgagtggca),

let-7 with primers 33872767 (accggatccacagtgtagaccgtccaccaatcg) and 33872768 (actgtcgacatttgtgttaaggcactcattgtgttgc),

lin-4 with F59G1.5658+.*SalI.lin-4* (gtcgacgagacgccgagtctcccttactg) and F59G1.6169-.*BamHI.lin-4* (ggatccaggccggaagcataaactcataaacc),

mir-237 with 44938-001 (ggatccctgaatcgacttctctaggaatcc) and 44938-002 (gtcgacgttcaaaacttctacattgcgtgg) and inserted into *ptk luc* reporter vector (Motola et al., 2006) upstream of a thymidine kinase (tk) minimal promoter that was followed by the firefly luciferase cDNA. The *mir-241* promoter was subcloned into Fire Lab vector L4053 (Fire Lab *C. elegans* Vector Kit, 1999 plate) using *BamHI* to generate *mir-241p::4xNLS::GFP*, called A215.

mir-241 truncations #1 (called A224) was generated with primers 44113-005 (cgggatcc_cggtgtcgtcgtgttctaaatgttcc) and 50390-002 (ggatcc_ggaagggattgaatgtcaccgagcatatat), #2 (called A225) was generated with primers 44113-007 (gtcgac_actagtctcaatgtactaatataaagtacca) and 46031-001 (cgggatcc_actttgacacccccgcggtttg), #3 (called A226) was generated with PCR primers 50390-001(gtcgac_cgaatgactgaacgattgagagaacgagag) and 46031-001 (cgggatcc_actttgacacccccgcggtttg), and truncation #4 (called A227) was generated with primers 44113-007 (gtcgac_actagtctcaatgtactaatataaagtacca) and 44116-006 (ggatccctctcgttctctcaatcgttcagtcattcg)

pG5 luc was obtained from the Mangelsdorf lab (Motola et al., 2006), *ptk luc daf-9 (*A194) contains a PCR product amplified primers 6555-084 (gtcgat cac cag ggt atc act tcg gta gac ac), and 6555-085 (ggatccgaagatattgaaggattgatgtgc), *ptk luc him-4* contains a PCR product amplified with primers 6555-082 (gtcgacagtaagcccaaactgcgactacg), and 6555-083 (ggatccccaaaatagtaagagatagtgccttcg), *ptk luc unc-5* (A195), contains a PCR product amplified

with primers 6555-080 (gtcgacacagaatcatgtagctcactactgt), and 6555-081 (gtcgacacagaatcatgtagctcactactgt).

5.2.2 Site directed mutagenesis of *daf-12*-like CRMs

Point mutations were introduced using Quikchange Multi. Vector A215 was mutated with primers 59450-001 (CTCAATGTACTAATATAAGGTACCATTTCTCTTTTTCTCTCTCACGC) and 59450-003 (GTCTGGCGTCCAAAGGTACCTTTTTCTCTCTGTTTCTCCACCG) to give *mir-241p(mut ab)::4xNLS::GFP* (A275). The insert was subclonated into *ptk luc* to give *ptk luc mir-241p(mu tab)* (A279). A275 was template for site directed mutagenesis using Quikchange II and primers 30037678 (ccaggctcggtgccgGgtacCtttataaaGgtAcCtccctgacg), 30037679 (cgtcagggaGgTacCtttataaaGgtacCcggcaccgagcctgg) to give *mir-241p(mut abcd)::4xNLS::GFP*, called A455. Luciferase reporter *ptk luc 241c* with one of two DAF-12 sites of the *241cd* CRM mutated (Figure 50) was generated using site directed mutagenesis as decribed above using primers 46031-002 (gccgtgtacttttataaaGGTACCtccctgacgcgcgggagacgc) and primer 46031-003 (gcgtctcccgcgcgtcagggaGGTACCtttataaaagtacacggc) to give vector A214. Luciferase reporter *ptk luc 84b* with the 84b DAF-12-RE mutated (following page: Figure 23) was generated using site directed mutagenesis (as decribed in Chapter 1) using primers 50622-001 (ccttcgcctttccccaaaGgtAcCagcaaacttgaagggcaag) and primer 50622-002(cttgcccttcaagtttgctGgTacCtttggggaaaggcgaagg) described above.

5.3 CRM-repeat generation

Repeat-PCR-products described in Chapter 3 were generated by using 50µl PCR reaction containing 50ng of plasmid DNA harboring any template containing sequence (e.g. the corresponding *ptk luc* vectors used in Chapter 2) 2.5µ *Taq* Precision or 1.25u *Pfu* Ultra, 5µl manufacturer supplied 10x PCR buffer, 1µl of each primer working solution (working solution is 10pmol/µl), 1µl of the 50 mM dNTPs solution. Cycling parameters were 2min initial denaturation at 95°C, then 35 cycles of 30sec 95°C denaturation, 1min 50°C primer annealing, 30sec 72°C extension time. PCR-products were separated on a 0.5x TBE 0.8% agarose gel, bands of different sizes corresponding to different repeat numbers were gel extracted and sub-clonated into *TOPO TA* or *TOPO BLUNT* vector according to used polymerase and sequenced to verify identity, repeat number and orientation. Inserts were then excised and sub-clonated into

the multiple cloning site of a modified *yfp* or *cfp* reporter plasmid upstream of a *Δpes-10* minimal promoter and the chromophore coding region.

The modified vectors containing a *yfp* coding region were called A423 and A424 depending on the orientation of the multiple cloning site. They were generated as the following: The original *yfp* (L4817, internal name A246) or *cfp* (L4816, internal name A245) reporter plasmids are taken from the 1999 Fire Lab Vector Kit. Vector backbone and chromophore cDNA were excised out of L4816 or L4817 by digestion with *HindIII* and *BamHI*, the *Δpes-10* minimal promoter sequence was excised out of Fire Lab vector L4053 (called A170) by digestion with *NheI* and *BamHI* and the 4x241ab repeat was excised out of *Topo TA* vector (called A384) by digestion with *HindIII* and *XbaI*. All fragments were gel purified and ligated in a single step with equimolar amount of DNA fragments. The *yfp* containing plasmid was called A391 (Figure 37), the *cfp* containing A388). Oligo nucleotides for forward and reverse strand of a multiple cloning site containing in 5' to 3' order restriction sites for *SalI, NehI, XbaI, ApaI, SpeI, HindIII* (forward oligo 28227516: agctctgcagagtcgacatgctagcatctagagggcccactagtttaagcttattgca, and reverse 28227517: ataagcttaaactagtgggccctctagatgctagcatgtcgactatgcag) were annealed as described for EMSA oligo annealing. The resulting double stranded oligo contained sticky end overhangs for 5' *HindIII* and a 3' *PstI* ligation. The oligo overhangs also had a mismatch in order to destroy the restriction sites they were annealed to. The double stranded oligo was ligated into A391/A388 backbone digested with *PstI* and *HindIII* and gel extracted to eliminate the insert. The *yfp* containing product was called A424 (Figure 37). A423 vector was generated using oligos 28227518 (agcttttactagtgggcccattctagaagctagcatgtcgactactgca) and 28227519 (gtagtcgacatgctagcttctagaatgggcccactagtaaa) with restriction sites in opposite orientation as A424 (*HindIII, SpeI, ApaI, XbaI, NheI, SalI* in 5' to 3' order, forming a 5' *HindIII* and a 3' *PstI* overhang that was not destroyed after ligation).

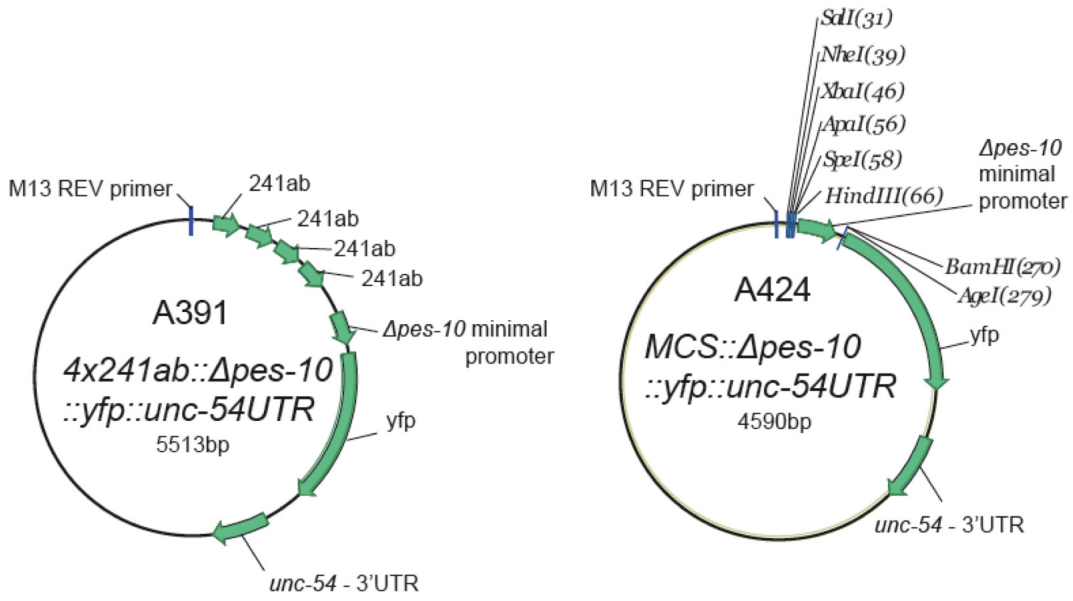

Figure 37: A391 and A424 vector map

Primers 42692097 (agccatcacc_tctctcctagtcgctggtcagtg, forward) and 42692097 ctaggagagag_gtgatggctgtaagagagaag, reverse) were used to PCR-generate reporter repeats "4x84d" and "6x84d". The PCR product was separated on a 1.2% agarose gel and DNA fragments between 500 and 1000bplength were gel-extracted, sub-clonated into TopoTA (A632 for 4x84d and A628 for 6x84d) and sequenced to verify identity, repeat number and orientation. *4x84d::Δpes-10::yfp* was generated by excising the inserts out of A632 and A628 with XbaI, SpeI and ligation into A424 digested with *XbaI*, followed by shrimp alkaline phosphatase treatment (SAP). *4x84d::Δpes-10::yfp* was called A634. The *6x84d::Δpes-10::yfp* vector was called A631, containing the 6x84d repeat in opposite orientation to the *yfp*.

Primers used to generate repeats "1x84e" to "4x84e"were 35910036 (gacaccccatcggcg_ctgcgcgttcgttcctctcttctcgand, forward) and 35910037(ggaacgaacgcg cagcgccgatggggtgtcctatccgccg, reverse). For the generation of 2x84eMut with a mutated DAF-12-like CRM were generated by using A479 as template. The PCR product was separated on a 1.2% agarose gel and DNA were gel-extracted corresponding to various fragment lengths (Figure 22), sub-clonated into *TopoTA* (A632 for 4x84d and A628 for 6x84d) and sequenced to verify identity, repeat number and orientation. Promoter repeats were sub-clonated into *TopoTA* (A520 for 1x84e, A521 for 2x84e, A523 for 4x84e). A424 vector and insert vectors were

digested with HindIII and XbaI and ligated. *1x84e::Δpes-10::yfp* vector was A529, *2x84e::Δpes-10::yfp* vector was A530 and *4x84e::Δpes-10::yfp* vector was called A532).

4x241ab repeat was generated with primers 87436-003(ccaaaaccattcgcatccccaacacttaccttcaataagg , forward) and 87436-004 (agtgttggggatgc_gaatggattttggttgaatgggttggtggattgatg, reverse), sub-clonated into *Topo TA* and called A384 and further processed as described above.

2x241cd was generated with *Pfu* Ultra polymerase and primers 87436-001 (gagcagaagta_actagtctcaatgtactaatataaagtacc, forward) and 87436-002 (gtacattgagactagt_tacctctgctctgaaactcggtggagaaacagagag, reverse), sub-clonated into *Topo BLUNT* and called A401. Backbone of A391 and insert of A401 were gel-purified and ligated after vector digestion with *HindIII* and *NotI* and the *2x241cd::Δpes-10::yfp* product was called A406.

4xTRE repeat was generated with primers 31355948 (ggtgtcacgcccaggtcaccgcaataaaatacc) and 31355949 (ggtgacctgggcgtgacacccgattaaattcg), and sub-clonate into *TOPO TA* to give vector A457. Backbone of A391 and insert of A457 were gel-purified and ligated after vector digestion with *HindIII* and *NotI* and the *4xTRE::Δpes-10::yfp* product was called A459.

5.4 Double-tagging constructs

The constructs listed in Table 2 were generated for the CFP/YFP double tagging-project described in Appendix 3. However, not all constructs were used during this project. The data is shown here to give a complete list of reagents created.

	promoter	chromophore	UTR	construct
1	*myo-3*	*cfp*	*unc-54*	A245
2	*myo-3*	*yfp*	*unc-54*	A246
3	*daf-12*	*cfp*	*unc-54*	A433
4	*daf-12*	*yfp*	*unc-54*	A434
5	*daf-12*	*cfp*	*daf-12*	A453
6	*daf-12*	*yfp*	*daf-12*	A454
7	*daf-12*	*cfp*	*hbl-1*	A443
8	*daf-12*	*yfp*	*hbl-1*	A444
9	*myo-3*	*cfp*	*daf-16*	A414
10	*myo-3*	*yfp*	*daf-16*	A415
11	*daf-16B*	*cfp*	*unc-54*	A437
12	*daf-16B*	*yfp*	*unc-54*	A438
13	*daf-16B*	*cfp*	*daf-16*	A435
14	*daf-16B*	*yfp*	*daf-16*	A436

Table 2: List of *cfp* / *yfp* tagging vector constructs

myo-3p::cfp/yfp::unc-54-UTR : Constructs *myo-3p::cfp-unc-54-UTR* (A245) *myo-3p::yfp-unc-54-UTR* (AA246) were taken out of the 1999 Fire Lab Vector Kit where they are called L4816 and L4817, respectively.

daf-12p::cfp/yfp::unc-54-UTR : A 5kb fragment upstream of the *daf-12* start codon was PCR amplified with Taq Precision using primers 22507-003 (cta GCT AGC cttccgaaccaatcatatgtattgtc) and 22507-004 (gg GGT ACC ttaattggcgcccgttgcgccgaaatgtg) and subclonated into *TOPO TA* vector to give vector A177.

The promoter was cut out of A177 with *SalI* and *BamHI* und sublonated into vector L4053 from the 1995 Fire Lab Vector Kit to give vector A249. The promoter was excised out of A249 with *HindIII* and *AgeI* and subclonated into vector A392 (*cfp*) and A393 (*yfp*) to give vector A433 (*cfp*) and A434 (*yfp*). A392 (*cfp*) and A393 (*yfp*) were derived previously from A312 (*cfp*) and A313 (*yfp*) by digestion with *BamHI* and relegation of the vector backbone. A312/A313

were derived from A245/A246 by digestion with *HindIII* and *XbaI* and ligation with *HindIII* and *XbaI* digested *TOPO TA* vector to exchange the *myo-3* promoter with the multiple cloning site of *TOPO TA.*

daf-12p::cfp/yfp::daf-12-UTR : Vectors A453 (*cfp*) and A454 (*yfp*) were derived by cutting the DAF-12 UTR out of vector Ba359 of the Antebi Lab Bacterial collection using *EcoRI* and *ApaI* and ligation into A304 (*cfp*) and A306 (*yfp*). A304 and A306 were obtained earlier by subclonation of the *daf-12* promoter out of A177 into A245 (*cfp*) and A246 (*yfp*) using *SalI* and *BamHI* to give vectors A251 and A252.

daf-12p::cfp/yfp::hbl-1-UTR : The *hbl-1*-UTR was PCR amplified using *Pfu* ultra polymerase and primers 29030250 (gggccc ctgatgatccgattaattgtgtactttg) and 29030249 (CGGCCG tgaggacgtcctcgttaaggaaacac) and subclonated into *TOPO BLUNT* to give vector A442. *hbl-1*-UTR was cut out of A442 with *ApaI* and *EcoRI* and ligated into A453 (*cfp*) and A454 (*yfp*) that were obtained earlier as described above to give A443 (*cfp*) and A444 (*yfp*).

myo-3p::cfp/yfp::daf-16-UTR : The *daf-16*-UTR was PCR amplified with Taq precicion and primers 84160-001 (GAATTCGTCGAcgatcagccactgatggatactatggatgttg) and 84160-002 (GTCGACtggtaaaatttcgcgcctgg) and subclonated into *TOPO TA* to give vector A355. A355 was digested with *EcoRI* and *SalI* and ligated into A392 (*cfp*) and *A393* (*yfp*) to give vector *A414* (*cfp*) and A415 (*yfp*).

daf-16p::cfp/yfp::unc-54-UTR : A 5kb fragment upstream of the start codon of the *daf-16 B*-isoform was PCR amplified using primers 87436-005 (CCCGGGcgtcttgtcctgcgctcttatcattcttatc) and 87436-004 (ACCGGTcgtcctcattcactcccgattcttcctcatcc) and subclonated into *TOPO X*L to give vector A432. The promoter was excised from A432 using *XbaI*, *AgeI* and ligated into only *AgeI* digested and Shrimp alkaline phosphatase treated A492 and A393 to give vectors A437 (*cfp*) and A438 (*yfp*).

daf-16p::cfp/yfp::daf-16-UTR : The promoter of *daf-16B* isoform was excised from A432 using *XbaI*, *AgeI* and ligated into only *AgeI* digested and Shrimp alkaline phosphatase treated A414 and A415 to give vectors A435 (*cfp*) and A436 (*yfp*)

Nematodes

Standard techniques were used to maintain nematodes (Brenner, 1974). For ligand supplemented plates, 10µl of 75µM Δ^4-DA (Motola et al., 2006) in ethanol were mixed with 90µl of over night OP50 culture in LB medium and seeded onto 3cm plates containing 3ml NGM agar.

5.5 RNAi knock-out

RNAi mediated gene knock out was achived by feeding, using *E. coli* strain *HT115(DE3)* that was transgenic for a vector containing a short, 100 to 500bp long stretch of DNA sequence of the coding region of the targeted gene, flanked by two T7 polymerase binding sites facing into the insert. An *HT115* culture was grown over night at 37°C in LB medium containing 75-100µg Ampicillin and 12.5µg Tetracyclin. The culture was pelleted and resuspended in LB in 1/5 of the original volume and plated onto NG plates supplemented with 50µg/ml Ampicillin and 1mM IPTG to induce the T7 polymerase to generate the double stranded RNA. RNAi clones were taken out of the "Arringer library" (Kamath et al., 2003). As a negative control, one RNAi plate was plated out with *HT115* transformed with 4440, the empty RNAi vector. Positive control was RNAi aginst *unc-22* to cause the easily scoreable "uncoordinated" phenotype

5.6 Analysis of GFP expression

10 to 20 gravid adult worms were placed on a 6cm NG agar plate for 6h at 20°C to lay eggs and then removed. Plates were incubated at desired temperature and scored when the worms reached desired stage. Used as a negative control was a plate that was For the analysis of extra chormosomal arrays in different mutant backgrounds, N2 worms transgenic with the same extra chromosomal array were used. GFP intensity was observed using a Leica FL-MZIIII binocular or the Zeiss Axioscope2 equipped with fluorescence filter sets described below.

5.7 Worm transformation

Worm lines transgenic with reporter constructs were generated using microinjection (Mello, 1991) of DNA mix with 100ng/µl total concentration into the germline. Germline injected animals gave offspring that at low frequency had plasmid DNA rearranged to form an extra

chromosomal array that shows relatively stable transmission. Each event of extra chromosomal array formation shows within limits an individual expression level and transmission rate, which is why each individual, array transmitting worm is considered an individual worm line that received a unique "*dhEx*" number after entering into the lab worm collection, identifying all offspring and crosses done with this line. For the individual variations between different *dhEx* lines, multiple *dhEx* lines of injections with the same construct were kept.

5.8 Worm lines transgenic with reporter used in Chapter 2

dhEx458 (= *mir-241p::4xNLS::gfp*), *dhEx480* (= *mir-241p(mut abcd) ::4xNLS::gfp*) were generated by injection of 20ng/µl reporter construct and 80ng/µl *coel::rfp* (Miyabayashi et al., 1999). Worm strain *GR1427* (=*mir-84p::gfp*) was obtained from Hayes (Hayes et al., 2006). Worm strains *BW1932* (*hbl-1p;;hbl-1::gfp*) and *BW1891* (*hbl-1p;;unc-54::gfp*) were obtained from Abrahante (Abrahante et al., 2003). Gene alleles /strains are listed in Table 4.

5.9 Worm lines transgenic with CRM-repeat reporter constructs

6x and 4x 84d repeats were injected with 10ng/µl A631 and A634 as well as 10ng/µl of A245 as marker. 1x84e, 2x84e, 2x84eMut and 4x84e were generated by injection of 2,5ng/µl of construct *A529*, *A530*, *A532* and *A532* with *A245* as marker. 4x241ab, 2x241cd and 4xTRE repeats were injected with 20ng/µl of vector *A391*, *A406* and *A459*, respectively, and 80ng/µl of *coel::rfp*.

Extra chromosomal arrays for 4x84d reporter are *dhEx500* till *dhEx504* and for the 6x84d reporter *dhEx513* and *dhEx514*.

Extra chromosomal arrays for 1x84e reporter are *dhEx521*, *dhEx522*. Extra chromosomal arrays for 2x84e reporter are dhEx501, dhEx502 (this one was used for crosses with other genetic backgrounds), dhEx503 and dhEx504. Extra chromosomal arrays for 2x84eMUT reporter are dhEx509 till dhEx512. Extra chromosomal arrays for 4x84e reporter are *dhEx500* till *dhEx504*.

4x241ab: Extra chromosomal array is *dhEx464*

2x241cd: Extra chromosomal array is *dhEx519*

4xTRE: Extra chromosomal arrays are *dhEx493* till *dhEx495*, the latter used for crosses with other genetic backgrounds.

5.10 Worm lines transgenic with double tagging constructs

The following worm lines were generated or planned to be generated for the CFP/YFP double tagging-project described in Appendix 3. Each chromophore vector is present in equimolar amounts relative to 10ng/µl *daf-12p::yfp::unc-54*-UTR, and filled up with *coel::rfp* vector construct to 100ng/µl. Not all constructs were used during this project. Worm lines were generated by injecting by injecting different mixes of one or two *yfp / cfp* vectors, a marker vector. *Coel::rfp w*as used as a marker. The data is shown here to give a complete list of reagents created. Table 3 shows of which reporter constructs the generated lines / *dhEx* lines consist, all lines contain the *coel::rfp* marker.

injection mix	reporter	dhEx
1	*daf-12p::yfp::unc-54-UTR* -	*467*
2	- *daf-12p::cfp::unc-54-UTR*	*471, 472, 473*
3	*daf-12p::yfp::unc-54-UTR* *daf-12p::cfp::unc-54-UTR*	*468, 474, 475*
4	*daf-12p::yfp::unc-54-UTR* *daf-12p::cfp::daf-12-UTR*	*469*
5	*daf-12p::yfp::unc-54-UTR* *daf-12p::cfp::hbl-1-UTR*	*470, 476*
6	*daf-12p::yfp::hbl-1-UTR* *daf-12p::cfp::unc-54-UTR*	*477, 478*

Table 3: Double tagging injected extra chromosomal arrays

Worm strains shown in **Error! Reference source not found.** of Appendix 3 were generated during the pilot experiment for the double tagging project by germline injection using 20ng/µl for each chromophore vector, 10 ng/µl A245 construct as marker and *pCR 2.1* vector to reach 100 ng/µl total concentration of injected DNA: "Y9-1" is transgenic with *daf-12p::yfp::daf-12-UTR*. Strains called "C1-4" and "C1-5" are individual lines transgenic with the reporter *daf-12p::cfp::daf-12-UTR*. Strains called "CY1-2", "CY1-3", "CY5-1" and "CY5-9" are individually

formed lines transgenic with equimolar amounts of both *daf-12p::yfp::unc-54-UTR* and *daf-12p::ycfp::unc-54-UTR* constructs.

Gene alleles / strains

N2

daf-2(e1368)

daf-7(e1372)

daf-12(rh61rh411)

daf-12(rh61)

din-1(dh14

daf-9(dh6), mir-48(n4097)

mir-48 mir-241(nDf51)

lin-29(n546)

daf-12rh61rh411; lin-29(n546)

lin-12(n137n460)

daf-16(mu86)

BW1932, ctIs39 hbl-1p;;hbl-1::gfp

BW1891, ctIs37 hbl-1p;;unc-54::gfp

ctIs39 daf-12(rh61)

ctIs37 daf-12(rh61)

dhEx458(mir-241(wt)::GFP), N2

dhEx458,daf-12(rh61rh411)

dhEx458,daf-9(dh6)

dhEx458,daf-9(dh6); din-1(dh149)

dhEx458, daf-2(e1368)

dhEx458, daf-7(e1372)

dhEx480(mir-241(mut-abcd)::GFP), N2

dhEx480,daf-12(rh61rh411)

dhEx480,daf-9(dh6)

dhEx480,daf-9(dh6); din1(dh149)

GR1427, mgEx674(mir-84::GFP), N2

mgEx674, daf-12(rh61rh411)

mgEx674, daf-9(dh6); din-1(dh149)

mgEx674, daf-7(e1372)

mgEx674, daf-2(e1368)

mgEx674, daf-9(dh6)

Table 4: Gene alleles / strains

Microscopy

5.11 Microscope

Microscopy was performed with a Zeiss Axioscope 2plus and an Axiocam MRm, using Axiovision 4.1 software. Excretory cell GFP expression (mir-241p::gfp) or seam cell expression (mir-84p::gfp) was scored by eye (n>20), as well as quantified by comparison of micrographs taken with 100X or 63X lens, usually 10 or more pictures per genotype/condition. Worm tissues scored as "off" had no detectable GFP, "low" as hardly detectable GFP, and “high” as everything else easily seen.

5.12 Fluorescence microscopy filter sets

The following filter sets were used together with the Zeiss Axioscope2 for fluorescence quantification by eye and by Axiovision software:

GFP – Chroma Technologies #41018 “Endow Longpass Emission”

YFP – Chroma Technologies #41028 “YFP/GFP BP (10C/TOPAZ)”

CFP – Chroma Technologies #31044v2 “Cya GFP”

dsRed - – Chroma Technologies “Filter Set 15”

5.13 Bionocular

A Leica MZ FLIII was used for fluorescence observation and analysis of worms on plates. The binocular was equipped with the following filter sets: GFP, dsRed, CFP

Cell culture and luciferase assay

HEK293T cells were cultivated in DMEM with 25mM glucose (GibcoBRL 11995-065) supplemented with 10% FBS (HyClone SH30088.03) for normal cultivation and 10% charcoal/dextran-treated FBS ("ssFBS", HyCloneSH30068.03). Luciferase assay was performed in white, clear bottom 96 well plates (Corning Costar 3610) with 30.000 cells in 100µl ssFBS-DMEM per well. Cells were transfected 16h after seeding with 0.4µl of a 2M $CaCl_2$ solution,

30ng transcription factor vector, 30ng luciferase reporter vector, 5ng beta-gal expression vector and 60ng *TOPO TA* vector (Invitrogen 45-0641) in 3.7µl total volume per well. This was combined while vortexing with an equal volume of 2xHBS buffer (280mM NaCl, 10mM KCl, 1.5mM Na_2HPO_4, 12mM dextrose, 42mM HEPES) to form calcium phosphate precipitate and directly applied to cells. 8h after transfection, a ssFBS-DMEM-ligand solution with 2.16x ligand concentration was prepared and 92.6µl were applied per well. Luciferase activity was assayed 16h after ligand addition: Medium was decanted and 50µl of assay buffer were added per well.

Assay buffer consisted of 10% "10x core buffer" (300mM Tricine pH7.8, 80mM Mg Acetate (Sigma M0631), 2mM EDTA), 1% Triton X-100, 0.5mM D-Luciferin (Invitrogen L2912), 1.5mM ATP (Sigma A8937), 0.5mM Coenzyme A Sodium salt (Sigma C3144), and 0.7% 2-Mercaptoethanol (Sigma M6250) and incubated for 1min at 24°C before reading in a Luminoskan Ascent (Lab Systems) luminometer. Subsequently, beta-galacotsidase activity as transfection control was measured after the luciferase reading in the same well by adding 125µl beta-gal buffer consisting of 60mM Na_2HPO_4, 40mM NaH_2PO_4, 8mM KCl, 0.8mM $MgCl_2$, 0.04% 2-Nitrophenyl-β-D-galacto-pyranoside (Sigma N1127), 0.3% 2-Mercaptoethanol. After 10min incubation at 24°C, absorption at 405nm was measured in a Power-Wave XS (Bio-Tek) plate reader. Relative luciferase units were divided by the beta-galactosidase OD_{405} to generate the luciferase activity corrected for variations in transcription efficiency.

5.14 Luciferase assay data

Four different combinations of transcription factor expression vector, luciferase reporter vector and ligand conditions were tested for each reporter including the empty *ptk-luc* luciferase vector:

a) DAF-12 expression vector, reporter vector, subsequent addition of Δ^4-DA (shown as solid green in Fig. 1) to see transcriptional effects dependent on both DAF-12 and ligand

b) GFP expression vector, reporter vector, subsequent addition of Δ^4-DA (shown as striped green in Fig. 1) to see transcriptional effects dependent only on the ligand and cell culture endogenous factors

c) DAF-12 expression vector, reporter vector, subsequent addition of ethanol as vehicle (shown as solid red in Fig. 1) to see transcriptional effects dependent on DAF-12 without ligand

d) DAF-12 expression vector, reporter vector, subsequent addition of ethanol as vehicle (shown as striped red in Fig. 1) to see transcriptional effects dependent only on ethanol and cell culture endogenous factors.

Each of these four conditions was tested in triplicate for each of the used promoter reporter constructs. Figure 7, Figure 26 A, Figure 31, Figure 33, Figure 41 and following page: Figure 42 show luciferase quantification values as "Relative Luciferase Units" to show transcriptional effect of any of the four tested conditions, while Figure 9 and Figure 50 show fold change of luciferase quantification values between DAF-12 expression vector transfected wells with ligand in presence of either wild type or mutant promoter to show the change caused by the promoter modifications. Figure 26 B shows fold induction of ligand supplemented versus ethanol control wells that were both transfected with DAF-12 expression vector and the same reporter.

Error bars of diagrams showing RLU are standard deviations, while error bars of diagrams showing fold-induction values reflect the compound error.

5.15 Gel Shift

Protocol for Electrophoretic Mobility Shift Assay was modified after Timchenko (Timchenko et al., 1999). A 10cm dish of HEK293T cells was transfected using Fugene6 reagent (Roche 11 814 443 001) according to manufacture´s protocols. 6µg DNA and 18µl Fugene6 were used for a 10cm culture. Cultures were placed on ice for nuclear extraction, washed with Buffer A (25mM Tris-HCl pH 7.5, 50ml KCl, 2mM $MgCl_2$, 1mM EDTA, 5mM Dithiothreitol in water) and detached with a cell scraper into 1ml Buffer A that was transferred into a 1.5ml tube. Cells were pelleted and supernatant aspirated before the cell pellet was passed eight times through a syringe (BD 1cc Insulin Syringe" U-100 28G 1/2") for cell rupture. Released nuclei were pelleted by 10min centrifugation at 10.000g and 4°C. The cytosolic fraction in the supernatant was removed and the pellet re-dissolved in Buffer B (25mM Tris-HCl pH 7.5, 420mM NaCl, 1.5mM MgCl2, 0.5mM EDTA, 1mM Dithiothreitol, and 25% sucrose in water) and incubated for 30 min with occasional vortexing for nuclei rupture and release of nuclear proteins. The suspension was centrifuged for 20min at 20.000g to pellet cell debris, and supernatant was frozen at -20°C for later use.

Single stranded oligos were annealed by heating 10µg of each oligo in 100µl with 10% 20xSSC to 95°C for 1min and returning to 24°C over three hours. Half the annealing mix was separated on a wide pocket 15% acryl amid gel (stock 30% Acrylamid/Bis 19:1, Bio-Rad 191-

0154) in 0.5x TBE and stained with ethidium bromide (Sigma E1385). The overloaded, unstained band of the ds oligo was cut out, transferred to a 0.5ml tube with the tip perforated and stuffed with glas wool (Supelco 2-0411) and placed inside a 1.5ml tube. Water / ssoligo was eluted by centrifugation at 20.000g for 10 min. 2µl of the eluted ds oligos were labeled by incubation with 2u Klenow(3´exo$^-$) fragment (NEB M0212S), NEBuffer 2, 2µl of each 10mM ATP, GTP, TTP and radio labeled CTP (Amersham, AA0075) for 1h at 24°C. The labeled oligo was purified by spinning through a G50 Sephadex Column (Roche #11 273 965 001) with 1100g for 4min after a 2min and 1100g column pre-run.

Following oligos were used:

241a (wt sequence forward: agg_tactaatataaagtaccatttct and reverse: agg_agaaatggtactttatattagta, mutant forward: agg_tactaatataaGgtaccatttct and reverse agg_agaaatggtacCttatattagta)

241b (wt sequence forward: agg_tccaaaagtgcgtttttctctctgt and reverse: agg_acagagagaaaaacgcacttttgga, mutant forward: agg_tccaaaGgtAcCtttttctctctgt and reverse agg_acagagagaaaaaGgTacCtttgga)

241cd(wt sequence forward: agg_tgtacttttataaaagtgcatccct and reverse: agg_agggatgcacttttataaaagtac, mutant for cd forward: agg_tgtacttttataaaGGTACCtccct and reverse agg_agggaGGTACCtttataaaagtaca, mutant for c only forward: agg_tactaatataaGgtaccatttct and reverse agg_agaaatggtacCttatattagta, mutant for d only forward: agg_tccaaaGgtAcCtttttctctctgt and reverse agg_acagagagaaaaaGgTacCtttgga)

TRE-wt (wt sequence forward: AGG_atcaaaagtggaacaaaagttccatttctt and reverse: AGG aagaaatggaacttttgttccacttttgat, negative mutant forward: AGG_atcaaaGgtACCacaaaGgtAccatttctt and reverse: AGG_aagaaatggTacCtttgtGGTacCtttgat, positive mutant forward: and reverse AGG_aagaaatTgCacttttgttGcacttttgat).

5-10µg Protein was bound to 1µl of the oligo labeling reaction by 30min incubation at 24°C with 20mM Tris-HCl ph 7.5, 100mM KCl, 2mM $MgCl_2$, 5mM DTT and 10% glycerol). The

whole annealing reaction was separated on a 18x20cm 5% acryl amide/TBE gel and stopped when bromophenol blue marker migrated 2/3 towards the gel bottom, transferred to 3MM chromatography paper (Whatman 3030347) and vacuum dried on a gel dryer (Bio-Rad Model 583). The dried gel was exposed for 10min to 1d onto 8x10in BioMax XAR film (Kodak F5513).

RNA extraction

For total RNA extraction, 20 young adult worms were picked to a new, seeded NGM plate and incubated at 20°C. After two and three days, 100µl of 10x over night OP50-LB culture was added to the plate and after four days now mostly adult staged worms were bleached and eggs were pipetted to plates with the final growth conditions, using glass Pasteur pipettes. When most worms reached the desired stage, worms were washed off the plate and sedimented for 15min in a vertical 5ml glass tube on ice to separate worms from OP50 bacteria. Sedimented worms were transferred with glass Pasteur pipettes into a new 1.5ml bullet tube and pelleted. M9 volume was aspirated until 100µl M9/worm pellet remained. This was mixed with 1ml TRIzol Reagent (Invitrogen 15596-018). Worms were freeze-thawed in liquid nitrogen and 37°C water bath six times, and RNA was extracted according to GibcoBRL Trizol Reagent manual #15596.

Taqman Q-PCR

Total RNA was DNase treated (Invitrogen 18068-015) and diluted to 2ng/µl as template for Q-PCR using Taqman MicroRNA Assay (Applied Biosystems) reagents and its protocols to quantify cel-mir-48 (#4373463), cel-mir-84 (#4373490), cel-mir-241 (#4373438), has-let-7a (#4373169), using Taqman microRNA RT Kit (4366597) and Taqman Universal PCR MasterMix (4324018). hsa-miR-1 (# 4373161) was used as endogenous control. PCR reactions were performed in a ABIprism 7000 machine controlled by ABI SDS software version 1.2.3 which was also used for data analysis. Each bar represents mean relative quantification value of a technical triplicate on a single biological experiment, with error bars indicating maximum and minimum RQ values of the triplicate. A test for cross-reativity of microRNA specific primers and probes is shown in Figure 38.

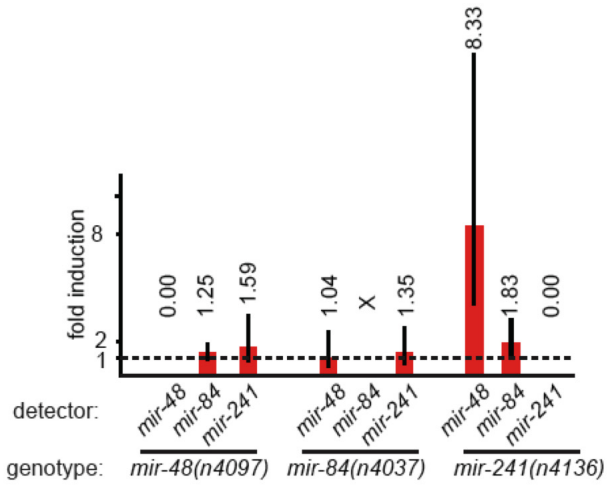

Figure 38: Cross reactivity of TaqMan Q-PCR primers and probes
Primers and probes were tested for cross reactivity by performing Q-PCR for *mir-48, -84, -241* on wild type and deletion strain with either one of the *mir-48, -84, -241* microRNAs deleted. One biological replicate with n>4000 L3 stage animals per genotype.

Data analysis

EC50 values were calculated using GraphPad5 to fit a non-linear least squares regression curve to the data values. Error bars in luciferase assay data plots are explained in the "Luciferase assay data" paragraph.

6. Appendices

Appendix 1: *Him4*/hemicentin is transcriptionally regulated by *daf-12*

The cytosekeleton and the extracellular matrix interact to give shape and movement to cells during development, since they can generate force and displacement. HIM-4 is an extracellular matrix protein with s size of 5198aa (Vogel and Hedgecock, 2001). It contains conserved domains, among others N-terminal secretion signal, 48x repeat of Ig modules and a 3fold repeat of EGF. HIM-4 is expressed and secreted from a wide variety of cells, where it induces hemidesmosome formation, or multimerises to form fine, linear tracks to guide cell migrations, e.g. for linker cell of male gonad that leads gonad migration, or to lesser extend migration of the distal tip cell (DTC) of hermaphrodite gonad. Defects of *him-4* lead to germline chromosome loss, tissue fragility and defective cell migration of the male linker cell. A GFP reporter consisting of a *him-4* promoter with in-frame *gfp* fused to the N-terminus lacking the excretion domain is expressed in hermaphrodite DTC during the migration turn towards dorsal and back to midbody. This expression coincides with the heterochronic "Mig" phenotype that certain *daf-12* signaling mutants show. The ligand binding domain truncation *daf-12(rh61)* or point mutation alleles *rh273* and *rh274* show this phenotype, as well as a *daf-9(rh50)* dafachronic acid synthesis hypomorphic allele. The *daf-12(rh61rh411)* null allele only shows a migration defect when in background of other heterochronic mutants, e.g. a null allele of the *lin-29*/ZiFi protein or a hypomorph of the *dre-1*/F-box protein.

When analyzing *him-4* promoter activation in different backgrounds I found a partial *daf-12* dependence. Wild type and *daf-12* null mutants do not show a Mig phenotype and 100% of all DTC express *him-4p::gfp* (Figure 39). RNAi knock down of *lin-29* and *dre-1* caused migration defects in *daf-12(rh61rh411)* null background, and loss of *lin-29* does not affect *him-4* DTC expression, while loss of *dre-1* does.

Dafachronic acid synthesis hypomorphic *daf-9(rh50)* allele and the *daf-12(rh61)* allele both cause highly penetrant Mig phenotype, and both can be rescued by RNAi knock down of *daf-12* co-repressor *din-1*, but only *daf-9(rh50)* is rescued for both, migration defect and *him-4* expression by ligand supplementation (Figure 39 E).

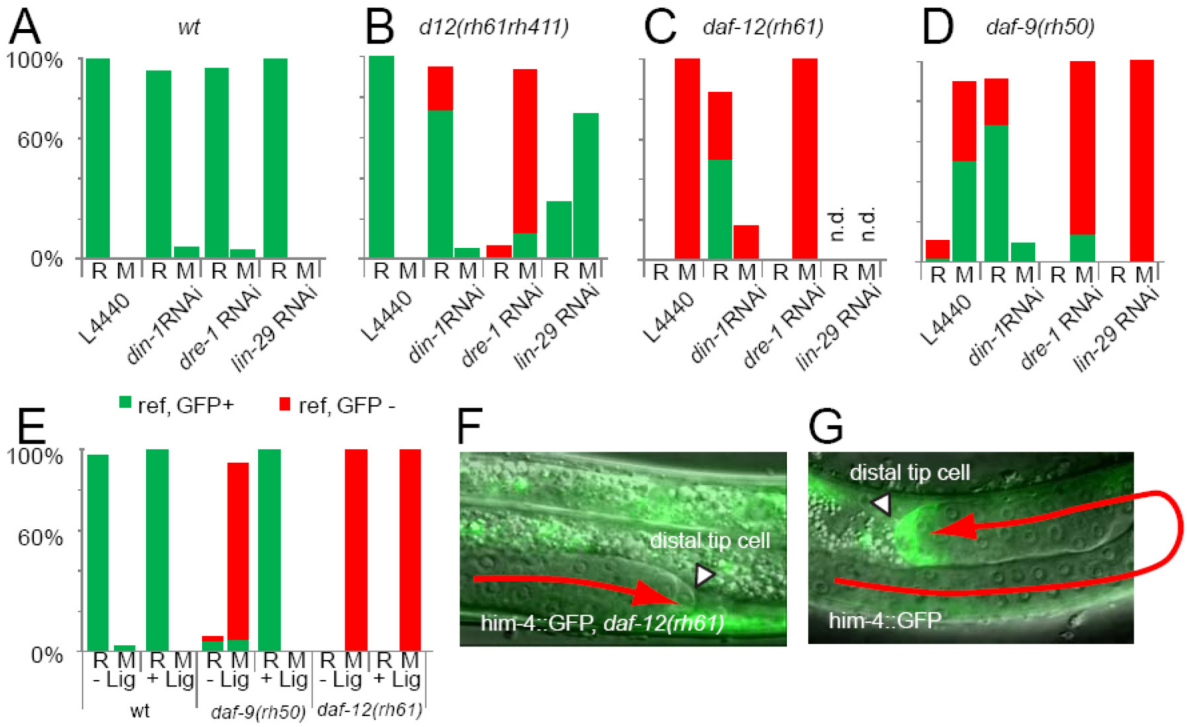

Figure 39: *Him-4* regulation is *daf-12* dependent
Him-4p::gfp expression in distal tip cell at 30h-45h of age in wild type (A), *daf-12(rh61rh411)* (B), *daf-12(rh61)* (C) and *daf-9(rh50)* (D) background on RNAi against *din-1, dre-1* or *lin-29*. Shown are percent of distal tip cells expressing GFP (green) or no GFP (red), percent of distal tip cells that are reflexed ("R") and non reflexed showing the Mig phenotype ("M"), n>20 for each bar. Only in mutations affecting upstream acting *daf-9*, but not in *daf-12lbd* mutants is *him-4p::gfp* reporter expression dafachronic acid dependent (E). A distal tip cell showing Mig phenotyp (F) or wild type reflexed migration (G) in *him-4p::gfp* reporter background.

However, DAF-12 and a *him-4* promoter luciferase reporter were co-transfected into human embryonic kidney cells, no luciferase activation was noticeable after ligand application, arguing for a either a non-direct *daf-12* regulation of the *him-4* promoter, or the requirement for *C. elegans* specific co-factors not available in human cell culture.

Appendix 2: Dafachronic acid derivatives and their effect on DAF-12

The luciferase assay used in Chapter 2 allows rapid *in vitro* testing if compounds can bind to DAF-12/NHR and influence its transcriptional activation. By using this assay, I tested several hypotheses.

6.1 Glycinoeclepin A drivatives as DAF-12 ligand

Δ^4- and Δ^7-dafachronic acid were suggested to be the natural ligands of DAF-12 (Motola et al., 2006). However, a structurally related compound, Glycinoeclepin A, was reported to act as a potent egg hatching factor in plant parasitic neamtodes (Fukuzawa et al., 1985; Masamune et al., 1982). The main structural difference of this compound compared to the dafachronic acids is a further oxidation and ring-opening. The structure and function of the egg hatching factor might be conserved in other nematode species, and similar compounds might be present in *C. elegans*, acting as natural DAF-12 ligands of even higher activity. This led the lab of E.J. Corey to wonder if a ring-opening reaction performed on the dafachronic acids, that converts them into Glycenoeclepin-like compounds, would turn them into more potent ligands for DAF-12, noticeable in higher transcriptional activation of DAF-12/NHR.

Simon Giroux of the E.J. Corey lab synthezised the Glycinoecleptin A-like oxidation product of dafachchronic acids and I tested the product along with intermediates and other derivatives for their biological activity *in vitro* and *in vivo*. Luciferase assay was performed with cells co-transfected with DAF-12 expression vector and *lit-1* promoter luciferase reporter (Shostak et al., 2004). Different concentrations of compounds were tested on these cells for their capacity to induce DAF-12 dependent transcriptional activation.

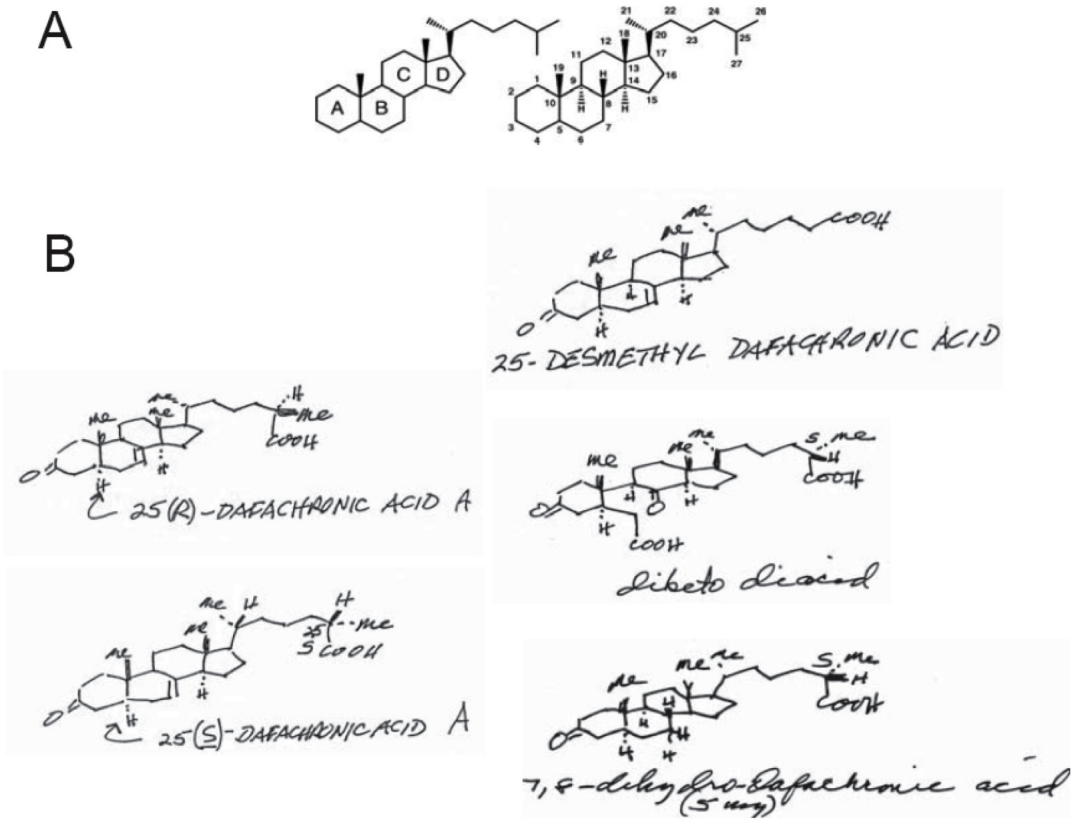

Figure 40: Dafachronic acid derivatives
Structure of the dafachronic acid derivates tested for the E.J. Corey lab. Panel A shows nomenclature of ring and carbon atom positions. Panel B: (25R)-Δ^7-dafachronic acid; (25S)-Δ^7-dafachronic acid; Δ^7-desmethyl dafachronic acid; (25S)-7,8-dihydro dafachronic acid; (25S)-diketodiacid-dafachronic acid. Drawings by E.J. Corey. Structures of (25S)-Δ^4-dafachronic acid is shown in Figure 2.

I found that compounds with a double bound in Δ^4- position are generally less active then those with a double bound in Δ^7-position: EC_{50} values of (25S)-Δ^7- and (25R)-Δ^7-dafachronic acid are 26 and 64 nM. (4S and 4R vs. 7S and 7R in Figure 41). Chirality at position 25 also influenced activity, with the R-configuration in all cases being more active then the S-configuration (4S and 7S vs. 4R and 7R in Figure 41). Removal of the methyl group at position 25 of Δ^7-dafachronic acid strongly decreased the activity (7DM in Figure 41 A). Saturation at the Δ^4- or Δ^7-double bound only mildly decreased activity to an EC_{50} value of 114nM (7,8DH in Figure 41 B), while ring opening at that position to a diKeto-diAcid derivative similar to Glycenoeclepin A lead to a total loss of activity (diKdiA Figure 41).

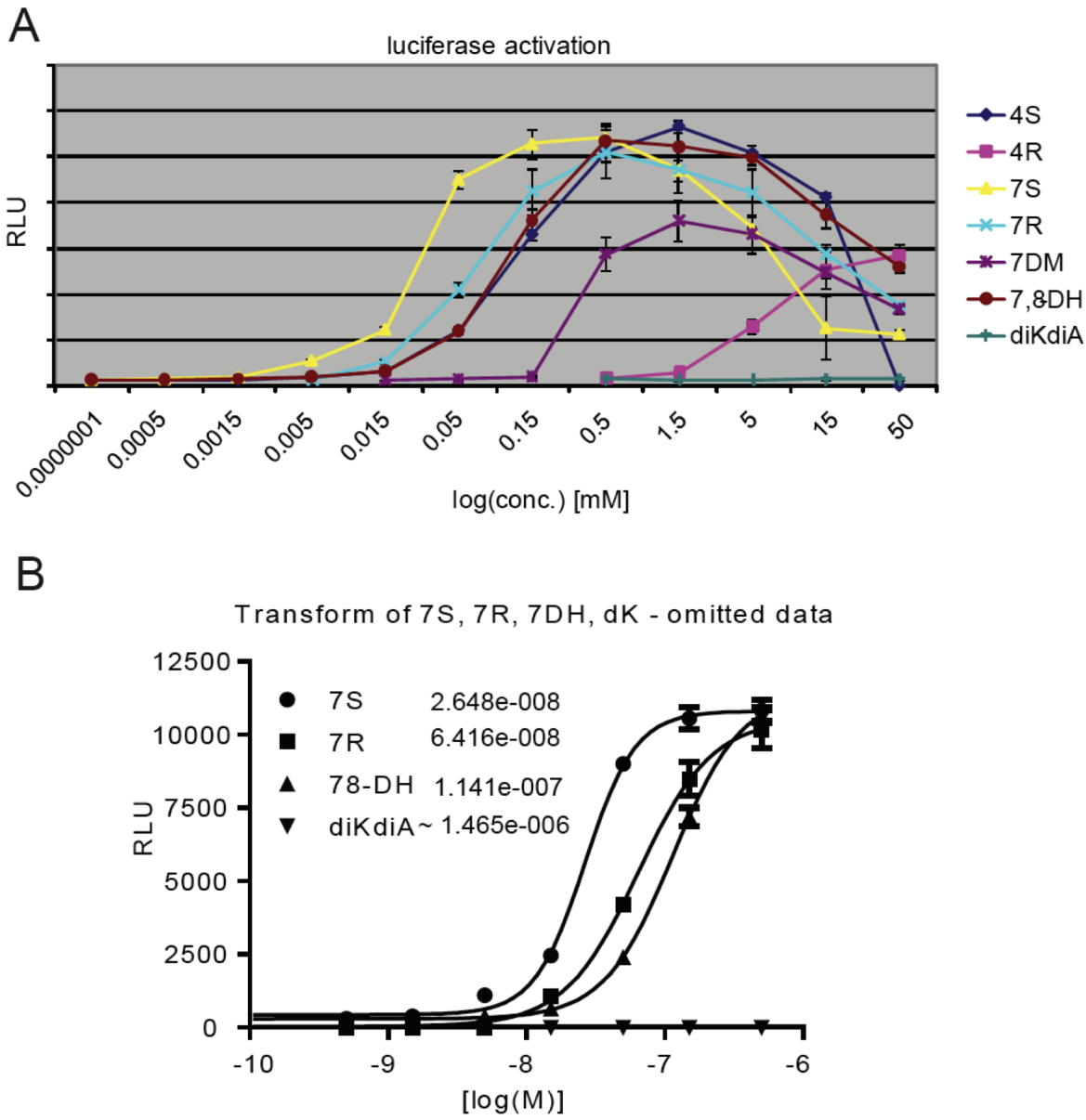

Figure 41: DAF-12 activation by dafachronic acid derivatives
Various dafachronic acid derivatives were tested for their transcriptional activation of DAF-12 in a luciferase assay with *mir-241* promoter luciferase reporter. "4S" = (25S)-Δ^4-dafachronic acid; "4R" = (25R)-Δ^4-dafachronic acid; "7S" = (25S)-Δ^7-dafachronic acid; "7R" = (25R)-Δ^7-dafachronic acid; "7DM" = Δ^7-desmethyl dafachronic acid; "7,8DH" = (25S)-7,8-dihydro dafachronic acid; "diKdiA" = (25S)-diketodiacid-dafachronic acid. EC_{50} values shown in B in Mol. Assays were repeated once with similar results

6.2 Ascr#3 interact and DAF-12/NHR or DAF-9/CYP450

C. elegans excretes compounds, called "dauer pheromones", that are capable of inducing dauer formation even during good environmental conditions. Recently, the chemical structures was elucidated for dauer pheromone component ascr#3, member of a compound class called

"ascarosides" (Butcher et al., 2007; Pungaliya et al., 2009; Srinivasan et al., 2008). I hypothesized that these compounds exert their effect by interacting with either one of the dauer preventing genes DAF-12/NHR or DAF-9/CYP450 to block dafachronic acid activation of DAF-12, or dafachronic acid production. I tested the ascarosides for interference with either DAF-12 transcriptional activation or with DAF-9/CYP450 mediated biosynthesis of the DAF-12-ligands in an *in vitro* luciferase assay. The co-repressor DIN-1/SHARP is the main co-regulator of DAF-12 during dauer formation (see Chapter 1.3.7), and candidate for ascaroside induced DAF-12 interaction. For that reason I co-expressed DIN-1/SHARP during several of the luciferase assays.

6.2.1 Ascr#3 and DAF-12/NHR

Dafachronic acid and DAF-12 activate transcription of the promoter of a luciferase reporter containing the promoter of *mir-241*, a direct transcriptional target of DAF-12 (Bethke et al., 2009). If ascarosides can interact with DAF-12, they are likely to suppress the dafachronic acid dependent activation. I found that increasing concentrations of ascr#3 do not strongly inhibit dafachronic acid dependent transcriptional activation by DAF-12, and conclude that ascr#3 does not interact directly with DAF-12 to prevent DAF-12 mediated promotion of developmental progression *in vivo* (following page: Figure 42 A). The ascr#3 concentrations used compare to up to 400nM found in a very dense *C. elegans* liquid culture under optimal cultivation conditions (Frank Schroeder, personal communication). Concentrations in nature are expected to be far lower.

6.2.2 Ascr#3 and DAF-9/CYPp450

DAF-12 is unable to activate the *mir-241* promoter reporter in presence of lathosterone instead of dafachronic acids (Motola et al., 2006). Lathoseterone is the direct precursor of dafachronic acid and substrate for DAF-9/CYP450 that oxidizes the 26 position carbon of lathosterone into a carboxy group to give the active dafachronic acids. Co-transfection of a daf-9 expression construct supplies enzymatic activity for the lathosterone conversion to dafachronic acid, and increasing doses of lathosterone lead to increased DAF-12 activation of the *mir-241* promoter reporter (following page: Figure 42 B). I used this co-transfection assay to test if ascr#3 can interact with DAF-9/CYP450 to prevent lathosterone turn over to dafachronic acids *in vivo* and this way prevent developmental progression and induce dauer formation. I found that increasing doses of ascr#3 do not inhibit the DAF-9/CYP450 mediate conversion of lathosterone to dafachronic acid (following page: Figure 42 C).

6.3 Δ^4- and Δ^7-dafachronic and DAF-9/CYPp450?

It is assumed that Δ^4- and Δ^7-dafachronic acid are the natural ligands of DAF-12/NHR and the final biosynthetic products of the DAF-9/CYPp450 oxidation that show maximum DAF-12 transcriptional activation (following page: Figure 42 D). To test if this is true, or of DAF-9/CYPp450 can further oxidize dafachronic acids to higher active ligands, I measured DAF-12 and Δ^4-dafachronic acid dependent activation of the *mir-241* promoter reporter in absence and in presence of DAF-9/CYPp450 expression vector. I found that DAF-9 co-transfection can increase Δ^4-dafachronic acid activation of DAF-12 (following page: Figure 42 F). This observation raises the possibility that dafachronic acids can be further modified to a yet undescribed compound that is a more potent ligand for DAF-12. However, I need to test if this result is not an artifact due to impurities of the Δ^4-dafachronic acid or quality variations of the DNA samples used to transfect cells.

following page: Figure 42: Ascaroside asc#3 does not interact with DAF-12 or DAF-9
A luciferase reporter containing the *mir-241* promoter is strongly activated when DAF-12, DIN-1 and 400nM Δ^4-dafachronic acid are present, and varying concentrations of ascr#3 (panel E for molecular structure) do not change the DAF-12 and ligand dependent activation (A). Activation of *mir-241* promoter luciferase reporter is strongest in presence DAF-9, DAF-12 and 10µM lathosterone (B). DAF-9 mediated turn over of lathosterone is not suppressed by different concentrations of ascr#3 (C). *mir-241* promoter luciferase reporter activation in DAF-12 presence is <10 fold stronger with Δ^7-dafachronic acid then with Δ^4-dafachronic acid (D), and presence of DAF-9 can increase DAF-12 dependent transcriptional activation of the *mir-241* promoter luciferase promoter in presence of Δ^4-dafachronic acid (F). Assays were repeated once with similar results.

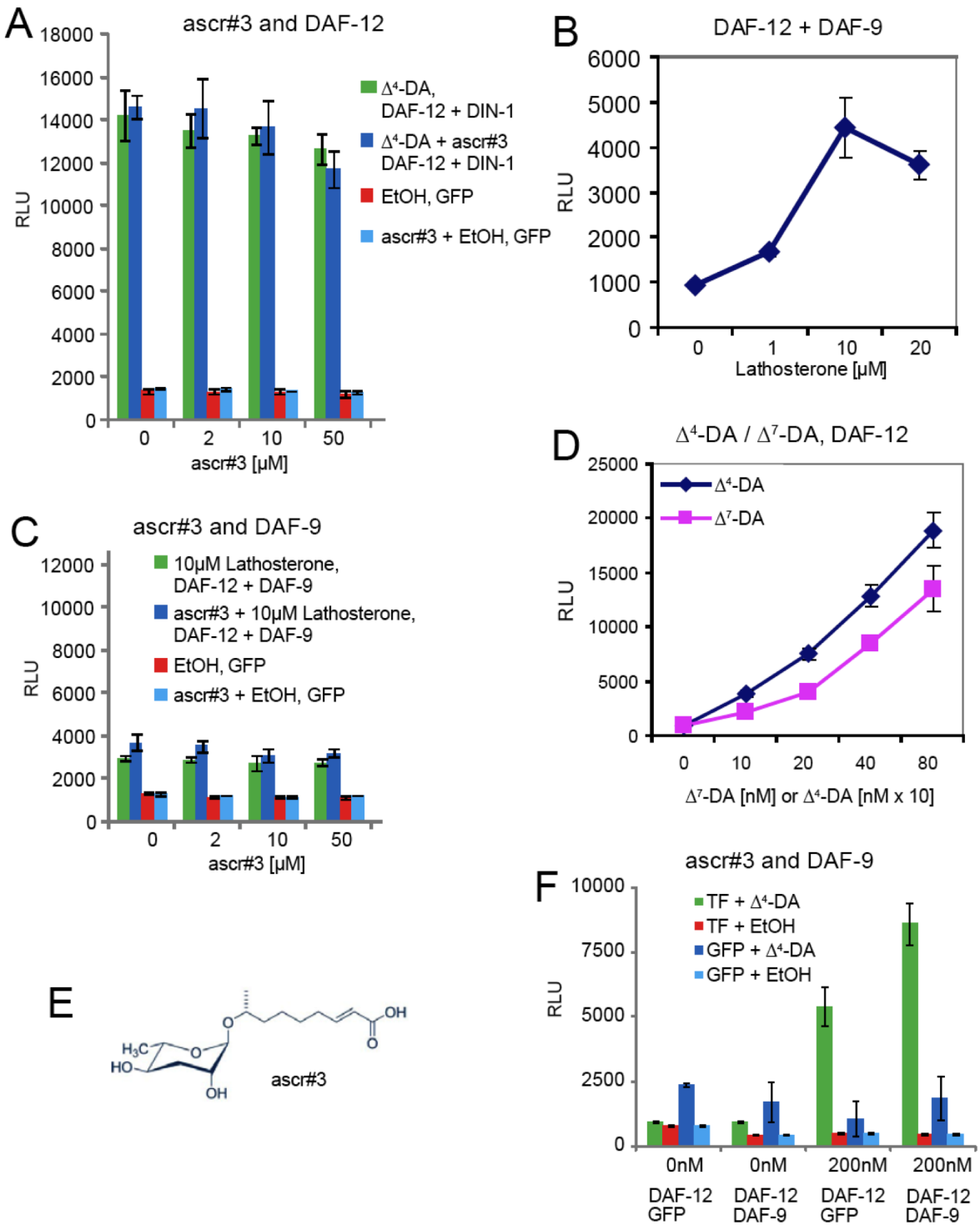
A
ascr#3 and DAF-12
RLU
18000
16000
14000
12000
10000
8000
6000
4000
2000
0
0
2
10
50
ascr#3 [μM]
Δ4-DA, DAF-12 + DIN-1
Δ4-DA + ascr#3 DAF-12 + DIN-1
EtOH, GFP
ascr#3 + EtOH, GFP
B
DAF-12 + DAF-9
RLU
6000
5000
4000
3000
2000
1000
0
0
1
10
20
Lathosterone [μM]
C
ascr#3 and DAF-9
RLU
12000
10000
8000
6000
4000
2000
0
0
2
10
50
ascr#3 [μM]
10μM Lathosterone, DAF-12 + DAF-9
ascr#3 + 10μM Lathosterone, DAF-12 + DAF-9
EtOH, GFP
ascr#3 + EtOH, GFP
D
Δ4-DA / Δ7-DA, DAF-12
RLU
25000
20000
15000
10000
5000
0
0
10
20
40
80
Δ7-DA [nM] or Δ4-DA [nM x 10]
Δ4-DA
Δ7-DA
E
ascr#3
F
ascr#3 and DAF-9
RLU
10000
7500
5000
2500
0
0nM
0nM
200nM
200nM
DAF-12 GFP
DAF-12 DAF-9
DAF-12 GFP
DAF-12 DAF-9
TF + Δ4-DA
TF + EtOH
GFP + Δ4-DA
GFP + EtOH

Appendix 3: Transcriptional activation versus UTR-mediated repression

During the work with microRNA and the translational repression they cause, it became important to measure both promoter derived transcriptional activation and separately from that promoter derived transcriptional activation minus UTR-mediated translational repression. To eliminate animal-to-animal variations, the perfect system would allow measuring both values in the same animal but independently of each other. To obtain cellular resolution and measurement in live animals, fluorescent proteins regulated by the promoters and 3'UTRs of interest appeared to be the tool of choice. A previous publication showed that two GFP variants, Cyan Fluorescent Protein (CFP) and Yellow Fluorescent Protein (YFP) are detectable separately without significant cross-activation (Miller et al., 1999) and I decided to use these two chromophores regulated by only the promoter or the promoter together with the 3'UTR. I generated two different types of constructs: one type contains a fusion of the *yfp* coding region to the promoter of interest and a stable, non-repressed *unc-54*-UTR to generate a stable mRNA that is translated to YFP according to transcriptional activation only. The second type of construct contains a CFP instead of a YFP coding region, and a UTR that is candidate for translational repression instead of the non-repressed *unc-54*-UTR (**Error! Reference source not found.** A).

When transforming *C. elegans* by germline injection, the injected plasmid DNA is re-arranged into long arrays and relatively stable inherited through mitosis and meiosis. To test for repeatable ratio of two plasmids injected in equimolar amounts, I used two nearly identical plasmids (A245 and A246) that only differed in a few base pairs defining the differences between CFP and YFP and measured fluorescence intensity in multiple, independently generated transgenic worm lines.

Fluorescence channel images for the CFP and for the YFP channel showed identical distribution that, when color coded and over layered gave a nearly homogenous mixed color showing equal distribution throughout all worm tissues (**Error! Reference source not found.** B-E). Pixel intensity measurement of the pharyngeal lobe of several animals of several independently derived transgenic worm lines also gave reproducible ration between CFP and YFP intensities (**Error! Reference source not found.** F). As a negative control, worm lines were generated carrying only one of the chromophore expression vectors, and animals of these strains gave strong signal in the channel corresponding to the chromophore expressed from the

injected plasmid, but no signal in the channel corresponding to the chromophore expression vector that was not injected (data not shown).

To introduce the 3'UTR-mediated repression component in this balanced system, I next injected an equimolar mix of the *yfp* plasmid with and a different *cfp* plasmid that had the un-repressed *unc-54*-UTR exchanged for a 3'UTR that is expected to mediate repression. Candidates were the *hbl-1*-UTR, the *daf-12*-UTR and the *daf-16*-UTR. I found that the newly introduced, repression-candidate UTRs led to a strong, partially tissue selective decrease of chromophore expression (**Error! Reference source not found.** G-J). The same decrease in chromophore expression level was observed for both chromophores when fused to the repression-candidate UTR (**Error! Reference source not found.** J). This repression was not alleviated by RNAi against key components of the RNAi machinery (*alg-2* and *dcr-1*, observation of YFP/CFP ratio by eye, n>10 animals per condition, RNAi positive control were severe tissue malformations on plates with RNAi against the mRNAs that were absent from plates with control vector).

I next tried to test *hbl-1*-UTR repression activity in the seam cells during L3 stage, as observed in Figure 18 of Chapter 2 . Unfortunately, the *daf-12* promoter used for chromophore expression constructs activated only very weakly in this tissue, preventing a use of this system for the measurement of *hbl-1*-UTR mediated repression.

Table 5: Double-tagging plasmid constructs

	promoter	chromophore	UTR	construct
1	*myo-3*	*cfp*	*unc-54*	A245
2	*myo-3*	*yfp*	*unc-54*	A246
3	*daf-12*	*cfp*	*unc-54*	A433
4	*daf-12*	*yfp*	*unc-54*	A434
5	*daf-12*	*cfp*	*daf-12*	A453
6	*daf-12*	*yfp*	*daf-12*	A454
7	*daf-12*	*cfp*	*hbl-1*	A443
8	*daf-12*	*yfp*	*hbl-1*	A444

In this appendix, I found that extrachromosomal arrays consisting of equimolar injected identical chromophore expression plasmids yield reproducible chromophore expression ratios

that is maintained during reproduction. This observation supports the feasibility of the double-tagging approach described above. However, expression level of the repression-candidate 3'UTR plasmids did not increase when key components of the machinery were knocked out that mediates the RNAi/microRNA mediate 3'UTR-repression. From this observation I cannot conclude if the initial loss of is due to 3'UTR-mediated repression, or simply a loss of mRNA stability compared to the *unc-54* UTR or any other mechanism negatively influencing the expression in a UTR dependent way. A possible test is to cross the array containing both chromophore plasmids into *daf-12(rh61)* background and look for chromophor expression level changes, as ibserved for hbl-1-UTR constructs in Figure 18.

following page: Figure 43: CFP/YFP tagging
The *yfp* expression vector contains a non-repressed UTR (green) and expression intensity of the chromophor*e in vivo* represents transcriptional activation of the promoter, while the *cfp* vector contains the repressed UTR (red) and expression intensity of the chromophore represents transcriptional activation minus UTR-mediated translational repression (A). DIC image (B) of a worm transgenic with a *yfp* and a *cfp* expression vector that carry both the *myo-3* promoter and the *unc-54*-UTR as regulatory sequences. CFP channel image (D) and YFP channel image (E) show identical chromophore fluorescence levels, and result in homogenous mixed color when colored channel images are over layered (C). The average ratio of measured pixel intensity was constant throughout three of four independently generated transgenic worm lines (CY1-2, CY5-1, CY1-3, CY5-9), transgenic with extra chromosomal arrays consisting of equimolar amounts of both *cfp* and *yfp* expression vectors containing the *daf-12* promoter and the *unc-54*-UTR (vectors A433 and A434) (F). G-I: A worm line transformed with an equimolar mix of *yfp* vector with the *daf-12* promoter and the *unc-54*-UTR, and *cfp* vector with the *daf-12* promoter and the *daf-12*-UTR (vectors A433 and A453). The YFP channel (H) shows strong expression in several tissues, while the strongly enhanced CFP channel image (I) shows loss of fluorescence in most tissues other then few cells, e.g. in the body wall (arrow). Panel G shows the corresponding DIC image.
Diagram J shows the average ratio of YFP over CFP pixel intensity in a defined tissue (big pharyngeal lobe) measured in three independently generated worm lines. Worm lines C1-4 and C1-5 were transgenic with equimolar mixes of *yfp* expression vector containing the *daf-12* promoter and the *unc-54*-UTR and *cfp* expression vector containing the *daf-12* promoter and the *daf-12*-UTR. Worm line Y9-1 was transgenic with an equimolar mix of *yfp* expression vector containing the *daf-12* promoter and the *daf-12*-UTR and *cfp* expression vector containing the *daf-12* promoter and the *unc-54*-UTR, shown in G-I. B-e, G-I: n>20 animals were observed and representative images are shown, F-J: count was performed once.

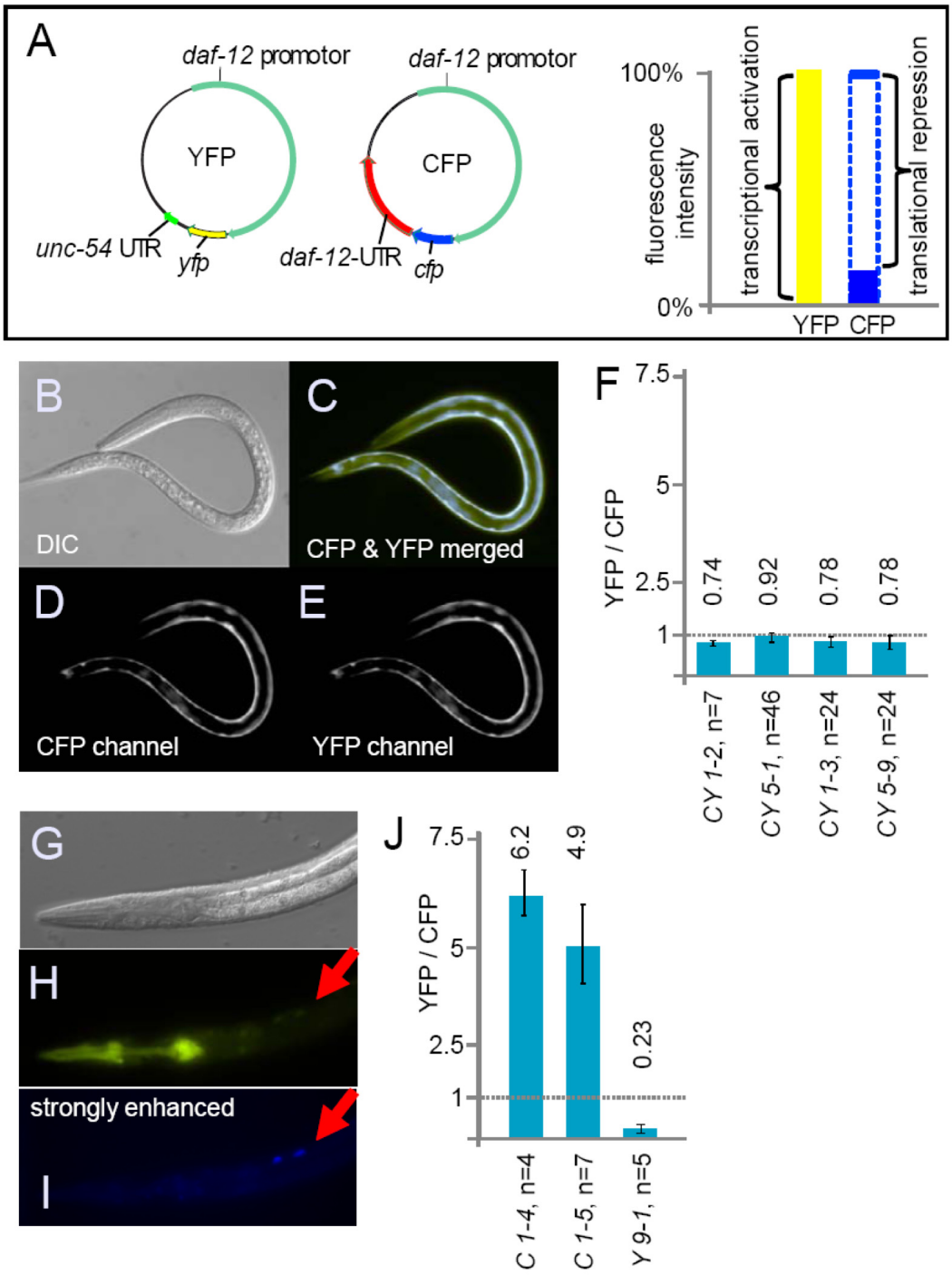
A
daf-12 promotor
YFP
unc-54 UTR
yfp
daf-12 promotor
CFP
daf-12-UTR
cfp
100%
0%
fluorescence intensity
transcriptional activation
translational repression
YFP
CFP
B
DIC
C
CFP & YFP merged
D
CFP channel
E
YFP channel
F
YFP / CFP
7.5
5
2.5
1
0.74
0.92
0.78
0.78
CY 1-2, n=7
CY 5-1, n=46
CY 1-3, n=24
CY 5-9, n=24
G
H
strongly enhanced
I
J
YFP / CFP
7.5
5
2.5
1
6.2
4.9
0.23
C 1-4, n=4
C 1-5, n=7
Y 9-1, n=5

Appendix 4: Conservation of *cis*-regulatory motifs in *let-7* family microRNA promoters

To test these candidate DAF-12 dependent and independent CRMs, I analyzed the promoters by sequence comparison to related nematode species. Clustalw alignment of *C. elegans*, *C. briggsea* and *C. brenneri* showed conservation between long regions of the *myo-2* promoter that was analysed in detail (Okkema et al., 1993; Thatcher et al., 1999) (Figure 44) to test if ClustalW is functional for testing promoter conservation between these three species.

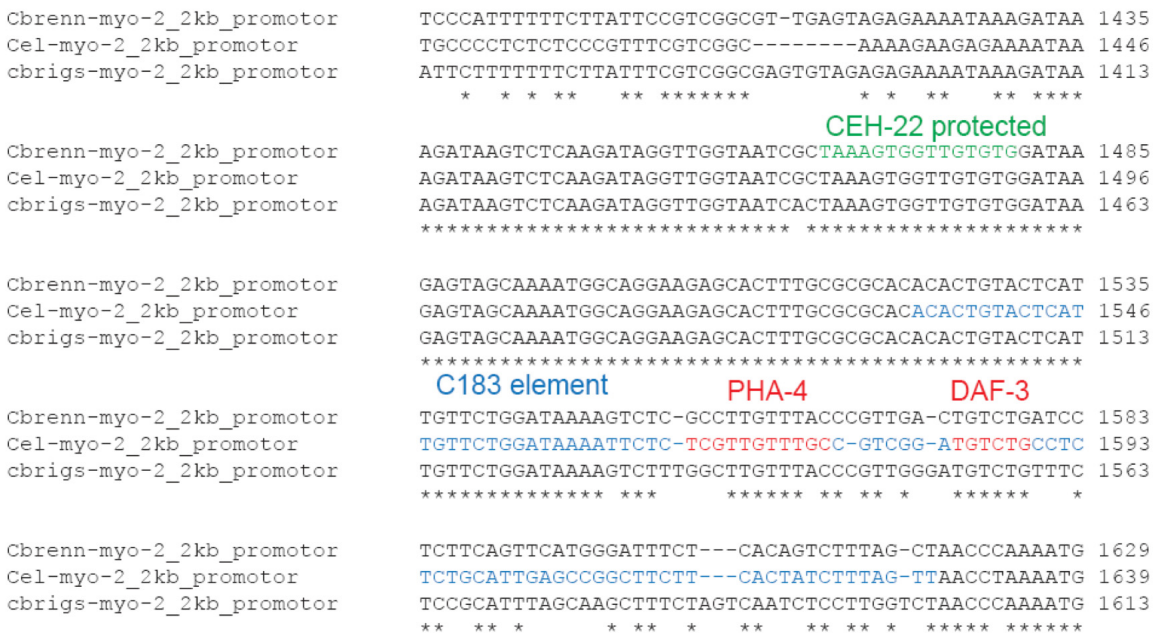

Figure 44: Cross-species alignment of *myo-2* promoter
Part of the ClustalW alignment of a 2kb *myo-2* promoter sequences from *C. brenneri* (Cbrenn), *C. briggsea* (Cbrigs) and *C. elegans* (Cel). The C183 element is marked in blue, and defined transcription factor binding sites are marked in red. Nucleotide numbers on the right indicate distance to start of alignment of 2kb sequence upstream of the *myo-2* start codon.

However, the same alignment strategy revealed a far lower conservation of promoters of the *mir-84*, *mir-241* and *let-7* microRNA promoters.

Figure 45: Cross-species alignment of 84e
Part of the ClustalW alignment of *mir-84* promoter sequences from *C. brenneri* (Cbren), *C. briggsea* (Cbrig) and *C. elegans* (Cel). Marked in blue is the sequence repeated in 84e reporter constructs. Nucleotide numbers on the right indicate distance to start of the alignment of 1.1kb sequence upstream of first nucleotide of the *mir-84* seed sequence. DAF-12-like a DAF-3-like CRMs are marked in red.

Only the pharyngeal expressed 84e CRM shows high conservation surrounding the DAF-12-like CRM (Figure 32). The seam and hypodermal expressed 84d CRM is much less conserved (Figure 46).

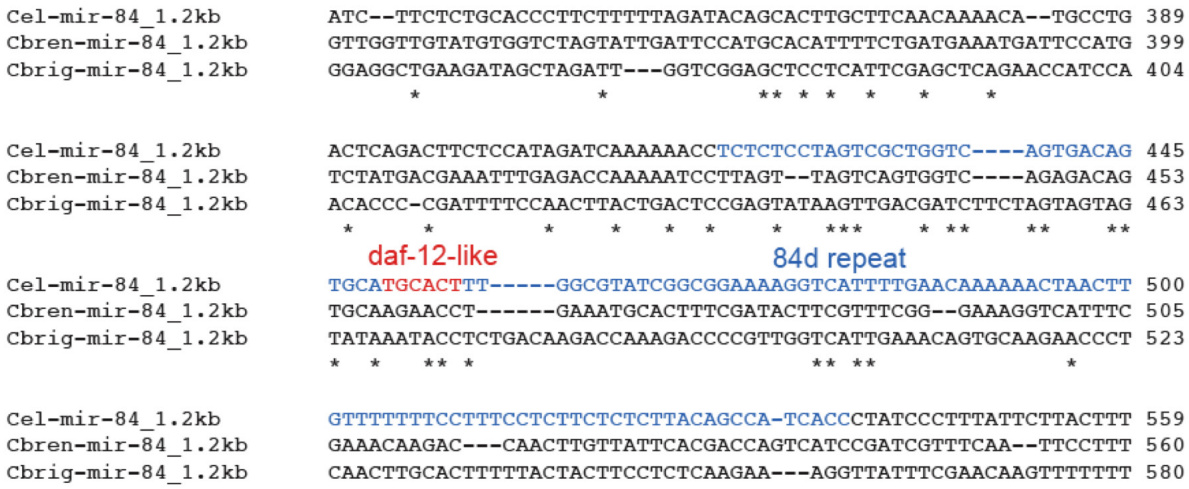

Figure 46: Cross-species alignment of 84d

Part of the ClustalW alignment of *mir-84* promoter sequences from *C. brenneri* (Cbren), *C. briggsea* (Cbrig) and *C. elegans* (Cel). Marked in blue is the sequence repeated in 84d reporter constructs. Nucleotide numbers on the right indicate distance to start of the alignment of 1.1kb sequence upstream of first nucleotide of the *mir-84* seed sequence. The DAF-12-like CRM is marked in red.

In the mir-241 promoter, the completely daf-12 dependent 241ab CRM construct shows a much lover conservation (Figure 47) then the less daf-12 dependent 241cd CRM (Figure 48).

```
Cbri-mir-241_1.1kb      CCCCT-TTTGATGACCTAGATAACTTATCATGGTCATCTTTTGCCTTCATAAC-TAGCCG 117
Cel-mir-241_1.1kb       CAATTGTTCAACCACTAACTTCCCCCAGCTTCATTGCCATAAATCCCCAAAACATACCTG 83
Cbre-mir-241_1.1kb      CAATCGTCATTCCATATATATCATTTATATTAATCAGAATGTA---CTAATACTCTCTTC 85
                        *     *      *   *  *     *   *  *     *        *  **

Cbri-mir-241_1.1kb      ACCCCTTACTTTACATCTCCATTTCGTTTTTGCTTTCCTTCC-TCAAATCTAATCTCAG- 175
Cel-mir-241_1.1kb       ATATTCTTCT----GATTACATTTCAAAT---CTCCTCGTCA-TCATAACTAGTCTCAAT 135
Cbre-mir-241_1.1kb      ATTTCTCTTT----CACTCTATTCCAAATGACATTCAATCCGGTGGCGCCGAGTGTCAG- 140
                        *        *       *  *** *   *    *      *  *     * * * ***
                                  DAF-12, 241a                241ab repeat
Cbri-mir-241_1.1kb      GTGCACTTTTTAGGCGAAATCACAGATTTGATTTCAAATAT-CACTCTTACT----AATC 230
Cel-mir-241_1.1kb       GTACTAATATAAAGTACCATTTCTCTTTTTCTCTCTCACGCATGTGCTTATTTCAGAATA 195
Cbre-mir-241_1.1kb      GAGCGGAT----AGCGCCTTCAAAGTGCTTCTTTCTC-----TGTTCCTCTC------TC 185
                        *  *   *     *     *        *  * **          * *         *
                                                    FLH-1
Cbri-mir-241_1.1kb      ACGGTGCACTTTCACATGCTACACGGGCGCCCGGTGC-CAAGCGCCGCGGAGTCTGGCGT 289
Cel-mir-241_1.1kb       TATATGCTCGGTGACATTCAATCCCTTCCTCCGCGGCGCCTGCGCCGAGAAGTCTGGCGT 255
Cbre-mir-241_1.1kb      CAAGTGCTTTCCGAAGTTTCAGAGCAATCC-----GCCCCGGCTCCG-----CTTCACAT 235
                            ***      *  *   *              ** *  ** ***       *  * *
                          DAF-12, 241b
Cbri-mir-241_1.1kb      CCAAAAGTGC--TTCTTCTTCTGTCTCTAGTC----TCTCCAGTCTGCTCCTGAACTTCC 343
Cel-mir-241_1.1kb       CCAAAAGTGCGTTTTTCTCTCTGTTTCTCCACCGAGTTTCAGAGCAGAAGTAGAAGAAGA 315
Cbre-mir-241_1.1kb      CCAGTGCCAGGCTCCTCCATCTGCC-CTCTTTGCTCTCTCCGGTGCCCTTTTTC-CTCGG 293
                        ***         *  *   ****   **        * **
```

Figure 47: Cross-species alignment of 241ab
Part of the ClustalW alignment of *mir-241* promoter sequences from *C. brenneri* (Cbre), *C. briggsea* (Cbri) and *C. elegans* (Cel). Marked in blue is the sequence repeated in 84d reporter constructs. Nucleotide numbers on the right indicate distance to start of the alignment of 1.2kb sequence upstream of the first nucleotide of the *mir-241* seed sequence. DAF-12 and FLH-1 CRMs are marked in red.

Figure 48: species alignment of 241cd
Part of the ClustalW alignment of *mir-241* promoter sequences from *C. brenneri* (Cbre), *C. briggsea* (Cbri) and *C. elegans* (Cel). Marked in blue is the sequence repeated in 84d reporter constructs. Nucleotide numbers on the right indicate distance to start of the alignment of 1.2kb sequence upstream of the first nucleotide of the *mir-241* seed sequence. The DAF-12 CRMs are marked in red.

When aligning the TRE containing *let-7* promoter, I did not detect the degree of conservation reported by Johnson (Johnson et al., 2003) (Figure 49).

Figure 49: Cross-species alignment of TRE
Part of the ClustalW alignment of *let-7* promoter sequences from *C. brenneri* (Cbren), *C. briggsea* (Cbr) and *C. elegans* (Cel). Marked in blue is the sequence repeated in TRE reporter constructs. Nucleotide numbers on the right indicate distance to start of the alignment of 1.9kb sequence upstream of the first nucleotide of the *let-7* seed sequence. The DAF-12;like CRMs are marked in red.

I tested the repeated promoter sequences for degree of sequence conservation between closely related nematode species to find CRMs that were functionally important and therefore conserved above non-important promoter regions.

Each CRM showed a different degree of conservation between different *Caenorhabditis* species, but the degree of conservation and functionality do not appear to correlate since the non-conserved 241ab CRM drives transcription in the most DAF-12 signaling dependent fashion.

This repeats the previous observation that CEH-10 and TTX-3 (Wenick and Hobert, 2004) motifs are conserved between *C. elegans* and *C. briggsea*, but that elements that are either lost or gained between species also are functional.

Appendix 5: Dimerization might influence DAF-12 transcriptional activation

The capacity of NHRs to form homo- or hetero dimers that change their ligand dependence (Forman et al., 1995) highlight the importance of the relative orientation of nuclear receptor REs inside specific CRM-constructs. I found that point mutation of a single DAF-12 RE that is part of a repeat (IR9 = 241cd, ER23 = 84ab) increases activity *in vitro* in promoter full length context, while mutation of other REs, e.g. 241ab, abolish *in vitro* activation (data shown above) (Figure 50).

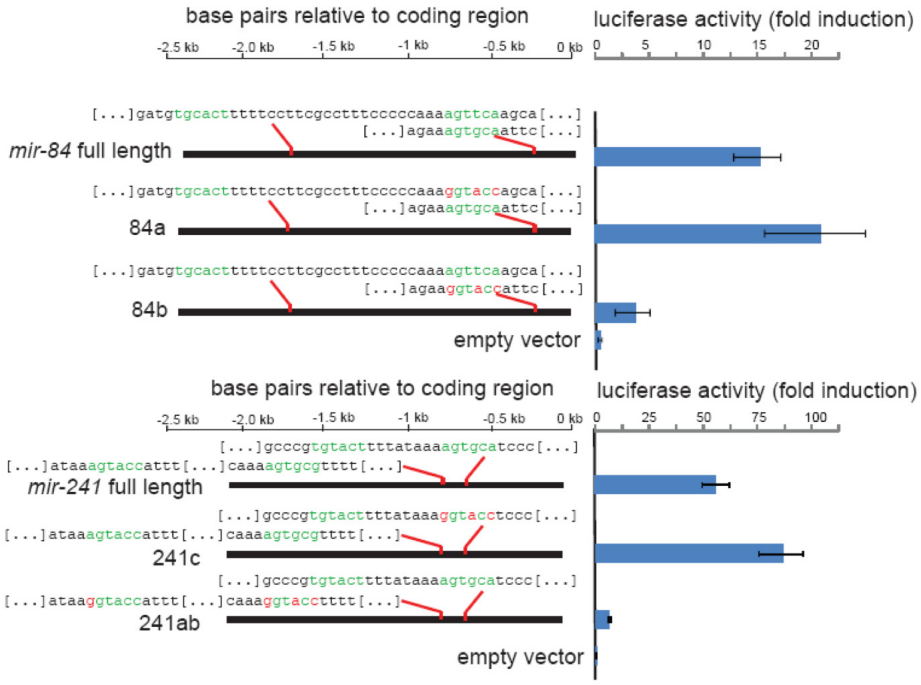

Figure 50: Luciferase assay of repeated response elements
Expression vectors for *daf-12* or *gfp* as control were transfected into Human Embryonic Kidney cell, along with vectors containing luciferase cDNA downstream of wild type or mutated versions of the *mir-84* or *mir-241* promoters followed by a minimal promoter. Displayed sequences are blown up from the marked full length promoter regions, with green marking wild type sequence of DAF-12-CRMs and red marking mutated nucleotides. Point mutation of the downstream RE of a repeat in both cases led to an increase of dafachronic acid dependent fold luciferase activation, while point mutation of the separately occurring RE lead to a strong loss of activation.

NHRs commonly bind to repeats of their REs and physically interact while bound to DNA(Forman et al., 1995). By showing that transcriptional activation through DAF-12 increases after loss of one REs out of a repeat, I indicate that dimerization might play a role in modulating

DAF-12 transcriptional activation. The *in vivo* regulation of the IR9 containing 241cd CRM is less stringent DAF-12 and ligand dependent then regulation of the 241ab site. A possible explanation is that a non-DAF-12 NRs is involved in DAF-12 hetero dimerisation, possibly connecting other NHR cascades to the 241cd CRM, or that the CRM sequence influences DAF-12 ligand responsiveness, as observed for the glucocorticoid receptor (Meijsing et al., 2009).

Appendix 6: List of heterochronic genes in *C. elegans*

name	time point	tissue	heterochronic phenotype	Molecular function	homolog	reference
ain-1	L1-Ad L2-L3?	vulva, neurons	retarded	microRNA processing	Drosophila GAWKY	(Ding et al., 2005)
ain-2	?					(Zhang et al., 2007)
alg-1/ alg-2		widely expressed from embryo to adult	retarded	RNA processing	Translation initiation factor 2C; Argnonaute like proteins in vertebrates	(Grishok et al., 2001)
cgh-1		germline		germline helicase		
daf-12	L2-L3	whole body, peaks at L2/L3	retarded	NHR	DHR96, LXR,VDR	(Antebi et al., 1998; Antebi et al., 2000)
daf-9	L2-L3	hypodermis, XXX neuron, spermatheca		CYP450		(Gerisch et al., 2001; Jia et al., 2002)
dcr-1		n.a.	retarded	RNA processing	DICER	(Grishok et al., 2001)

name	time point	tissue	heterochronic phenotype	Molecular function	homolog	reference
din-1	L2-L3	whole body		co-repressor	SHARP	(Ludewig et al., 2004)
dre-1	L2-L3	whole body	precocious	ubiquitinylation	human FBX011	(Fielenbach et al., 2007)
flh-1, -2, -3		embryogenesis	precocious	DNA binding	FLYWCH transcription factor	(Ow et al., 2008)
hbl-1	L1, L2-L3, L4-Ad	hypodermal syncytium neurons later muscle	precocious	nucleic acid binding	hunchback	(Fay et al., 1999) (Frand et al., 2005)
Kin-20	L4-Ad	hypodemis	precocious	circadian rhythm	drosophila timeless & doubletime	(Banerjee et al., 2005)
let-7	L4,-Ad	weak expression in most tissues, stronger in seam cells starting at L4	retarded	microRNA	*let-7*	(Pasquinelli et al., 2000; Reinhart et al., 2000)
lin-12	L4-Ad	vulva, hypodemis	precocious (gf)	notch ligand		(Solomon et al., 2008)
lin-14	L1-L2	neurons, intestine hypodermis	precocious	nuclear protein		(Ruvkun and Giusto, 1989)

name	time point	tissue	heterochronic phenotype	Molecular function	homolog	reference
lin-28	L1-Ad	hypodermis, muscle, neurons	precocious	RNA binding	human LIN28	(Arasu et al., 1991; Moss et al., 1997)
lin-29	L4-Ad	gonad at L3, hypodermis at L4, vulva & goand L4	retarded	ZiFi	EGR2	(Rougvie and Ambros, 1995)
lin-4	L2-Ad	everywhere	retarded	microRNA		(Lee et al., 1993)
lin-41	L4-Ad	hypodemis pharynx pharynx, intestine at L2/L3, L4	precocious	RBBC, RING finger, B-box, coiled-coil domain, translational inhibition	TRIM71	(Slack et al., 2000)
lin-42	each molt	seam cells, hyp. syncitium,	precocious	transcriptional regulator	period	(Jeon et al., 1999)
lin-46	L3, Ad	seam cell	retarded	Scaffolding protein	MoeA, gephyrin	(Pepper et al., 2004)
lin-58	L2-L3, L4-Ad	see *mir-48*	precocious	*mir-48 gf*	*let-7*	(Abrahante et al., 1998; Li et al., 2005)

name	time point	tissue	heterochronic phenotype	Molecular function	homolog	reference
Lin-66	L2/L3	body vulva muscle, intestine, neurons, hypodermis	retarded	novel	nematode specific	(Morita and Han, 2006)
mir-241	L2-L3	widely expressed after L2	retarded	microRNA	*let-7*	(Abbott et al., 2005)
mir-48	L2-L3	widely expressed after L2	retarded	microRNA	*let-7*	(Abbott et al., 2005)
mir-84	L2-L3, L4-Ad	widely expressed after L2	retarded	microRNA	*let-7*	(Abbott et al., 2005)
nhl-2		neurons, body muscle, pharynx		microRNA processing		(Hammell et al., 2009)
nhr-23	L4-Ad	germline during embryogenesis, intesitine and pharynx of all stages, peaks during intermolts	retarded	NHR, molting	*Drosophila* DHR3, ecdysone responsive	(Frand et al., 2005; Gissendanner et al., 2004)

name	time point	tissue	heterochronic phenotype	Molecular function	homolog	reference
nhr-25	L4-Ad	widely expressed during all stages, peaks during molts, succeeding *nhr-23* peaks	retarded	NHR, molting	*Drosophila* Ftz-F1, human LRH-1	(Frand et al., 2005; Gissendanner et al., 2004)
sop-2	L4-Ad	whole body	?	DNA binding HOX gene expression	related to Polycomb genes	(Zhang et al., 2004)
tim-1	L4-Ad	hypodermis	precocious	circadian rhythm	mammalian timeless / *Drosophila* doubletime	(Banerjee et al., 2005)

Nuclear Hormone Receptor Regulation of MicroRNAs Controls Developmental Progression

Axel Bethke,[1,2] Nicole Fielenbach,[1] Zhu Wang,[3] David J. Mangelsdorf,[3] Adam Antebi[1,4]*

In response to small-molecule signals such as retinoids or steroids, nuclear receptors activate gene expression to regulate development in different tissues. MicroRNAs turn off target gene expression within cells by binding complementary regions in messenger RNA transcripts, and they have been broadly implicated in development and disease. Here we show that the *Caenorhabditis elegans* nuclear receptor DAF-12 and its steroidal ligand directly activate promoters of *let-7* microRNA family members to down-regulate the microRNA target *hbl-1*, which drives progression of epidermal stem cells from second to third larval stage patterns of cell division. Conversely, the receptor without the ligand represses microRNA expression during developmental arrest. These findings identify microRNAs as components of a hormone-coupled molecular switch that shuts off earlier developmental programs to allow for later ones.

Lipophilic hormones coordinate organism-wide developmental progression in metazoans by binding to nuclear hormone receptors (NHRs), converting the presence or absence of ligand into changes in gene expression patterns (*1*). This regulation is conserved in the nematode *Caenorhabditis elegans*, where the nuclear hormone receptor DAF-12, a homolog of vertebrate liver X and vitamin D receptors, regulates developmental progression or arrest in response to the environment (*2*, *3*). In favorable environments, activation of transforming growth factor-β (TGF-β) and insulin/insulin-like growth factor (IGF) signaling cascades results in production of the DAF-12 steroidal ligands, the dafachronic acids (e.g., Δ^4-DA), which promote rapid progression through four larval stages (L1 to L4) to reproductive adults (*4*). In unfavorable environments, endocrine systems are suppressed, and DAF-12 without the ligand causes arrest at a stress-resistant, long-lived alternative third larval stage, called the dauer diapause (L3d) (*5*).

A more cell-intrinsic level of developmental control is exerted by microRNAs. MicroRNAs are ~20- to 22-nucleotide-long RNA molecules that bind to the 3′ untranslated region (3′UTR) of target messenger RNAs (mRNAs) and decrease their expression (*6*–*8*). Null mutants for several microRNA genes show tissue-selective failure of progression from one stage-specific program to the next, generally described as heterochronic phenotypes. These phenotypes are most visible in the hypodermis, where hypodermal seam cells undergo invariant asymmetric stem cell division patterns, in which one daughter cell fuses to the hypodermal syncytium, whereas the other retains stem cell character and its capacity to divide (*9*). Only during L2 do seam cells undergo one proliferative division before stem cell division, and repetition or loss of this program leads to changes in overall seam cell number in later stages. Finally, seam cell division ceases altogether by adulthood. Seam cells in animals with mutation of the microRNA *lin-4* repeat L1 programs of asymmetric cell division during L2 stage; a triple deletion of the *let-7* microRNA homologs *mir-48*, *-84*, *-241* (referred to as *let-7s*) repeat L2 programs of cell proliferation during L3 stage; and *let-7* null mutants repeat larval stage divisions and molting behavior in adults (*10*–*12*).

[1]Huffington Center on Aging, Department of Molecular and Cellular Biology, Baylor College of Medicine, One Baylor Plaza, Houston, TX 77030, USA. [2]University of Osnabrück, Fachbereich Biologie/Chemie, Barbarastrasse 11, 49069 Osnabrück, Germany. [3]Department of Pharmacology and Howard Hughes Medical Institute, University of Texas Southwestern Medical Center, 6001 Forest Park Road, Dallas, TX 75390, USA. [4]Max-Planck-Institute for Biology of Ageing, Gleulerstrasse 50a, D-50931 Cologne, Germany.

*To whom correspondence should be addressed. E-mail: aantebi@bcm.edu

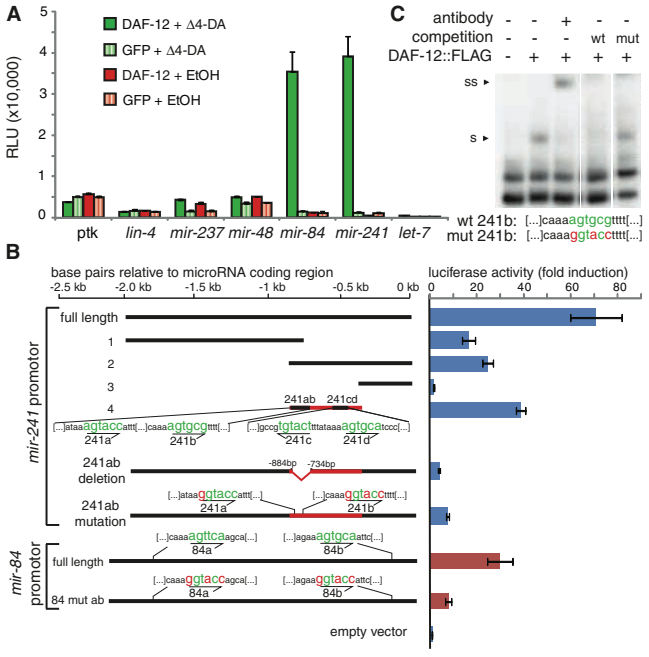

Fig. 1. DAF-12 and dafachronic acid (Δ^4-DA) activate microRNA promoters in vitro. (**A**) Activation of microRNA promoters in HEK293T cells. Promoters of *let-7* homologs, *mir-84* and *mir-241*, were strongly activated in the presence of DAF-12 and 400 nM Δ^4-DA, whereas other microRNAs were relatively unaffected. Luciferase assays were measured in triplicate and are shown with SD. EtOH, ethanol vehicle control; ptk, empty luciferase vector. (**B**) Mutation analysis of *mir-241p* and *mir-84p* reveals DAF-12–Δ^4-DA–activating elements. Deletion analysis of the *mir-241p* showed that the highest relative induction occurs with fragment 4, which contains four DAF-12 REs, 241a, b, c, and d. Deletion or point mutation of *241ab* elements (in red) abolished activation (blue bars). Similarly, point mutation of DAF-12 REs in *mir-84p*, 84a and b, reduced expression (red bars). (**C**) Gel mobility shift assay of DAF-12 and *mir-241p*. ^{32}P-radiolabeled oligomers containing the WT 241b element were shifted (s) by nuclear extracts expressing DAF-12::FLAG and supershifted (ss) in the presence of FLAG-specific antibody. Unlabeled WT 241b-oligomer prevented the shift, but addition of an oligomer with a point mutation did not.

daf-12(*rh61rh411*) null mutants exhibit a heterochronic phenotype similar to triple deletion of *let-7* family members *mir-48*,*mir-241*(*nDf51*); *mir-84*(*n4037*), resulting in extra seam cells at the L3 stage (table S1) (*2*, *11*). This observation suggested that *daf-12* might directly activate the *let-7s* microRNAs. To test this hypothesis, we fused the microRNA promoters *mir-241p* and *mir-84p* to the luciferase gene and co-transfected the reporters with DAF-12 into human cells (*13*). DAF-12 and Δ^4-DA strongly activated *mir-241p* and *mir-84p*, whereas other promoters gave little or no signal (Fig. 1A). Deletion analysis of the *mir-241p* revealed that, whereas several deletion mutations retained transcriptional activity in the presence of DAF-12 and Δ^4-DA, fragment 4 produced the highest fold induction, and its removal substantially reduced activity (Fig. 1B). This fragment contained two pairs of DAF-12 response elements (REs), as described by Shostak (*14*). In the full-length promoter context, mutation of one RE pair in *mir-241p* and two REs in *mir-84p* led to a decrease in activation of about seven- and threefold, respectively. Gel mobility shift assays confirmed in vitro binding of DAF-12 to these REs, whereas mutated versions abolished the interaction (Fig. 1C).

To examine microRNA expression in vivo, we generated transgenic worms containing the microRNA promoters fused to green fluorescent protein (GFP). Wild-type (WT) worms containing *mir-241p::GFP* gave a broad expression pattern as described (*15*). However, *daf-12* nulls showed decreased expression, most noticeably in the excretory cells (exc), as well as in muscles, pharynx, and intestine, although neuronal expression seemed less affected, which reveals the tissue selectivity of *daf-12* regulation (Fig. 2, A to D). Null mu-

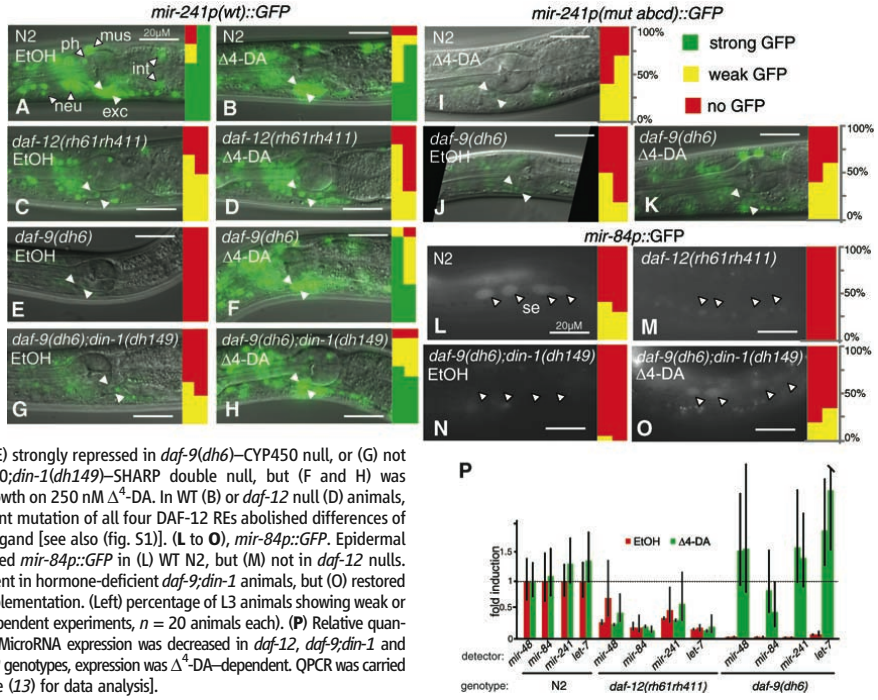

Fig. 2. DAF-12 and Δ^4-DA regulate microRNA promoters in vivo. (**A** to **K**) *mir-241p::GFP*. Images show representative L3 animals, with indicated cell types (white arrowheads and exc, excretory cell; outlined arrowheads, neu, neuron; mus, muscle; int, intestine; ph, pharynx). Bar graphs alongside the images quantify the percentage of worms with excretory cell GFP expression as either strong (green), weak (yellow), or off (red) (two independent experiments, left and right, $n = 10$ animals each). For *mir-241p::GFP* expression level in worms grown without ligand (EtOH) or with ligand (Δ4-DA). (A and B) WT (N2-type). (C) Expression was decreased in *daf-12*(*rh61rh411*)–NHR null, (E) strongly repressed in *daf-9*(*dh6*)–CYP450 null, or (G) not activated in *daf-9*(*dh6*)–CYP450;*din-1*(*dh149*)–SHARP double null, but (F and H) was rescued nearly to WT level by growth on 250 nM Δ^4-DA. In WT (B) or *daf-12* null (D) animals, Δ^4-DA had no effect. (I to K) Point mutation of all four DAF-12 REs abolished differences of tested genetic backgrounds or ligand [see also (fig. S1)]. (**L** to **O**), *mir-84p::GFP*. Epidermal seam cells (arrowheads) expressed *mir-84p::GFP* in (L) WT N2, but (M) not in *daf-12* nulls. (N) Seam cell expression was absent in hormone-deficient *daf-9;din-1* animals, but (O) restored to nearly WT levels by Δ^4-DA supplementation. (Left) percentage of L3 animals showing weak or no seam cell expression (two independent experiments, $n = 20$ animals each). (**P**) Relative quantification of microRNAs by QPCR. MicroRNA expression was decreased in *daf-12*, *daf-9;din-1* and repressed in *daf-9* mutants. In *daf-9* genotypes, expression was Δ^4-DA–dependent. QPCR was carried out using the TaqMan system [see (*13*) for data analysis].

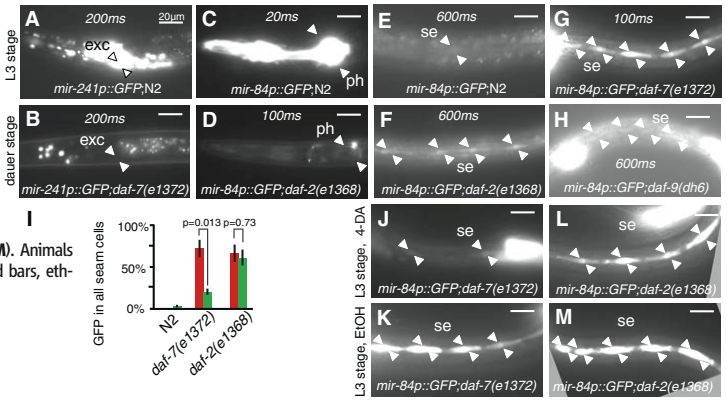

Fig. 3. MicroRNA regulation by dauer signaling pathways. *mir-241p::GFP* showed high expression in continuously growing WT (**A**), but low expression in *daf-7*(*e1372*) dauer larvae (**B**). *mir-84p::GFP* showed high expression in the pharynx of continuously growing WT (**C**) but low expression in *daf-2*(*e1368*) dauers (**D**). *mir-84p::GFP* seam cell expression (**E**) was elevated in *daf-2* and *daf-9* mutants during dauer stage (**F** and **H**) and was even higher in *daf-7* mutants during reproductive growth at 20°C (**G**). Penetrant seam expression was reversed by 500 nM Δ^4-DA in *daf-7*, but not *daf-2*, during reproductive growth (**I** to **M**). Animals were assayed during L3 and/or L3d stages, $n > 20$. Red bars, ethanol vehicle, green bars, Δ^4-DA (SEM).

tants for cytochrome P-450 (CYP450) *daf-9*(*dh6*) fail to produce dafachronic acids, and DAF-12 without the ligand interacts with its co-repressor DIN-1–SHARP to repress transcriptional targets; together they cause constitutive developmental arrest and dauer larvae formation (*16*–*18*). In these hormone-deficient larvae, *mir-241p::GFP* expression was tightly repressed in most tissues (Fig. 2E). Supplementation with Δ^4-DA rescued this arrest and brought *mir-241p::GFP* expression back to WT levels (Fig. 2F). Tight repression was also relieved in *daf-9*(*dh6*);*din-1*(*dh149*) double-null mutants lacking the corepressor, with *mir-241p::GFP* expression levels similar to *daf-12* nulls (Fig. 2, G and H). Unlike *daf-12* nulls, however, Δ^4-DA supplementation of *daf-9;din-1* worms restored *mir-241p::GFP* expression back to WT levels. Point mutation of all four *daf-12*-REs in *mir-241p* resulted in the same weak expression level in WT, *daf-12* null with ligand, as well as *daf-9* null, and *daf-9*;*din-1* doubles with or without ligand (Fig. 2, I to K, and fig. S1), which revealed that these REs mediate both activation and repression. Thus, DAF-12 with the ligand works through its REs to mildly activate *mir-241p* in some tissues, whereas DAF-12 without the ligand, together with DIN-1, tightly represses expression in nearly all tissues.

As reported, *mir-84p::GFP* was expressed in pharynx, somatic gonad, seam cells, vulva cells, and, occasionally, in the intestine (*15*, *19*). Seam cell expression was absent in *daf-12* null and *daf-9;din-1* null worms, and expression was increased almost to WT levels in *daf-9;din-1* animals by addition of Δ^4-DA (Fig. 2, L to O), which explains *daf-12* heterochronic phenotypes as a failure to activate the microRNAs in temporally patterned tissues. By contrast, expression in other tissues, such as the pharynx, was less affected, which shows again tissue-specific *daf-12* regulation (fig. S2). The transcriptional regulation of the *let-7s* is also reflected in the abundance of total mature microRNAs as measured by TaqMan fluorescence-based quantitative real-time polymerase chain reaction (QPCR). *daf-12* mutants and *daf-9;din-1* animals showed decreased levels compared with WT, whereas *daf-9* nulls showed tight repression of *let-7* family of microRNAs (Fig. 2P and figs. S3 to S5). As expected, expression in *daf-9*, *daf-9;din1*, but not *daf-12*, mutants was rescued by Δ^4-DA.

The dauer signaling pathways work upstream of *daf-12* to govern organismal developmental progression and Δ^4-DA production. We therefore wanted to see if *let-7s* expression was affected by dauer constitutive mutant backgrounds of *daf-7*–TGF-β, *daf-2*–insulin/IGF-I receptor, and *daf-9*–CYP450. *mir-241p::GFP* expression was nearly completely repressed in these dauer larvae, whereas *mir-84p::GFP* was down-regulated in some tissues, such as the pharynx (Fig. 3, A to D), but consistently up-regulated and more penetrant in others such as the seam (Fig. 3, E to H). Even in reproductively growing L3 larvae, seam cell expression was more penetrant in *daf-2*(*e1368*) and *daf-7*(*e1372*) mutants than in WT (Fig. 3G). Δ^4-DA supplementation largely reversed this effect in *daf-7*, but not in the *daf-2* background (Fig. 3, I to M), which suggests that insulin/IGF and TGF-β signaling distinctly regulate *mir-84p* expression in a Δ^4-DA–independent and Δ^4-DA–dependent manner.

The zinc finger protein *hbl-1* (hunchback) is responsible for L2 proliferative programs of seam cells (*11*). *hbl-1* loss leads to a loss of proliferative programs and, hence, a decreased seam cell number (table S1). *let-7s* are proposed to inhibit *hbl-1*, through microRNA-mediated repression of its 3′UTR, because *let-7s* mutants have both increased seam number and *hbl-1::GFP* expression at L3 (*11*, *20*). Given that DAF-12 activates *let-7s*, we examined interactions with *hbl-1*. Consistent with the notion that *hbl-1* inhibition is promoted by NHR signaling, *daf-12* mutants and *daf-9;din-1* double-mutants have extra seam cells, the latter reversed by Δ^4-DA (table S1). Moreover, the penetrant extra seam phenotype of the *daf-12*(*rh61*) ligand–binding domain mutant was dependent on functional *hbl-1*(+), placing *daf-12* upstream of *hbl-1* by genetic epistasis. Accordingly, we observed consistent up-regulated hypodermal expression of *hbl-1p::GFP::hbl-1*–3′UTR during L3 in *daf-12*(*rh61*), but not in WT (Fig. 4, A and B). This up-regulation was likely due to loss of UTR-mediated repression, as exchange of the *hbl-1*–3′UTR for a nonrepressed *unc-54*–3′UTR led to equal hypodermal expression levels in both WT and the *daf-12*(*rh61*) background (Fig. 4, C and D).

In this work, we show that the NHR DAF-12 directly regulates the *let-7* relatives, *mir-84* and *mir-241*, and connects organism-wide commitments to cell intrinsic programs (Fig. 4E). These studies suggest a model whereby, in unfavorable environments, down-regulated insulin/IGF-1 and TGF-β pathways suppress dafachronic acid production and DAF-12 without the ligand together with co-repressor DIN-1 repress microRNA expression in most tissues and specify developmental arrest. Conversely, in favorable environments, stimulation of insulin/IGF-1 and TGF-β growth signaling pathways results in dafachronic acid production. DAF-12 with the ligand activates *let-7* homologs, which, in turn, down-regulate their target, *hbl-1*, and allows L2 to L3 transitions in the hypodermis. The use of this NHR-microRNA–coupled molecular switch to turn off earlier programs to allow for later ones is a function likely to be conserved and may be a paradigm for understanding hormone-dependent developmental progression, stem cell differentiation, maturation, or tumor formation in metazoans. In particular, activation of new programs and inhibition of earlier ones are critical for the fidelity of distinct developmental states, which may be less apparent in more complex animals whose cell lineages are unknown. In fact, DAF-12 itself is down-regulated by *let-7* at later stages, which suggests that both feedforward and feedback loops drive transitions (*21*). In *Drosophila melanogaster*, the steroid hormone ecdysone and its cognate receptor regulate developmental progression in part via *mir-14*, but it is not known whether regulation is direct or indirect (*22*). Our studies also reveal the intricacy of NHR signaling in an organismal context. They give visible evidence that receptors with the ligand can activate their targets, whereas receptors without the ligand can repress them, with vastly different outcomes for progression or arrest. This hormone-dependent modulation of target gene expression around basal transcription mirrors that seen with the vertebrate homolog LXR (*23*). Finally, DAF-12–NHR regulation of the microRNAs is highly tissue- and stage-specific, implicating other transcription factors, coregulators, and chromatin factors in the control of microRNA expression.

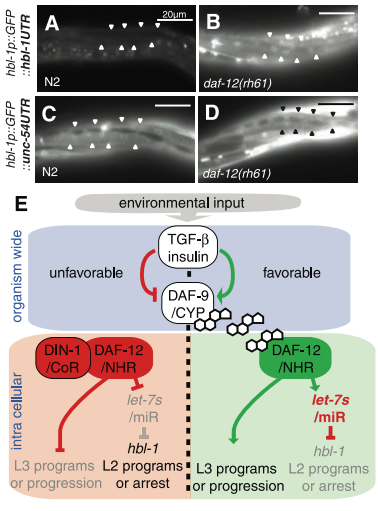

Fig. 4. *let-7s* repression target, *hbl-1*, is regulated by DAF-12. A GFP-fusion to *hbl-1* promoter and 3′UTR was repressed in the hypodermis at mid L3 (28 hours) in WT (**A**). In the *daf-12*(*rh61*) mutant, reporter signal was up-regulated in the hypodermis (arrows) and other tissues (**B**) (exposure 250 ms). A GFP-fusion to the *hbl-1* promoter, containing the *unc-54*–3′UTR lacked substantial up-regulation in the hypodermis (**C** and **D**), although body muscles showed modest reporter up-regulation (D) (exposure time 50 ms). (**E**) Model for NHR-microRNA signaling cascades (E). In response to favorable environmental signals, activated insulin/IGF and TGF-β pathways induce Δ^4-DA biosynthesis through DAF-9–CYP450. (Right) DAF-12 with the ligand activates L3 programs and expression of *let-7s* and thereby inhibits HBL-1 and genes of L2 programs, which result in developmental progression (E). (Left) During unfavorable conditions, DAF-12 without the ligand, together with DIN-1, repress L3 programs and *let-7s*, which allows derepression of L2 programs or developmental arrest. Dauer signaling also has Δ^4-DA–independent outputs onto microRNAs.

References and Notes

1. D. J. Mangelsdorf *et al.*, *Cell* **83**, 835 (1995).
2. A. Antebi, J. G. Culotti, E. M. Hedgecock, *Development* **125**, 1191 (1998).
3. A. Antebi, W. H. Yeh, D. Tait, E. M. Hedgecock, D. L. Riddle, *Genes Dev.* **14**, 1512 (2000).
4. D. L. Motola *et al.*, *Cell* **124**, 1209 (2006).
5. N. Fielenbach, A. Antebi, *Genes Dev.* **22**, 2149 (2008).
6. D. P. Bartel, *Cell* **116**, 281 (2004).
7. R. C. Lee, R. L. Feinbaum, V. Ambros, *Cell* **75**, 843 (1993).
8. B. Wightman, I. Ha, G. Ruvkun, *Cell* **75**, 855 (1993).
9. A. E. Rougvie, *Development* **132**, 3787 (2005).
10. M. Chalfie, H. R. Horvitz, J. E. Sulston, *Cell* **24**, 59 (1981).
11. A. L. Abbott *et al.*, *Dev. Cell* **9**, 403 (2005).
12. B. J. Reinhart *et al.*, *Nature* **403**, 901 (2000).
13. Materials and methods are available as supporting material on *Science* Online.
14. Y. Shostak, M. R. Van Gilst, A. Antebi, K. R. Yamamoto, *Genes Dev.* **18**, 2529 (2004).
15. A. Esquela-Kerscher *et al.*, *Dev. Dyn.* **234**, 868 (2005).
16. B. Gerisch, C. Weitzel, C. Kober-Eisermann, V. Rottiers, A. Antebi, *Dev. Cell* **1**, 841 (2001).
17. K. Jia, P. S. Albert, D. L. Riddle, *Development* **129**, 221 (2002).
18. A. H. Ludewig *et al.*, *Genes Dev.* **18**, 2120 (2004).
19. G. D. Hayes, A. R. Frand, G. Ruvkun, *Development* **133**, 4631 (2006).
20. M. Li, M. W. Jones-Rhoades, N. C. Lau, D. P. Bartel, A. E. Rougvie, *Dev. Cell* **9**, 415 (2005).
21. H. Grosshans, T. Johnson, K. L. Reinert, M. Gerstein, F. J. Slack, *Dev. Cell* **8**, 321 (2005).
22. J. Varghese, S. M. Cohen, *Genes Dev.* **21**, 2277 (2007).
23. J. J. Repa *et al.*, *Science* **289**, 1524 (2000).
24. Our thanks go to G. Hayes, G. Ruvkun, V. Ambros, and A. Rougvie for strains; N. Timchenko for gel shift support; and D. Magner, S. Greene, and F. Schroeder for manuscript comments. This work was supported by NIH grant GM077201 and the Ellison Medical Foundation (A.A.), and the Howard Hughes Medical Institute and the Robert A. Welch Foundation (D.J.M.).

Supporting Online Material

www.sciencemag.org/cgi/content/full/324/5923/95/DC1
Materials and Methods
Figs. S1 to S5
Tables S1 and S2
References

20 August 2008; accepted 11 February 2009
10.1126/science.1164899

Evidence for Cardiomyocyte Renewal in Humans

Olaf Bergmann,[1]* Ratan D. Bhardwaj,[1]* Samuel Bernard,[2] Sofia Zdunek,[1] Fanie Barnabé-Heider,[1] Stuart Walsh,[3] Joel Zupicich,[1] Kanar Alkass,[4] Bruce A. Buchholz,[5] Henrik Druid,[4] Stefan Jovinge,[3,6] Jonas Frisén[1]†

It has been difficult to establish whether we are limited to the heart muscle cells we are born with or if cardiomyocytes are generated also later in life. We have taken advantage of the integration of carbon-14, generated by nuclear bomb tests during the Cold War, into DNA to establish the age of cardiomyocytes in humans. We report that cardiomyocytes renew, with a gradual decrease from 1% turning over annually at the age of 25 to 0.45% at the age of 75. Fewer than 50% of cardiomyocytes are exchanged during a normal life span. The capacity to generate cardiomyocytes in the adult human heart suggests that it may be rational to work toward the development of therapeutic strategies aimed at stimulating this process in cardiac pathologies.

Myocardial damage often results in chronic heart failure due to loss and insufficient regeneration of cardiomyocytes. This has prompted efforts to devise cardiomyocyte replacement therapies by cell transplantation or by the promotion of endogenous regenerative processes. The development of cell transplantation strategies is advancing rapidly, and some are currently being evaluated in clinical trials (*1*, *2*). Stimulating endogenous regenerative processes is attractive as it potentially could provide a noninvasive therapy and circumvent the immunosuppression required for allografts. However, it is unclear whether such regenerative strategies are realistic because it has been difficult to establish whether cardiomyocytes can be generated after the perinatal period in humans.

Stem/progenitor cells with the potential to generate cardiomyocytes in vitro remain in the adult rodent and human myocardium (*3*, *4*). Moreover, mature cardiomyocytes have been suggested to be able to reenter the cell cycle and duplicate (*5*). However, studies over several decades in rodents with labeled nucleotide analogs have led to conflicting results, ranging from no to substantial generation of cardiomyocytes postnatally (*6*). A recent genetic labeling study, which enabled detection of cardiomyocyte generation by stem/progenitor cells (but not by cardiomyocyte duplication), demonstrated cardiomyocyte renewal after myocardial injury, but not during 1 year in the healthy mouse (*7*).

It is possible that humans, who live much longer than rodents, may have a different requirement for cardiomyocyte replacement. Cell turnover has been difficult to study in humans because the use of labeled nucleotide analogs and other strategies commonly used in experimental animals cannot readily be adapted for studies in humans owing to safety concerns. The limited functional recovery after loss of myocardium and the fact that primary cardiac tumors are very rare indicate limited proliferation within the adult human heart (*8*). Several studies have described the presence of molecular markers associated with mitosis in the human myocardium (*5*), but this provides limited information because it is difficult to deduce the future fate of a potentially dividing cell in terms of differentiation and long-term survival.

We have measured carbon-14 (^{14}C) from nuclear bomb tests in genomic DNA of human myocardial cells, which allows retrospective birth dating (*9*–*11*). ^{14}C concentrations in the atmosphere remained relatively stable until the Cold War, when aboveground nuclear bomb tests caused a sharp increase (*12*, *13*). Even though the detonations were conducted at a limited number of locations, the elevated amounts of ^{14}C in the atmosphere rapidly equalized around the world as $^{14}CO_2$. After the Limited Nuclear Test Ban Treaty in 1963, the ^{14}C concentrations dropped exponentially, not primarily because of radioactive decay (half-life of 5730 years), but by diffusion from the atmosphere (*14*). Newly created atmospheric ^{14}C reacts with oxygen to form $^{14}CO_2$, which is incorporated by plants through photosynthesis. Humans eat plants, and animals that live off plants, so the ^{14}C concentration in the human body mirrors that in the atmosphere at any given time (*15*–*18*). Because DNA is stable after a cell has gone through its last cell division, the concentration of ^{14}C in DNA serves as a date mark for when a cell was born and can be used to retrospectively birth date cells in humans (*9*–*11*).

We first carbon-dated left ventricle myocardial cells, including cardiomyocytes and other cell types, to determine the extent of postnatal DNA synthesis in the human heart. DNA was extracted, and ^{14}C concentrations were measured by accelerator mass spectrometry (see tables S1 and S2 for ^{14}C values and associated data). The cellular birth dates can be inferred by determining the time at which the sample's ^{14}C concentration corresponded to the atmospheric concentration (Fig. 1A). ^{14}C concentrations from all individuals born around or after the nuclear bomb tests corresponded to atmospheric concentrations several years after the subjects' birth (Fig. 1B), indicating substantial postnatal DNA synthesis. Analysis of individuals born before the period of nuclear bomb tests allows for sensitive detection of any turnover after 1955, due to the marked increase in ^{14}C concentrations. By analyzing individuals born at different times before 1955 it is possible to establish the age up to which DNA synthesis occurs, or whether it continues beyond that age.

[1]Department of Cell and Molecular Biology, Karolinska Institutet, SE-171 77 Stockholm, Sweden. [2]CNRS UMR5208, Institut Camille Jordan, Université Claude Bernard Lyon 1, 69622 Villeurbanne cedex, France. [3]Lund Strategic Research Center for Stem Cell Biology and Cell Therapy, Lund University, SE-221 84 Lund, Sweden. [4]Department of Forensic Medicine, Karolinska Institutet, SE-171 77 Stockholm, Sweden. [5]Center for Accelerator Mass Spectrometry, Lawrence Livermore National Laboratory, 7000 East Avenue, L-397, Livermore, CA 94551, USA. [6]Department of Cardiology, Lund University Hospital, SE-221 85 Lund, Sweden.

*These authors contributed equally to this work.
†To whom correspondence should be addressed. E-mail: jonas.frisen@ki.se

ORGANIC LETTERS

2008
Vol. 10, No. 16
3643−3645

Syntheses and Biological Evaluation of B-Ring-Modified Analogues of Dafachronic Acid A

Simon Giroux,[†] Axel Bethke,[‡] Nicole Fielenbach,[‡] Adam Antebi,[‡] and E. J. Corey*,[†]

Department of Chemistry and Chemical Biology, Harvard University, 12 Oxford Street, Cambridge, Massachusetts 02138, and Huffington Center on Aging, Department of Molecular and Cellular Biology, Baylor College of Medicine, Houston, Texas 77030

corey@chemistry.harvard.edu

Received June 24, 2008

ABSTRACT

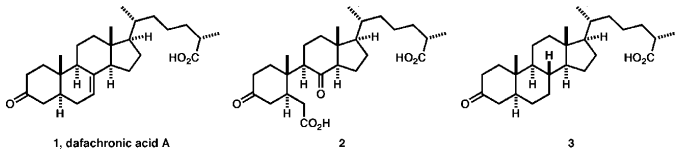

1, dafachronic acid A 2 3

Synthesis and testing of dafachronic acid A (1) and its derivatives 2 and 3 have revealed that 1, and not a further oxidation product, is the natural ligand for the DAF-12 receptor of *Caenorhabditis elegans*.

Remarkably, the life span of the nematode *Caenorhabditis elegans* can be increased significantly by loss of function of a handful of genes that affect endocrine function. Among them, the daf-9 gene encodes a cytochrome P450 enzyme which is responsible for the biosynthesis of the bile acid-like steroid, dafachronic acid A (**1**). Based on various analytical techniques, it has been recently proposed by Mangelsdorf and Antebi that **1** is the major ligand for the nuclear receptor DAF-12, which in its ligand bound form regulates genes that prevent entry into the dauer stage, a long-lived quiescent mode.[1] However, synthesis of the proposed ligand remained elusive until a later work, in which the 25-(*S*) structure of **1** and its 25-(*R*)-diastereomer were made.[2,3]

In this research, we address the question of whether dafachronic acid A is the true ligand for the nuclear hormone receptor DAF-12 or just a precursor of a further biooxidation product which is the actual ligand. We were intrigued by the fact that dafachronic acid A, with its Δ^7-olefinic linkage, might be further oxidized biologically to a seco acid structure resembling that of glycinoeclepin A,[4,5] a potent hatching factor for the eggs of the nematode *Heterodera glycines*

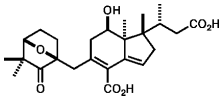

Figure 1. Structure of glycinoeclepin A.

[†] Harvard University.
[‡] Baylor College of Medicine.

(1) (a) Motola, D. L.; Cummins, C. L.; Rottiers, V.; Sharma, K. K.; Li, T.; Li, Y.; Suino-Powell, K.; Xu, H. E.; Auchus, R. J.; Antebi, A.; Mangelsdorf, D. J. *Cell* **2006**, *124*, 1209–1223. (b) Gerisch, B.; Rottiers, V.; Li, D.; Motola, D. L.; Cummins, C. L.; Lehrach, H.; Mangelsdorf, D. J.; Antebi, A. *Proc. Natl. Acad. Sci. U.S.A.* **2007**, *104*, 5014–5019. (c) Rottiers, V.; Motola, D. L.; Gerisch, B.; Cummins, C. L.; Nishiwaki, K.; Mangelsdorf, D. J.; Antebi, A. *Developmental Cell* **2006**, *10*, 473–482. (d) (c) For an online resource on *C. elegans*, see: http://www.wormbook.org.

(2) Giroux, S.; Corey, E. J. *J. Am. Chem. Soc.* **2007**, *129*, 9866–9867.
(3) Giroux, S.; Corey, E. J. *Org. Lett.* **2008**, *10*, 801–802.
(4) Glycinoeclepin A, a natural product that is released into soil from the roots of the soybean plant, is active at 10^{-12} g/mL as a hatching factor for *H. glycines*; see: (a) Fukuzawa, A.; Furusaki, A.; Ikura, M.; Masamune, T *J. Chem. Soc. Chem. Commun.* **1985**, *221−222*, 748. (b) Masamune, T.; Anetai, M.; Takasugi, M.; Katsui, N. *Nature* **1982**, *297*, 495–496.

10.1021/ol801425v CCC: $40.75
Published on Web 07/19/2008

Scheme 1. Synthesis of Analogues **2** and **3** from β-Stigmasterol

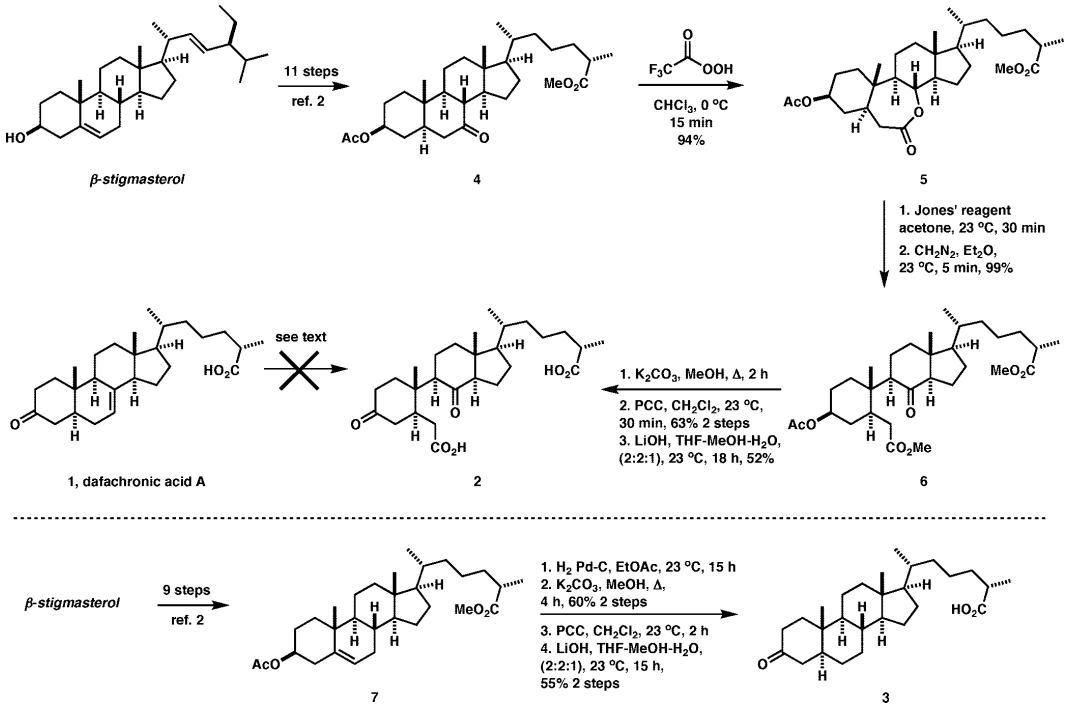

(Figure 1). Consequently, we became interested in exploring the biological activity of the β-seco dafachronic acid A derivative **2**, as an analogue of glycinoeclepin A, which might even be a more active metabolite of **1**. In this paper, we describe the synthesis and biological evaluation of **2**. For comparison, we have also synthesized the 7,8-dihydro derivative of dafachronic acid A, **3**, which would be expected to be devoid of activity if the seco acid **2** were the real ligand for DAF-12, rather than dafachronic acid A (**1**).

The synthesis of the diketo diacid **2** started with the previously reported 6-keto steroid **4**.[2] Baeyer−Villiger oxidation of **4** with trifluoroperacetic acid ($(CF_3CO)_2O$, H_2O_2, 0 °C, $CHCl_3$) afforded the desired 7-membered lactone **5** in 94% yield and as a sole regioisomer. Lactone **5** was cleaved to a ketoacid intermediate by treatment with Jones' reagent (2 equiv, 23 °C, acetone) which was esterified by diazomethane (CH_2N_2, Et_2O) to give ketoester **6** in essentially quantitative yield over two steps. Saponification of the 3β-acetate, oxidation of the resulting alcohol to the ketone, and hydrolysis gave the diketo diacid **2** in 52% overall yield (three steps, Scheme 1). Our initial strategy for the synthesis of **2** involved the oxidation of the Δ^7-olefinic linkage in **1** by various methods. Surprisingly, all attempts to directly oxidize the Δ^7 bond to the diketo diacid **2** using O_3 then H_2O_2, $KMnO_4$, NBu_4MnO_4, and $RuCl_3-NaIO_4$ were unsuccessful.

To synthesize the 7,8-dihydro analogue **3**, we have also used an intermediate from our synthesis of **1**.[2] Thus, the Δ^5-double bond in **7** was reduced (H_2, 1 atm, Pd−C, EtOAc) to give the fully saturated steroid, and the same three steps as above were performed to give analogue **3** in 33% overall yield for the four steps. It should also be mentioned that the hydrogenation of **1** to **3** failed under several conditions.[6]

Next, samples of the synthetic dafachronic acid A **1**, the *seco*-diacid **2**, and 7,8-dihydrodafachronic acid A **3** were evaluated for their bioactivity. First, the ability of synthetic ligands to rescue daf-9 hormone biosynthetic mutants from the dauer state was measured. Consistent with **1** being a natural ligand for DAF-12, dafachronic acid A rescued dauer formation in the nanomolar range, with half-maximal activity of 18.5 nM (Figure 2). Similarly, the 7,8-dihydrodafachronic acid A also gave substantial rescue with half-maximal rescue at 292 nM. By contrast, the *seco*-diacid **2** was found *not* to rescue *C. elegans* from the dauer state, indicating that it is not a ligand. Second, the ability of synthetic ligands to activate DAF-12 in transcriptional assays on a target gene,

(5) For the syntheses of glycinoeclepin A, see: (a) Murai, A; Tanimoto, N.; Sakamoto, N.; Masamune, T. *J. Am. Chem. Soc.* **1988**, *110*, 1985–1986.

(6) To the best of our knowledge, no successful hydrogenation of isolated Δ^7 double bonds has been reported in the literature. (b) Mori, K.; Watanabe, H. *Pure Appl. Chem.* **1989**, *61*, 543–546. (c) Corey, E. J.; Houpis, I. N. *J. Am. Chem. Soc.* **1990**, *112*, 8997–8998.

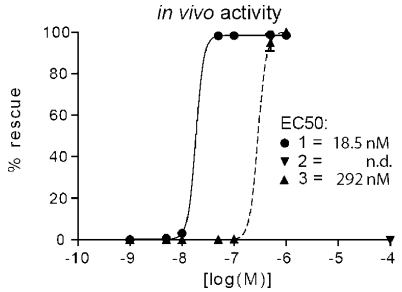

Figure 2. In vivo activity of sterols **1**−**3** measured as the percentage of rescue of *daf-9(dh6)* null worms from dauer to wild-type gravid adults.

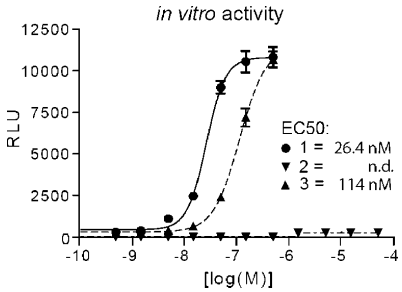

Figure 3. Transcriptional activation of DAF-12 by **1**−**3** on lit-1::ptk-luciferase reporter constructs, measuring relative luciferase units with and without ligand (RLU) vs concentration.

lit-1, was measured. To do this, plasmid constructs containing the daf-12 gene and the lit-1 gene fused to a luciferase reporter were cotransfected into human embryonic kidney cells (HEK293T) and treated with various doses of the compounds and luciferase induction measured by light emission.[1] In accord with the dauer rescue results, **2** showed *no activity* even at 100 μM concentration (Figure 3), whereas 7,8-dihydrodafachronic acid A (**3**) showed activity similar to that of dafachronic acid A (**1**). Specifically, measurement of the dose−response revealed EC_{50} values for daf-12 activation to be 114 nM for 7,8-dihydrodafachronic acid A and 26 nM for dafachronic acid A.

These results taken together allow the following conclusions: (1) dafachronic acid A is a natural ligand for DAF-12 nuclear receptor, (2) in contrast to the soybean nematode case, ring B oxidative cleavage products are not the active agents for gene activation of *C. elegans* DAF-12, and (3) the $\Delta^{7,8}$ double bond is not essential for dafachronic acid activity on *C. elegans*.

Acknowledgment. S.G. is grateful to NSERC (Canada) for a postdoctoral fellowship. A.A. is grateful for support from NIH and the Ellison Foundation. We thank Dongling Li (Baylor College of Medicine) for technical assistance.

Supporting Information Available: Experimental protocols, characterization for all new compounds, and methods for performing the dauer assays. This material is available free of charge via the Internet at http://pubs.acs.org.

OL801425V

7. Erklärung über die Eigenständigkeit der erbrachten wissenschaftlichen Leistung

Ich erkläre hiermit, dass ich die vorliegende Arbeit ohne unzulässige Hilfe Dritter und ohne Benutzung anderer als der angegebenen Hilfsmittel angefertigt habe. Die aus anderen Quellen direkt oder indirect übernommenen Daten und Konzepte sind unter Angabe der Quelle gekennzeichnet.

Bei der Auswahl und Auswertung folgenden Materials haben mir die nachstehend aufgeführten Personen in der jeweils beschriebenen Weise entgeltlich / unentgeltlich geholfen.

1. Nicole Fielenbach, a postdoctoral fellow of the Antebi Lab, contributed to genetics to generate worm strains and to analyzing GFP intensities.

2. Zhu Wang is a graduate student in David Mangelsdorf's lab and assisted in performing initial luciferase assays.

3. David Mangelsdorf provided the Δ4-dafachronic acid.

4. Adam Antebi supervised the study and supervised the text writing for the publication, but also contributed directly by generating worm strains and analysis of GFP intensities.

5. For Chapter 2 , Mary Wiese, a graduate student of the Antebi lab and the Zheng lab at Baylor College of Medicine contributed by germline injection of several constructs.

6. For Chapter 4 , Linyan Meng, a rotation student in the Antebi Lab, contributed to luciferase assays and GFP intensity analysis.

7. For Appendix 2, the Corey lab at Harvard University provided Δ7-dafachronic acid and all tested derivatives. The Schroeder lab at Cornell University provided ascaroside ascr#3.

8. For Appendix 3, Dongling Li, research assistant of the Antebi lab, contributed by germline injection of some of the constructs.

9. Christopher Henseley, an undergrad student of the Department of Biology of the Rice University in Houston, Tx, contributed to the molecular biology required to generate various

reporter construct plasmids used for Appendix 3 and to germline injection to transform the generated constructs into C. elegans.

Weitere Personen waren an der inhaltlichen materiellen Erstellung der vorliegenden Arbeit nicht beteiligt. Insbesondere habe ich hierfuer nicht die entgeltliche Hilfe von Vermittlungs- bzw. Beratungsdiensten (Promotionsberater oder andere Personen) in Anspruch genommen. Niemand hat von mir unmittelbar oder mittelbar geldwerte Leistungen für Arbeiten erhalten, die im Zusammenhang mit dem Inhalt der vorgelegten Dissertation stehen.

Die Arbeit wurde bisher weder im In- noch im Ausland in gleicher oder ähnlicher Form einer anderen Prüfungsbehörde vorgelegt.

....

(Ort. Datum) (Unterschrift)

7.1 Publication of Data presented in Chapter 2

Science. 2009 Apr 3;324(5923):95-8.
Axel Bethke, Nicole Fielenbach, Zhu Wang, David J. Mangelsdorf, Adam Antebi :
"Direct nuclear hormone receptor regulation of microRNAs controls developmental progression"

7.2 Publication of Data presented in Appendix 2

Org Lett. 2008 Aug 21;10(16):3643-5.
Simon Giroux, Axel Bethke, Nicole Fielenbach, Adam Antebi, and E. J. Corey :
“Syntheses and Biological Evaluation of B-Ring-Modified Analogues of Dafachronic Acid A”

8. References

Abbott, A.L., Alvarez-Saavedra, E., Miska, E.A., Lau, N.C., Bartel, D.P., Horvitz, H.R., and Ambros, V. (2005). The let-7 MicroRNA family members mir-48, mir-84, and mir-241 function together to regulate developmental timing in Caenorhabditis elegans. Dev Cell *9*, 403-414.

Abrahante, J.E., Daul, A.L., Li, M., Volk, M.L., Tennessen, J.M., Miller, E.A., and Rougvie, A.E. (2003). The Caenorhabditis elegans hunchback-like gene lin-57/hbl-1 controls developmental time and is regulated by microRNAs. Dev Cell *4*, 625-637.

Abrahante, J.E., Miller, E.A., and Rougvie, A.E. (1998). Identification of heterochronic mutants in Caenorhabditis elegans. Temporal misexpression of a collagen::green fluorescent protein fusion gene. Genetics *149*, 1335-1351.

Adam, G., Perrimon, N., and Noselli, S. (2003). The retinoic-like juvenile hormone controls the looping of left-right asymmetric organs in Drosophila. Development *130*, 2397-2406.

Allen, B.M. (1925). The effects of extirpation of the thyroid and pituitary glands upon the limb development of anurans. Journal of Experimental Zoology *42*, 13-30.

Ambros, V., and Horvitz, H.R. (1984). Heterochronic mutants of the nematode Caenorhabditis elegans. Science *226*, 409-416.

Anderson, R.C. (1984). The origins of zooparasitic nematodes. The Canadian Journal of Zoology *62*, 317-328.

Antebi, A. (2006). Nuclear hormone receptors in C. elegans. WormBook, 1-13.

Antebi, A., Culotti, J.G., and Hedgecock, E.M. (1998). *daf-12* regulates developmental age and the dauer alternative in *C. elegans*. Development *125*, 1191-1205.

Antebi, A., Yeh, W.H., Tait, D., Hedgecock, E.M., and Riddle, D.L. (2000). daf-12 encodes a nuclear receptor that regulates the dauer diapause and developmental age in C. elegans. Genes Dev *14*, 1512-1527.

Ao, W., Gaudet, J., Kent, W.J., Muttumu, S., and Mango, S.E. (2004). Environmentally induced foregut remodeling by PHA-4/FoxA and DAF-12/NHR. Science *305*, 1743-1746.

Arasu, P., Wightman, B., and Ruvkun, G. (1991). Temporal regulation of lin-14 by the antagonistic action of two other heterochronic genes, lin-4 and lin-28. Genes Dev *5*, 1825-1833.

Banerjee, D., Kwok, A., Lin, S.Y., and Slack, F.J. (2005). Developmental timing in C. elegans is regulated by kin-20 and tim-1, homologs of core circadian clock genes. Dev Cell *8*, 287-295.

Bargmann, C.I., and Horvitz, H.R. (1991). Control of larval development by chemosensory neurons in Caenorhabditis elegans. Science *251*, 1243-1246.

Bethke, A., Fielenbach, N., Wang, Z., Mangelsdorf, D.J., and Antebi, A. (2009). Nuclear hormone receptor regulation of microRNAs controls developmental progression. Science *324*, 95-98.

Blacque, O.E., Perens, E.A., Boroevich, K.A., Inglis, P.N., Li, C., Warner, A., Khattra, J., Holt, R.A., Ou, G., Mah, A.K.*, et al.* (2005). Functional genomics of the cilium, a sensory organelle. Curr Biol *15*, 935-941.

Bourguet, W., Ruff, M., Chambon, P., Gronemeyer, H., and Moras, D. (1995). Crystal structure of the ligand-binding domain of the human nuclear receptor RXR-alpha. Nature *375*, 377-382.

Brenner, S. (1974). The genetics of Caenorhabditis elegans. Genetics *77*, 71-94.

Brown, D.D., and Cai, L. (2007). Amphibian metamorphosis. Dev Biol *306*, 20-33.

Brugarolas, J., Chandrasekaran, C., Gordon, J.I., Beach, D., Jacks, T., and Hannon, G.J. (1995). Radiation-induced cell cycle arrest compromised by p21 deficiency. Nature *377*, 552-557.

Buchholz, D.R., Hsia, S.C., Fu, L., and Shi, Y.B. (2003). A dominant-negative thyroid hormone receptor blocks amphibian metamorphosis by retaining corepressors at target genes. Mol Cell Biol *23*, 6750-6758.

Butcher, R.A., Fujita, M., Schroeder, F.C., and Clardy, J. (2007). Small-molecule pheromones that control dauer development in Caenorhabditis elegans. Nat Chem Biol *3*, 420-422.
Cassada, R.C., and Russell, R.L. (1975). The dauerlarva, a post-embryonic developmental variant of the nematode Caenorhabditis elegans. Dev Biol *46*, 326-342.
Chalfie, M., Horvitz, H.R., and Sulston, J.E. (1981). Mutations that lead to reiterations in the cell lineages of C. elegans. Cell *24*, 59-69.
Chang, T.C., Wentzel, E.A., Kent, O.A., Ramachandran, K., Mullendore, M., Lee, K.H., Feldmann, G., Yamakuchi, M., Ferlito, M., Lowenstein, C.J*., et al.* (2007). Transactivation of miR-34a by p53 broadly influences gene expression and promotes apoptosis. Mol Cell *26*, 745-752.
Christensen, S., Kodoyianni, V., Bosenberg, M., Friedman, L., and Kimble, J. (1996). lag-1, a gene required for lin-12 and glp-1 signaling in Caenorhabditis elegans, is homologous to human CBF1 and Drosophila Su(H). Development *122*, 1373-1383.
Couse, J.F., Hewitt, S.C., Bunch, D.O., Sar, M., Walker, V.R., Davis, B.J., and Korach, K.S. (1999). Postnatal sex reversal of the ovaries in mice lacking estrogen receptors alpha and beta. Science *286*, 2328-2331.
Couse, J.F., and Korach, K.S. (2001). Contrasting phenotypes in reproductive tissues of female estrogen receptor null mice. Ann N Y Acad Sci *948*, 1-8.
Crosby, S.D., Puetz, J.J., Simburger, K.S., Fahrner, T.J., and Milbrandt, J. (1991). The early response gene NGFI-C encodes a zinc finger transcriptional activator and is a member of the GCGGGGGCG (GSG) element-binding protein family. Mol Cell Biol *11*, 3835-3841.
da Graca, L.S., Zimmerman, K.K., Mitchell, M.C., Kozhan-Gorodetska, M., Sekiewicz, K., Morales, Y., and Patterson, G.I. (2004). DAF-5 is a Ski oncoprotein homolog that functions in a neuronal TGF beta pathway to regulate C. elegans dauer development. Development *131*, 435-446.
Darimont, B.D., Wagner, R.L., Apriletti, J.W., Stallcup, M.R., Kushner, P.J., Baxter, J.D., Fletterick, R.J., and Yamamoto, K.R. (1998). Structure and specificity of nuclear receptor-coactivator interactions. Genes Dev *12*, 3343-3356.
Davidson, E. (2006). The Regulatory Genome (Elsevier).
Ding, L., Spencer, A., Morita, K., and Han, M. (2005). The developmental timing regulator AIN-1 interacts with miRISCs and may target the argonaute protein ALG-1 to cytoplasmic P bodies in C. elegans. Mol Cell *19*, 437-447.
Emery, P., Strubin, M., Hofmann, K., Bucher, P., Mach, B., and Reith, W. (1996). A consensus motif in the RFX DNA binding domain and binding domain mutants with altered specificity. Mol Cell Biol *16*, 4486-4494.
Esquela-Kerscher, A., Johnson, S.M., Bai, L., Saito, K., Partridge, J., Reinert, K.L., and Slack, F.J. (2005). Post-embryonic expression of C. elegans microRNAs belonging to the lin-4 and let-7 families in the hypodermis and the reproductive system. Dev Dyn *234*, 868-877.
Fay, D.S., Stanley, H.M., Han, M., and Wood, W.B. (1999). A Caenorhabditis elegans homologue of hunchback is required for late stages of development but not early embryonic patterning. Dev Biol *205*, 240-253.
Fazi, F., Rosa, A., Fatica, A., Gelmetti, V., De Marchis, M.L., Nervi, C., and Bozzoni, I. (2005). A minicircuitry comprised of microRNA-223 and transcription factors NFI-A and C/EBPalpha regulates human granulopoiesis. Cell *123*, 819-831.
Fielenbach, N., and Antebi, A. (2008). C. elegans dauer formation and the molecular basis of plasticity. Genes Dev *22*, 2149-2165.
Fielenbach, N., Guardavaccaro, D., Neubert, K., Chan, T., Li, D., Feng, Q., Hutter, H., Pagano, M., and Antebi, A. (2007). DRE-1: an evolutionarily conserved F box protein that regulates C. elegans developmental age. Dev Cell *12*, 443-455.
Fire, A. (1986). Integrative transformation of Caenorhabditis elegans. EMBO J *5*, 2673-2680.
Fire, A., Harrison, S.W., and Dixon, D. (1990). A modular set of lacZ fusion vectors for studying gene expression in Caenorhabditis elegans. Gene *93*, 189-198.

Fisher, C.R., Graves, K.H., Parlow, A.F., and Simpson, E.R. (1998). Characterization of mice deficient in aromatase (ArKO) because of targeted disruption of the cyp19 gene. Proc Natl Acad Sci U S A *95*, 6965-6970.
Flames, N., and Hobert, O. (2009). Gene regulatory logic of dopamine neuron differentiation. Nature *458*, 885-889.
Forman, B.M., Umesono, K., Chen, J., and Evans, R.M. (1995). Unique response pathways are established by allosteric interactions among nuclear hormone receptors. Cell *81*, 541-550.
Frand, A.R., Russel, S., and Ruvkun, G. (2005). Functional genomic analysis of C. elegans molting. PLoS Biol *3*, e312.
Fukuzawa, A., Furusaki, A., Ikura, M., and Masamune, T. (1985). Glycinoeclepin A, a Natural Hatching Stimulus for the Soybean Cyst Nematode. J CHEM SOC, CHEM COMMUN, 221-223.
Furuyama, T., Nakazawa, T., Nakano, I., and Mori, N. (2000). Identification of the differential distribution patterns of mRNAs and consensus binding sequences for mouse DAF-16 homologues. Biochem J *349*, 629-634.
Gaudet, J., Muttumu, S., Horner, M., and Mango, S.E. (2004). Whole-genome analysis of temporal gene expression during foregut development. PLoS Biol *2*, e352.
Gems, D., Sutton, A.J., Sundermeyer, M.L., Albert, P.S., King, K.V., Edgley, M.L., Larsen, P.L., and Riddle, D.L. (1998). Two pleiotropic classes of daf-2 mutation affect larval arrest, adult behavior, reproduction and longevity in Caenorhabditis elegans. Genetics *150*, 129-155.
Gerisch, B., and Antebi, A. (2004). Hormonal signals produced by DAF-9/cytochrome P450 regulate C. elegans dauer diapause in response to environmental cues. Development *131*, 1765-1776.
Gerisch, B., Weitzel, C., Kober-Eisermann, C., Rottiers, V., and Antebi, A. (2001). A hormonal signaling pathway influencing C. elegans metabolism, reproductive development, and life span. Dev Cell *1*, 841-851.
Gilbert, S.F. (2003). Developmental Biology, Seventh Edition edn (Sinauer Associates, Inc.).
Girard, L.R., Fiedler, T.J., Harris, T.W., Carvalho, F., Antoshechkin, I., Han, M., Sternberg, P.W., Stein, L.D., and Chalfie, M. (2007). WormBook: the online review of Caenorhabditis elegans biology. Nucleic Acids Res *35*, D472-475.
Giroux, S., Bethke, A., Fielenbach, N., Antebi, A., and Corey, E.J. (2008). Syntheses and biological evaluation of B-ring-modified analogues of dafachronic acid A. Org Lett *10*, 3643-3645.
Giroux, S., and Corey, E.J. (2007). Stereocontrolled synthesis of dafachronic acid A, the ligand for the DAF-12 nuclear receptor of Caenorhabditis elegans. J Am Chem Soc *129*, 9866-9867.
Gissendanner, C.R., Crossgrove, K., Kraus, K.A., Maina, C.V., and Sluder, A.E. (2004). Expression and function of conserved nuclear receptor genes in Caenorhabditis elegans. Dev Biol *266*, 399-416.
Greenwald, I.S., Sternberg, P.W., and Horvitz, H.R. (1983). The lin-12 locus specifies cell fates in Caenorhabditis elegans. Cell *34*, 435-444.
Grishok, A., Pasquinelli, A.E., Conte, D., Li, N., Parrish, S., Ha, I., Baillie, D.L., Fire, A., Ruvkun, G., and Mello, C.C. (2001). Genes and mechanisms related to RNA interference regulate expression of the small temporal RNAs that control C. elegans developmental timing. Cell *106*, 23-34.
Grosshans, H., Johnson, T., Reinert, K.L., Gerstein, M., and Slack, F.J. (2005). The temporal patterning microRNA let-7 regulates several transcription factors at the larval to adult transition in C. elegans. Dev Cell *8*, 321-330.
Hammell, C.M., Lubin, I., Boag, P.R., Blackwell, T.K., and Ambros, V. (2009). nhl-2 Modulates microRNA activity in Caenorhabditis elegans. Cell *136*, 926-938.
Harington, C.R. (1928). Resolution of dl-Thyroxine. Biochemical Journal *22*, 1429-1435.
Harris, C.C. (1996). p53 tumor suppressor gene: from the basic research laboratory to the clinic--an abridged historical perspective. Carcinogenesis *17*, 1187-1198.
Harris, T.D., and Horvitz, B. (2007). *mab-10*, a Heterochronic Gene Required For the Terminal Differentiation of Hypodermal Cells and the Cessation of Molting, Encodes a Member of the NAB Family of Transcription Factors. (International Worm Meeting 2007).

Hayes, G.D., Frand, A.R., and Ruvkun, G. (2006). The mir-84 and let-7 paralogous microRNA genes of Caenorhabditis elegans direct the cessation of molting via the conserved nuclear hormone receptors NHR-23 and NHR-25. Development *133*, 4631-4641.
He, L., He, X., Lim, L.P., de Stanchina, E., Xuan, Z., Liang, Y., Xue, W., Zender, L., Magnus, J., Ridzon, D.*, et al.* (2007). A microRNA component of the p53 tumour suppressor network. Nature *447*, 1130-1134.
Hedgecock, E.M., Culotti, J.G., Hall, D.H., and Stern, B.D. (1987). Genetics of cell and axon migrations in Caenorhabditis elegans. Development *100*, 365-382.
Henderson, S.T., and Johnson, T.E. (2001). daf-16 integrates developmental and environmental inputs to mediate aging in the nematode Caenorhabditis elegans. Curr Biol *11*, 1975-1980.
Herndon, L.A., Schmeissner, P.J., Dudaronek, J.M., Brown, P.A., Listner, K.M., Sakano, Y., Paupard, M.C., Hall, D.H., and Driscoll, M. (2002). Stochastic and genetic factors influence tissue-specific decline in ageing C. elegans. Nature *419*, 808-814.
Hodgkin, J. (2007). Introduction to genetics and genomics. WormBook.
Horner, M.A., Quintin, S., Domeier, M.E., Kimble, J., Labouesse, M., and Mango, S.E. (1998). pha-4, an HNF-3 homolog, specifies pharyngeal organ identity in Caenorhabditis elegans. Genes Dev *12*, 1947-1952.
Hsia, S.C., Tomita, A., Obata, K., Paul, B., Buchholz, D., and Shi, Y.B. (2003). Role of chromatin disruption and histone acetylation in thyroid hormone receptor action: implications in the regulation of HIV-1 LTR. Histol Histopathol *18*, 323-331.
Hutvagner, G., McLachlan, J., Pasquinelli, A.E., Balint, E., Tuschl, T., and Zamore, P.D. (2001). A cellular function for the RNA-interference enzyme Dicer in the maturation of the let-7 small temporal RNA. Science *293*, 834-838.
Inoue, T., and Thomas, J.H. (2000). Targets of TGF-beta signaling in Caenorhabditis elegans dauer formation. Dev Biol *217*, 192-204.
J. Sambrook, E.F.F., T. Maniatis (1989). Molecular Cloning - A Laboratory Manual, Second Edition edn (Cold Spring Harbour Laboratory Press).
Jeon, M., Gardner, H.F., Miller, E.A., Deshler, J., and Rougvie, A.E. (1999). Similarity of the C. elegans developmental timing protein LIN-42 to circadian rhythm proteins. Science *286*, 1141-1146.
Jia, K., Albert, P.S., and Riddle, D.L. (2002). DAF-9, a cytochrome P450 regulating C. elegans larval development and adult longevity. Development *129*, 221-231.
Johnson, S.M., Lin, S.Y., and Slack, F.J. (2003). The time of appearance of the C. elegans let-7 microRNA is transcriptionally controlled utilizing a temporal regulatory element in its promoter. Dev Biol *259*, 364-379.
Johnston, R.J., Jr., Chang, S., Etchberger, J.F., Ortiz, C.O., and Hobert, O. (2005). MicroRNAs acting in a double-negative feedback loop to control a neuronal cell fate decision. Proc Natl Acad Sci U S A *102*, 12449-12454.
Kalb, J.M., Lau, K.K., Goszczynski, B., Fukushige, T., Moons, D., Okkema, P.G., and McGhee, J.D. (1998). pha-4 is Ce-fkh-1, a fork head/HNF-3alpha,beta,gamma homolog that functions in organogenesis of the C. elegans pharynx. Development *125*, 2171-2180.
Kamath, R.S., Fraser, A.G., Dong, Y., Poulin, G., Durbin, R., Gotta, M., Kanapin, A., Le Bot, N., Moreno, S., Sohrmann, M.*, et al.* (2003). Systematic functional analysis of the Caenorhabditis elegans genome using RNAi. Nature *421*, 231-237.
Kenyon, C. (2005). The plasticity of aging: insights from long-lived mutants. Cell *120*, 449-460.
Kenyon, C., Chang, J., Gensch, E., Rudner, A., and Tabtiang, R. (1993). A C. elegans mutant that lives twice as long as wild type. Nature *366*, 461-464.
Kimble, J., and Hirsh, D. (1979). The postembryonic cell lineages of the hermaphrodite and male gonads in Caenorhabditis elegans. Dev Biol *70*, 396-417.
Kimura, K.D., Tissenbaum, H.A., Liu, Y., and Ruvkun, G. (1997). daf-2, an insulin receptor-like gene that regulates longevity and diapause in Caenorhabditis elegans. Science *277*, 942-946.

Kurokawa, R., DiRenzo, J., Boehm, M., Sugarman, J., Gloss, B., Rosenfeld, M.G., Heyman, R.A., and Glass, C.K. (1994). Regulation of retinoid signalling by receptor polarity and allosteric control of ligand binding. Nature *371*, 528-531.
Larsen, P.L., Albert, P.S., and Riddle, D.L. (1995). Genes that regulate both development and longevity in Caenorhabditis elegans. Genetics *139*, 1567-1583.
Lau, N.C., Lim, L.P., Weinstein, E.G., and Bartel, D.P. (2001). An abundant class of tiny RNAs with probable regulatory roles in Caenorhabditis elegans. Science *294*, 858-862.
Le, N., Nagarajan, R., Wang, J.Y., Svaren, J., LaPash, C., Araki, T., Schmidt, R.E., and Milbrandt, J. (2005). Nab proteins are essential for peripheral nervous system myelination. Nat Neurosci *8*, 932-940.
Lee, D.L. (2002). The Biology of Nematodes (Leeds, University of Leeds).
Lee, R.C., Feinbaum, R.L., and Ambros, V. (1993). The C. elegans heterochronic gene lin-4 encodes small RNAs with antisense complementarity to lin-14. Cell *75*, 843-854.
Lee, R.Y., Hench, J., and Ruvkun, G. (2001). Regulation of C. elegans DAF-16 and its human ortholog FKHRL1 by the daf-2 insulin-like signaling pathway. Curr Biol *11*, 1950-1957.
Lehmann, R., and Nusslein-Volhard, C. (1987). hunchback, a gene required for segmentation of an anterior and posterior region of the Drosophila embryo. Dev Biol *119*, 402-417.
Lewis, B.P., Burge, C.B., and Bartel, D.P. (2005). Conserved seed pairing, often flanked by adenosines, indicates that thousands of human genes are microRNA targets. Cell *120*, 15-20.
Li, M., Jones-Rhoades, M.W., Lau, N.C., Bartel, D.P., and Rougvie, A.E. (2005). Regulatory mutations of mir-48, a C. elegans let-7 family MicroRNA, cause developmental timing defects. Dev Cell *9*, 415-422.
Li, W., Kennedy, S.G., and Ruvkun, G. (2003). daf-28 encodes a C. elegans insulin superfamily member that is regulated by environmental cues and acts in the DAF-2 signaling pathway. Genes Dev *17*, 844-858.
Lin, K., Hsin, H., Libina, N., and Kenyon, C. (2001). Regulation of the Caenorhabditis elegans longevity protein DAF-16 by insulin/IGF-1 and germline signaling. Nat Genet *28*, 139-145.
Lin, S.Y., Johnson, S.M., Abraham, M., Vella, M.C., Pasquinelli, A., Gamberi, C., Gottlieb, E., and Slack, F.J. (2003). The C elegans hunchback homolog, hbl-1, controls temporal patterning and is a probable microRNA target. Dev Cell *4*, 639-650.
Liu, Z., Kirch, S., and Ambros, V. (1995). The Caenorhabditis elegans heterochronic gene pathway controls stage-specific transcription of collagen genes. Development *121*, 2471-2478.
Liu, Z.C., and Ambros, V. (1989). Heterochronic genes control the stage-specific initiation and expression of the dauer larva developmental program in Caenorhabditis elegans. Genes Dev *3*, 2039-2049.
Ludewig, A.H., Kober-Eisermann, C., Weitzel, C., Bethke, A., Neubert, K., Gerisch, B., Hutter, H., and Antebi, A. (2004). A novel nuclear receptor/coregulator complex controls C. elegans lipid metabolism, larval development, and aging. Genes Dev *18*, 2120-2133.
Mader, S., Chen, J.Y., Chen, Z., White, J., Chambon, P., and Gronemeyer, H. (1993). The patterns of binding of RAR, RXR and TR homo- and heterodimers to direct repeats are dictated by the binding specificites of the DNA binding domains. EMBO J *12*, 5029-5041.
Mak, H.Y., and Ruvkun, G. (2004). Intercellular signaling of reproductive development by the C. elegans DAF-9 cytochrome P450. Development *131*, 1777-1786.
Mangelsdorf, D.J., and Evans, R.M. (1995). The RXR heterodimers and orphan receptors. Cell *83*, 841-850.
Mangelsdorf, D.J., Thummel, C., Beato, M., Herrlich, P., Schutz, G., Umesono, K., Blumberg, B., Kastner, P., Mark, M., Chambon, P*., et al.* (1995). The nuclear receptor superfamily: the second decade. Cell *83*, 835-839.
Marri, S., and Gupta, B.P. (2009). Dissection of lin-11 enhancer regions in Caenorhabditis elegans and other nematodes. Dev Biol *325*, 402-411.

Masamune, T., Anetai, M., Takasugi, M., and Katsui, N. (1982). Isolation of a natural hatching stimulus, glycinoelepin A, for the soy bean cyst nematode. Nature *297*, 495-496.
Meijsing, S.H., Pufall, M.A., So, A.Y., Bates, D.L., Chen, L., and Yamamoto, K.R. (2009). DNA binding site sequence directs glucocorticoid receptor structure and activity. Science *324*, 407-410.
Miller, D.M., 3rd, Desai, N.S., Hardin, D.C., Piston, D.W., Patterson, G.H., Fleenor, J., Xu, S., and Fire, A. (1999). Two-color GFP expression system for C. elegans. Biotechniques *26*, 914-918, 920-911.
Mitteroecker, P., Gunz, P., Bernhard, M., Schaefer, K., and Bookstein, F.L. (2004). Comparison of cranial ontogenetic trajectories among great apes and humans. J Hum Evol *46*, 679-697.
Miyabayashi, T., Palfreyman, M.T., Sluder, A.E., Slack, F., and Sengupta, P. (1999). Expression and function of members of a divergent nuclear receptor family in Caenorhabditis elegans. Dev Biol *215*, 314-331.
Morita, K., and Han, M. (2006). Multiple mechanisms are involved in regulating the expression of the developmental timing regulator lin-28 in Caenorhabditis elegans. EMBO J *25*, 5794-5804.
Moss, E.G. (2007). Heterochronic genes and the nature of developmental time. Curr Biol *17*, R425-434.
Moss, E.G., Lee, R.C., and Ambros, V. (1997). The cold shock domain protein LIN-28 controls developmental timing in C. elegans and is regulated by the lin-4 RNA. Cell *88*, 637-646.
Motola, D.L., Cummins, C.L., Rottiers, V., Sharma, K., Sunino, K., Xu, E., Auchus, R., Antebi, A., and Mangelsdorf, M. (2006). Identification of DAF-12 ligands that govern dauer formation and reproduction in C. elegans. Cell *124*, 1209-1223.
Muscatelli, F., Strom, T.M., Walker, A.P., Zanaria, E., Recan, D., Meindl, A., Bardoni, B., Guioli, S., Zehetner, G., Rabl, W*., et al.* (1994). Mutations in the DAX-1 gene give rise to both X-linked adrenal hypoplasia congenita and hypogonadotropic hypogonadism. Nature *372*, 672-676.
Nachtigal, M.W., Hirokawa, Y., Enyeart-VanHouten, D.L., Flanagan, J.N., Hammer, G.D., and Ingraham, H.A. (1998). Wilms' tumor 1 and Dax-1 modulate the orphan nuclear receptor SF-1 in sex-specific gene expression. Cell *93*, 445-454.
Newman, M.A., Thomson, J.M., and Hammond, S.M. (2008). Lin-28 interaction with the Let-7 precursor loop mediates regulated microRNA processing. RNA *14*, 1539-1549.
O'Malley, B.W. (2006). Molecular biology. Little molecules with big goals. Science *313*, 1749-1750.
Ogawa, A., Streit, A., Antebi, A., and Sommer, R.J. (2009). A conserved endocrine mechanism controls the formation of dauer and infective larvae in nematodes. Curr Biol *19*, 67-71.
Ogg, S., Paradis, S., Gottlieb, S., Patterson, G.I., Lee, L., Tissenbaum, H.A., and Ruvkun, G. (1997). The Fork head transcription factor DAF-16 transduces insulin-like metabolic and longevity signals in C. elegans. Nature *389*, 994-999.
Ohler, U., Yekta, S., Lim, L.P., Bartel, D.P., and Burge, C.B. (2004). Patterns of flanking sequence conservation and a characteristic upstream motif for microRNA gene identification. RNA *10*, 1309-1322.
Okkema, P.G., and Fire, A. (1994). The Caenorhabditis elegans NK-2 class homeoprotein CEH-22 is involved in combinatorial activation of gene expression in pharyngeal muscle. Development *120*, 2175-2186.
Okkema, P.G., Harrison, S.W., Plunger, V., Aryana, A., and Fire, A. (1993). Sequence requirements for myosin gene expression and regulation in Caenorhabditis elegans. Genetics *135*, 385-404.
Okkema, P.G., and Krause, M. (2005). Transcriptional regulation. WormBook, 1-40.
Olsen, P.H., and Ambros, V. (1999). The lin-4 regulatory RNA controls developmental timing in Caenorhabditis elegans by blocking LIN-14 protein synthesis after the initiation of translation. Dev Biol *216*, 671-680.
Onate, S.A., Tsai, S.Y., Tsai, M.J., and O'Malley, B.W. (1995). Sequence and characterization of a coactivator for the steroid hormone receptor superfamily. Science *270*, 1354-1357.
Ouellet, J., Li, S., and Roy, R. (2008). Notch signalling is required for both dauer maintenance and recovery in C. elegans. Development *135*, 2583-2592.

Ow, M.C., Martinez, N.J., Olsen, P.H., Silverman, H.S., Barrasa, M.I., Conradt, B., Walhout, A.J., and Ambros, V. (2008). The FLYWCH transcription factors FLH-1, FLH-2, and FLH-3 repress embryonic expression of microRNA genes in C. elegans. Genes Dev *22*, 2520-2534.
Page, A.P., and Johnstone, I.L. (2007). The cuticle. WormBook, 1-15.
Paradis, S., and Ruvkun, G. (1998). Caenorhabditis elegans Akt/PKB transduces insulin receptor-like signals from AGE-1 PI3 kinase to the DAF-16 transcription factor. Genes Dev *12*, 2488-2498.
Paris, M., and Laudet, V. (2008). The history of a developmental stage: metamorphosis in chordates. Genesis *46*, 657-672.
Pasquinelli, A.E., Reinhart, B.J., Slack, F., Martindale, M.Q., Kuroda, M.I., Maller, B., Hayward, D.C., Ball, E.E., Degnan, B., Muller, P.*, et al.* (2000). Conservation of the sequence and temporal expression of let-7 heterochronic regulatory RNA. Nature *408*, 86-89.
Patterson, G.I., Koweek, A., Wong, A., Liu, Y., and Ruvkun, G. (1997). The DAF-3 Smad protein antagonizes TGF-beta-related receptor signaling in the Caenorhabditis elegans dauer pathway. Genes Dev *11*, 2679-2690.
Pepper, A.S., McCane, J.E., Kemper, K., Yeung, D.A., Lee, R.C., Ambros, V., and Moss, E.G. (2004). The C. elegans heterochronic gene lin-46 affects developmental timing at two larval stages and encodes a relative of the scaffolding protein gephyrin. Development *131*, 2049-2059.
Perkins, L.A., Hedgecock, E.M., Thomson, J.N., and Culotti, J.G. (1986). Mutant sensory cilia in the nematode Caenorhabditis elegans. Dev Biol *117*, 456-487.
Pungaliya, C., Srinivasan, J., Fox, B.W., Malik, R.U., Ludewig, A.H., Sternberg, P.W., and Schroeder, F.C. (2009). A shortcut to identifying small molecule signals that regulate behavior and development in Caenorhabditis elegans. Proc Natl Acad Sci U S A.
Raver-Shapira, N., Marciano, E., Meiri, E., Spector, Y., Rosenfeld, N., Moskovits, N., Bentwich, Z., and Oren, M. (2007). Transcriptional activation of miR-34a contributes to p53-mediated apoptosis. Mol Cell *26*, 731-743.
Reinhart, B.J., Slack, F.J., Basson, M., Pasquinelli, A.E., Bettinger, J.C., Rougvie, A.E., Horvitz, H.R., and Ruvkun, G. (2000). The 21-nucleotide let-7 RNA regulates developmental timing in C. elegans. Nature *403*, 901-906.
Reith, W., Kobr, M., Emery, P., Durand, B., Siegrist, C.A., and Mach, B. (1994). Cooperative binding between factors RFX and X2bp to the X and X2 boxes of MHC class II promoters. J Biol Chem *269*, 20020-20025.
Riddle, D.L., Blumenthal, T., Meyer, B.J., and Priess, J.R. (1997). *C. elegans* II (Cold Spring Harbor Monograph Series).
Riddle, D.L., Swanson, M.M., and Albert, P.S. (1981). Interacting genes in nematode dauer larva formation. Nature *290*, 668-671.
Rosenfeld, M.G., Lunyak, V.V., and Glass, C.K. (2006). Sensors and signals: a coactivator/corepressor/epigenetic code for integrating signal-dependent programs of transcriptional response. Genes Dev *20*, 1405-1428.
Rougvie, A.E. (2001). Control of developmental timing in animals. Nat Rev Genet *2*, 690-701.
Rougvie, A.E., and Ambros, V. (1995). The heterochronic gene lin-29 encodes a zinc finger protein that controls a terminal differentiation event in Caenorhabditis elegans. Development *121*, 2491-2500.
Ruvkun, G., and Giusto, J. (1989). The Caenorhabditis elegans heterochronic gene lin-14 encodes a nuclear protein that forms a temporal developmental switch. Nature *338*, 313-319.
Savage-Dunn, C. (2005). TGF-beta signaling. WormBook, 1-12.
Savkur, R.S., and Burris, T.P. (2004). The coactivator LXXLL nuclear receptor recognition motif. J Pept Res *63*, 207-212.
Schackwitz, W.S., Inoue, T., and Thomas, J.H. (1996). Chemosensory neurons function in parallel to mediate a pheromone response in C. elegans. Neuron *17*, 719-728.

Shi, Y., Downes, M., Xie, W., Kao, H.Y., Ordentlich, P., Tsai, C.C., Hon, M., and Evans, R.M. (2001). Sharp, an inducible cofactor that integrates nuclear receptor repression and activation. Genes Dev *15*, 1140-1151.
Shiau, A.K., Barstad, D., Loria, P.M., Cheng, L., Kushner, P.J., Agard, D.A., and Greene, G.L. (1998). The structural basis of estrogen receptor/coactivator recognition and the antagonism of this interaction by tamoxifen. Cell *95*, 927-937.
Shostak, Y., Van Gilst, M.R., Antebi, A., and Yamamoto, K.R. (2004). Identification of C. elegans DAF-12-binding sites, response elements, and target genes. Genes Dev *18*, 2529-2544.
Slack, F.J., Basson, M., Liu, Z., Ambros, V., Horvitz, H.R., and Ruvkun, G. (2000). The lin-41 RBCC gene acts in the C. elegans heterochronic pathway between the let-7 regulatory RNA and the LIN-29 transcription factor. Mol Cell *5*, 659-669.
Solomon, A., Mian, Y., Ortega-Cava, C., Liu, V.W., Gurumurthy, C.B., Naramura, M., Band, V., and Band, H. (2008). Upregulation of the let-7 microRNA with precocious development in lin-12/Notch hypermorphic Caenorhabditis elegans mutants. Dev Biol *316*, 191-199.
Srinivasan, J., Kaplan, F., Ajredini, R., Zachariah, C., Alborn, H.T., Teal, P.E., Malik, R.U., Edison, A.S., Sternberg, P.W., and Schroeder, F.C. (2008). A blend of small molecules regulates both mating and development in Caenorhabditis elegans. Nature *454*, 1115-1118.
Sulston, J.E., and Horvitz, H.R. (1977). Post-embryonic cell lineages of the nematode, Caenorhabditis elegans. Dev Biol *56*, 110-156.
Sulston, J.E., Schierenberg, E., White, J.G., and Thomson, J.N. (1983). The embryonic cell lineage of the nematode Caenorhabditis elegans. Dev Biol *100*, 64-119.
Swain, A., Narvaez, V., Burgoyne, P., Camerino, G., and Lovell-Badge, R. (1998). Dax1 antagonizes Sry action in mammalian sex determination. Nature *391*, 761-767.
Swoboda, P., Adler, H.T., and Thomas, J.H. (2000). The RFX-type transcription factor DAF-19 regulates sensory neuron cilium formation in C. elegans. Mol Cell *5*, 411-421.
Talbot, W.S., Swyryd, E.A., and Hogness, D.S. (1993). Drosophila tissues with different metamorphic responses to ecdysone express different ecdysone receptor isoforms. Cell *73*, 1323-1337.
Tanenbaum, D.M., Wang, Y., Williams, S.P., and Sigler, P.B. (1998). Crystallographic comparison of the estrogen and progesterone receptor's ligand binding domains. Proc Natl Acad Sci U S A *95*, 5998-6003.
Tarasov, V., Jung, P., Verdoodt, B., Lodygin, D., Epanchintsev, A., Menssen, A., Meister, G., and Hermeking, H. (2007). Differential regulation of microRNAs by p53 revealed by massively parallel sequencing: miR-34a is a p53 target that induces apoptosis and G1-arrest. Cell Cycle *6*, 1586-1593.
Tautz, D., Tautz, C., Webb, D., and Dover, G.A. (1987). Evolutionary divergence of promoters and spacers in the rDNA family of four Drosophila species. Implications for molecular coevolution in multigene families. J Mol Biol *195*, 525-542.
Tewari, M., Hu, P.J., Ahn, J.S., Ayivi-Guedehoussou, N., Vidalain, P.O., Li, S., Milstein, S., Armstrong, C.M., Boxem, M., Butler, M.D*., et al.* (2004). Systematic interactome mapping and genetic perturbation analysis of a C. elegans TGF-beta signaling network. Mol Cell *13*, 469-482.
Thatcher, J.D., Haun, C., and Okkema, P.G. (1999). The DAF-3 Smad binds DNA and represses gene expression in the Caenorhabditis elegans pharynx. Development *126*, 97-107.
Thomas, H.E., Stunnenberg, H.G., and Stewart, A.F. (1993). Heterodimerization of the Drosophila ecdysone receptor with retinoid X receptor and ultraspiracle. Nature *362*, 471-475.
Timchenko, N.A., Wilde, M., and Darlington, G.J. (1999). C/EBPalpha regulates formation of S-phase-specific E2F-p107 complexes in livers of newborn mice. Mol Cell Biol *19*, 2936-2945.
Topilko, P., Schneider-Maunoury, S., Levi, G., Baron-Van Evercooren, A., Chennoufi, A.B., Seitanidou, T., Babinet, C., and Charnay, P. (1994). Krox-20 controls myelination in the peripheral nervous system. Nature *371*, 796-799.
Truman, J.W., Talbot, W.S., Fahrbach, S.E., and Hogness, D.S. (1994). Ecdysone receptor expression in the CNS correlates with stage-specific responses to ecdysteroids during Drosophila and Manduca development. Development *120*, 219-234.

Vainio, S., Heikkila, M., Kispert, A., Chin, N., and McMahon, A.P. (1999). Female development in mammals is regulated by Wnt-4 signalling. Nature *397*, 405-409.
Valadi, H., Ekstrom, K., Bossios, A., Sjostrand, M., Lee, J.J., and Lotvall, J.O. (2007). Exosome-mediated transfer of mRNAs and microRNAs is a novel mechanism of genetic exchange between cells. Nat Cell Biol *9*, 654-659.
Varghese, J., and Cohen, S.M. (2007). microRNA miR-14 acts to modulate a positive autoregulatory loop controlling steroid hormone signaling in Drosophila. Genes Dev *21*, 2277-2282.
Vogel, B.E., and Hedgecock, E.M. (2001). Hemicentin, a conserved extracellular member of the immunoglobulin superfamily, organizes epithelial and other cell attachments into oriented line-shaped junctions. Development *128*, 883-894.
Waldman, T., Kinzler, K.W., and Vogelstein, B. (1995). p21 is necessary for the p53-mediated G1 arrest in human cancer cells. Cancer Res *55*, 5187-5190.
Wenick, A.S., and Hobert, O. (2004). Genomic cis-regulatory architecture and trans-acting regulators of a single interneuron-specific gene battery in C. elegans. Dev Cell *6*, 757-770.
Wightman, B., Ha, I., and Ruvkun, G. (1993). Posttranscriptional regulation of the heterochronic gene lin-14 by lin-4 mediates temporal pattern formation in C. elegans. Cell *75*, 855-862.
Winston, W.M., Molodowitch, C., and Hunter, C.P. (2002). Systemic RNAi in C. elegans requires the putative transmembrane protein SID-1. Science *295*, 2456-2459.
Winston, W.M., Sutherlin, M., Wright, A.J., Feinberg, E.H., and Hunter, C.P. (2007). Caenorhabditis elegans SID-2 is required for environmental RNA interference. Proc Natl Acad Sci U S A *104*, 10565-10570.
Wood, W.B. (1988). The Nematode Caenorhabditis Elegans (Cold Spring Harbor Laboratory).
Yao, T.P., Forman, B.M., Jiang, Z., Cherbas, L., Chen, J.D., McKeown, M., Cherbas, P., and Evans, R.M. (1993). Functional ecdysone receptor is the product of EcR and Ultraspiracle genes. Nature *366*, 476-479.
Yoo, A.S., and Greenwald, I. (2005). LIN-12/Notch activation leads to microRNA-mediated down-regulation of Vav in C. elegans. Science *310*, 1330-1333.
Yuan, A., Farber, E.L., Rapoport, A.L., Tejada, D., Deniskin, R., Akhmedov, N.B., and Farber, D.B. (2009). Transfer of microRNAs by embryonic stem cell microvesicles. PLoS ONE *4*, e4722.
Zamir, I., Harding, H.P., Atkins, G.B., Horlein, A., Glass, C.K., Rosenfeld, M.G., and Lazar, M.A. (1996). A nuclear hormone receptor corepressor mediates transcriptional silencing by receptors with distinct repression domains. Mol Cell Biol *16*, 5458-5465.
Zanaria, E., Muscatelli, F., Bardoni, B., Strom, T.M., Guioli, S., Guo, W., Lalli, E., Moser, C., Walker, A.P., McCabe, E.R.*, et al.* (1994). An unusual member of the nuclear hormone receptor superfamily responsible for X-linked adrenal hypoplasia congenita. Nature *372*, 635-641.
Zhang, H., Azevedo, R.B., Lints, R., Doyle, C., Teng, Y., Haber, D., and Emmons, S.W. (2003). Global regulation of Hox gene expression in C. elegans by a SAM domain protein. Dev Cell *4*, 903-915.
Zhang, H., Christoforou, A., Aravind, L., Emmons, S.W., van den Heuvel, S., and Haber, D.A. (2004). The C. elegans Polycomb gene SOP-2 encodes an RNA binding protein. Mol Cell *14*, 841-847.
Zhang, L., Ding, L., Cheung, T.H., Dong, M.Q., Chen, J., Sewell, A.K., Liu, X., Yates, J.R., 3rd, and Han, M. (2007). Systematic identification of C. elegans miRISC proteins, miRNAs, and mRNA targets by their interactions with GW182 proteins AIN-1 and AIN-2. Mol Cell *28*, 598-613.
Zhao, R., Gish, K., Murphy, M., Yin, Y., Notterman, D., Hoffman, W.H., Tom, E., Mack, D.H., and Levine, A.J. (2000). Analysis of p53-regulated gene expression patterns using oligonucleotide arrays. Genes Dev *14*, 981-993.